REFERENCE ONLY

UNIVERSITY OF LONDON THESIS

Degree PhD Year 2006 Name of Author SOLANKI Dina

COPYRIGHT

This is a thesis accepted for a Higher Degree of the University of London. It is an unpublished typescript and the copyright is held by the author. All persons consulting the thesis must read and abide by the Copyright Declaration below.

COPYRIGHT DECLARATION

I recognise that the copyright of the above-described thesis rests with the author and that no quotation from it or information derived from it may be published without the prior written consent of the author.

LOANS

Theses may not be lent to individuals, but the Senate House Library may lend a copy to approved libraries within the United Kingdom, for consultation solely on the premises of those libraries. Application should be made to: Inter-Library Loans, Senate House Library, Senate House, Malet Street, London WC1E 7HU.

REPRODUCTION

University of London theses may not be reproduced without explicit written permission from the Senate House Library. Enquiries should be addressed to the Theses Section of the Library. Regulations concerning reproduction vary according to the date of acceptance of the thesis and are listed below as guidelines.

A. Before 1962. Permission granted only upon the prior written consent of the author. (The Senate House Library will provide addresses where possible).

B. 1962 - 1974. In many cases the author has agreed to permit copying upon completion of a Copyright Declaration.

C. 1975 - 1988. Most theses may be copied upon completion of a Copyright Declaration.

D. 1989 onwards. Most theses may be copied.

This thesis comes within category D.

☐ This copy has been deposited in the Library of UCL

☐ This copy has been deposited in the Senate House Library, Senate House, Malet Street, London WC1E 7HU.

Cyanide and Dithiocarbamate Complexes as Potential Catalysts for Ring-Opening Polymerisation of Epoxides

A thesis presented to the University of London in partial fulfillment of the requirements for the degree of Doctor of Philosophy

Dina Solanki

University College London
Christopher Ingold Laboratories
20 Gordon Street
London WC1H 0AJ

2006

ProQuest LLC
789 East Eisenhower Parkway
P.O. Box 1346
Ann Arbor, MI 48106-1346

I, Dina Solanki, confirm that the work presented in this thesis is my own. Where information has been derived from other sources, I confirm that this has been indicated in the thesis.

For Nishma, Kiran and Deepa

Mum and Dad

Abstract

This thesis investigates the potential catalysis of the ring-opening polymerisation (ROP) of propylene oxide (PO). Numerous industrial and academic research groups have investigated the mechanism and developed more efficient catalysis, the leading catalysts at the moment being Double-Metal Cyanides (DMC). This thesis has considered variations to DMC catalysts as well as other potential catalysts. A combination of metal cyanides and amines were also used to form complexes, which were then characterised and tested for polymerisation.

The process of ring-opening one unit of PO was examined using organic dithiocarbamates. A range of amines was used to synthesise dithiocarbamates, which were found to ring-open PO along with other epoxides. The scope was extended to include metal bis(dithiocarbamates) and consider any catalytic properties they may have towards polymerisation. Organic dithiocarbamates ranging from small groups such as methyl to rings like piperidine were attached *via* (bromomethyl)benzene units to form arenes with multifunctional arms. The number of bromomethyl units on the benzene varied from two to six, which allowed the arrangement of the arms to be studied and form iniferters for living polymerisation reactions. The dithiocarbamate chemistry was extended to include other transition metals, namely ruthenium and palladium. This work was developed using bidenetate phosphine ligands as well as allyl groups acting as capping end groups. Various substituted piperazine dithiocarbamates were reacted to potentially act as linking units to form multimetallic arrays.

Acknowledgements

Firstly, I would like to thank my supervisor Dr. Graeme Hogarth for, well everything! For taking me on half-way through my Ph.D and teaching me how to be a real synthetic chemist. I thank him for the immense patience he has shown me over the years along with his enthusiasm and support. His guidance and creativity with regards to my project has been invaluable and I am sure I would not have completed this thesis without his eye for detail and phenomenal memory. Thank you.

I thank Cognis Ltd and EPSRC for the financial sponsorship of my Ph.D. I thank Dr. Andrew Small and Dr. Muriel Ecormier for all their help and support throughout this project. I acknowledge Dr. Nicholas Leadbeater for securing industrial sponsorship and EPSRC funding.

I want to thank my family. I am eternally grateful to my sisters; Nishma, Kiran, Deepa and my parents for putting up with me over the last few years. I thank them for their love, support and encouragement over the years and their apparent unshakeable belief in me. For their kind words, hugs and shoulders and not forgetting the tough love when I needed it. I thank them for the sacrifices they have made for me and having my back. A special thank you to Nish-Moo for keeping me company during the marathon midnight printing session! Cheers sweety!

I would also like to thank my "honorary" supervisor, Dr. James Wilton-Ely for his support and encouragement over the years. I thank him for teaching me the tricks of the trade and all his work in our collaborative research. I also thank him for the interesting discussions about life and the pep-talks. My thanks go to Dr. Andrea Sella for also

teaching me how to be a real chemist and his enthusiasm for science, which I have found to be contagious. Will never forgot the liquid nitrogen ice cream!

I am forever grateful to my good friend, Dr. Christina Baskaran for being my own personal post-doc. I thank her for her text-book knowledge of chemistry and proofing my thesis. For the constant encouragement, support and kindness she has shown me over the years.

My thanks go to my friends for their support and encouragement over the years. I would like to thank the soon-to-be Doctors: Asthi Rampaul, Siama Basharat, Jalpa Patel, Naima Narband and Robert D'Rozario for all their help and support over the years. For the offers of reading the thesis to running TGA samples to having people to lunch with. I thank them for their friendship and easing my return to UCL. I am grateful to Dr. Supti Sarkar and Dr. Krishna Balakrishnan for their advice and support for my Ph.D and their valuable friendship. Many thanks to Peter Mark for listening over the years and guiding me through.

I would like to thank my best friend, Arti Patil for her love and patience, support and encouragement over the years. I thank her for carrying our friendship over the last few years. For giving me space when I needed it and checking in, to see I was still kicking.

I would like to thank Dr. Jonathan Dallimore for his belief in me and fighting my corner. Without his help, I simply would not have been here. I would also like to thank Prof. Mike Ewing for all his help in the past and aiding my return to UCL.

I would like to thank Dr. Chris Blackman for making my time in the office enjoyable. For helping me with my food so I didn't get fatter and the entertaining discussions about life. I also thank him for acknowledging my computer ignorance and taking care of Wonder Woman (my laptop!). I thank Dr. Jesus J. Gil-Tomas, Paolo Melgari, Robert Palgrave, Dr. Geoff Hyett and Kristopher Page for all their technical help through the years and during the thesis writing. My thanks go to all the past and present members of the Hogarth / Sella / Parkin and Carmalt groups as well as the Leadbeater group for making the last few years enjoyable.

I thank Dr. Abil Aliev for all his help elucidating my spectra and David Butler for NMR support and advice. I thank John Hill and Lisa Harris for Mass Specs and Jill Maxwell for elemental analysis. I thank Steve Frith for running my TGA samples and the useful discussions about thermal analysis. I would also like to thank Phil Hayes and Glen Greeves for their help and guidance over the years and to Phil, especially for looking out for my safety and reminding me to lock the door.

Thank you all!

If I have forgotten anyone, I'm sorry and thank you.

Table of Contents

List of Figures, Schemes, Tables and Equations

Chapter 1

Chapter 2

Chapter 3

Chapter 4

Chapter 5

Chapter 6

Chapter 7

Abbreviations

BO	butylene oxide
br (IR)	broad
Bu	butyl
Calc.	Calculated
CI	chemical ionisation
d (NMR)	doublet
dd (NMR)	doublet of doublets
DMC	Double metal cyanide
dppe	bis(diphenylphosphino)ethane
dppm	bis(diphenylphosphino)methane
dt (NMR)	doublet of triplets
EI	electron impact
en	ethylenediamine
Et	ethyl
FAB	fast atom bomardment
^{i}Bu	*iso*-butyl
^{i}Pr	*iso*-propyl
IR	Infra-red
J	coupling constant
m (IR)	medium absorption
m (NMR)	multiplet
Me	methyl
mm (NMR)	multiplet of mulplets
MS	mass spectrometry
NMR	nuclear magnetic resonance
PO	propylene oxide
ppm	parts per million
PPO	poly(propylene oxide)
Pr	propyl
q (NMR)	quartet
quin (NMR)	quintet

Recalc.	recalculated
ROP	ring-opening polymerisation
s (IR)	strong absorption
s (NMR)	singlet
sept (NMR)	septet
sex (NMR)	sextet
SO	styrene oxide
t (NMR)	triplet

Chapter 1

General Introduction

1.0 General Introduction

Polymers are macromolecules formed from the linking together of numerous smaller molecules (monomers) to form chains and rings[1]. The number of monomers linked together can vary greatly, depending on the reaction conditions utilised as well as any catalysts used. Thousands of both naturally occurring and synthetic polymers are now known which have become invaluable materials in today's world.

Polymers can be traced back to the ancient Mayan civilisation in 16th century Central America who used the natural polymer rubber harvested from trees[2] while another natural polymer, cellulose was identified to be a chain of linked smaller units by Polanyi[3]. In 1839, Charles Goodyear discovered the process of vulcanisation, in which natural rubber was reacted with sulfur and heated to produce sturdy polymers still used in industry today for cars tyres amongst other things. In 1907, Leo Baekeland prepared the first synthetic polymer, Baekeland, the hardness and high heat resistance of which gave it excellent electrical insulator properties.

Publication in 1920 of Staudinger's research, "Uber Polymerisation" on polymers initiated great interest in polymer science leading to the industrial production of polyvinyl chloride (PVC). Following this, many other well-known polymers were designed such as polystyrene (1930), Nylon (1938), polyethylene (1941), Ekomol (1970) and Kevlar (1971). The polymer industry grew at a rapid rate such that in 1976, the polymer/plastics industry produced more material than the steel, aluminium and copper industries combined.

There is no agreed uniform method of classification of polymers but there are different ways in which the polymers can be organised. One method is to use the terms thermoplastics and thermosets. Thermoplastics are generally linear chains of monomers that melt when heated and resolidify when cooled, while thermosets are cross-linked materials that do not melt at high temperatures but decompose irreversibly.

A second method of distinguishing polymers is by the process of formation. Carothers[4] introduced addition and condensation polymerisation as two processes of polymer formation. Addition polymerisation affords polymers in which the composition of monomeric units are identical to the monomers (e.g. polymerisation of vinyl chloride), while condensation polymerisation forms polymers, such as polyamide, in which the monomeric units are different from the monomers e.g. the condensation reaction forms small molecules such as water that are excluded.

Flory[5] emphasised the polymerisation mechanisms by introducing chain and step reactions mechanisms to loosely resemble addition and condensation polymerisation respectively. In chain reactions, there are limited active sites and so the monomers gradually react and the high-molecular weight is not realised until the end. In the case of step reactions, there can be a number of different polymer chains depending on the number of functional groups on the parent monomer. Multiple active sites results in polymers, which are unbranched linear chains or multi-cross-linked networks or a mixture of both.

Another type of polymer classification is the way in which the monomers arrange themselves, their tactity. This type of classification can only be used for asymmetric

monomers, such as propylene oxide. Depending on the approach of attack, the polymer has three possible arrangements: isotactic, syndiotactic and atactic. Isotactic is when all the chiral centres have the same configuration and the pedant groups in the monomer arrange themselves in an identical way. Syndiotactic polymers have a regular alternating arrangement of the pedant groups in the monomer and finally atactic in which all the molecules are randomly ordered (Figure 1).

Figure 1: Three forms of tacticity of poly α-olefins

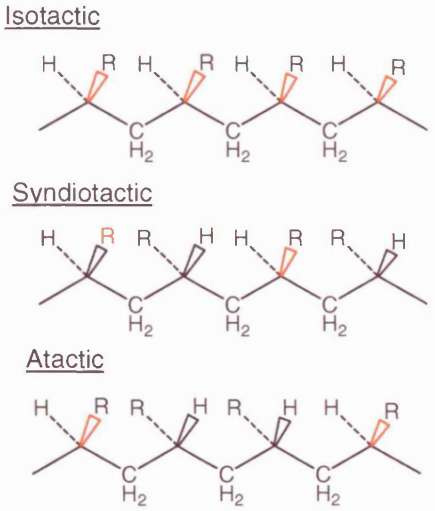

Research in polymer science has continued with great speed aided by the development of instrumentation such as gel permeation chromatography (GPC). This has allowed in-depth analysis of polymers formed in terms of the number of units in the polymer (molecular weight (M_w)), the number of polymer molecules (M_n) and the ratio of the M_w and M_n being termed the polydispersity. If all the polymer molecules are of equal size, then the number average molecular weight is equal to the weight average molecular weight to give a polydispersity index (PDI) of 1[6]. However, all synthetic and many natural polymers have a greater molecular weight average and thus PDI is

greater than 1. This value can be used to assess the quality and uniformity of the polymers formed.

1.1 Catalysts in Polymer Synthesis

There are hundreds of examples of catalysts in industry that produce polymers used in everyday life. The catalyst offers an alternative reaction path that requires less energy, thus lowering the activation barrier and allowing it to proceed more rapidly. Catalysts are vital in polymer synthesis and can form polymers with specifically desirable properties. These include polymer structure (linear or rings), M_n, M_w, PDI, temperature sensitivity and flexibility to name a few.

An example of a catalyst being used to create a polymer with specific properties would be the production of poly(propylene) (PP). PP is a thermoplastic polymer used for a wide variety of applications. It has found uses in areas as diverse as flexible and rigid packaging, large moulded parts for automotive and numerous consumer products. Its properties include excellent chemical resistance, high strength, high melting point of 160°C and the lowest density of all plastics used in packaging.

The tacitity of a polymer is vital in controlling the properties and uses of the product. The organisation and orientation of the chiral centres in the backbone of the polymer and the steric configuration of the pendant methyl groups affect the polymer's ability to form crystals[7]. Controlling the orientation of monomers to the catalyst controls the tacticity of PP and therefore its properties.

Ziegler-Natta catalysts are used for PP production because these catalysts only allow monomers with the correct orientation to join the polymer chain. Early Ziegler-Natta catalysts were formed from titanium chloride and gave atactic polymers of PP. Some zirconium-based Ziegler-Natta catalysts form isotactic polymers with all the methyl groups on one side, causing the polymer to form helices. The arrangement of these helices next to each other results in the great strength of PP. Further to this, Kaminsky catalysts based on metallocenes of group 4 transition metals with methylaluminium oxane (MAO), such as Cp_2ZrCl_2 (Figure **2a**) are catalytic. These complexes use chiral metallocenes and bridged cyclopentadienyl rings to control tacticity of polymers formed. For PP, variation of these complexes generates polymers with atactic, isotactic and syndiotactic tacticity (Figure **2a-c**)[8].

Figure 2: Kaminsky catalysts producing PP polymers with different tacticity[9]

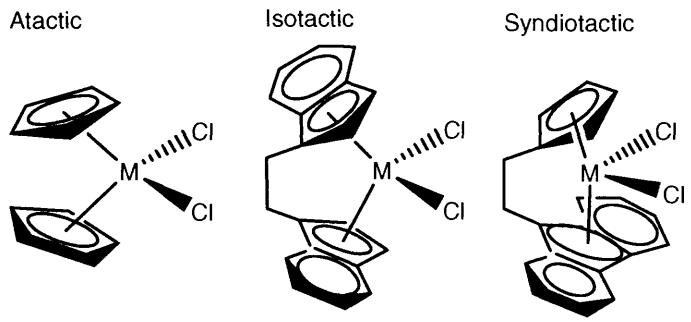

1.2 Poly(propylene oxide)

In collaboration with Cognis, we have concentrated on the polymerisation of propylene oxide (PO) *via* ring-opening polymerisation (ROP). Approximately 4.5 million tonnes of poly(propylene oxide) (PPO) was produced internationally in 2003[10]. It nets millions of pounds annually and continues to increase production and profitability each

year. Around 40% of PPO products find uses in surfactants and oil demulsifiers, the further 60% being used for polyurethanes, which have a great number of uses in flexible foam, coatings, adhesives, sealants and elastomers[4]. These are developed and used in many household goods such as furniture, car seating, paints, ski suits and waterproof leisurewear etc. There has been fierce competition in PO polymerisation catalysis due to the growing demands of China and its economy. As China's industry continues to grow faster than any other country in the world, they have attempted to set up PPO production in their country to meet the demands but they continue to be the biggest importer of PPO.

Propylene oxide is a three-membered ring, consisting of oxygen and two carbons, bonded *via* σ bonds. The C-O bond is polar due to the high electronegativity of the oxygen bond measuring 1.4 Å and the C-C bond measures 1.5 Å (Figure 3). There is significant ring strain in the three-membered ring giving a more reactive species compared to other simple ethers. The energy required to break the C-O bond of monomer PO is 26.7 kcal/mol[11]. The strain is therefore relieved by ring-opening, which can be achieved in different ways.

Figure 3: The bond lengths and angles of propylene oxide[12]

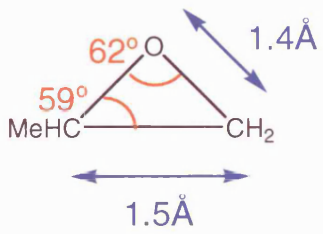

1.3 Mechanisms of PO ROP

There are two possible sites of attack on PO, the C_α which is the chiral centre and more sterically hindered due to the methyl group compared to methylene C_β (Scheme 1).

Scheme 1: Two routes to ring-opening PO monomer with KOH

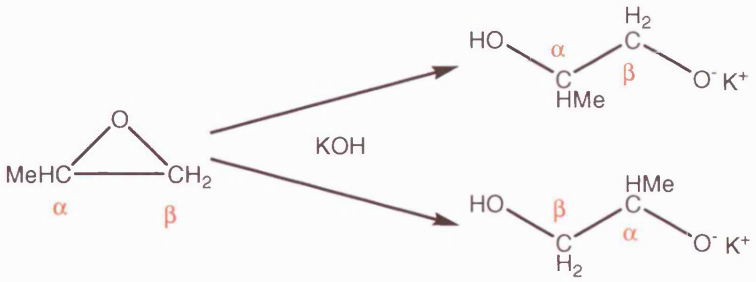

Depending on the type of catalyst and mechanism followed, the organisation and orientation of the monomers in the polymer chain (tacticity) can be controlled. This is known as regioselectivity and strongly affects the quality and properties of the polymer formed. Most catalysts attack the sterically less hindered C_β of PO, forming "head-to-tail" (HT) polymers. If each monomer is ring-opened in this manner, a regular crystalline polymer (isotactic) is formed. Using specific catalysts such as Et_2Zn/H_2O[13, 14], it is possible for the C_α to be the site of ring opening. The amorphous PPO formed has "head-to-head" (HH) and "tail-to-tail" (TT) configurations but this is rare for PO (Figure 4).

Figure 4: Representations of different configurations

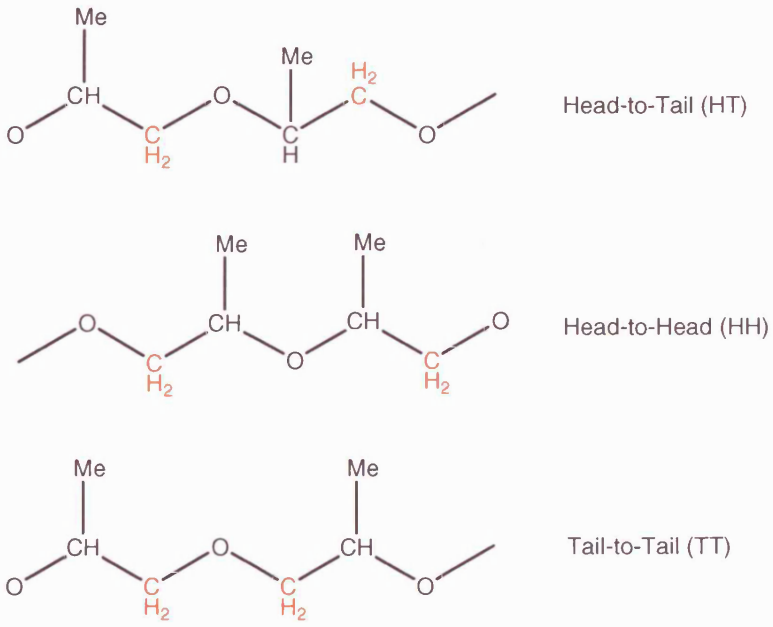

Generally, when PO is ring-opened, there is an inversion of the configuration at the carbon where the cleavage occurs. Most catalysts, regardless of it being mononuclear, multinuclear, or chelating ring systems have inversion at the C_β. There are very few examples of stereoretention[15, 16] of the polymer backbone. Both homogenous and heterogeneous catalysts have been used and mechanistic speculation drawn about their activity. These epoxides react to form polymers known as polyether polyol *via* cationic, anionic and coordination routes[17].

Cationic Mechanism: In the cationic route, many different types of catalysts can be used to polymerise PO yielding low-molecular weight polymers. These catalysts can be strong protic acids such as trifluoroacetic, fluorosulfonic and trimethanesulfonic (triflic) acids[1] that create secondary oxonium ion. The reaction mechanism for proton donor initiation is outlined below where the carbon with the methyl substituent group is regiospecific (Scheme 2).

Scheme 2: Mechanism of cationic polymerisation using acid [1]

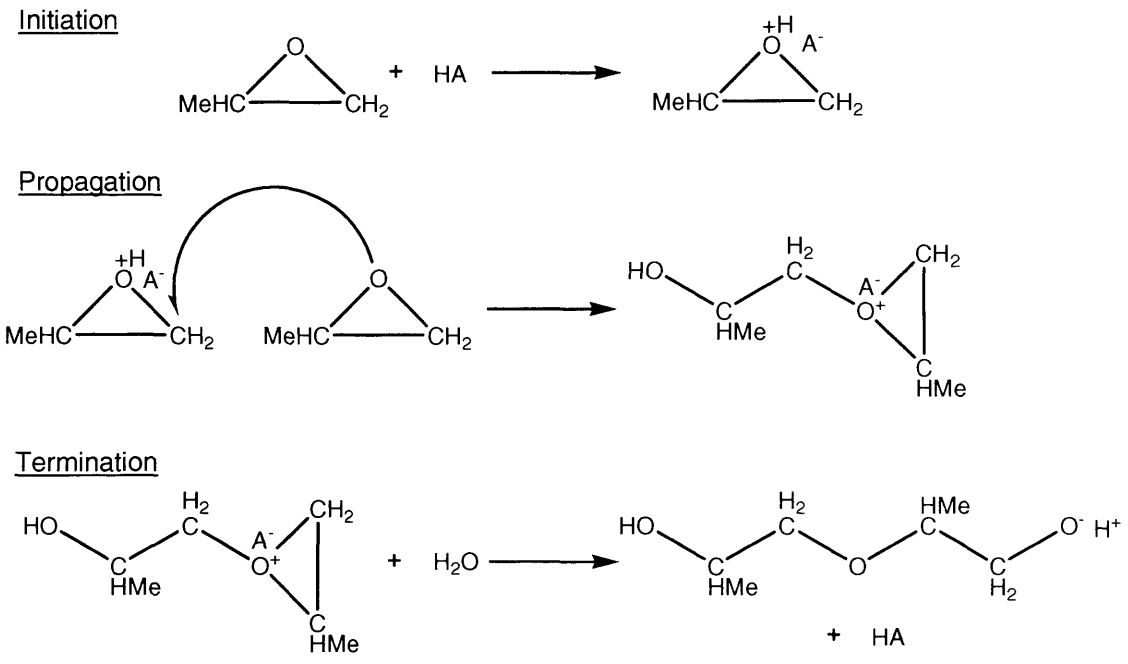

The nucleophilicity of the anion can limit the reaction if the anion is weakly nucleophilic as it can compete with PO for the proton or the secondary /tertiary oxonium anions. This results in a very low degree of polymerisation and low-molecular weight polymers. The nucleophilicity of water also allows competition with PO monomers for the oxonium ions, resulting in premature ending of polymerisation.

Lewis acids have been investigated in ROP of PO and complexes such as BF_3 with water or some other protogen (e.g. allyl halide) have been successful in polymerisation[1]. BF_3 with water forms $H^+[BF_3OH]^-$ ionic system that produces the cation for PO coordination. The mechanism for $H^+[BF_3OH]^-$ shows the formation of the secondary and tertiary oxonium ion, which reacts with the PO monomer to ring-open the epoxide (Scheme 3).

Scheme 3: Mechanism of cationic polymerisation using Lewis acids

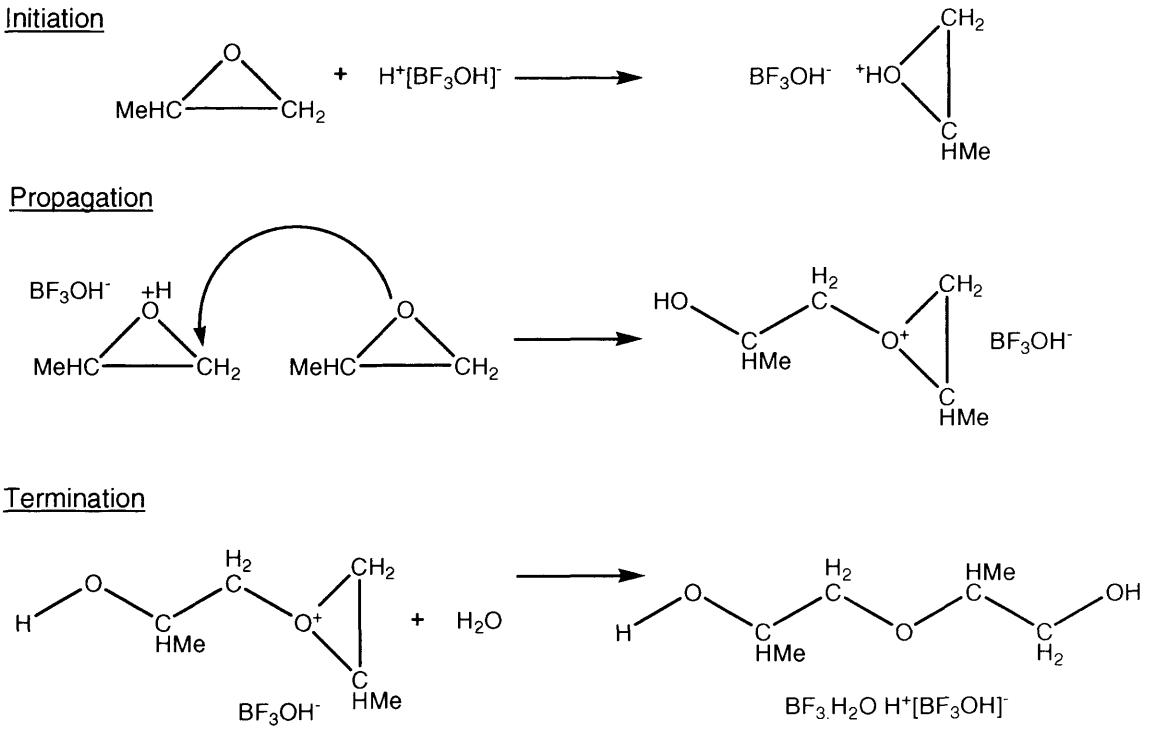

Other examples of these catalysts would be complexes of alkyl halide with a Lewis acid to give carbocations (see below).

Equation 1: Examples of Lewis acid [1]

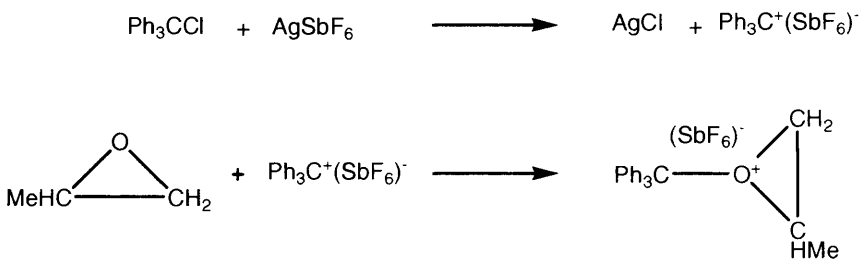

Anionic mechanism: The anionic polymerisation route produces low-molecular weight polymers and uses basic catalysts such as KOH or alkoxides. The formation of an alkoxide ion by S_N2 displacement in the initiation stage allows the nucleophilic displacement in the propagation stage (Scheme 4). PO exhibits stereoregularity due to the nucleophilic substitution preferring the less hindered C_β, which produces chains with pendant methyl groups [17].

Scheme 4: Mechanism of anionic polymerisation

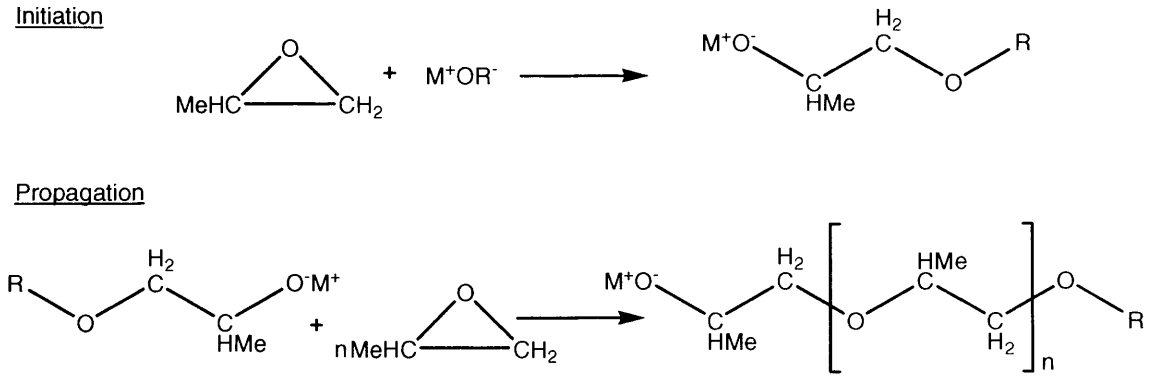

This process forms low-molecular weight polymers (<6,000) due to the competition between the initiation and propagation stages, resulting in chain transfer. Chain transfer occurs when the proton from the methyl group of the PO is extracted, followed by rapid ring-opening producing an alkyl alkoxide anion. This can partially isomerise to form the enolate (Scheme 5).

Scheme 5: Mechanism of chain transfer [1]

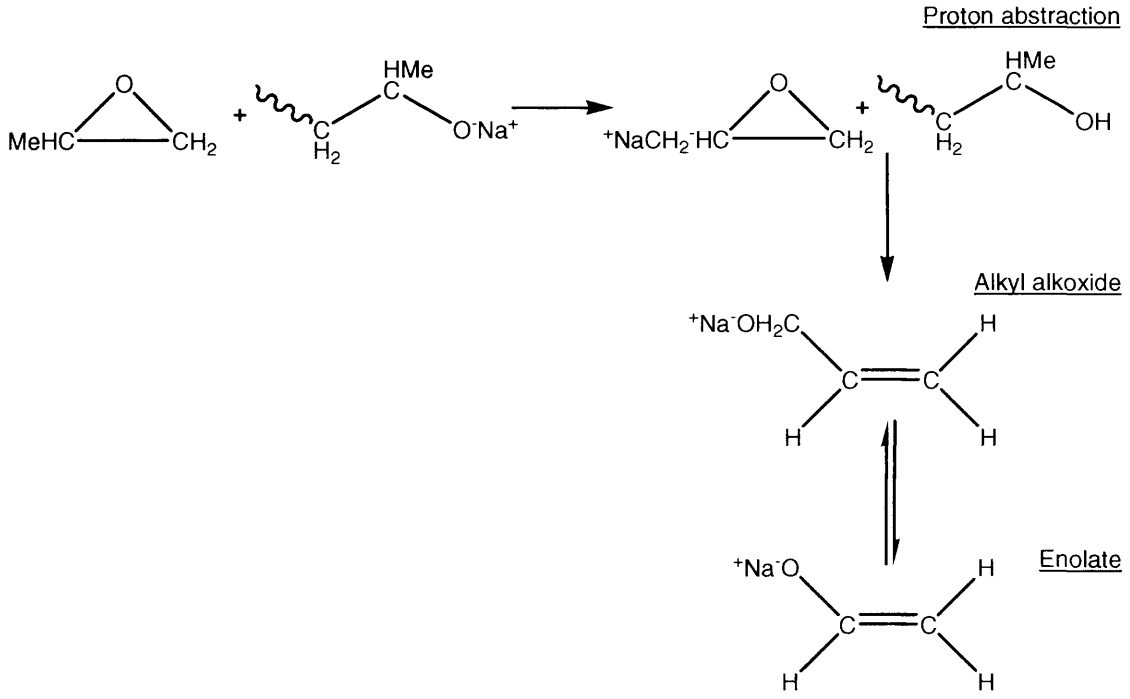

The addition of more monomer units allows the active end of the chains to react and increase its molecular weight. Co-block polymers can easily be formed using this process, resulting in a variety of polymers with different properties.

Coordination Mechanism: Coordination catalysts encompass a wide range of compounds such as alkaline earth complexes [18-20] calcium amide[21-25], calcium amide-alkoxide[21, 26] as well as Ziegler-Natta types catalysts[27-29]. Other examples would be dialkylzinc compounds[30-34] and metal porphyrins[35-37].

Coordination catalysts polymerise epoxides by forming σ bonds between the catalyst's active sites, the electrophilic metal atom and the heteroatom oxygen of PO[38] Nucleophilic attack at the catalyst and the ring-opening of the epoxide follows. This process is commonly known as coordinated anionic mechanism allowing the production of high-molecular weight PPO attributed to the lack of any simple termination step (Scheme 6).

Scheme 6: Mechanism of coordinate anionic polymerisation [6]

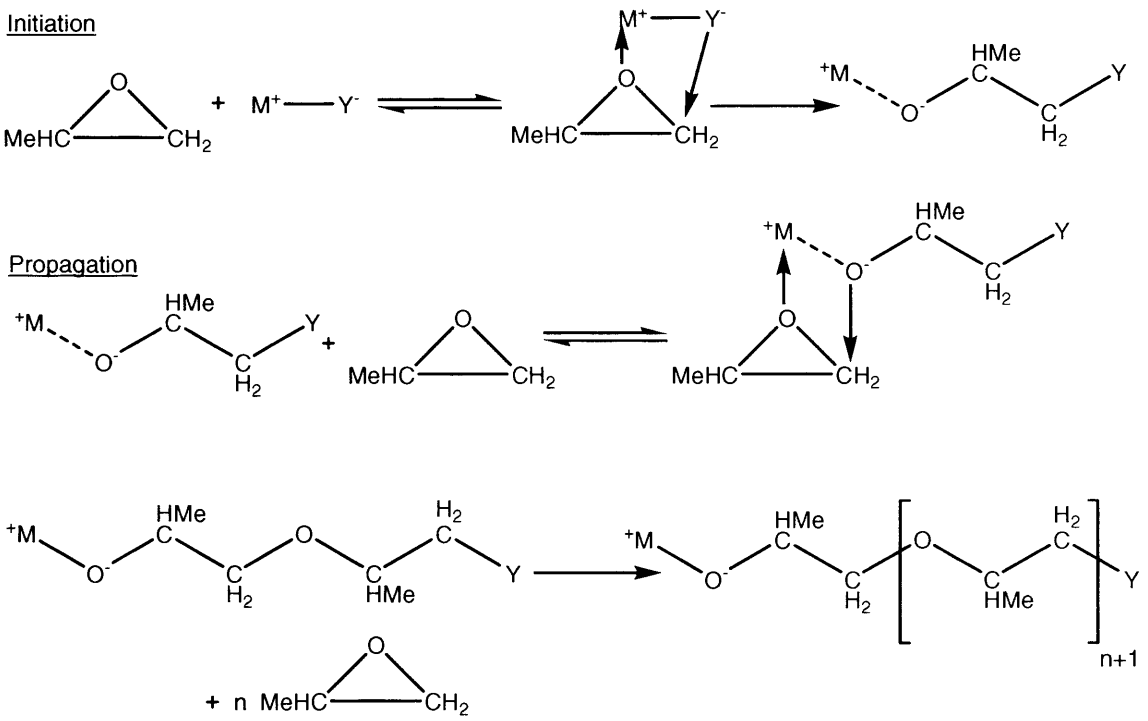

Coordinated cationic mechanism has also been proposed for PO polymerisation using $O(ZnEt)_2$ as the catalyst[6] (Scheme 7).

Scheme 7: Mechanism of coordinate cationic polymerisation[6]

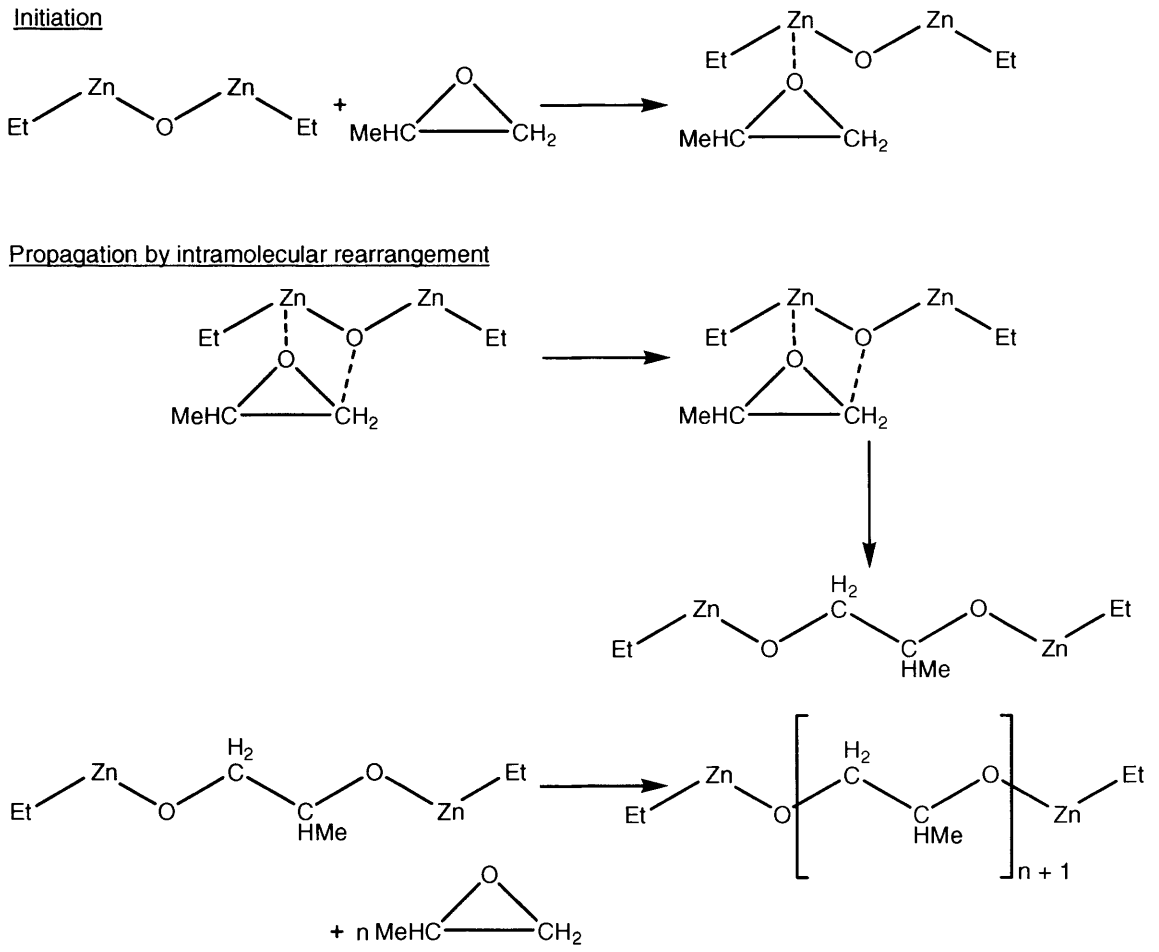

Numerous coordination catalysts provide high quality PPO with high-molecular weights. Many catalyst complexes are regiospecific, forming large portions of crystalline isotactic and syndiotactic polymers; however, amorphous polymers are also formed. It has been proposed that catalysts such as $Et_2Zn.H_2O$ form both isotactic and syndiotactic polymers from specific sites and a mixture of racemic polymers from other sites. Further work is being carried out to fully understand the mechanism involved in polymer formation[6].

1.4 Traditional Catalyst - Potassium Hydroxide

Like many other companies, Cognis uses the conventional catalyst KOH for PO ROP following a base (anionic) polymerisation process. Polymers are formed in reasonable yields with low to medium molecular weight. Advantages of using this catalyst are that it is inexpensive and produces good regiospecific polymer due to the S_N2 nucleophilic attack on the less hindered C_β atom. Some catalysts require a mixing time with an initiator or monomer before forming the active species (induction period), which is unnecessary for KOH, thus making it more economical. However, there are numerous disadvantages of base catalysis such as the mediocre molecular weight of polymers formed. The basicity of catalyst also causes the abstraction of a methyl proton generating unsaturated ends, which leads to chain transfers, resulting in the decrease in the degree of polymerisation and therefore reducing M_w. When PPO has high-unsaturated terminal ends and is reacted with isocyanates to make polyurethane (PU), there is a significant decrease in PU polymer quality and properties[39].

There are increasing governmental regulations requiring companies to minimise the affects of industrial processes on the environment. Cognis take this responsibility very seriously and hope to invest in an environmentally benign catalyst system. Using KOH in industry results in undesirable by-products, such as dimethyldioxane (formed by two PO rings opening to form a six-membered ring) requiring costly disposal. Therefore, a recyclable catalyst that is easily extracted from the polymer would be ideal. Another possibility would be to leave trace amounts of catalyst in the final polymer that has no affect on further manufacturing of products. A lack of an extraction stage in the industrial process would be time saving and economical.

1.5 Double Metal Cyanide (DMC)

Leading catalysts for ROP of PO are double metal cyanides (DMC). Typical DMC complexes are $Zn_3[Co(CN)_6]_2.12H_2O$ and $Zn_3[Fe(CN)_6]_212H_2O$. There are various combinations of DMC complexes following the general formula $[(M)_aM'(CN)_b]$. In the formula, M is an alkali metal ion, alkaline earth metal ion or a transition metal, M' is transition metal ion, typically Zn(II), Fe(III), Co(III) or Ni(II) and a = 1 - 3; b = 4, 6. Their simple synthesis involves the reaction of aqueous solutions of metal salts and metal cyanides to produce DMC precipitate.

DMC compounds were first discovered to catalyse the ROP of epoxides by General Tyre and Rubber Co. in the early 1960s[40]. Companies such as Shell[41-43] and Arco Co.[39, 44, 45] altered the DMCs to improve their activity and in 1983 implemented them in PPO production. DMCs are more expensive than KOH so they have to be more active to be economically viable. Various papers and patents[46-48] have exhausted the different combinations of these DMC complexes and found that the most effective in ROP of epoxides to produce polyether polyols is $Zn_3[Co(CN)_6]_2.12H_2O$ and more recently, $Zn_3[Fe(CN)_6]_212H_2O$[39, 43, 49] being marginally more catalytic.

Transition metal cyanide complexes date back to 1704 when Diesbach serendipitously discovered Prussian blue [50]. There are many advantages of using cyanides as ligands such as its ability to act as both σ-donors and π-acceptors (Figure 5). It also has a single negative charge and its ambidentate nature makes it a highly versatile ligand. In the ground state, CN^-, has triple bond character between carbon and nitrogen atoms [51]. The negative charge is almost evenly distributed over the two atoms [C (-0.501) and N (-0.499)]. The carbon is the site for bonding as the highest energy lone pair (5σ) is

localised at carbon with a lower ionisation potential of 11.26 eV versus 14.3 eV of the nitrogen. In the spectrochemical series, cyanide is positioned at the high end, so forming low-spin complexes. Due to their anionic nature, cyanides are better σ donors and poor π acceptors compared to carbon monoxide, which form strong M-L σ bonds, stabilising low and high oxidation states.

Figure 5: π back-bonding from dπ orbital to the pπ of CN^-

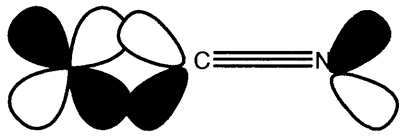

Filled metal d-orbital Empty π* orbital

The structures of DMC complexes have been investigated but limited information is available. A crystal structure of $Zn_3[Co(CN)_6]_2.12H_2O$ has been obtained [52], exhibiting a rocksalt cubic structure with divalent zinc metals linked to cobalt atoms by cyanides. Each cobalt (III) centre is bound to six cyanides through the carbon, forming an octahedron. The four nitrogen ends of the cyanides bind to the zinc centre in the planar manner. The two oxygen atoms from the water occupy the sites above and below the plane leading to an overall octahedral array.

Based on the formula, zinc has occupancy of 1 in the cubic structure and cobalt is ⅔. There are eight water molecules and three uncoordinated water molecules per unit cell. As the zinc and cobalt occupancy is unbalanced, there are empty cobalt coordinate sites in the cubic structure. Therefore, there are two basic structural units. The first is a completely ordered arrangement of metals and cyanides, occurring ⅓ of the time in the overall structure. The bond lengths of the various DMC atoms are 1.901(14) Å for Co-C; 2.089(9) Å for Zn-N; 1.135(13) Å for C-N and 2.134(10) Å for Zn-O (Figure **6a**).

The second structural unit occurs when two cobalt atoms are missing from each cubic unit. In this unit, a water molecule (H_2O{2}) fills the empty cobalt coordination site with a further nine water molecules ($6H_2O$ {1} and $3H_2O$ {3}) forming strong hydrogen bonds. The other two water molecules (H_2O {4}) are clathrated in the cavities of the network, linked by hydrogen bonding (Figure **6b**). These water molecules are considered to be important in stabilising the structure of the DMC. Thermal gravimetric analysis has found that the structure can be partially and completely dehydrated with decreases in the bond lengths of Zn-N but the structure can be rehydrated to its original form.

Figure 6: Crystal lattice of $Zn_3[Co(CN)_6]_2.12H_2O$[52]

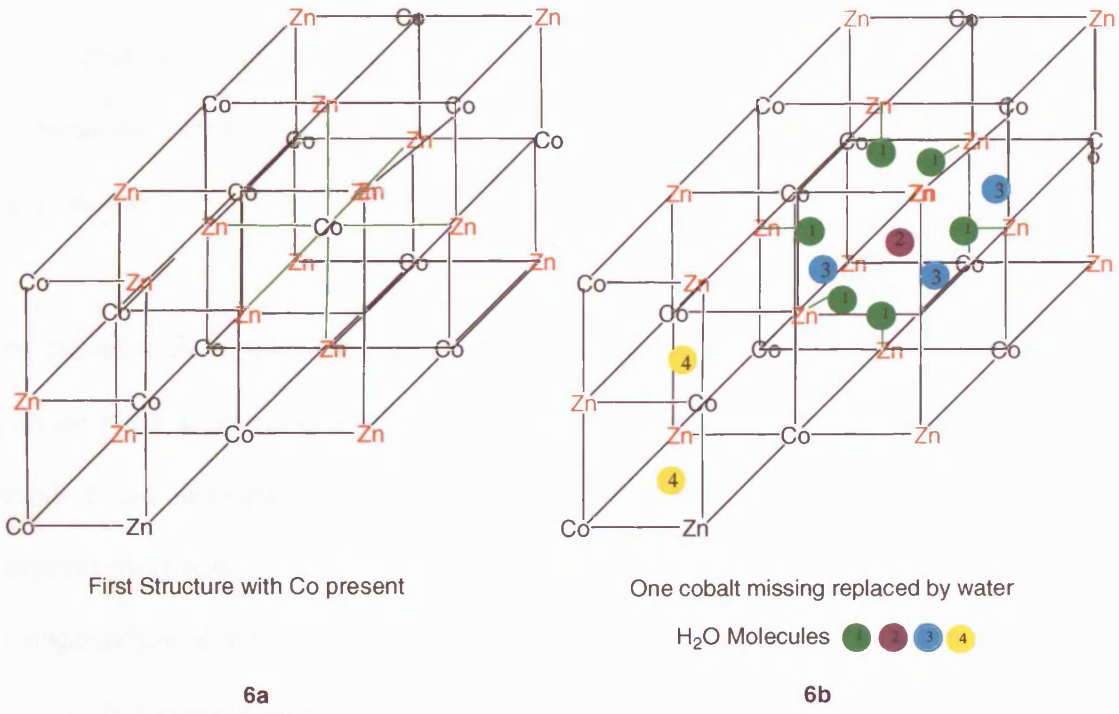

Analogous manganese and cadmium [53] salts of $[Co(CN)_6]^{3-}$ and $Fe_4[Fe(CN)_6]_3.xH_2O$ [54] adopt the same structural features, indicating these structures are uniform in this class of compounds. The zinc centre in $Zn_3[Co(CN)_6]_2$ is believed to be the catalytically

active site, the axial water molecules being readily lost generating active sites for alkoxide addition and polymer growth. The network holds the zinc centre in a square-planar arrangement, allowing the two vacant axial positions for further bonding (Scheme 8).

Scheme 8: Square-planar arrangement of the zinc centre with two water molecules (above and below)

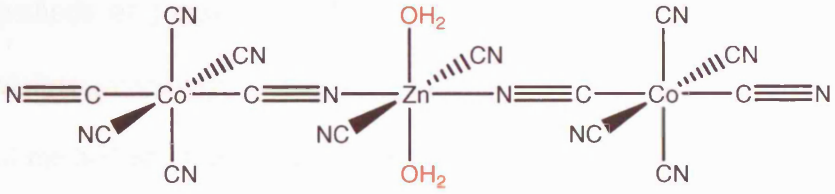

Other DMC-type structures such as $[\{CpCo(CN)_2(\mu\text{-}CN)\}_2Zn(py)_4]$ [55] display similar cubic character with zinc adopting an octahedral arrangement, indicting the desirable constrained tetra-nitrogen coordination at this centre, allowing the axial positions to react further.

As the network of the DMC compounds have vacant cavities, various organic solvents can be used as guest molecules. The advantage of this is better interface between catalyst and monomer. The increased miscibility of the catalyst with the monomer exposes more active sites and potentially increases the rate of polymerisation. Organic compounds used for this purpose are termed "complexing agents". A typical example of this is a combination of ^tBuOH, poly(ethylene glycol) (PEG) and H_2O, known as glyme which has a high surface area of 50 - 200m^2/g. The formation of these complexes involves similar procedures to traditional DMC complexes, however, the complexing agents are stirred with the individual metal salts and metal cyanides prior to their combination. Once these have been added together, they are stirred with more

complexing agent. The precipitate is filtered and reacted with more complexing agent several times before finally being filtered and dried[56]. This process ensures the maximum amount of complexing agent has been incorporated so that the catalytic properties are boosted. The general formula for these types of DMC complexes are $Zn_3[Co(CN)_6]_2.xH_2O.y^tBuOH.z$PEG.

Different methods of preparing DMC complexes have been introduced in order to increase catalyst reactivity. Sugiyama *et al.*[57] synthesised DMCs using the conventional method and then heated them with the complexing agent at 60°C. Heating the mixture encourages greater uptake of the complexing agent, which in turn increases miscibility and reactivity. Other methods[58] of complexing DMC compounds include layering the DMC compound with a solvent immiscible with water, the DMC compound being dissolved leaving the water molecules behind. The removal of water results in an increased number of active site accessible and therefore reactivity.

Various types of organic complexing agents [49] [59-64] have been shown to increase solubility such as bifunctional glycol [65], β-cyclodextrin, PEG 1,000, Tween-60 [66] and organic ethers [67]. Many researchers [43, 49, 56, 68] have found that the organic complexing agent played an important role in the morphologies of the complexes. Hua *et al.* [59] postulated that organic ligands determined the crystallinity of the complex. They found the quantity and electronegativity of atoms in the organic ligands affect the morphology; large quantities of complexing agent reducing the crystallinity. The highly electronegative atoms in the complexing agent also reduce crystallinity and in the absence of a complexing agent, highly crystalline DMC complexes are formed which have been found to be inactive as catalysts [46]. In our research, we have found evidence

to the contrary, the standard DMC complexes without a complexing agent catalysing the ROP of PO (discussed later).

The combinations and amounts of various components of DMC complexes have been investigated. Using an excess of $ZnCl_2$ in DMC [45] formation provides additional metal cation sites that interacting with ^tBuOH and offering more active sites for polymerisation. Chen *et al.* [39] found that changing the ratio of $ZnCl_2$: $K_3[Fe(CN)_6]$ influenced the viscosity of the polymer and polymerisation reaction time. A 6:1 ratio produced the highest viscosity and shortest reaction time. The resulting catalyst which including $ZnCl_2$ is represented in the formula $Zn_3[Fe(CN)_6]_2.wZnCl_2xH_2O.y^tBuOH.z$PEG.

The preparation and drying conditions can also alter the ratios of the different components but small variations had no appreciable effect on the activity [45]. The ratio of monomer: initiator was claimed to dictate the molecular weight of the polymer and not the monomer: catalyst ratio as might be expected. Since the number of moles of polymers is nearly equivalent to that of initiator, each initiator participates in the propagation and very few new chains are formed. The ratios of initiator to monomer can dictate the quality of the polymer and the aim of this research is to optimise the production of PPO, thus balancing the ratios can play a vital role.

The complexing agent can affect the morphology of the DMC complex. Using X-ray diffraction, it was found that amorphous DMC complexes were more catalytically active than their crystalline counterparts. Researchers [39, 45] found that the order in which the reactants are added together also affects the morphology. When the

complexing agent is added to the individual aqueous solutions of metal salts and cyanides before they react together, the product is more amorphous than when the complexing agent is added after the reaction between the metal salt and cyanides [43, 45, 49, 56].

Polymerisation of PO involves ring-opening of a strained epoxide, which is an extremely exothermic. To control the excess heat and energy formed in an industrial process, an induction period is used. DMC catalysts utilise this induction period, a small quantity reacting with ^{t}BuOH and PO to form oxonium ions and prepare for monomer addition. After a period, the bulk monomer is added and polymerisation is completed. Although DMC catalysts are very effective in forming PPO, this induction period is time consuming and uneconomical.

The method of monomer addition to the catalyst can alter the quality and molecular weight of the polymer formed. It was found that monomer addition in one-step resulted in a broader molecular weight distribution compared to that formed when stepwise monomer addition was used. Huang *et al.* [45] have suggested an explanation for the broad molecular weight distribution upon one step addition. They proposed that when there is a high concentration of PO, an increase in the rate of chain propagation ensues making it faster than the rate of formation of active centres. As the catalyst concentration decreases, the exchange rate decreases and this therefore decreases the number of active centres propagating together.

Many of the existing patents for DMC complexes have examined catalyst formulation and preparation, uses of various complexing agents, reaction conditions, as well as

methods of monomer addition. Hofmann *et al.* [69] recognised the Lewis basicity of the oxygen atom in PO and included an additional component, Lewis acidic lanthanide triflate. Ranges of lanthanides were investigated along with some early transition metals such as scandium and yttrium. These triflates were reacted with monomer to form low-molecular weight oligomers ranging from 200 to 1,000, which were then reacted with DMC catalyst and more monomer to form long-chain PPO. The advantages of using triflates are that they are highly reactive and do not require an induction period. Also, very small quantities of catalyst are required and hence do not deactivate the DMC catalysts added later.

1.5.1 Mechanism of DMC catalysts

There has been great controversy over the mechanism by which the DMC catalysts ring-open PO. Numerous industrial and academic groups have attempted to propose mechanisms and provide a consensus [39, 43, 45, 46, 48]. Various active sites have been suggested such as Zn^{2+}, $[Fe(CN)_6]^{3-}$, Cl^- and even the complexing agent [49].

Huang *et al.* [45] examined the mechanism behind the polymerisation of PO. DMC catalysts yielded polymers with a head-to-tail regiosequence and a random distribution of tacticity, indicating that the active centre had both cationic and coordinate character. They used GPC to determine the presence of only one type of active centre. IR studies identified a lack of metal-alkoxide bonds, suggesting a coordination-insertion mechanism was unlikely. Therefore, they have suggested that the DMC active centre is coordinating cationic. Kim *et al.*[70] proposed a detailed mechanism for these types of polymerisation. They also observed that the active sites in the DMC catalyst had cationic and coordinate properties (Scheme 9).

Scheme 9: Proposed mechanism for DMC catalysts *via* coordinate cationic polymerisation [70]

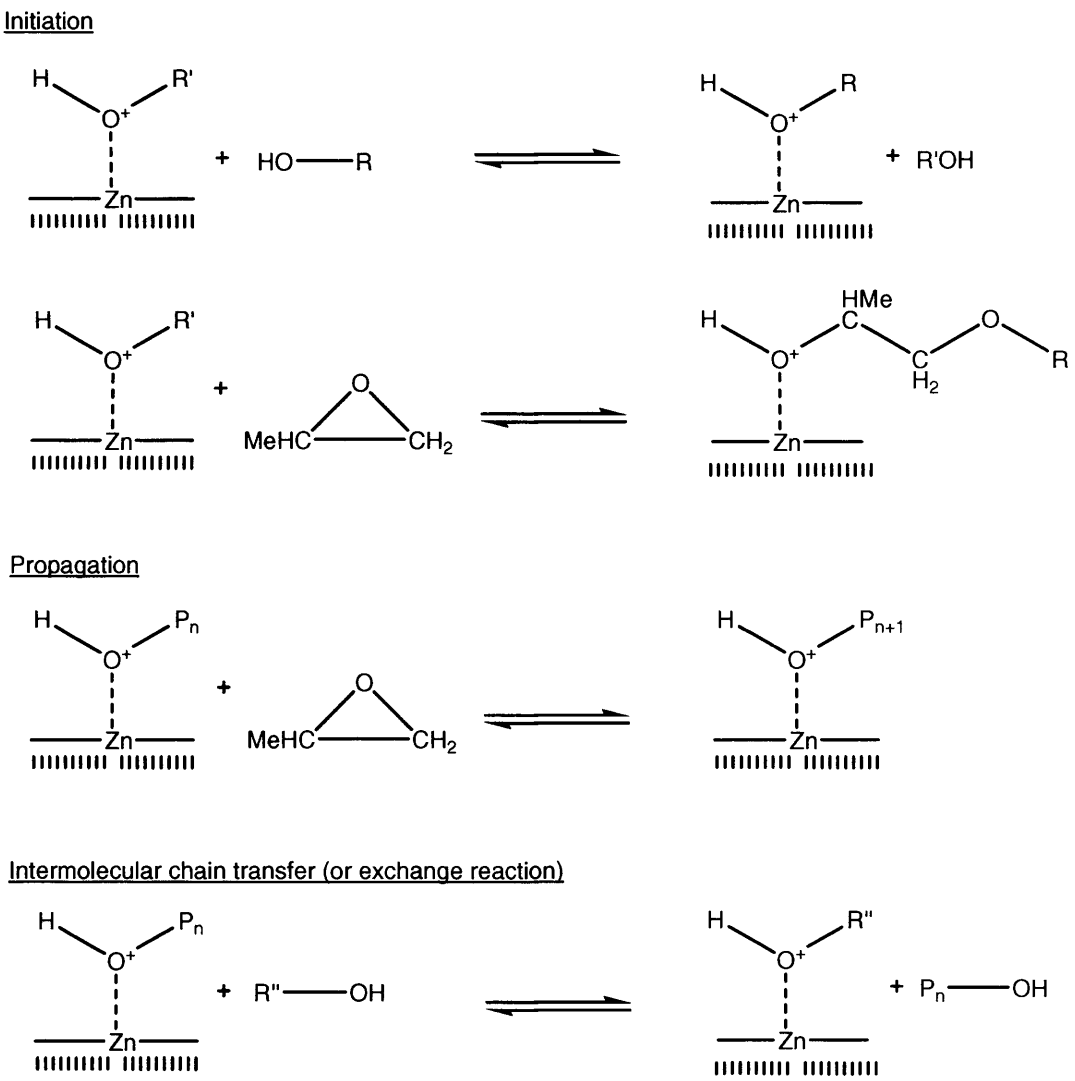

Although there is no uniform agreement, researchers that actually commit to a mechanism prefer one with a combination of coordinate and cationic polymerisation. After reviewing the literature, the author believes that this mechanism is the most probable with substantial evidence presented in literature.

1.5.2 Evaluation of DMC

DMC catalysts are preferred for PO polymerisation and subject of numerous patents [43, 46-48]. They have proved to be the most reactive producing high yields with high M_w

(1,500-10,000), narrow molecular weight distributions and low unsaturated polymers. There has been research [71-76] in catalyst extraction but methods found resulted in deactivation. One of the greatest advantages of DMC catalysts is that they are highly reactive so can be used in very small amounts, in the range of 15-100 ppm. When catalytic amounts are so small and relatively inert to further manufacturing, DMC catalysts can be left in the final polymer, therefore avoiding time and money spent on catalyst extraction.

In spite of the great advantages of DMC catalysts, there is room for improvement. The induction period is costly in terms of increased cycle time and although these polymers have less terminal unsaturation compared to polymers produced by KOH catalysts, reducing this further would be desirable. Many of the industrial leaders have invested time and resources into DMC catalysts and have secured many patents. Other companies will have to pay a large sum of money to use these patented catalysts, which is not financially viable. Therefore, different classes of chemical compounds have been investigated as potential catalysts to compete against the DMC catalysts and provide a market advantage to smaller companies.

Cognis wishes to increase their market share and become more competitive with the market leaders in this economy. This would be achieved by using a catalyst that produces high-molecular weight polymers in excellent yield with the desired properties. Cognis also wishes to use catalysts in very small amount so that it can be left in the polymer mixture. Ideally, this will be inert to allow for further manufacturing processes of the polymer and so catalyst extraction is not necessary and economical.

1.6 Alternative Catalysts

As well as conventional alkali metal hydroxides and DMC catalysts, a number of other compounds have been shown to successfully ring-open PO [36, 77-79]. Many follow clear pathways, which allow classification of the catalyst behaviour and polymerisation mechanism. These can be organised into three main processes: cationic, anionic and coordination polymerisation. There are, however, further examples indicating a combination of mechanisms using various techniques, such as coordination-anionic polymerisation and then there are instances in which the mechanism is not clear. Below is an outline of the three classes of mechanisms that can clearly be identified with examples.

1.6.1 Mechanisms of polymerisation

Cationic Polymerisation

Much work has been carried out on Lewis acids that ring-open heterocycles [80]. Both Lewis acids such as $BF_3.Et_2O$ and Brønsted acids such as HBF_4 [81, 82] catalyse PO polymerisation *via* ROP. Unfortunately, they tend to give oligomers and by-products such as dimethyldioxane. A range of different sizes of cyclic oligomers is formed due to "backbiting" reactions whereby the growing polymer chain reacts with itself, terminating the polymerisation [83] and their use in industry is limited.

Researchers[84-86] have devised cationic "activated monomer" ROP where a Brønsted acid is used to activate PO. Here, the neutral hydroxyl group replaces the electrophilic oxonium ion on the growing chain end. In this active chain mechanism, the reaction is carried out under strict control of the monomer, to the extent that it is starved of monomer (Scheme 10).

Scheme 10: Mechanism of RO polymerisation of PO using Brønsted acid

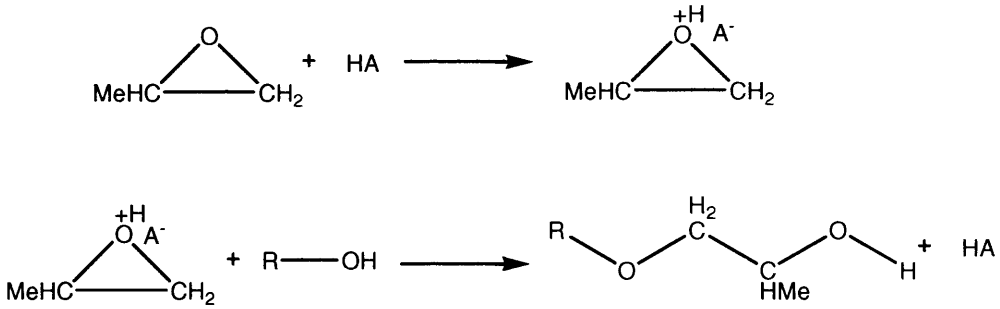

Examples of cationic catalysts for ROP of PO are the mono- and dimeric chromium complexes (Figure 7)[87]. These have been investigated using gas and solution phase polymerisation. Both complexes formed polymers, the greater activity being shown by the dinuclear complex. Oligomer formation was high and the turnover numbers (TON) larger for the dinuclear complex.

Figure 7: Mono and di- chromium salen complexes [88]

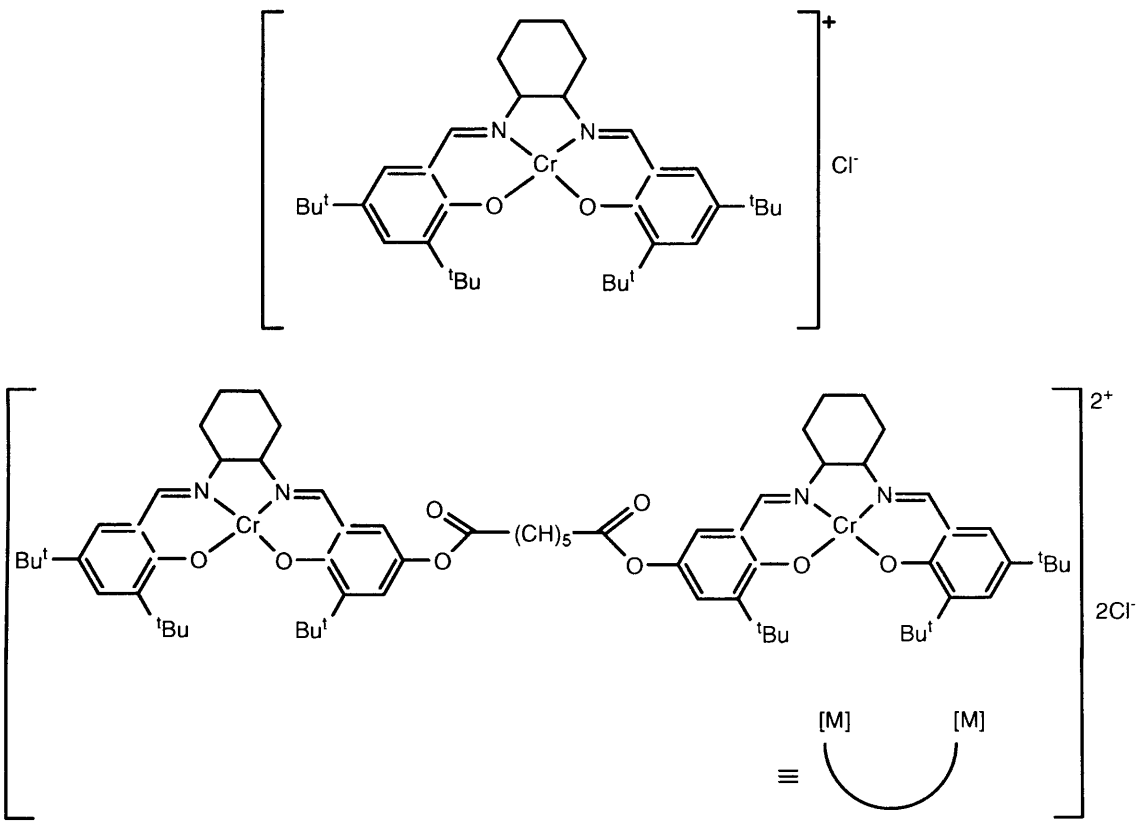

The mechanism proposed is cationic for the binuclear complex. The two metal centres are the active sites for catalyst. The coordination of the first PO initiates the polymerisation, forming oxonium ions. Using two active metal sites reduces backbiting of the polymer chain by defining the orientation *via* the formation of a μ_2 alkoxide (Scheme 11).

Scheme 11: Proposed mechanism of ROP of PO using bimetallic chromium salen complex [88]

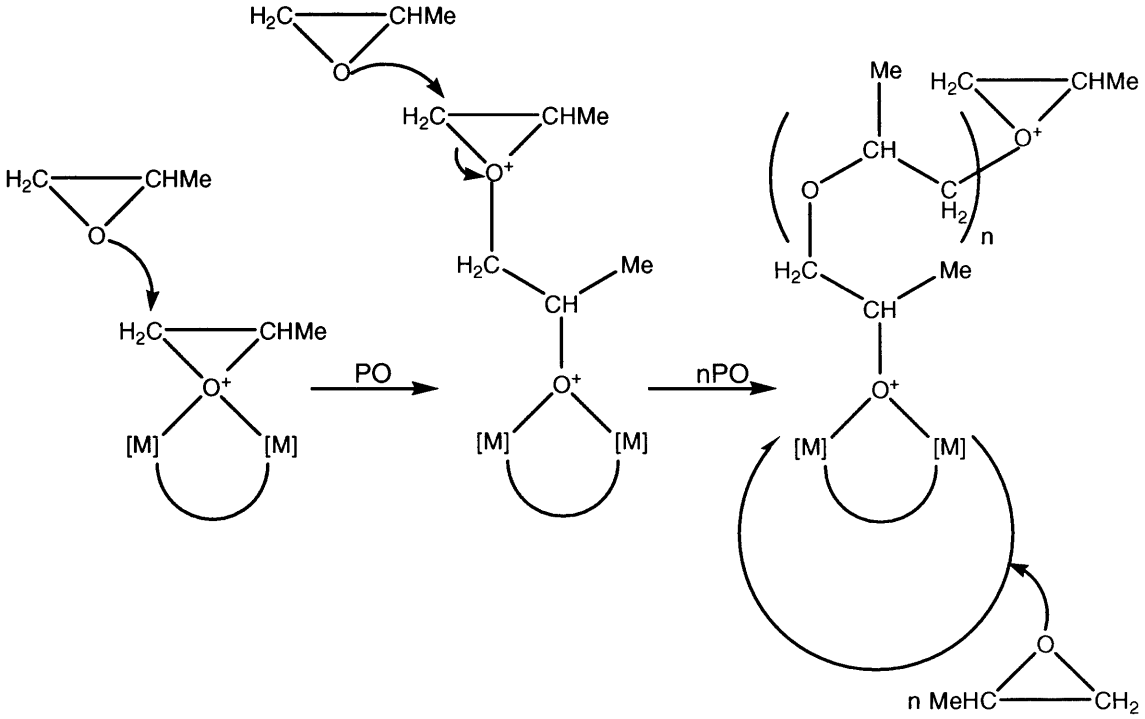

Anionic Polymerisation

In anionic polymerisation, PO is combined with an organic solvent rich in OH^- groups, (hydroxylic initiator) and a strong basic catalyst, such as KOH. An example of a catalyst following an anionic mechanism is potassium hydride with various crown ethers [37, 89]. A wide range of crown ethers has been considered such as 12-crown-4, 15-crown-5, dicyclohexano-18-crown-6 and dicyclohexano-24-crown-8, the most successful being 18-crown-6 combined with potassium glycidoxide, the latter acting as

an inimers (initiator-monomer). These complexes can initiate the polymerisation as an alkoxide and partake in the propagation step (Scheme 12) [77].

Scheme 12: Potassium glycidoxide with 18-crown-6 in ring-opening PO[35]

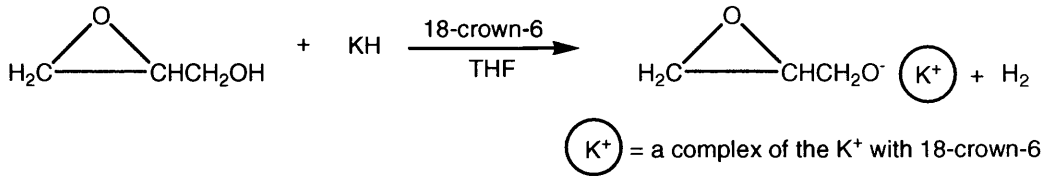

When crown ether: inimer ratios are 1:1, there is one species of unimodal molecular weight indicating one active species. The optimal ratio of crown ether: inimer is 6:1 producing polymers of PDI = 1.2. Stolarzewicz *et al.* [77] have suggested two active species; one on the surface of the insoluble part of potassium glycidoxide and the second species possibly in the THF solution.

Using K^-, $K^+(15\text{-crown-5})_2$ [90], PO polymerisation can also be achieved but results in a low polydispersity polymer. During the initiation step, potassium crown ether forms numerous types of oxides such as potassium isopropoxide and potassium tetraethylene glycoxide vinyl ether [90]. These oxides form different anionic chains, which lead to low PDI values. The low PDI is further reduced due to the strong tendency of oxides to undergo chain transfers. The end groups are determined by quenching groups, however, all these polymers have hydroxyl functional groups.

Anionic catalysts have the disadvantage of requiring the removal of base after polymerisation is completed as it hinders further reactions with diisocyanates in

polyurethane formation. Another major problem is the formation of terminal unsaturated ends of polymers due to deprotonation of the methyl groups.

Coordination Polymerisation

In 1955, Pruitt and Baggett[91] introduced coordination polymerisation of PO using ferric chloride. This catalyst gave mixtures of amorphous and crystalline polymers with the retention of the polymer backbone. As some crystalline polymers are formed, it is proposed that there must be asymmetric catalytic sites, which have preferred reactivity for different racemic PO. The polymers formed using optical isomers produce crystalline polymers of identical optical activity. Price and Osgan [92] postulated that heterogeneous asymmetric centres form catalytic sites producing crystalline PPO with the amorphous PPO being formed in solution. Kinetic data indicated the rate was dependant on the initial catalyst concentration as was the molecular weight. The initiation of this catalyst involved the reaction of ferric chloride with four to five PO units to form the oligomer.

Figure 8: Ferric chloride with two chains of growing PPO [6]

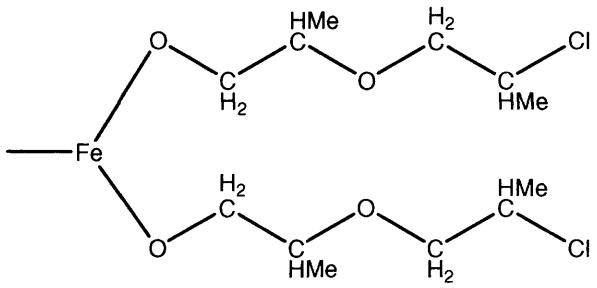

The formation of two different chains with individual chloride ends was assumed. The addition of an alcohol results in the displacement of the chloride to form alkoxides. The mechanism is believed to involve PO coordinating to iron, increasing the cationic nature of the secondary carbon of the epoxide and the anionic character of the alkoxide

oxygen. This encourages the anionic alkoxide to migrate to form the propagation step (Scheme 13).

Scheme 13: Ring-opening of PO using iron complex [6]

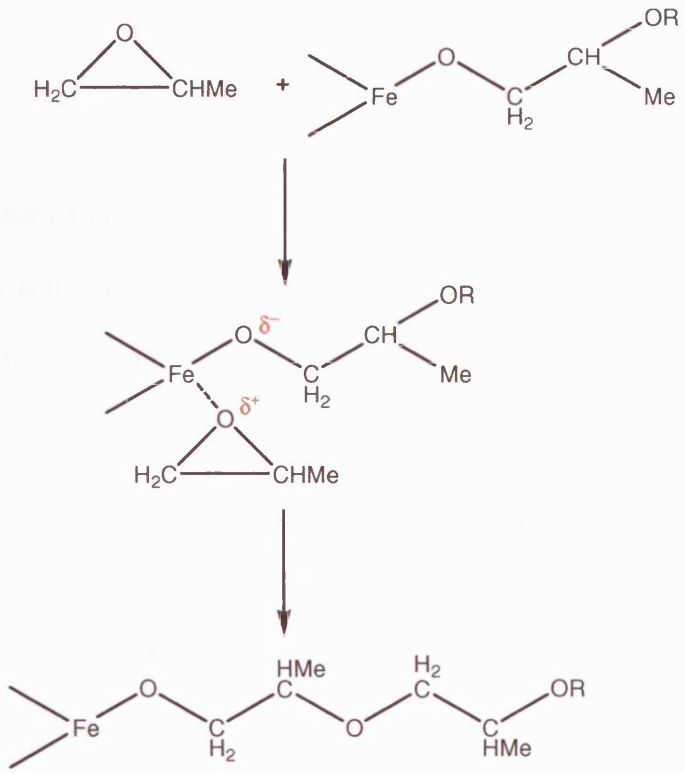

It has been proposed that heterogeneous sites on the surface of the iron catalyst forms crystalline PPO. Researchers postulated [92] that the surface of the catalyst has limited space due to its highly coordinated nature. Therefore, the accommodation of PO is restricted and only a specific orientation of the PO would be acceptable. Configuration of the adjacent asymmetric centre in the alkoxide will determine the configuration and orientation of the PO. This process produces highly isotactic polymers. Formation of amorphous PPO is attributed to activity sites in solution. This would result in less steric rigid requirements for coordination, forming PPO with a mixture of tacticities. This system also is more susceptible to displacement of the growing alkoxide group, leading to chain termination and low-molecular weight polymers, typical for amorphous PPO.

Despite these clearly defined catalyst systems, there are many other examples of catalysts that polymerise PO with less defined mechanisms and in some cases, a combination of mechanisms. The following sections are divided into classes of complexes.

1.6.2 Aluminium

There are numerous examples of catalysts with aluminium centres that polymerise PO *via* ROP such as aluminium porphyrins [93, 94], aluminium isopropoxide/zinc chloride [95], trialkylaluminium / H_2O [96, 97] and trialkylaluminium / H_2O / acetylacetone [98].

Aluminium porphyrin complexes consist of a centralised aluminium ion, surrounded by an organic, planar ring with a rigid structure. One of the key examples of these types of catalysts is 5,10,15,20 (tetraphenylporphinato)aluminium chloride [(TPP)AlCl] for epoxide polymerisation (Figure 9).

Figure 9: [(TPP)AlCl] porphyrin [94]

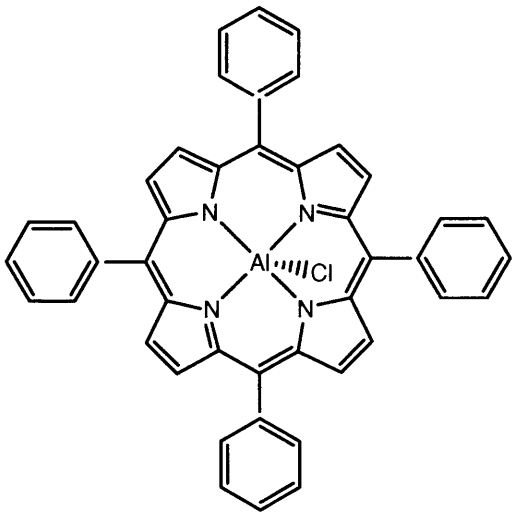

These complexes have been reported to have good activity as catalysts for epoxide polymerisation [94, 99, 100]. Their advantages are that they produce polymers of narrow molecular weight distribution and the molecular weight of the polymer can be controlled by altering the epoxide: catalyst molar ratio.

Aida and Inoue [101] used extensive NMR techniques to investigate the mechanism of PO polymerisation. The [(TPP)AlCl] system was found to react with PO to form (tetraphenylporphinato) aluminium alkoxide [(TPP)Al(OR)], a living propagating species. It is at this site that successive PO monomers react to form high-molecular weight polymers of 10,200 with very low polydispersity (PDI = 1.13) and a 100% conversion rate[94]. The scope of the system was tested with substituted phenyls on the porphyrin ligand and it was found that the use of para-substituted chloride or methoxide complexes reduced the conversion rate and M_w, but had little affect on polydispersity. The introduction of Lewis acidic organoaluminium compounds with bulky substituents such as methylaluminium di(2,6-di-*t*-butylphenoxide) can accelerate the rate of polymerisation [38, 88, 102-104].

A few years later, the first example of "immortal" polymerisation was found using an anionic growth species [36]. Researchers found that the addition of a protic compound (alcohol) reacting with the growing species did not terminate the polymerisation as would be expected. The ROP of PO with [(TPP)AlCl]-MeOH yielded polymers of controlled molecular weight and narrow distribution. In this system, the number of polymer chains exceeded the number of aluminium porphyrin complexes. It was also found that increasing the amount of methanol decreased the molecular weight of polymer. Due to the narrow molecular weight distribution (PDI = 1.07 - 1.17), the

number of polymer molecules (N_p) was calculated based on the number average molecular weight. Absence of methanol resulted in the ratio of polymer molecules (N_p) and [(TPP)AlCl] (N_{Al}) being equal. However, as methanol is increased in the reaction, the ratio of $(N_p)/(N_{Al})$ increases suggesting that methanol participates in the reaction as a chain transfer agent [36].

Furthermore, Asano *et al.* [36] found that the number of the polymer molecules found corresponds to the ratio {[MeOH] + [(TPP)AlCl]}/ [(TPP)AlCl]. Therefore, the polymer molecules grow from [(TPP)AlCl] and all the molecules of methanol. The active propagating species of the polymerisation is the [(TPP)Al(OR)] and this suggests a rapid exchange between the aluminium alkoxide and methanol, forming numerous aluminium alkoxides [36]. By use of NMR experiments it was found that this rapid exchange is faster than propagation i.e. insertion of epoxide into [(TPP)Al(OR)] (Scheme 14).

Scheme 14: Mechanism of ROP of PO using [(TPP)AlCl] and alcohol [36]

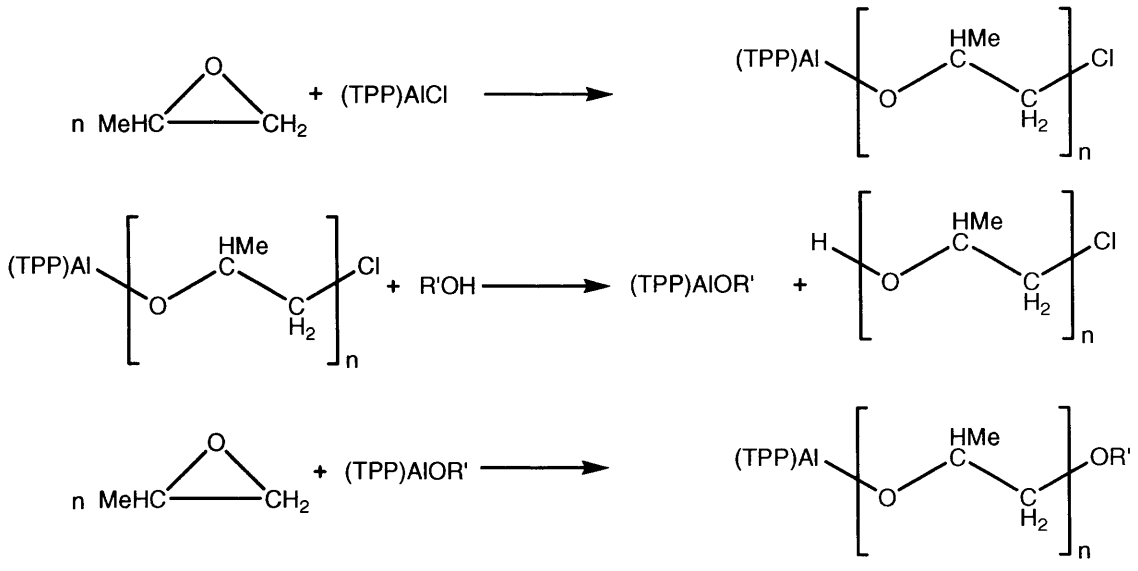

The proposed immortality of polymerisation stems from the fact that the liberated polymer chain has an alcohol end allowing further chain transfers by reversing the reaction. Therefore, the reaction can become temporarily "dormant" but not terminated.

A variety of aluminium porphyrin catalysts with different substituents were investigated to provide further evidence of the chain transfer ability of these systems [93]. They confirmed the active catalytic site as the alkoxide and that these alkoxides were able to exchange between porphyrins and other tetradentate ring systems.

Other tetradentate ligands that coordinate aluminium are salens and related N-,O-ligands[79, 105-107]. A typical salen ligand is *N*, *N*'-ethylenebis(2-hydroxyphenylene-imine) (Salen) composed of salicyclic aldehyde and ethylene diamine. These ligands are typcially dianionic and react with metals to form planar complexes with the metal in the centre of the ligand (Figure 10).

Figure 10: Typical Salen ligand

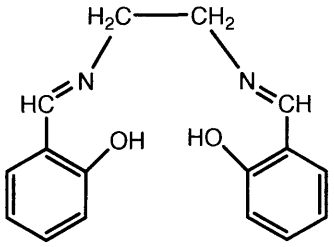

Many variations of [(Salen)AlCl][108] have been synthesised by altering the substituents. These can be reacted with MeOH or H_2O to give a six-coordinate distorted octahedral cations. Crystal structures show that two solvent units are coordinated to the aluminium centre; above and below the plane. When testing for ROP of PO, the mechanism

proposed was comparable to that with [(TPP)AlCl]. Inoue *et al.* [99, 109] found that [(Salen)AlCl] and [(TPP)AlCl] had similar reactivity giving narrow molecular weight distribution of polymers[99, 109].

Other salen-type ligands, which are penta-coordinate such as 1, 2-ethylene for $SalenN_3H_3$ and 1, 3-propylene for $SalpenN_3H_3$ were reacted with aluminium to form complexes **11a** and **11b** respectively (Figure 11). These complexes form six-coordinate monometallic ion pairs [107] with Lewis acidic character. Combination of these complexes with organic aluminium compounds forms bimetallic complexes. The complexes that successfully catalyses PO polymerisation were $[(Salen)N_3H\{Al(THF)\}][AlMe_2Cl_2]$ and $[(Salpen)N_3H\{Al(THF)\}][AlMe_2Cl_2]$ yielding polymers of 700 M_n and PDI = 1.5.

Figure 11: Salen and Salpen ligands with aluminium cation [107]

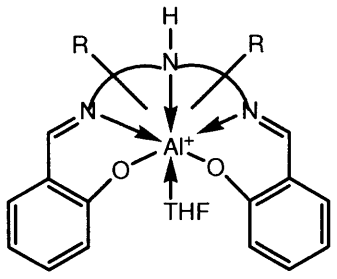

$SalenN_3H_3$ (**11a**) R = 1,2-ethylene
$Salpen\ N_3H_3$ (**11b**) R = 1,3-propylene

Other aluminium complexes using multidentate N, N and N, O- ligands have been used to investigate the polymerisation of epoxides [78, 80, 97, 107, 110, 111]. In one example, Me_3Al reacts with various bidentate N, N- and N, O- ligands to form active species (Figures **12a-c**) [110].

Figure 12: Examples of aluminium bidentate catalysts [110]

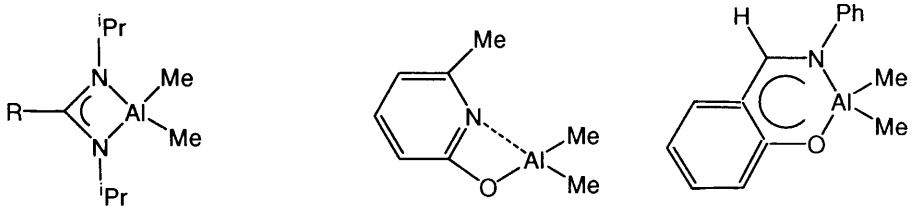

R = Me, ^{t}Bu

12a **12b** **12c**

These compounds were tested for PO polymerisation in neutral and borane-activated cationic forms. The neutral complexes were inactive with the exception of **12c** which produced (*via* abstraction of Me) a broad molecular weight distribution, PDI = 1.44 and M_n = 680. When activated with $B(C_6H_5)_3$ and $[Ph_3C]^+[B(C_6H_5)_4]^-$ successful catalysts were generated, producing polymers of M_w = 1,500. The mechanism suggested for the polymerisation was cationic based on NMR studies.

Emig *et al.* [80] investigated catalysts (Figure **13a**) with tridentate ligands based on a diamidoamine $[(RNCH_2CH_2)_2NR']$ moieties and group 13 metals. The unusual structure of trigonal-monopyramidal geometry provides an empty axial coordination site for PO monomer to enter the complex and insert into the M-Cl bond.

Figure 13: Examples of aluminium-based catalysts [80]

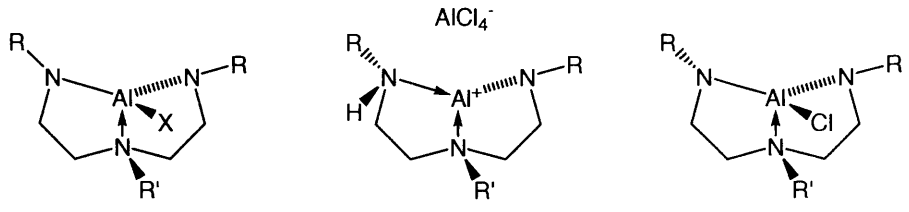

R = R' = $SiMe_3$, CH_3, ^{i}Pr

13a

R = R' = $SiMe_3$
R = $SiMe_3$, R' = Me
R = ^{i}Pr, R' = $SiMe_3$

13b

R = R' = $SiMe_3$

13c

The neutral complexes were not catalysts suggesting that cation formation is instrumental in polymer formation. Complexes **13b** and **13c** (Figure 13) had the highest reactivity, producing polymers of $M_n \cong 2{,}000$, PDI $\cong 1.20$ and ~60% conversion rate.

Chisholm *et al.* [112, 113] investigated complexes formed from 2,2'-ethylidenebis(4,6-di-*tert*-butylphenol), 2,2'-methylidene-bis(4-dimethyl-6-di-*tert*-butylphenol) and Et_2AlCl, forming bimetallic phenoxide complexes (Figure 14).

Figure 14: Bimetallic phenoxide complexes [113]

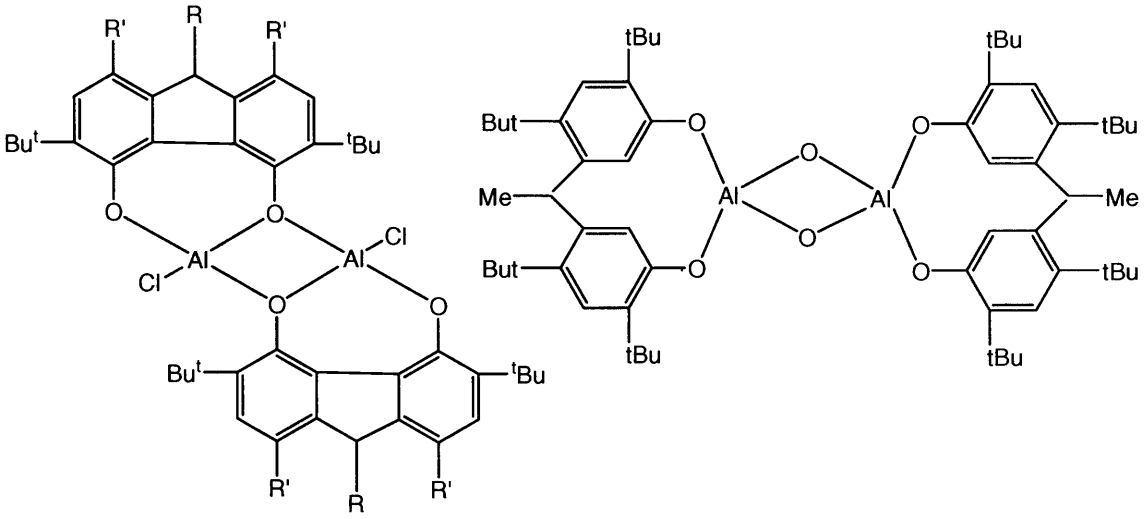

R = H, Me; R' = Me, ^{t}Bu

In these complexes, a cationic coordination mechanism was observed for the ring-opening process *via* backside attack on the activated PO monomer, resulting in inversion of substituted carbon centre. These researchers compared the tacticity and catalytic activity of the complexes with other systems such as [(TPP)AlCl] [94] and calcium amide-alkoxide [21, 26]. In comparison, their catalyst was less reactive generating regio-irregular polymers.

In conclusion, numerous examples of aluminium-based catalysts have been studied with varying reactivity. The ligands involved in these complexes varied from porphyrins, N'N''- and N'O-ligands as well as bimetallic phenoxide complexes. These resulted in different tacticities and M_w. When these catalysts are compared to KOH and DMC complexes, their reactivity and quality of polymers were much lower, precluding industrial application.

1.6.3 Zinc

A host of zinc systems with the general formula $[Zn(OR)_2].[EtZn(OR)]_6$ [114] (R = Me, CH_2CH_2OMe) [15, 114-117] and $[Zn(OR)_2].[EtZn(OR)]_2$ (R = $CH(Me)CH_2OMe$) have been utilised as catalysts. The structures of $[Zn(OMe)_2].[EtZn(OMe)]_6$ and $[Zn(OCH_2CH_2OMe)_2].[EtZn(OCH_2CH_2OMe)]_6$ have been shown by X-ray diffraction to contain two enantiomorphic distorted cubes which share a corner, the centre of symmetry being the octahedral zinc atom (Figure **16a**). However, the structure of $[Zn(OCH(Me)CH_2OMe)_2].[EtZn(OCH(Me)CH_2OMe)]_2$ is a centrosymmetric chair-form skeleton consisting of four zinc and four oxygen atoms (Figure **16b**)[38].

Figure 15: $[Zn(OR)_2].[EtZn(OR)]_6$ and $[Zn(OCH(Me)CH_2OMe)_2].[EtZn(OCH(Me)CH_2OMe)]_2$ [38]

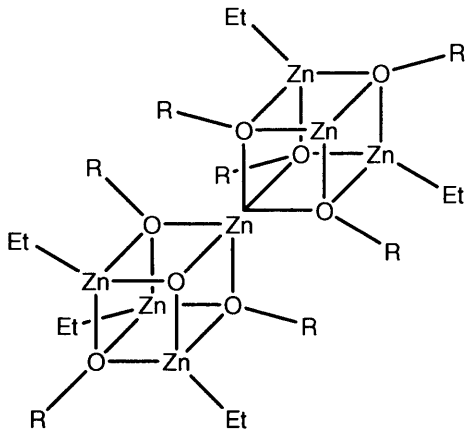

$[Zn(OR)_2][EtZn(OR)]_6$

R = Me, CH_2CH_2OMe

16a

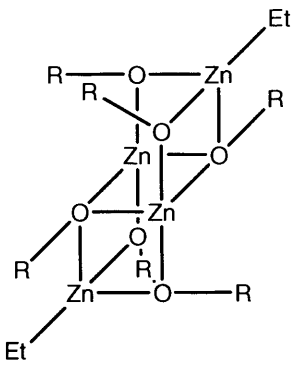

$[Zn(OR)_2]_2.[EtZn(OR)]_2$

R = $MeOCH_2CH(Me)$

16b

These zinc complexes are catalysts for the ROP of PO producing very high-molecular weight polymers with a broad distribution which indicates numerous active catalytic sites [99]. Extensive studies were undertaken to determine the mechanisms involved. Tsuruta *et al.* [15, 114, 116, 118-121] suggested that PO and the polymer chain were coordinated to the same zinc atom and this chiral octahedral centre controlled the stereochemistry[122, 123]. The mechanism for $[Zn(OR)_2].[EtZn(OR)]_6$ complexes is known as Tsuruta mechanism (Scheme 15).

Scheme 15: Tsuruta mechanism for ROP of PO (l-cube methyl groups deleted for clarity) [6]

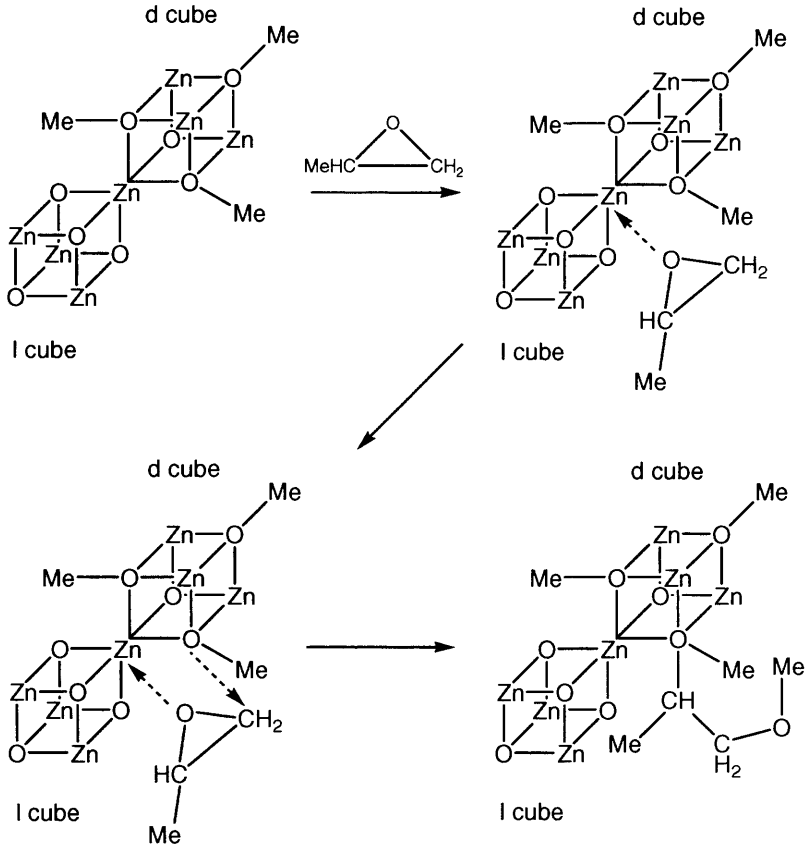

The oxygen of the PO attacks the centre octahedral zinc atom at the centre of the structure and undergoes ring-opening *via* cleavage of the O-CH_2 bond. Depending on which side the bonds weaken at the centred zinc, the *R* or *S* catalytic sites are identified and determine the tacticity of polymer. If the bonds weaken at the d-cube and the nucleophilic attack is at one of the methoxy groups on the d-cube, the l-monomer will

be favoured at this l-site. Vice-versa would be expected if bonds were weakened at the l-cube.

The $[Zn(OCH(Me)CH_2OMe)_2].[EtZn(OCH(Me)CH_2OMe)]_2$ complex has a higher rate of polymerisation compared to other zinc systems, due to the exposed position of the zinc atom. Hence, the zinc atoms are located on the corner of the chair-structure and easily accessible compared to the zinc atoms in the cube-type structure of $[Zn(OR)_2].[EtZn(OR)]_6$[32, 34, 117]. It is believed the PO attacks the more electrophilic zinc atom. As PO is activated, the adjacent zinc atom attacks the nucleophilic oxygen of PO *via* backside attack, leading to the inversion of the configuration at carbon atom of the epoxide ring.

Other zinc complexes have been considered as catalysts for PO polymerisation. Chisholm *et al.*[124] used zinc glutarate complexes formed from the reaction of zinc oxide and glutaric acid[125]. The formation of Zn-OH groups is proposed to be responsible for the highly active catalyst in initiating polymerisation, rapidly producing long chains *via* backside attack with a high-level regiocontrol and regioregularity.

Arylzinc alkoxides $[ArZn(OCH^iPr_2)]_2$ and $[Ar_2Zn_3(OCH^iPr_2)_4]$ (Ar = C_6H_5, *p*-$CF_3C_6H_4$, 2,4,6-$Me_3C_6H_2$ and C_6F_5) (Figure 16) have proved to be limited catalysts for ROP of PO[126]. Electron-withdrawing groups increase the Lewis acidity of the metal centres, encouraging ring-opening of monomers. This process causes the C-O bonds of the epoxide to break from both carbons, forming regio-irregular polymers. With weaker electron-withdrawing groups like phenyl, the attack is on the methylene carbon atom, forming regioregular polymers. The proposed mechanism is metal-promoted base

catalysis. Polymers formed had a broad molecular weight distribution with a low monomer conversion rate (10 - 48%). When comparing these catalysts to DMC and KOH, they are not active enough to be considered for the industrial production of PPO.

Figure 16: Structure of $[ArZn(OCH^iPr_2)]_2$ and $[Ar_2Zn_3(OCH^iPr_2)_4]$[126]

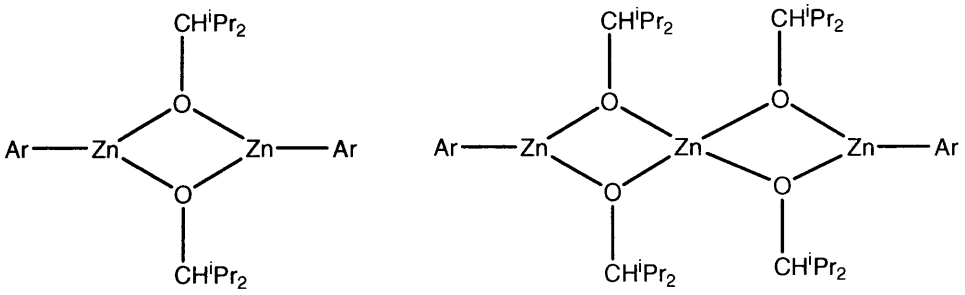

Ar = C_6H_5
p-$CF_3C_6H_4$
2,4,6-$Me_3C_6H_2$
C_6F_5

16a

Ar = *p*-$CF_3C_6H_4$
C_6F_5

16b

Zinc porphyrin complexes such as *N*-methylated tetraphenylporphyrin [(NMTPP)ZnX] (X = SPr, OPr^i) polymerise PO (Figure 17). Watanabe *et al.* [88] found that it was possible to accelerate the rate of epoxide polymerisation upon photoexcitation (visible light) of the porphyrin ring. Similar to the aluminium porphyrins, metal porphyrin-alkoxide systems are formed with the alkoxide in the axial position.

Figure 17: [Zn(NMTPP)X][88]

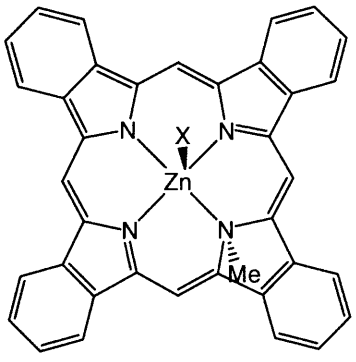

X = SPr, O^{i}Pr

Irradiating the complex with visible light accelerated both the initiation and propagation steps of the living polymerisation. Visible light enhances the reactivity of the zinc-axial ligand bonds, encouraging polymerisation. Polymers formed using irradiation produced had uniform lengths and the ratio of weight- and number-average molecular weights (PDI) was generally constant at 1.05 [88]. By NMR, polymers generated in the dark and upon irradiation were found to be identical with head-to-tail linkage [88] but irradiation lead to a significantly faster reaction.

1.6.4 Platinum, Rhodium and Cobalt

There are examples in the literature that show platinum-based catalysts can initiate ROP of various epoxides after addition of silanes which acts as reducing agents [127, 128]. Trace amounts (10 - 20 ppm) of platinum catalysts can be used so long as at least one silane is present. Examples of platinum catalysts are $[PtCl_2(C_6H_5CN)_2]$, $H[PtBr_6]$ and PtI_2. Different types of silanes can be used as reducing agents such as mono-, di- and trialkylsilanes and aryl, halo- and alkoxy substituted silanes[128].

After numerous mechanistic work, a colloidal platinum species was proposed as the active catalyst working *via* a cationic mechanism. Firstly, the silane reduces the platinum(II) to give a platinum colloid in an inhibition period. This is the rate determining step and can be altered by varying the type of silane and its reducing strength; the stronger the reducing agent, the faster the rate determining step. A useful way of avoiding this slow inhibition period is to mix the platinum complex and silane together, forming the colloid before monomer addition[128]. To this, the epoxide is added to form a 3-centre-2-electron bond. The oxygen of the epoxide monomer continues to attack the oxonium ion *via* nucleophilic attack to form the polymer. In this

mechanism, molecular oxygen is required to aid stabilisation of the colloid by ligating with the platinum[129].

Rhodium (I) complexes including $[RhCl(1,5\text{-cyclooctadiene})]_2$, $[RhCl(norbornadiene)]_2$ and $[RhCl(C_2H_4)_2]_2$ can similarly be used for ROP of epoxides in the presence of silanes[130]. They follow the same mechanism as the platinum compounds with silane but do not require molecular oxygen to stabilise the colloid. A range of silanes acting as reducing agents for rhodium can be used such as triethylsilane, 1,1,3,3-tetramethyldisiloxane and *n*-butylsilane as well as cyclic and linear polyermic siloxanes oligomers.

Cobalt carbonyls were also found to polymerise epoxides with silane compounds. These include $[Co_2(CO)_8]$ and $[Co_4(CO)_{12}]$, with the former being most active. The combination of $[Co_2(CO)_8]$ with a silane reducing agent produces a highly active catalyst that ring-opens epoxide very rapidly at room temperature. This system followed the colloid platinum and rhodium species and their interaction with silane compounds as reducing agents forming polymers[131].

These metal systems with silanes were able to catalyse epoxide polymerisation. However, when comparing the rate at which the polymer is formed and the quality of the product, these systems are deemed unsuitable for industrial formation of PPO.

1.6.5 Titanium

Following the success of Ziegler-Natta metallocenes, there has been great interest in zwitterionic metallocenes for catalysis. Zwitterionic titanoxanes were found to be

catalytic for ε-caprolactone[132]. They are highly active at room temperature with the optimal temperature being 60°C. When tested for PO polymerisation, only Figure 18 was found to be active. A very small quantity of this was added to PO at room temperature resulting in an extremely violent reaction followed by an explosion! Burlakov *et al.*[132] found that cooling the reaction vessel to <0°C controlled the reaction but produced liquid oligomers. Even when the temperature range examined was between –30 to +20°C and the ratio of PO: catalyst was 500 - 2,000:1 only liquid oligomers were formed. The mechanism proposed for this catalyst system is cationic polymerisation.

Figure 18: Structure of catalytically active[[Cp[η^5-$C_5H_4B(C_6F_5)_3$]Ti]$_2$O][132]

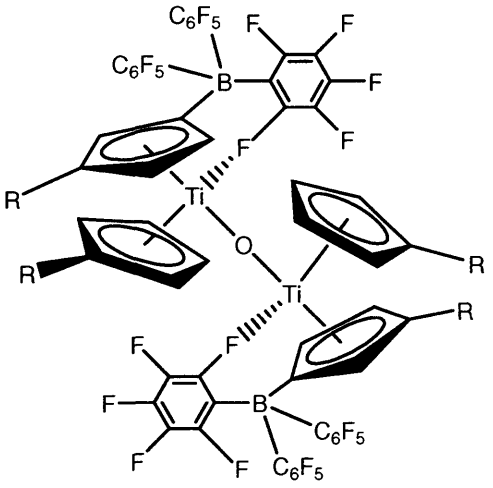

R = H, ^{i}Pr

1.6.6 Rare Earth Metals

Rare earth metals have been used for PO/CO_2 co-polymerisation reactions forming polycarbonates[133-135]. However, few have successfully been used as catalysts for PO polymerisation. There are numerous examples of polymer-supported metal catalysts that provide highly active catalysts with good selectivity. Zeng *et al.*[133] have investigated these systems with Chitosan-supported rare earth complexes (Cs-RE),

tri*iso*butyl aluminium (Al^iBu_3) and acetylacetone (acac) to give [Cs-RE-Al^iBu_3-acacH] (RE = Y, La, Pr, Nd, Er) systems. Different conditions and ratios of reactants were carefully examined to optimise the reactivity. All metal systems were highly active, yielding higher molecular weight polymers than conventional rare earth metal systems. The reaction conditions and ratios of the individual components strongly effect the polymerisation reactions and polymer quality. Increasing the ratio of Al/RE, increased monomer conversion and produces high molecular weight polymers. Also increasing reaction temperature resulted in increased catalytic activity but a decrease in polymer isotacticity. The isotactic quality of these polymers are still better than conventional rare earth metal catalysts[133], indicating greater regioselectivity of the former. There is a maximum level at which increasing RE, increases catalysis. After this point, catalysis decreases due to the embedment of RE atoms, a widespread problem in heterogeneous catalysis.

Various patents have been obtained that use a combination of lanthanide and organic aluminium compounds, such as trialkylaluminium or their hydrates[97, 133, 136]. The most effective combination is samarium trifluoroacetylacetonate (acac-F_6) with Et_3Al [Sm(acac-F_6)/ Et_3Al/H_2O] to give PPO of 8,000 M_n and PDI = 1.88. Another example of rare earth metals in catalysis of PO polymerisation is yttrium (III) ethylhexanoate[136] with Et_3Al to produce PPO with M_n = 121,000 but a very high PDI (4.05).

Lanthanide compounds [Cp_2LnX] containing various cyclopentadienyl ligands combined with organic aluminium compounds[137] have also been patented, producing 2,000 M_w and PDI of 1.41 but with relatively low isotacticity. Other systems include [$Ln(acac)_3$/BuMgCl] (Ln = Y, Nd, Sm)[138], [$Sm(OR)_3/AlR_3$-H_2O] (R = alkyl)[139],

neodecanoate/butyl aluminoxanes systems[140], $[Nd(P_2O_4)_3/\ ^iBu_3Al/\ H_2O]$[141], Nd napthenate/ $Al^iBu_3/\ H_2O$[142] and Calixarene-Neodymium complex/ $Al^iBu_3/\ H_2O$ (Figure 19)[143].

Figure19: Calixarene-Neodymium complex[143]

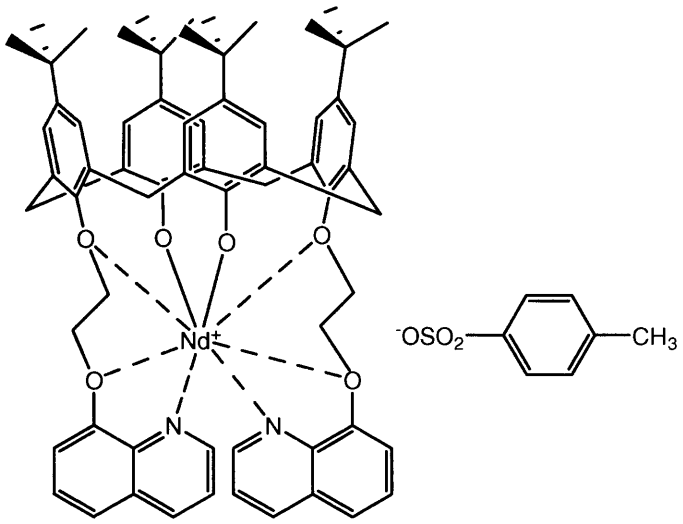

Although rare earth metal compounds in their various formulas are catalytic for PO polymerisation, the expense of the catalyst, low yields and poorer quality of polymer do not compare well with the conventional KOH systems or DMC complexes, therefore not viable catalysts.

1.6.7 Boron

There has been great interest in the Group 13 elements over the years[144-146]. As aluminium cations[108] are successful catalysts for PO polymerisation, boron cations were also investigated using nitrogen ligands, producing "borinium" compounds with two-coordinate cations and "borenium" as three-coordinated cations[147]. The compounds considered are of the form LBOR (L = a tridentate ($-O_2N$) ligand, i.e. *N*-salicylidene-*o*-aminophenol (LH_2), *N*-(5-chlorosalicylidene)-*o*-aminophenol ($L(Cl)H_2$) and *N*-(5-bromosalicylidene)-*o*-aminophenol ($L(Br)H_2$))[79]. LBOR, L(Cl)BOR and

L(Br)BOR (R = Me, Et, ^{n}Pr and ^{n}Bu) were combined with HOTf produce active catalysts for PO polymerisation (Scheme 16).

Scheme 16: Reaction of boron tridentate compound with HOTf [79]

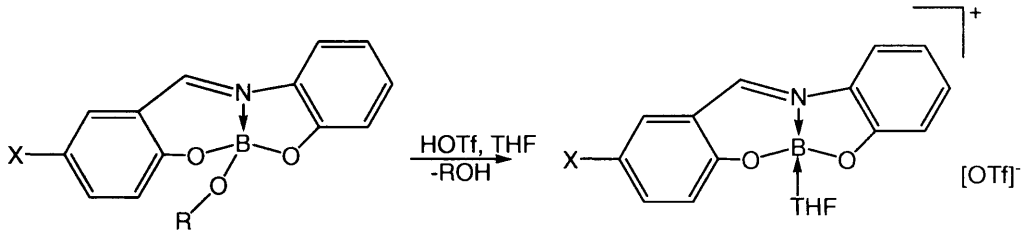

X = H = LH_2
X = Cl = $L(Cl)H_2$
X = Br = $L(Br)H_2$

R = Me, Et, ^{n}Pr, ^{n}Bu

The reaction and quality of polymer is limited as many of the complexes do not show activity even under harsh conditions. When these compounds are compared to the commercially available Lewis acid, [$^{n}Bu_2B$]OTf, they have limited use in polymerisation of epoxides.

Chakraborty *et al.*[83] investigated the highly Lewis acidic organoborane, $B(C_6F_5)_3$ which when combined with hydroxylic initiators gave highly active catalysts yielding low to medium-molecular weight polymers with narrow distributions. In the absence of a hydroxylic initiator, only isomerisation of PO to propionaldehyde and a mixture of oligomers were formed[83]. Using a range of Lewis acids and hydroxylic initiators, it was established that the rate of PO polymerisation is proportional to the Lewis acidity of the borane catalyst and the Brønsted acidity of the hydroxylic initiator (Scheme 14).

Scheme 17: Lewis acidity of various boron compounds

$$B(C_6F_5)_3 > B(2,4,6\text{-}F_3\text{-}C_6H_2)_3 > B(4\text{-}F\text{-}C_6H_4)_3 > B(OC_6F_5)_3,\ BPh_3$$

Excess water and carboxylic acid initiator is found to deactivate the borane catalyst, reducing polymerisation and forming atactic and regio-irregular polymers. Aluminium derivatives of the same catalysts are less successful than the borane species due to the instability with the hydroxylic initiators.

1.6.8 Phosphonium

As previously discussed, KOH is the conventional catalyst for PO polymerisation. It is first reacted with alcohol to form a potassium alkoxide initiator, which instigates anionic polymerisation producing polymers with high-unsaturated end groups. The initiator consists of two charged parts, known as the contact ion pair: the cation K^+ and anion RO^-. It has been suggested [148] that reducing the strong charge interaction between these ions, allows the alkoxide to react faster with monomers. The separation of this interaction in the contact ion pair can be achieved by using a softer, less electropositive cation.

A variety of counterions [149, 150] and complexes [151-153] have been considered. Soft counterions designed by Schwesinger *et al.* [154] have a lower tendency to form ion-pair association and polyaminophosphazene bases i.e. $P_2^+BF_4^-$ (Figure **20a**) and $^tBuP_4$ (Figure **20b**) have been shown to polymerise ethylene oxide to give high quality polymers [155, 156]. Rexin and Mulhaupt [148] have used dipropylene glycol (DPG) with phosphonium cation ($Cy_4P_1^+$) (Figure **20c**) to investigate the contact ion interaction. The charge is delocalised over the five central atoms, which induces charge separation, increasing the nucleophilicity and reactivity of anionic chain. When comparing the potassium cation to $Cy_4P_1^+$ (Figure **20c**), the latter is less electrophilic and has a higher

propagating rate for polymerisation while the quality of polymer formed is good with low PDI (1.03 - 1.09).

Figure 20: Examples of phosphonium cation with counter-anions [148]

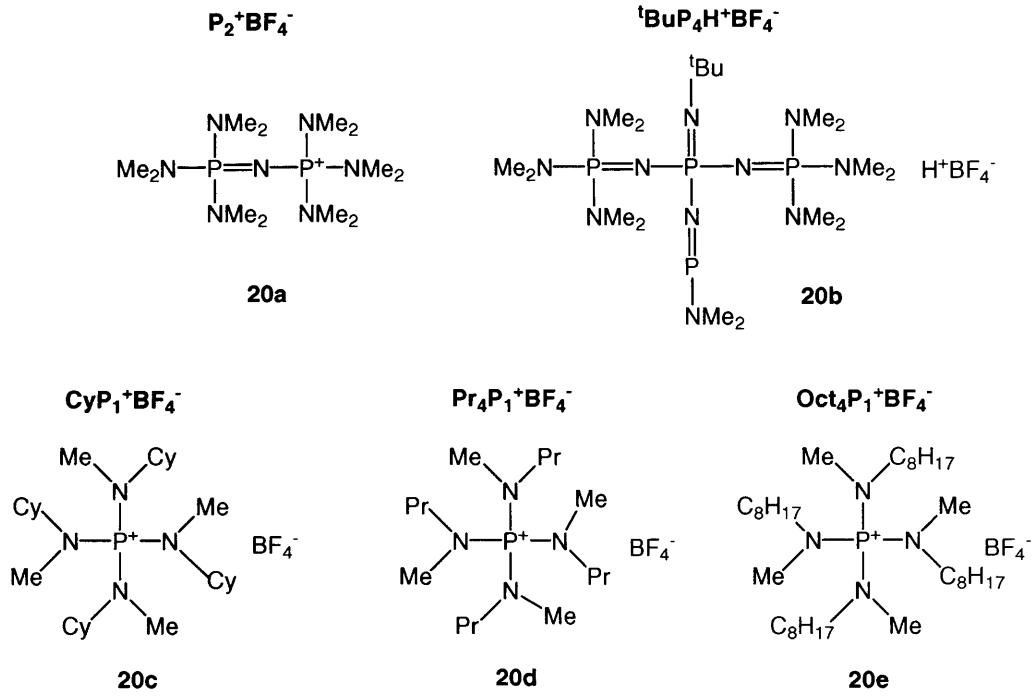

This work has been extended to include ($Cy_4P_1^+BF_4^-$) (Figure **20c**), ($Pr_4P_1^+BF_4^-$) (Figure **20d**) and ($Oct_4P_1^+BF_4^-$) (Figure **20e**). The various counterions have been tested for the anionic ROP at different temperatures and found that increasing temperature decreases activity but does not lead to complete dissociation of the cation. All phosphonium counterions worked optimally at 70°C with high M_w in the range of 2,800 - 4,410 and PDI = 1.03 – 1.06. There is no evidence to suggest that the alkyl, propyl, octyl or cyclohexyl groups influence rate of propagation or the degree of unsaturation.

In conclusion, numerous research groups have investigated the polymerisation of PO with varying degrees of success. It has been clearly demonstrated that many classes of chemical groups and complexes have the ability to ring-open epoxides. However, the generating of a polymer chain with any form of regioselectivity greatly depends on the

structure and occupancy of the active site. In the case of zinc-alkoxide systems with enantomeric cubes[15, 115-117], there is regioselectivity for both *R* and *S* polymers. Other catalysts systems form a mixture of tacticities and varying M_w. Some of these systems have been patented but there is no evidence these are active in industrial production as the conventional KOH and DMC complexes out-perform significantly. Our research aims to investigate other potential systems that can be used on an industrial scale to compete with the market leaders.

1.7 References

[1] G. Odian, *Principles of Polymerization*, 4th ed., Wiley, New York, **2004**.
[2] http://matse1.mse.uiuc.edu/polymers/time.html
[3] M. Polanyi, *Science* **1968**, *160*, 1308.
[4] J. W. Nicholson, *The Chemistry of Polymers*, 3rd ed., **2006**.
[5] P. J. Flory, *Principles of Polymer Chemistry*, **1953**.
[6] A. Ravve, Editor, *Principles of Polymer Chemistry, Second Edition*, 2nd ed., Kluwer Academic/Plenum Publishers, Dordrecht, Neth., **2000**.
[7] http://en.wikipedia.org/wiki/Tacticity
[8] http://en.wikipedia.org/wiki/Ziegler_Natta
[9] http://en.wikipedia.org/wiki/Kaminsky_catalyst
[10] J. Watanabe, A. Okuda, S. Nakayama, Y. Takizawa, Application: JP, 2003013052, **2003**.
[11] M. A. Munoz-Hernandez, M. L. McKee, T. S. Keizer, B. C. Yearwood, D. A. Atwood, *Journal of the Chemical Society-Dalton Transactions* **2002**, 410.
[12] P. Carlsson, J. Swenson, L. Borjesson, L. M. Torell, R. L. McGreevy, W. S. Howells, *Journal of Chemical Physics* **1998**, *109*, 8719.
[13] S. Tsuchiya, T. Tsuruta, *Makromolekulare Chemie* **1967**, *110*, 123.
[14] Z. Jedlinski, A. Dworak, M. Bero, *Makromolekulare Chemie-Macromolecular Chemistry and Physics* **1979**, *180*, 949.
[15] M. Ishimori, T. Hagiwara, T. Tsuruta, Y. Kai, N. Yasuoka, N. Kasai, *Bulletin of the Chemical Society of Japan* **1976**, *49*, 1165.
[16] J. J. Eisch, Z. R. Liu, M. Singh, *Journal of Organic Chemistry* **1992**, *57*, 1618.
[17] M. P. Stevens, *Polymer Chemistry: An Introduction*, Addison-Wesley Reading, Mass, **1999**.
[18] M. Fedtke, H. Schreiber, D. Hartwig, B. Bichowski, *Plaste und Kautschuk* **1983**, *30*, 488.
[19] I. G. Hargis, R. A. Livigni, Application: DE, 2144332, **1972**.
[20] H. Daimon, K. Kamio, S. Kojima, US, 3230207, **1966**.
[21] D. G. McCollum, M. H. Chisholm, J. K. Crandall, M. Pagel, *Book of Abstracts, 217th ACS National Meeting, Anaheim, Calif., March 21-25* **1999**, INOR.
[22] J. H. McCain, D. J. Foster, Application: EP, 80-200910 26546, **1981**.
[23] F. E. Bailey, Jr., F. N. Hill, J. T. Fitzpatrick, Application: US, 3256211, **1966**.

[24] F. N. Hill, F. E. Bailey, Jr., J. T. Fitzpatrick, Application: US, 3167519, **1965**.
[25] F. E. Bailey, Jr., H. G. France, *Journal of Polymer Science* **1960**, *45*, 243.
[26] F. N. Hill, J. T. Fitzpatrick, F. E. Bailey, Jr., GB, 839171, **1960**.
[27] G. L. Baker, F. S. Bates, Application: US, 4525538, **1985**.
[28] A. Shiga, M. Kadogo, T. Suzuki, Application: JP, 52154886, **1977**.
[29] J. Kresta, L. Ambroz, K. Obrucova, *Chemicky Prumysl* **1967**, *17*, 25.
[30] J. G. Bots, L. Vanderdoes, A. Bantjes, J. Boersma, *Makromolekulare Chemie-Macromolecular Chemistry and Physics* **1987**, *188*, 1665.
[31] W. Kuran, T. Listos, *Macromolecular Chemistry and Physics* **1994**, *195*, 401.
[32] Y. Hasebe, T. Tsuruta, *Makromolekulare Chemie-Macromolecular Chemistry and Physics* **1988**, *189*, 1915.
[33] T. Tsuruta, Y. Hasebe, *Macromolecular Chemistry and Physics* **1994**, *195*, 427.
[34] N. Yoshino, C. Suzuki, H. Kobayashi, T. Tsuruta, *Makromolekulare Chemie-Macromolecular Chemistry and Physics* **1988**, *189*, 1903.
[35] A. Stolarzewicz, B. Morejko-Buz, Z. Grobelny, W. Pisarski, M. Lanzendorfer, A. Muller, *Rapid Communications in Mass Spectrometry* **2004**, *18*, 716.
[36] S. Asano, T. Aida, S. Inoue, *Journal of the Chemical Society-Chemical Communications* **1985**, 1148.
[37] Z. Grobelny, A. Stolarzewicz, B. Morejko-Buz, A. Maercker, S. Krompiec, T. Bieg, *Journal of Organometallic Chemistry* **2003**, *672*, 43.
[38] W. Kuran, *Progress in Polymer Science* **1998**, *23*, 919.
[39] S. Chen, P. Zhang, L. Chen, *Progress in Organic Coatings* **2004**, *50*, 269.
[40] R. J. Herold, Application: US, 3278459, **1966**.
[41] R. J. Belner, Application: US, 3278458, **1966**.
[42] B. Le-Khac, Application: US, 5714428, **1998**.
[43] S. Chen, N. P. Xu, J. Shi, *Progress in Organic Coatings* **2004**, *49*, 125.
[44] B. Le-Khac, Application: US, 5693584, **1997**.
[45] Y. J. Huang, G. R. Qi, Y. H. Wang, *Journal of Polymer Science Part A-Polymer Chemistry* **2002**, *40*, 1142.
[46] B. Le-Khac, Application: EP, 654302, **1995**.
[47] J. Hofmann, P. Gupta, R.-J. Kumpf, P. Ooms, W. Schafer, M. Schneider, Application: WO, 98-EP6312 9919063, **1999**.
[48] P. Ooms, J. Hofmann, P. Gupta, L. Groenendaal, Application: EP, 1029871, **2000**.
[49] S. Chen, L. Chen, *Colloid and Polymer Science* **2004**, *282*, 1033.
[50] M. B. Robin, *Inorg. Chem.* **1962**, *1*, 337.
[51] K. R. Dunbar, R. A. Heintz, in *Progress in Inorganic Chemistry, Vol. 45*, **1997**, pp. 283.
[52] D. F. Mullica, W. O. Milligan, G. W. Beall, W. L. Reeves, *Acta Crystallographica Section B-Structural Science* **1978**, *34*, 3558.
[53] G. W. Beall, W. O. Milligan, J. Korp, I. Bernal, *Inorganic Chemistry* **1977**, *16*, 2715.
[54] H. J. Buser, D. Schwarzenbach, W. Petter, A. Ludi, *Inorganic Chemistry* **1977**, *16*, 2704.
[55] D. J. Darensbourg, M. J. Adams, J. C. Yarbrough, *Inorganic Chemistry* **2001**, *40*, 6543.
[56] Y.-J. Huang, G.-R. Qi, Y.-H. Wang, *Journal of Polymer Science, Part A: Polymer Chemistry* **2002**, *40*, 1142.
[57] K. Sugiyama, S. Ikai, Application: JP, 2003073469, **2003**.

[58] M. B. Eleveld, R. A. De Groot, R. Van Kempen, J. P. Smit, Application: WO, 2001072418, **2001**.
[59] Z. Hua, S. Chen, Y. Min, G. Qi, *Zhejiang Daxue Xuebao, Lixueban* **2004**, *31*, 74.
[60] S. Chen, X. W. Xia, N. P. Xu, *Abstracts of Papers, 226th ACS National Meeting, New York, NY, United States, September 7-11, 2003* **2003**, POLY.
[61] S. Chen, L. Chen, *Fenzi Cuihua* **2002**, *16*, 374.
[62] J. Milgrom, Application: US, 3427256, **1969**.
[63] R. J. Belner, Application: US, 3427334, **1969**.
[64] H. F. Reinhardt, Application: US, 3278559, **1966**.
[65] J. M. O'Connor, D. E. Laycock, M. H. McAdon, *Conference Proceedings - Polyurethanes Expo, Columbus, OH, United States, Sept. 30-Oct. 3, 2001* **2001**, 227.
[66] H. Liu, X. Wang, Y. Gu, W. Guo, *Molecules* **2003**, *8*, 67.
[67] X.-H. Liu, M.-Q. Kang, X.-K. Wang, *Gaodeng Xuexiao Huaxue Xuebao* **2000**, *21*, 1748.
[68] J. D. Darensbourg, M. J. Adams, C. J. Yarbrough, A. L. Phelps, *Inorganic chemistry* **2003**, *42*, 7809.
[69] J. Hofmann, P. Gupta, Application: WO, 99-EP2397 9954383, **1999**.
[70] I. Kim, J. T. Ahn, C. S. Ha, C. S. Yang, I. Park, *Polymer* **2003**, *44*, 3417.
[71] J. W. Reisch, M. M. Martinez, M. Raes, Application: US, 5144093, **1992**.
[72] L. E. Katz, J. W. Reisch, Application: US, 5099075, **1992**.
[73] J. L. Schuchardt, Application: EP, 385619, **1990**.
[74] T. Watabe, H. Takeyasu, T. Doi, N. Kunii, Application: EP, 383333, **1990**.
[75] S. D. Harper, S. H. Harris, Application: US, 4721818, **1988**.
[76] R. J. Herold, R. E. Bingham, Application: US, 4355188, **1982**.
[77] A. Stolarzewicz, B. Morejko-Buz, Z. Grobelny, W. Pisarski, H. Frey, *Polymer* **2004**, *45*, 7047.
[78] A. V. Korolev, E. Ihara, I. A. Guzei, V. G. Young, R. F. Jordan, *Journal of the American Chemical Society* **2001**, *123*, 8291.
[79] P. R. Wei, D. A. Atwood, *Inorganic Chemistry* **1998**, *37*, 4934.
[80] N. Emig, H. Nguyen, H. Krautscheid, R. Reau, J. B. Cazaux, G. Bertrand, *Organometallics* **1998**, *17*, 3599.
[81] S. D. Gagnon, *Kirk-Othmer Encyclopedia of Chemical Technology, Vol. 6*, 4th ed., John Wiley and Sons, New York, **1986**.
[82] P. Kubisa, *Cationic Polymerisations: Mechanism, Synthesis and Applications*, Marcel Dekker, New York, **1996**.
[83] D. Chakraborty, A. Rodriguez, E. Y. X. Chen, *Macromolecules* **2003**, *36*, 5470.
[84] M. Wojtania, P. Kubisa, S. Penczek, *Makromolekulare Chemie-Macromolecular Symposia* **1986**, *6*, 201.
[85] S. Penczek, *Journal of Polymer Science Part A-Polymer Chemistry* **2000**, *38*, 1919.
[86] P. Kubisa, S. Penczek, *Progress in Polymer Science* **1999**, *24*, 1409.
[87] E. Schon, X. Y. Zhang, Z. P. Zhou, M. H. Chisholm, P. Chen, *Inorganic Chemistry* **2004**, *43*, 7278.
[88] Y. Watanabe, T. Aida, S. Inoue, *Macromolecules* **1990**, *23*, 2612.
[89] A. Stolarzewicz, D. Neugebauer, *Macromolecular Chemistry and Physics* **1998**, *199*, 175.
[90] Z. Grobelny, A. Stolarzewicz, B. Morejko-Buz, G. Buika, J. V. Grazulevicius, A. Maercker, *European Polymer Journal* **2002**, *38*, 2359.

[91] M. E. Pruitt, J. M. Baggett, US, 2706181, **1955**.
[92] C. C. Price, M. Osgan, *Journal of the American Chemical Society* **1956**, *78*, 4787.
[93] S. Asano, T. Aida, S. Inoue, *Macromolecules* **1985**, *18*, 2057.
[94] T. Aida, S. Inoue, *Accounts of Chemical Research* **1996**, *29*, 39.
[95] M. Osgan, C. C. Price, *Journal of Polymer Science* **1959**, *34*, 153.
[96] R. O. Colclough, G. Gee, A. H. Jagger, *Journal of Polymer Science* **1960**, *48*, 273.
[97] B. Wu, C. J. Harlan, R. W. Lenz, A. R. Barron, *Macromolecules* **1997**, *30*, 316.
[98] E. J. Vandenberg, *Journal of Polymer Science* **1960**, *47*, 486.
[99] S. Inoue, *ACS Symposium Series* **1992**, *496*, 194.
[100] S. Inoue, T. Aida, *Ring-Opening Polymerization*, Hanser Verlag, Munich, **1993**.
[101] T. Aida, S. Inoue, *Macromolecules* **1981**, *14*, 1166.
[102] M. Kuroki, T. Watanabe, T. Aida, S. Inoue, *Journal of the American Chemical Society* **1991**, *113*, 5903.
[103] S. Inoue, T. Aida, *Chemtech* **1994**, *24*, 28.
[104] S. Inoue, T. Aida, H. Sugimoto, C. Kawamura, M. Kuroki, *Macromolecular Symposia* **1994**, *88*, 117.
[105] M. A. Munoz-Hernandez, B. Sannigrahi, D. A. Atwood, *Journal of the American Chemical Society* **1999**, *121*, 6747.
[106] J. A. Jegier, M. A. Munoz-Hernandez, D. A. Atwood, *Journal of the Chemical Society-Dalton Transactions* **1999**, 2583.
[107] S. M. Liu, M. A. Munoz-Hernandez, D. A. Atwood, *Journal of Organometallic Chemistry* **2000**, *596*, 109.
[108] D. A. Atwood, J. A. Jegier, D. Rutherford, *Journal of the American Chemical Society* **1995**, *117*, 6779.
[109] V. Vincens, A. Le Borgne, N. Spassky, *ACS Symposium Series* **1992**, *496*, 205.
[110] L. S. Baugh, J. A. Sissano, *Journal of Polymer Science Part A-Polymer Chemistry* **2002**, *40*, 1633.
[111] S. Dagorne, L. Lavanant, R. Welter, C. Chassenieux, P. Haquette, G. Jaouen, *Organometallics* **2003**, *22*, 3732.
[112] B. Antelmann, M. H. Chisholm, S. S. Iyer, J. C. Huffman, D. Navarro-Llobet, M. Pagel, W. J. Simonsick, W. Q. Zhong, *Macromolecules* **2001**, *34*, 3159.
[113] M. H. Chisholm, D. Navarro-Llobet, W. J. Simonsick, *Macromolecules* **2001**, *34*, 8851.
[114] H. Kageyama, Y. Kai, N. Kasai, C. Suzuki, N. Yoshino, T. Tsuruta, *Makromolekulare Chemie-Rapid Communications* **1984**, *5*, 89.
[115] M. Ishimori, T. Hagiwara, T. Tsuruta, *Makromolekulare Chemie-Macromolecular Chemistry and Physics* **1978**, *179*, 2337.
[116] T. Hagiwara, M. Ishimori, T. Tsuruta, *Macromolecular Chemistry and Physics-Makromolekulare Chemie* **1981**, *182*, 501.
[117] H. Kageyama, K. Miki, N. Tanaka, N. Kasai, M. Ishimori, T. Heki, T. Tsuruta, *Makromolekulare Chemie-Rapid Communications* **1982**, *3*, 947.
[118] T. Tsuruta, S. Inoue, M. Ishimori, N. Yoshida, *Journal of Polymer Science* **1964**, *No. 4*, 267.
[119] M. Ishimori, G. Hsiue, T. Tsuruta, *Makromolekulare Chemie* **1969**, *124*, 143.
[120] M. Ishimori, T. Tsuruta, *Makromolekulare Chemie* **1963**, *64*, 190.
[121] T. Tsuruta, S. Inoue, N. Yoshida, J. Furukawa, *Makromolekulare Chemie* **1962**, *55*, 230.

[122] L. G. Donaruma, B. P. Block, K. L. Loening, N. Plate, T. Tsuruta, K. C. Buschbeck, W. H. Powell, J. Reedijk, *Pure and Applied Chemistry* **1981**, *53*, 2283.
[123] T. Tsuruta, *Journal of Polymer Science Part C-Polymer Symposium* **1980**, 73.
[124] M. H. Chisholm, D. Navarro-Llobet, Z. P. Zhou, *Macromolecules* **2002**, *35*, 6494.
[125] M. Ree, J. Y. Bae, J. H. Jung, T. J. Shin, *Journal of Polymer Science, Part A: Polymer Chemistry* **1999**, *37*, 1863.
[126] M. H. Chisholm, J. C. Gallucci, H. Yin, H. Zhen, *Inorganic Chemistry* **2005**, *44*, 4777.
[127] J. V. Crivello, M. Fan, *Journal of Polymer Science Part A-Polymer Chemistry* **1991**, *29*, 1853.
[128] J. V. Crivello, M. X. Fan, *Makromolekulare Chemie-Macromolecular Symposia* **1992**, *54-5*, 179.
[129] L. N. Lewis, *Journal of the American Chemical Society* **1990**, *112*, 5998.
[130] J. V. Crivello, M. Fan, *Journal of Polymer Science Part A-Polymer Chemistry* **1992**, *30*, 1.
[131] J. V. Crivello, M. X. Fan, Application: US, 5412054, **1995**.
[132] V. V. Burlakov, A. V. Letov, P. Arndt, W. Baumann, A. Spannenberg, C. Fischer, L. I. Strunkina, M. K. Minacheva, Y. S. Vygodskii, U. Rosenthal, V. B. Shur, *Journal of Molecular Catalysis A-Chemical* **2003**, *200*, 63.
[133] X. Zeng, Y. Zhang, Z. Shen, *Journal of Polymer Science, Part A: Polymer Chemistry* **1997**, *35*, 2177.
[134] H. Kawamukai, S. Miyanaga, T. Oda: JP, 2001048974, **2001**.
[135] N. Takizawa, S. Miyanaga, T. Oda: JP, 2001011170, **2001**.
[136] T. Asanuma, H. Yasuda, E. Ihara: JP, 11012352, **1999**.
[137] T. Asanuma, H. Yasuda, E. Ihara: JP, 11012353, **1999**.
[138] J. Sun, *Yingyong Huaxue* **1995**, *12*, 68.
[139] H. Yasuda, E. Ihara, *Macromolecular Chemistry and Physics* **1995**, *196*, 2417.
[140] D. K. Jenkins, Application: GB, 2247024, **1992**.
[141] J. Peng, Y. Zhang, Z. Shen, *Gaofenzi Cailiao Kexue Yu Gongcheng* **1991**, *2*, 184.
[142] M. Yang, C. Zha, Z. Shen, *Shiyou Huagong* **1990**, *19*, 218.
[143] B. Teng, C. Chen, Y. Zheng, X. Liu, W. Zhang, Z. Jiang, Z. Wu, *Polymer Preprints* **2000**, *41*, 111.
[144] K. Maruoka, A. B. Concepcion, N. Hirayama, H. Yamamoto, *Journal of the American Chemical Society* **1990**, *112*, 7422.
[145] H. Yamamoto, *Organometallics in Synthesis-A Manual*, John Wiley & Sons New York, **1994**.
[146] K. Maruoka, S. Nagahara, H. Yamamoto, *Tetrahedron Letters* **1990**, *31*, 5475.
[147] H. Noth, S. Weber, B. Rasthofer, C. Narula, A. Konstantinov, *Pure and Applied Chemistry* **1983**, *55*, 1453.
[148] O. Rexin, R. Mulhaupt, *Journal of Polymer Science Part A-Polymer Chemistry* **2002**, *40*, 864.
[149] J. Furukawa, T. Saegusa, *Polymer Reviews. Vol. 3. Polymerization of Aldehydes and Oxides*, **1963**.
[150] J. T. Patton, *Chemtech* **1976**, *6*, 780.
[151] H. Koinuma, K. Naito, H. Hirai, *Makromolekulare Chemie-Macromolecular Chemistry and Physics* **1982**, *183*, 1383.

[152] T. Tsuruta, Y. Kawakami, *Comprehensive Polymer Science: The Synthesis, Characterisation, Reactions & Applications of Polymers, Vol. 3*, Pergamon, Oxford, **1989**.
[153] J. Ding, F. Heatley, C. Price, C. Booth, *European Polymer Journal* **1991**, *27*, 895.
[154] R. Schwesinger, H. Schlemper, *Angewandte Chemie-International Edition* **1987**, *26*, 1167.
[155] B. Eβwein, A. Molenberg, M. Moller, *Macromolecular Symposia* **1996**, *107*, 331.
[156] B. Eβwein, M. Moller, *Angew. Chem* **1996**, *108*, 703.

Chapter 2

Polymerisation

2.0 Potential catalysts for Ring-Opening Polymerisation for Propylene Oxide

Wide ranges of compounds are known to catalyse the ring-opening of epoxides. As discussed in Chapter 1, the leading catalysts are Double Metal Cyanides complexes (DMC). Our objective was to investigate and develop highly active catalysts for ring-opening polymerisation (ROP) of propylene oxide (PO). There are numerous patents for this reaction and we hoped to develop our own catalyst.

In our investigation, we designed experiments to examine the catalytic activity for epoxide polymerisation. We developed and used three methods to test for PO polymerisation.

Test tube method 1: PO (2 ml) was added to the potential catalyst (approximately 0.01-0.05 g) in a test tube, sealed and stirred for 17 h. with a magnetic stirrer. Each catalyst was tested twice, once with ethanol (EtOH) (2 ml) to initiate the reaction and without. The product was dissolved in dichloromethane (DCM) (2 ml) and placed on the vacuum line for 10 min. to remove residual PO. The product was characterised using ^{1}H NMR and IR spectroscopy. This very simple process of testing catalysts allowed a wide range of complexes to be screened. Cognis wanted a catalyst active at room temperature to be worthy of further investigation. Any catalyst found needed to be as reactive, if not more active than KOH and DMC to be viable industrially. A reactive catalyst at room temperature could be optimised to further increase catalysis and productivity with different conditions.

Different conditions for optimisation were investigated. First, the effects of temperature were considered by heating the catalyst, initiator and PO under nitrogen atmosphere,

ranging from room temperature to 100°C over a period of 8 h. Aliquots of the solution were collected and tested for polymerisation using ^{1}H NMR spectroscopy.

The quantity of the initiator in the reaction mixture was also examined using the methodology from a leading research group[1]. It was found that large quantities of initiators actually inhibit polymerisation and so the monomer and catalyst amounts were kept constant with variation in the initiator amount. In this case, the initiator, EtOH was used in the molar ratios [PO]:[Catalyst]:[Initiator]; [5,000]:[1]:[X], where X = 30 - 7,500. Aliquots of the solution were collected and tested for polymerisation using ^{1}H NMR spectroscopy.

Pilot Plant: Cognis has an excellent industrial plant at their site in Southampton that have polymerisation vessels of various sizes. The main plant has three alkoxylation vessels with the nominal capacities of 30, 20 and 10 tonnes. The pilot plants have three alkoxylation vessels of 80, 10 and 5 litres. The pilot plant we used has the 5 litres vessel, which required a minimum of 10 g of catalysts to react with PO and butanol. The vessel was charged with butanol and catalyst and heated to 120°C under nitrogen atmosphere. Half the quantity of PO monomer was added and stirred until constant pressure was achieved. The other portion of PO was added and stirred to yield poly(propylene oxide). The access to these facilities was very important but due to the large quantities of complex (~10 g) required to test potential catalysts, only a limited use of these facilities could be made.

2.1 Characterisation of polymers

The conventional methods of polymer characterisation are Gel Permeation Chromatography (GPC) and MaliTOF-MS, which yields information about the molecular weights (M_w, M_n and PDI). Unfortunately, as we did not have access to these specialised techniques, characterisation had to be limited to Gas Chromatography (GC), Nuclear Magnetic Resonance (NMR) and Infra-red (IR) spectroscopy. These techniques were found to give reliable data on the polymers formed and were used extensively in this study.

NMR spectroscopy: The polymer product was dissolved in $CDCl_3$ and ^1H and ^{13}C NMR spectroscopy were used to identify polymer formation. The ^1H NMR spectrum was expected to showed multiplets in the range of δ 1.00 – 1.40 ppm for pendant Me and multiplets between δ 3.00 – 3.70 ppm for methylene / methine protons. The ^{13}C NMR spectrum would show peaks at δ 16.00 – 24.00 ppm for pendant methyl group and δ 70.00 - 77.00 ppm for the methylene / methine carbon. Many papers [2-6] have used NMR techniques to determine the tacticity of the polymers formed. This is a complicated process involving ^{13}C NMR and various 2D techniques. Our interest rested with finding an active catalyst for polymerisation and the tacticity of polymers formed was considered a lesser priority at this stage.

Infra-red (IR) spectroscopy was used for identify the C-O bond of the ether formed in the polymer as well as the C-H peaks of the polymer. The peaks were in the range 1150 - 1085 cm^{-1} for ν(C-O) ether bond and between 2980 - 2850 cm^{-1} for the ν(C-H) bond. The range of 4,000 cm^{-1} to 450 cm^{-1} was used to record IR spectra of the liquid product.

Gas Chromatography (GC) is used by Cognis to identify the smaller polymers and follow the addition of each monomer unit to the butanol initiator. Using the HP 6890 GC system with a mid-polar column, we were able to follow monomer addition (Figure 1). The characterisation of polymers was limited with GC as the addition of monomer units could be followed up to a particular molecular mass but then the polymer got stuck on the column and the peaks became indistinguishable.

Figure 1: GC spectrum for the polymerisation of PO with $Zn_3[Co(CN)_6]_2.xH_2O.y^tBuOH.zPEG$

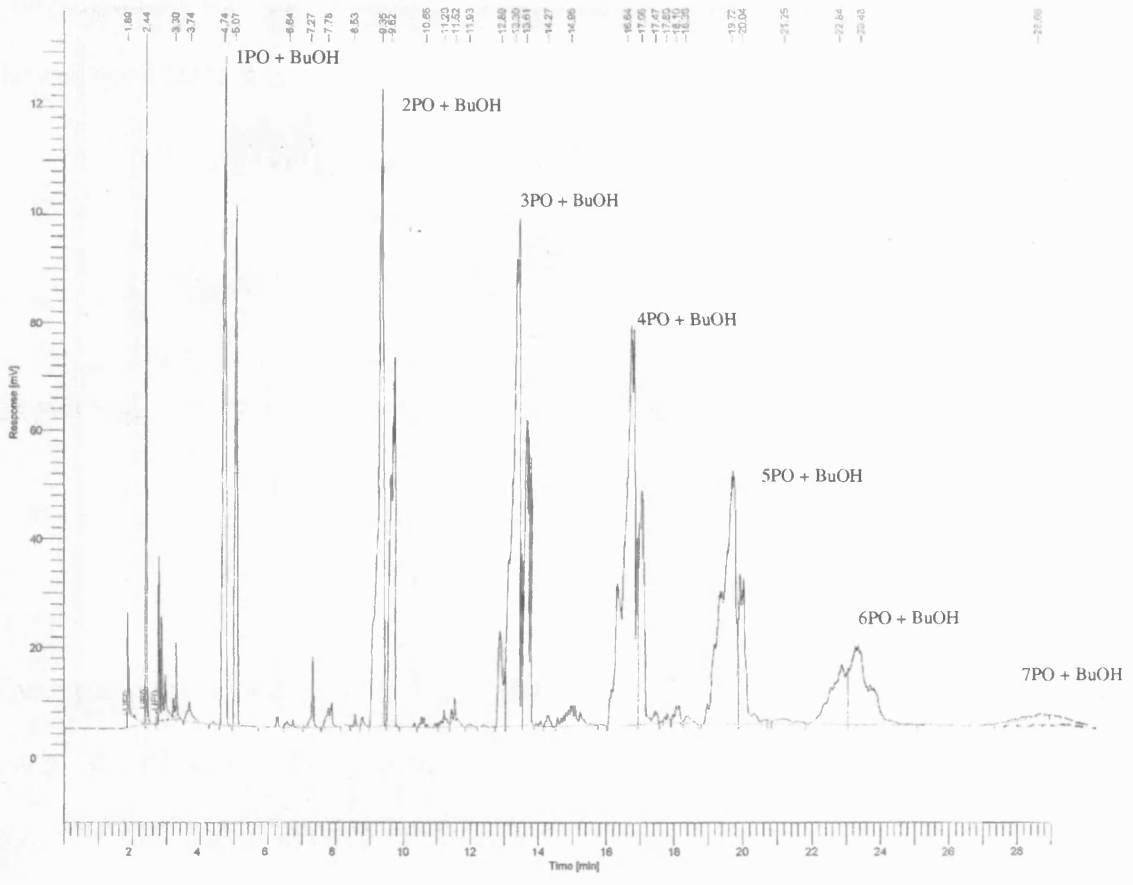

2.2 DMC Compounds

Once the methods of polymerisation testing were established, we needed to create standards that displayed poly(propylene oxide). DMC complexes were selected to form

these standards, as the starting materials were inexpensive and easily prepared. Using standard experimental methods reported in literature[7], DMC complexes were successfully formed in high yields. There are various combinations of DMC complexes and we choose the most successful complexes, namely $Zn_3[M(CN)_6]_2$, $Zn_3[M(CN)_6]_2.xH_2O.y^tBuOH.zPEG$ (M = Co, Fe; PEG = Polyethylene glycol) as well as $Zn[Ni(CN)_4]$ and $Zn[Ni(CN)_4].xH_2O.y^tBuOH.zPEG$ (Equation 1). These complexes were poorly soluble and IR spectroscopy was used to characterise them. The expected ν(CN) stretch for this type of functional group was in the range 2150 - 2200 cm^{-1} [8-10]. Comparison between the synthesised DMC compounds and values reported in literature showed good agreement.

Equation 1: Formation of standard and glymed DMC complexes

$$2K_3[M(CN)_6] + 3ZnCl_2 \longrightarrow Zn_3[M(CN)_6]_2 + 3KCl$$

$$2K_3[M(CN)_6] + 3ZnCl_2 + xH_2O + y^tBuOH + zPEG \longrightarrow Zn_3[M(CN)_6]_2.xH_2O.y^tBuOH.zPEG$$

M = Co / Fe

These compounds were tested using all three methods and polymerisation was followed using GC, IR and NMR spectroscopy. The data confirmed that both standard and glymed DMC complexes proved to be very effective catalysts in ROP of PO in all cases. For example, the reaction involving the compound $Zn_3[Co(CN)_6]_2.xH_2O.y^tBuOH.zPEG$ showed the appropriate IR stretches for ν(CH) at 2871 and 2971 cm^{-1} and the ν(C-O) at 1100 cm^{-1}. The ^1H NMR spectrum showed the methylene and methine protons as a large multiplet of multiplets between δ 3.27 – 3.54 and the pendant methyl groups appeared as a multiplet at δ 1.06. The ^{13}C NMR

spectrum showed numerous carbons peaks between δ 73.2 and 76.2 for the methylene / methine carbons and the methyl carbons in the range δ 17.3 – 18.9, corroborating the IR data and confirming polymerisation. Using test tube reactions, the DMC complexes were also reacted with butylene oxide (BO) and styrene oxide (SO) to confirm polymerisation of different epoxides. All this data allowed the creation of standards of polymerisation to compare with future polymer data.

Having investigated and formed many DMC complexes that are utilised in industry and heavily patented, we were now in a position to consider alternative catalysts that still provided high-molecular weight polymers with low unsaturation as well as be economically viable.

2.3 Cation vs. Anion Investigation

As the DMC compounds can be divided into cationic (Zn^{2+}) and anionic ($[Co(CN)_6]^{3-}$) fragments, we investigated the part played by each component by varying one whilst keeping the other part constant. By systematically exchanging cations and anions, we were hoping to identify the active part of the catalyst. For example, we wanted to establish whether it is the anionic $[Co(CN)_6]^{3-}$ that determines the catalytic activity or just a large anion that is required but not specifically a cyanometallate. Once this was established, new catalyst systems could be developed according.

The cation component was examined by substituting it for other large cations, while keeping the cyanometallate anion constant. The starting point of this investigation was the potassium salts; $K_3[Co(CN)_6]$, $K_3[Fe(CN)_6]$ and $K_2[Ni(CN)_4]$. All of these complexes were readily available and tested in the polymerisation reaction with PO. As

expected, no polymerisation was observed from the IR and ^{1}H NMR spectroscopy, confirming that potassium cyanometallate salts were not catalytically active for the ROP of PO.

We considered using bis(diphenylphosphino) ammonium ions (PPN) which have many uses in organometallic chemistry as stabilisers for large anions. By replacing the potassium cation in $K_3[Co(CN)_6]$ with PPN cation, it was expected to improve the solubility of the complex in organic solvents. Compounds formed were $[PPN]_3[Co(CN)_6]$, $[PPN]_3[Fe(CN)_6]$ and $[PPN]_2[Ni(CN)_4]$ in high yields, confirmed by IR and NMR data [11]. The IR data showed the ν(CN) stretch of $[PPN_3][Co(CN)_6]$ at 2112 cm^{-1}, $[PPN]_3[Fe(CN)_6]$ at 2104 cm^{-1} and $[PPN]_2[Ni(CN)_4]$ at 2115 cm^{-1} consistent with literature [11]. The ^{31}P NMR peaks were virtually identical, $[PPN]_3[Co(CN)_6]$ was δ 21.81 ppm, $[PPN]_3[Fe(CN)_6]$ was δ 21.82 ppm and $[PPN]_2[Ni(CN)_4]$ was δ 21.81 ppm compared to PPNCl at δ 22.72 ppm. These PPN complexes were tested for PO polymerisation but unfortunately the data showed that they were inactive catalysts.

As PPN complexes were formed in good yields, we wanted to consider other large cations, which could be complexed with cyanometallates. The tetrabutylammonium halides were reacted with $K_3[Co(CN)_6]$. However, both the chloride and bromide equivalents failed to form the required compound.

We then turned our attention to consider the role of anions with a transition metal cation such as Zn^{2+}. Various anions were investigated to identify the active catalytic component of DMC complexes. The anion component was investigated by the use of simple halides. $ZnCl_2$ with PO was highly exothermic and polymerised PO. Excess

quantities of $ZnCl_2$ in proportion to PO led to a discolouration of the polymer (orange/brown). The compound $ZnCl_2$ was very fast but indiscriminate and so not practical for use as a catalyst in industry. Larger tetrahedral and octahedral halide groups were considered. $ZnCl_2$ was reacted with $NaBF_4$ and $NaPF_6$ in distilled water but failed to form the desired compounds.

Another large anion considered was K_3PO_4 which was reacted with $ZnCl_2$ to form the complex $Zn_3(PO_4)_2$ which was characterised by IR stretches and elemental analysis. Attempts to polymerise PO and SO were unsuccessful.

Zinc acetate was tested in the polymerisation reaction with and without ethanol initiation. However, this complex did not display any catalytic properties. The reaction of $ZnCl_2$ with KOH produced $Zn(OH)_2$ in yield of 78% which was confirmed by IR data. This compound was tested in for PO polymerisation and showed mixed results that indicated some polymerisation. Another compound considered was the commercially available $Zn(CN)_2$ but tests showed negative results.

Phosphotungstic acid hydrate ($H_3PO_4.12WO_3.xH_2O$) was dissolved in distilled water and reacted with aqueous solutions of $K_3[Co(CN)_6]$. This formed a white precipitate, anticipated to be $K_3PO_4.12WO_3.xH_2O$. This complex was tested for polymerisation but the results were negative. This compound was then reacted with $ZnCl_2$ to attempt the formation of $Zn_3PO_4.12WO_3.xH_2O$. This was tested for polymerisation, which was also negative.

Interestingly, the addition of phosphotungstic acid directly to PO resulted in a vigorous, exothermic reaction, resulting in PO polymerisation. This vigorous reaction was exothermic, resulting in the discoloured orange/ brown polymer liquid, similar to the product from $ZnCl_2$ reaction. However, the addition of ethanol to the phosphotungustic acid first, then PO addition resulted in a more controlled reaction. It was thought that a cationic polymerisation mechanism was followed, producing oligomers, typical of this mechanistic route.

One of the most successful finds of this investigation was the Lewis acid, zinc triflate $[Zn(CF_3SO_3)_2]$ which is readily available. Following the trends of large anions, zinc triflate was tested for the polymerisation reaction with PO, BO and SO. The quality of IR, ^1H and ^{13}C NMR data showed a strong degree of polymerisation. As the zinc triflate proved to be successful, we considered other triflates, such as ytterbium triflate. This was tested for polymerisation of PO and proved to be a very good catalyst confirmed by ^1H NMR and IR spectroscopy.

Unfortunately, Hofmann *et al.*[8] patented this triflate work by combining the reactivity of both the triflates and DMC complexes. After investigating a range of metal triflates, they used $[Yb(CF_3SO_3)_2]$ in the first stages of the reaction to bring the molecular weight up to 1,000 M_w and then used the $Zn_3[Co(CN)_6]_2$.glyme to increase the molecular weight to the required value. The success of $[Yb(CF_3SO_3)_2]$ led to the revision of our observations that Zn^{2+} ion was key to the ROP. Perhaps, it is more accurate to propose the metal cation was responsible for the polymerisation than zinc ion specifically.

From the anion investigation, there are many potential anions that can be complexed with a metal cation to form active complexes catalysing the ROP of PO. Although there has been no conclusive evidence, the widely accepted mechanism is that these complexes react *via* the metal cation attaching to the epoxide oxygen [12, 13].

2.4 Metal Amines

Our research showed a potential catalyst needed to combine a metal cation with a large anion. Our attention turned to the possibility of various amines combined with zinc metal centre. Work by Cernak *et al.*[14] suggested that the metal amines could be combined with cyanometallates in a complex structure, which we thought could be excellent catalyst candidates.

The reaction of $ZnCl_2$ with primary amines in distilled water proved to be unsuccessful with yields as low as 10% and mixed with impurities. We decided to use $Zn(NO_3)_2.xH_2O$ as the zinc source and reacted this with a range of amines (ammonia (NH_3), diethylamine ($NHEt_2$) and triethylamine (NEt_3). The compounds $[Zn(NH_3)_6][NO_3]_2$, $[Zn(NHEt_2)_6][NO_3]_2$ and $[Zn(NEt_3)_6][NO_3]_2$ were partially soluble and characterisation data was limited. These were reacted with PO in test tube reactions and characterised by IR and ^1H NMR spectroscopy. The results from the data showed some indication of polymerisation but no conclusive results could be drawn in the absence of GPC and Maldi TOF data.

We reacted these zinc amines complexes with $K_3[Fe(CN)_6]$ to substitute the NO_3^- anion with $[Fe(CN)_6]^{3-}$. All the zinc amines complexes were reacted with aqueous solution of the cyanometallates and formed a range of complexes of the form

$[Zn(amine)_6]_3[Fe(CN)_6]_2$. Standard IR and ^1H NMR spectroscopy showed good levels of polymerisation in the IR and ^1H NMR spectra.

With these positive results, we extended the range of compounds by reacting these metal amines with potassium salts of cyanometallates $[M(amine)_6]_a[M'(CN)_b]_c$ (M = Zn, Co, Fe; M' = Co, Fe, a = 3, b = 6, c = 2; M = Ni, a = 0, b = 4, c = 0; amine = NH_3, $NHEt_2$, NEt_3). These were all tested for PO polymerisation and it was found that many compounds did show evidence of polymerisation. The next stage was to form metal compounds with multidentate amines such as ethylenediamine and cyclam ligands, which could constrain the metal centre in a specific geometry conducive to polymerisation. The compounds synthesised were of the form $[M(amine)_a][NO_3]_3$ and $[M(amine)_a][M'(CN)_b]_c$ (M = Zn, Co, Fe; amine = ethylenediamine (a = 3) , cyclam; M' = Co, Fe, a = 3, b = 6, c = 2; M = Ni, a = 0, b = 4, c = 0) and tested for polymerisation. Similar to the other metal amine complexes, there were some positive results for polymerisation.

Unfortunately, after substantial amounts of work on these metal amine compounds and mixed polymerisation results, a more in-depth characterisation of the products using elemental analysis showed that the structural formulae for these complexes could not be confirmed. A review of literature revealed that the method followed for the synthesis of the complexes was flawed. Studying zinc chemistry, it was found that dissolving $ZnCl_2$ / $Zn(NO_3)_2$ in distilled water and adding an amine forms a white precipitate, which we took to be $[Zn(amine)_6][NO_3]_2$ but in fact was considered to be $Zn(OH)_2$[15]. Only on excess addition of the amine was the $[Zn(amine)_4]^{2+}$ formed as a solution and therefore

the use of the white solid, now known to be $Zn(OH)_2$ resulted in all subsequent compounds having incorrect chemical formula.

It is thought that the polymerisation observed in many of the reaction with these metal-amine complexes could be due to the amines acting as a base and ring-opening PO to form PPO. However, interestingly, the three amines were used as catalysts in test tube reactions to yield polymers in small quantities. In addition, if the polymerisation observed was due to the amines in all the metal amine complexes, some compounds did not show polymerisation. Therefore, this suggests that the white precipitate is a mixture of hydroxide and amine complex.

Comparison of the polymerisation data using amines as catalysts and the polymerisation results of metal amine complexes showed the latter to be more catalytic. Having already established that the cyanometallate compounds, namely $K_3[Co(CN)_6]_2$, $K_3[Fe(CN)_6]_2$ and $K_2[Ni(CN)_4]$ do not catalyse PO polymerisation, it is plausible the metal hydroxide may coordinate with the amine to catalyse PO polymerisation. Another possibility is the $Zn(OH)_2$ catalyses the polymerisation as there is no evidence to suggest that $Zn(NO_3)_2$ ring-opens PO. Unfortunately, it was very difficult to identify which part was responsible for the polymerisation. The elemental analysis showed no pattern of formula and so without vast amounts of research and time, it was not possible to clearly identify the mechanism.

Overall, we established a system for testing the polymerisation of PO in a simple laboratory experiment. We developed standards of polymerisation, which allowed a comparison of polymerisation between a well-established catalyst and new potential catalysts.

The investigation of cation and anion moieties found that the most successful compounds for polymerisation had a metal centre and a large anion. The synthesis of metal amine investigation was flawed however yielded some interesting results. It is proposed that a combination of the components could form a complex that is catalytic. The combination of metal amine with cyanometallate was further investigated in Chapter 3.

2.5 References

[1] D. Chakraborty, A. Rodriguez, E. Y. X. Chen, *Macromolecules* **2003**, *36*, 5470.

[2] C. Billouard, S. Carlotti, P. Desbois, A. Deffieux, *Macromolecules* **2004**, *37*, 4038.

[3] W. Braune, J. Okuda, *Angewandte Chemie-International Edition* **2003**, *42*, 64.

[4] M. H. Chisholm, D. Navarro-Llobet, W. J. Simonsick, *Macromolecules* **2001**, *34*, 8851.

[5] B. Antelmann, M. H. Chisholm, S. S. Iyer, J. C. Huffman, D. Navarro-Llobet, M. Pagel, W. J. Simonsick, W. Q. Zhong, *Macromolecules* **2001**, *34*, 3159.

[6] Z. Oktem, K. Alyuruk, *Polymer* **1998**, *39*, 583.

[7] Y.-J. Huang, G.-R. Qi, Y.-H. Wang, *Journal of Polymer Science, Part A: Polymer Chemistry* **2002**, *40*, 1142.

[8] P. Ooms, J. Hofmann, P. Gupta, L. Groenendaal, Application: EP, 1029871, **2000**.

[9] J. Hofmann, P. Gupta, R.-J. Kumpf, P. Ooms, W. Schafer, M. Schneider, Application: WO, 98-EP6312 9919063, **1999**,

[10] B. Le-Khac, Application: EP, 654302, **1995**,

[11] D. A. Cauzzi, G. Mori, G. Predieri, A. Tiripicchio, F. Cavatorta, *Inorganica Chimica Acta* **1993**, *204*, 181.

[12] N. Yoshino, C. Suzuki, H. Kobayashi, T. Tsuruta, *Makromolekulare Chemie-Macromolecular Chemistry and Physics* **1988**, *189*, 1903.

[13] Y. Hasebe, T. Tsuruta, *Makromolekulare Chemie-Macromolecular Chemistry and Physics* **1988**, *189*, 1915.

[14] J. Cernak, J. Chomic, M. Dunajjurco, C. Kappenstein, *Inorganica Chimica Acta* **1984**, *85*, 219.

[15] F. A. Cotton, G. Wilkinson, *Advanced Inorganic Chemistry: A Comprehensive Text. 4th Ed*, **1987**.

Chapter 3

Cyanides

3.1 Introduction

As previously discussed, (Chapter 1), Double Metal Cyanide (DMC) complexes are deemed the most effective catalysts for ROP of PO. Much research has been undertaken to establish their structure and polymerisation mechanisms in the hope of further enhancing catalysis and productivity. Reaction of aqueous metal salts and metal cyanides resulted in the formation of networks consisting of metal centres bridged by cyanide ligands with cavities. For example, in $Zn_3[Co(CN)_6]_2.12H_2O$, the three zinc centres are held in position by the nitrogen end of the cyanide bridges. This results in an octahedral geometry about the zinc centre with the axial positions available for the water molecules.

The versatility of the bridging cyanide ligand has led to a whole host of networks with various shapes and sizes [1-3]. To better understand these metal-cyanide networks, researchers have proposed numerous transition metal complexes with cyanide ligands. For example, structural studies on analogous $[M(CN)_6]^{3-}$ (M = Cr to Co) complexes showed a steadily decrease of M-C bond lengths (1.89 – 2.08 Å). Using IR studies, the free CN stretch was identified at 2080 cm^{-1} with terminal M-CN in the range 2200 – 2000 cm^{-1}. Researchers[4] also used homologous series $[V(CN)_6]^{n-}$ (n = 3 - 5) to consider the effect of metal oxidation state on the cyanide stretch. It was proposed that as the oxidation state increased, the metal centre became more electropositive, resulting in the enhancement of the M-C σ bonding and therefore increasing the $\nu(C\equiv N)$. The frequency of the C≡N vibration also increased as the mode of binding changed, as terminal CN binding was lower frequency than linear binding.

The cyanide ligand has numerous modes of binding, most of which are through the carbon atom, as terminal (**a**) and linear bridged (**b**) with atypical binding modes also represented (**c-g**) [2] (Figure 1).

Figure 1: Modes of binding for the cyanide ligand [2]

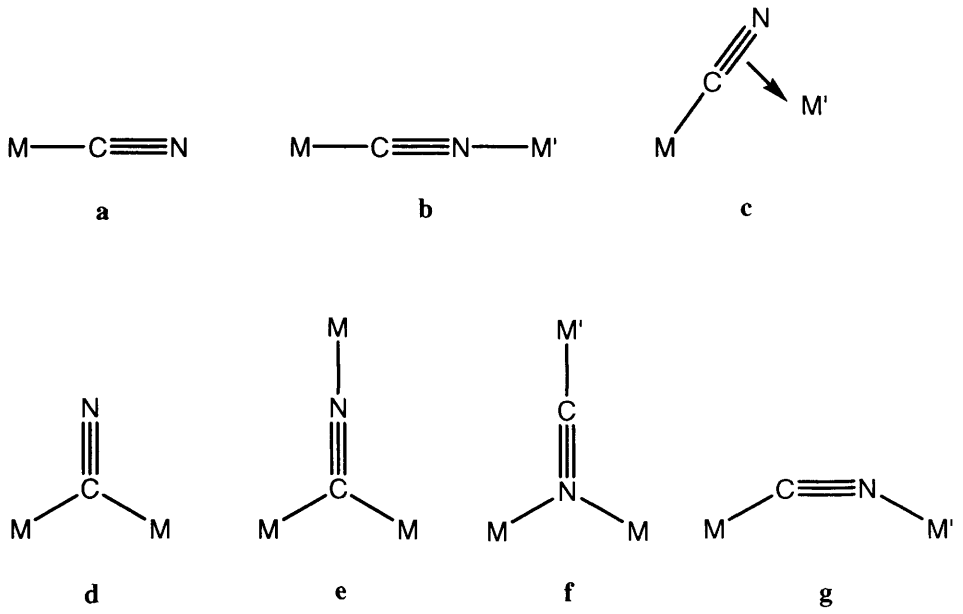

Interesting and useful features of these types of metal-cyanide compounds were their examples of linkage isomers such as $Fe_3[Mn(CN)_6]_2$, $Co[Cr(CN)_6]_2$ and $Fe[Cr(CN)_6]_2$ [5]. For example, $KFeCr(CN)_6$ has two isomers, a green one best represented by the bonding Fe^{II}-CN-Cr^{III} (ν(C≡N) 2092cm^{-1}) and a red one by Cr^{III}-CN-Fe^{II} (ν(C≡N) 2168, 2114 cm^{-1}) [6].

Transition metals can accommodate between two to eight cyanide ligands, offering a host of geometries. Two-coordinate complexes involve d^{10} linear structures such as $Hg(CN)_2$ or $[M(CN)_2]^-$ (M = Ag, Au) [7-9], while $[Hg(CN)_3]^-$ is a planar anion forming chains with weak interactions between Hg-N, giving a chain trigonal pyramidal structure[10]. Tetra–coordinate cyanide compounds can be either tetrahedral or square

planar geometries, examples of the former including $[M(CN)_4]^{3-}$ (M = Cu, Ag) [11] and $[M(CN)_4]^{2-}$ (M = Zn, Cd, Hg) [7]. Square planar d^8 metal complexes are very common and include anions such as $[Au(CN)_4]^-$ [12] and $[M(CN)_4]^{2-}$ (M = Ni, Pd, Pt) [13-15].

Penta-coordinate cyanide complexes have two possible geometries, namely square pyramidal [16-18] and trigonal bipyramidal. The anion $[Ni(CN)_5]^{3-}$ exhibits both geometries until heated or put under pressure at which point it reverts to the more stable square pyramidal. Most common hexacyanometal anions display an octahedral or distorted octahedral structure in different oxidation states and charges $[M(CN)_6]^{n-}$ (n = 2 - 4) [19-22].

The hepta-coordinated cyanometal complexes observe a pentagonal bipyramidal structure determined by X-ray diffraction. Examples of these compounds include $[V(CN)_7]^{n-}$ (n = 4, 5) [23, 24], $[Mo(CN)_7]^{5-}$ [25] and $[Re(CN)_7]^{4-}$ [26]. Finally, the octacyanometalate is a dodecahedron or square antiprism, depending on the packaging forces. For example, $[Mo(CN)_8]^{4-}$ is a dodecahedron with K^+ salt but a square antiprism with Cd^{2+} ions [27]. Another interesting example is $[Mo(CN)_8]^{3-}$ which is dodecahedron with $[(Bu_4N)_3]^{3+}$ [28], square antiprism with $[Na_3]^{3+}$ [29] and approximately bicapped trigonal prismatic with $[Cs_3]^{3+}$ [30].

The range of metallic cyanide compounds previously discussed displays a multitude of diverse combinations. As the cyanide ligand generally has a linear coordination, depending upon the orientation of the cyanides and coordination number of the metal centres, this can lead to potentially different motifs (1D, 2D or 3D). The amidentate nature of cyanide which permits bonding *via* the carbon and the lone pair interaction of

the nitrogen with the second metal centre. The length of the linear M-CN-M' is approximately 5.0 – 5.6 Å leading to cavities in a polymeric structure allowing the trapping of guest solvent molecules. Materials of this nature are commonly known as inclusion compounds or clathrates [2].

In 1897, Hofmann serendipitously prepared clathrate-type compounds with the general formula $[M(NH_3)_2][M'(CN)_4]$ (M' = square planar metal). Hofmann mixed ammonical solutions of $Ni^{(II)}$ tetracyanide with guest molecules: benzene, thiophene, pyrrole and furan to form so-called Hofmann-type compounds with included guest molecules [31, 32]. Other potential guest molecules such as alkylbenzenes, halobenzenes and naphthalenes failed to form the desired compounds. Through various studies, he identified that the reaction was selective, allowing only certain guest molecules to fill the void cavities, being dependent on their size and shape.

Powell and Rayner [33, 34] elucidated the Hoffmann structure, $[Ni(NH_3)_2][Ni(CN)_4]$ (Figure 2). The square planar $Ni^{(II)}$ metal centre is encased with four cyanides bonded *via* the carbon atom. The octahedral $Ni^{(II)}$ centre is bridged to the square planar $Ni^{(II)}$ through the nitrogen end of the cyanide. Consequently, the equatorial positions on the octahedral $Ni^{(II)}$ are occupied by cyanides and the two axial positions, above and below are occupied by NH_3 molecules. This arrangement forms a 2D network with holes between the layers, filled with guest molecules (typically aromatic molecules), held in place by NH_3 ligands. In addition to this, the electronic effect of M-C orbitals restricts the benzene molecules ability to diffuse out of the network.

Figure 2: Hoffmann 2D motif with square planar $[Ni(CN)_4]^{2+}$ and octahedral $[Ni(CN)_4][(NH_3)_2]$

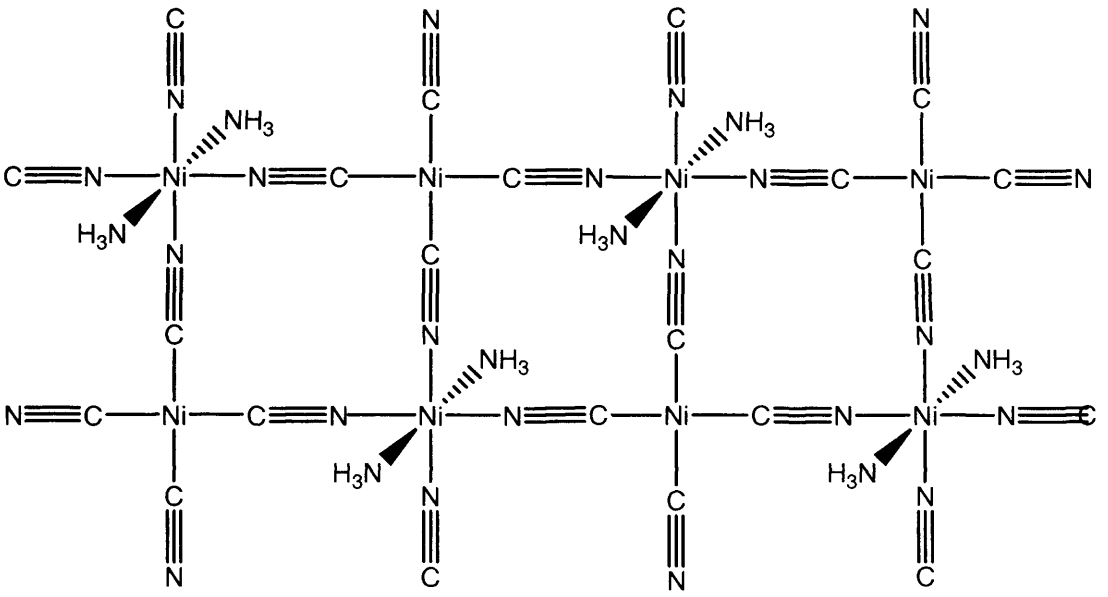

The original synthesis involved mixing aqueous solutions of $[Ni(NH_3)_6]^{2+}$ and $[Ni(CN)_4]^{2-}$ with the organic guest molecules producing impure and incomplete clathrated compounds with hydrated metal compounds[2]. Attempting different syntheses, it was found that the best method was to grow crystals at the interface of the organic and aqueous phases. Crystals formed were not very stable as they slowly decomposed and some guest molecules diffuse out over a period of time.

Further studies found that water can be clathrated. These compounds were characterised as $[Ni(NH_3)_2][M'(CN)_4].½H_2O$, containing a highly distorted tetragonal structure with a puckered layer [35]. A water molecule has also been found to replace NH_3 from the octahedral metal centre to act as a terminal ligand e.g. $[Ni(H_2O)_2][M'(CN)_4].nH_2O$ [36, 37].

Extension of the different types of Hofmann compounds by Iwamoto *et al.* [38-40] followed the general formula $[M(NH_3)_2][M'(CN)_4].2G$ (M = Mn, Fe, Co, Ni, Cu, Zn,

Cd; M' = Ni, Pd, Pt: G = C_4H_5N, C_4H_4S, C_6H_6, $C_6H_5NH_2$). Evolution of the Hofmann-type clathrates led to a new class of compounds known as "modified-Hofmann clathrates" [39-42], within which NH_3 was replaced with other ligands or substitute the square planar metal [M'$(CN)_4$] with tetrahedral metal centred tetracyanide compound. For example, the replacement of NH_3 with the monodentate methylamine formed [Cd$(MeNH_2)_2$][Ni$(CN)_4$].1.5$MeNH_2$. The network formed permitted larger aromatic guest molecules such as *o*-toluidine to be incorporated. Structural analysis showed the distorted network had four vacant cavities but was only able to accommodate three guest units, resulting in the presence of 1.5 guest molecules [41].

The most common modified-Hofmann clathrate involves the bidentate ligand, ethylenediamine (en = $H_2N(CH_2)_2NH_2$) in the general formula [M(en)][M'$(CN)_4$].2G. The interesting feature of these ligands is their ability to expand and contract in length between 7.86 – 8.06 Å to accommodate different aromatic guest molecules such as pyrrole and benzene, however they are unable to accommodate aniline.

Other bidentate ligands used were 2-methyl-ethylenediamine (pn = $H_2NCH_2CH(Me)NH_2$), trimethylenediamine (tn = $H_2N(CH_2)_3NH_2$) and monoethanolamine (mea = $H_2NCH_2CH_2OH$)[41]. Variation in the general formula is observed when using the bidentate ligand pn, in which the methyl moiety occupies one of the vacant cavities, resulting in a reduced number of guest molecules, i.e. [Cd(pn)][Ni$(CN)_4$].1.5G. In these compounds, both the amine and the guest molecules can alter the network structure of the compound.

When bidentate ligands with more than three carbon atoms are used, ($H_2N(CH_2)_nNH_2$), (n = 4 - 9), larger cavities are formed. These allow the incorporation of bigger aromatic guest molecules such as substituted or fused aromatics [43-47]. The long chain bidentates provide greater flexibility and distortion in the structure leading to slanting columns and pillars, effecting the puckering of the layers and inclusion of guest molecules. With the increase in different types of guest molecules clathrated in these compounds, accurate determination of the number and type of guest molecules clathrated becomes difficult. However, researchers [41, 47] have observed an interesting effect in which diamines with an even number of carbon atoms are more easily crystallised than those with an odd-number.

Our interest in these Hofmann-type clathrates stems from DMC compounds and their ability to catalyses PO polymerisation. As DMC compounds form networks of metal centres bridged with cyanide, we have attempted to also form networks of metals bridged with cyanides based on the Hofmann-type compounds. Once these crystals were formed, we hoped to characterise them and investigate their catalytic properties.

3.2 Results and Discussion

Following the Hofmann-type synthesis[48], a range of complexes were formed. Depending on the type of transition metal and the amine used, the shape and colour of the crystals were created. The two different amines used were ammonia and ethylenediamine (en).

3.21 Ammonia compounds

For the ammonia compounds, two methods were utilised. The first set of compounds were formed using Method A. This involved adding ammonia solution (35%) to the aqueous solution of metal chloride and potassium tetracyanonickelate hydrate. The second method (Method B) used pure liquid ammonia added directly to the aqueous solution of metal chloride and potassium tetracyanonickelate. These solutions were sealed airtight for a period of one to three months, until crystal formation was observed.

Comparison of the cadmium compounds (**1a** and **1b**) formed *via* both methods showed in each case the successful formation of $[Cd(NH_3)_2][Ni(CN)_4]$. Both elemental analyses were in good agreement between the calculated percentages. An interesting observation was that from Method A (**1a**), shiny fine yellow needles were formed that were different to the yellow-orange needles (**1b**) formed by Method B. The theoretical number of IR active bonds in $K_2Ni(CN)_4$, based on D_{4h} symmetry is one but a solid (KBr) spectrum displayed two stretches. This was attributed to the interaction of the potassium ions present and the constraint of the solid form. Comparison of the IR spectra of the starting material $K_2Ni(CN)_4$ for ν(CN) (2121 and 2085 cm^{-1}) and those of **1a** and **1b** showed an increase in wavenumbers of 30 - 70 cm^{-1}, each exhibiting two bands to indicate a symmetrical square planar system. Infra-red spectroscopy of both clearly identified two appropriate ν(CN) stretches in the range of 2200 – 2000 cm^{-1} as well as the corresponding peaks for ν(NH) and hydrogen bonding.

The formation of $[Zn(NH_3)_2][Ni(CN)_4]$ proved to be difficult. Method A failed to give any kind of solid. The compound did form *via* Method B giving a small quantity of golden brown needles but the analytical data were not in accordance with the expected

formulation. However, IR data identified two sharp bands at 2193 and 2152 cm^{-1}, which indicated there was a symmetrical square planar cyanometallate and was not $K_2Ni(CN)_4$. In addition to this, there was also a broad peak at 3273 cm^{-1}, which suggested the presence of N-H bonds of the NH_3 ligands. Therefore, although the elemental analysis did not verify the composition of **2b**, there is some evidence to suggest the compound was formed (discussed later in TGA section) as the similar complexes $[Zn(NH_3)_2][Ni(CN)_4].2G$ (G = benzene, aniline) were synthesised by Nakano *et al.* [49].

The nickel complex $[Ni(NH_3)_2][Ni(CN)_4]$ exhibited the greatest difference in crystal type between the two methods of formation. Method A gave a fluffy purple precipitate (**3a**) while Method B afforded fine blue-green needles (**3b**). However, the analytical data were in good agreement with the calculated values and both IR spectra displayed two identical stretches for ν(CN) at 2160 and 2120 cm^{-1}.

From all the experimental detail above, compounds of the general formula, $[M(NH_3)_2][Ni(CN)_4]$ were formed, however, this was not the case when copper was used. Method A gave small dark blue rod-like crystals (**4a**) with the formula $[Cu(NH_3)][Ni(CN)_4]$ based on elemental analysis. Method B gave blue fine needles (**4b**) with the formula $[Cu(H_2O)][Ni(CN)_4]$. This was unexpected, as all other compounds contained ammonia. However, the literature [50] offers some evidence to substantiate this structure as the crystal of $[Cd(H_2O)_2][Ni(CN)_4]$ was determined and other Hoffmann-type compounds have been shown to incorporate water molecules as both ligands and guest molecules [36, 37]. The IR spectra of these two compounds were different from the other ammonia-based compounds which as they all exhibited two

bands to represent ν(CN) of $[Ni(CN)_4]^{2-}$ as symmetrical. These copper-based compounds exhibited three bands at 2174, 2145, 2122 cm^{-1} for **4a** and 2172, 2152 and 2127 cm^{-1} for **4b** (further discussed in section 3.211).

Table 1 gives the values for the calculated and found percentages of the elements carbon, hydrogen and nitrogen in these compounds, showing good correlation.

Table 1: Elemental analysis for ammonia compounds

Structure	C %	H %	N %
$[Cd(NH_3)_2][Ni(CN)_4]$ (calculated)	15.54	1.96	27.18
1a	15.37	1.62	25.02
1b	15.56	1.72	25.61
$[Ni(NH_3)_2][Ni(CN)_4]$ (calculated)	18.80	2.37	32.89
3a	18.28	2.21	30.46
3b	18.22	2.09	30.06
$[Cu(NH_3)_2][Ni(CN)_4]$(calculated)	18.45	2.34	32.28
4a	18.96	1.46	28.12
4a $[Cu(NH_3)][Ni(CN)_4]$ (recalculated)	19.74	1.24	28.78
4b	18.90	0.73	23.71
4b $[Cu(H_2O)][Ni(CN)_4]$ (recalculated)	19.66	0.83	22.93

*3.211 Crystal structure of $[Cu(NH_3)_4][Ni(CN)_4]$ (**4b**)*

The variation of the elemental analysis percentages of the ammonia compounds led to further investigations into the composition and structure of the crystals formed. Crystal structures were possible as similar compounds with the general formula $[M(NH_3)_2][Ni(CN)_4].2G$ (M = $Cu^{(II)}$, $Cd^{(II)}$, $Zn^{(II)}$)(G = benzene, aniline) have been reported[49].

Only one of the above compounds was suitable for single crystal X-ray diffraction, namely, $[Cu(NH_3)_2][Ni(CN)_4]$ (**4b**). Blue rod-like crystals were found to be orthorhombic with the space group Pnma. The data collected was of high quality with the low R_1 value of 0.0159. Somewhat surprisingly, given the elemental analysis above, the compound was identified as $[Cu(NH_3)_4][Ni(CN)_4]$. The presence of the two additional ammonia molecules could be easily justified based on the excess ammonia present during crystal formation. The preparation of the compound for elemental analysis required it to be exposed to the atmosphere for a considerable amount of time, which could facilitate the loss of ammonia. When this sample was prepared for X-ray diffraction, it was quickly removed from the solution and covered in Fomblin® YR-1800 to prevent exposure to air and ammonia loss.

This structure clearly shows the slightly distorted square planar copper (II) centre ligated by four ammonia molecules. Each copper centre is bound to a nitrogen of one of the cyanide ligands from tetracyanonickelate, forming an overall square-based pyramidal geometry. The tetracyanonickelate is square planar, angles between the cyanides at 90° as expected (Figure 3).

Figure 3: Crystal structure of $[Cu(NH_3)_4][Ni(CN)_4]$ (4b)

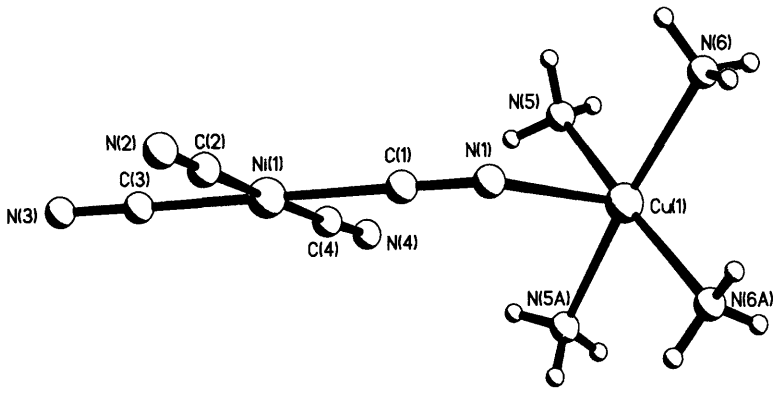

Reviews of the literature found many other examples of these types of compounds based on copper-amine systems with various tetracyanometalates[41]. A compound which had a close resemblance to this structure is $\{[Cu(NH_3)_4][cis\text{-}Ni(CN)_2(\mu\text{-}CN)_2]\text{-}cyclo\text{-}[trans\text{-}Cu(NH_3)_2]\text{-}[cis\text{-}Ni(CN)_2(\mu\text{-}CN)_2]\}_2$[51] (Figure 4). Comparison of the bond length and angles of this compound with **4b** demonstrated excellent agreement.

Figure 4: $\{[Cu(NH_3)_4][cis\text{-}Ni(CN)_2(\mu\text{-}CN)_2]\text{-}cyclo\text{-}[trans\text{-}Cu(NH_3)_2]\text{-}[cis\text{-}Ni(CN)_2(\mu\text{-}CN)_2]\}_2$ structure[52]

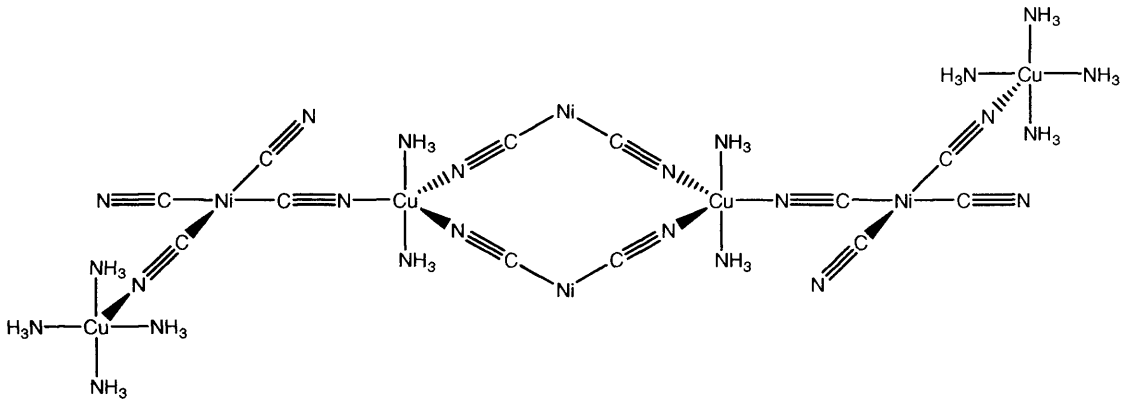
NH3
H3N—Cu—NH3
NH3
N≡C—Ni—C≡N—Cu—N≡C—Ni—C≡N
NH3
NH3
NH3
NH3
Ni
Ni
N
N
N
N
N
N
C
C
C

between the copper centre and the *cis*-cyanide ligand of the tetracyanonickelate at 3.383(19) Å, which formed 1D chains. The stacking arrangement also highlighted the linking of sheets *via* the Ni-Ni interaction with the distance of 3.711Å (Figure 5).

Figure 5: Stacking arrangement of $[Cu(NH_3)_4][Ni(CN)_4]$ (4b)

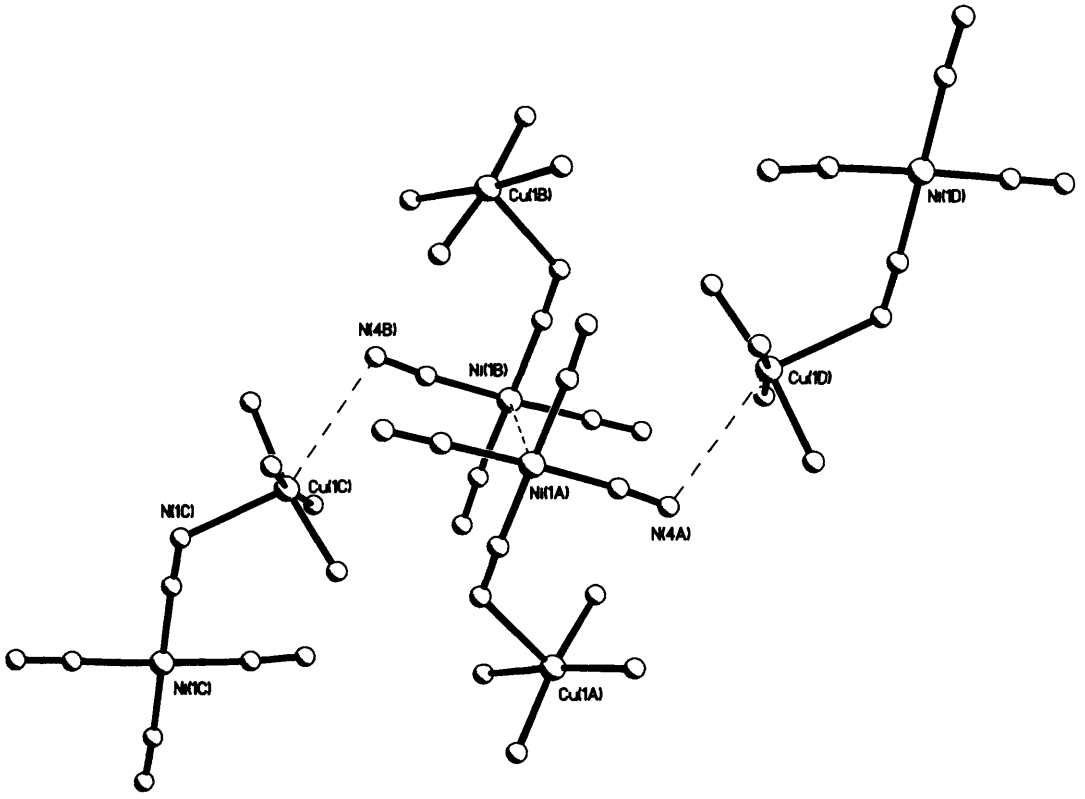

The bond angles were consistent with the literature values. The square planar geometry of the $[Ni(CN)_4]^{2-}$ was observed with angles at 177.49(7) Å (C(2)–Ni(1)–C(4)). The angles across the copper square planar geometry was slightly distorted at 172.06(5) Å (N(6A)–Cu(1)–N(5)). The angle between the two ammonia molecules through the copper centre was approximately 89.51(5) Å (N(6)–Cu(1)–N(5)) and the angle between two cyanides *via* the nickel centre were in good agreement at 90.07(7) Å (C(2)–Ni(1)–C(3)). The angle between the copper center and the attached NC ligand in our structure was 124.48(12) whereas the literature equivalent was 140.00(4)°.

3.22 Ethylenediamine compounds

Following on from the ammonia compounds, ethylenediamine (en) was used as the ligand. Synthesis outlined by Iwamoto *et al.*[48] was followed which involved the addition of the amine, en, to aqueous solutions of metal halide and potassium tetracyanonickelate. This was stoppered and left for a period of one to three months. The general formula of synthesised compounds anticipated was $[M(en)][Ni(CN)_4]$ (M = cadmium, zinc, nickel and copper), however, characterisation of these compounds indicated a number of variations were formed. Different coloured crystals were produced in different shapes, for example, the zinc compound (**6**) formed flat orange crystals whereas the copper compound (**8**) formed short, thick purple rod crystals (see below).

Figure 6: Photographs of compounds 6 and 8

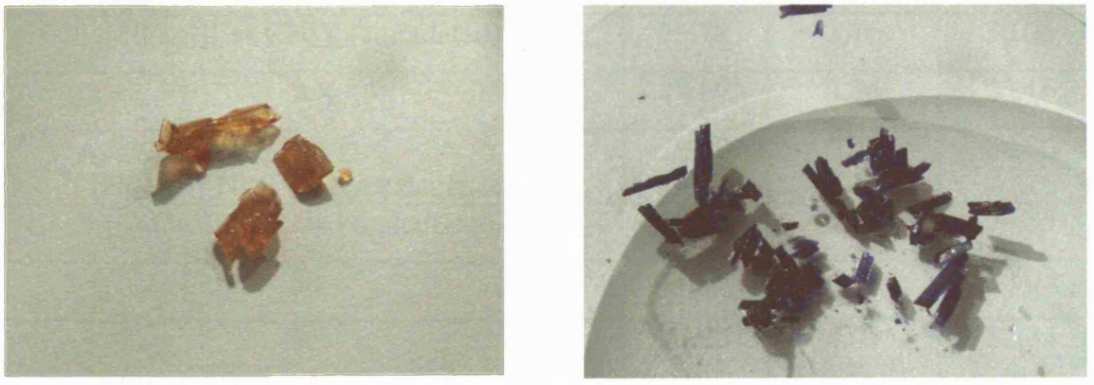

Characterisation of these compounds found that only one compound (**5**) displayed the desired formula. This compound $[Cd(en)][Ni(CN)_4]$ formed a fine cream precipitate instead of crystals. The elemental analysis values indicated that there was one en ligand. Elemental analysis data confirmed formulation of $[Zn(en)_2][Ni(CN)_4]$ (**6**) and $[Cu(en)_2][Ni(CN)_4]$ (**8**) with two en ligands. These formed orange and purple crystals respectively and were suitable for single crystal X-ray diffraction. In addition to this, **7**

formed pink plates characterised as $[Ni(en)_3][Ni(CN)_4]$ by elemental analysis; bearing two en ligands more than expected (Table 2). IR spectroscopy was used to further characterise these compounds clearly showing three stretches for the ν(CN) stretches in the range of 2200 – 2000 cm^{-1} and the corresponding peaks for ν(NH) between 3350 – 3250 cm^{-1} and ν(CH) 3000 – 2850 cm^{-1}.

Table 2: Elemental analysis for ethylenediamine compounds

Structure	C %	H %	N %
$[Cd(en)][Ni(CN)_4]$ (calculated)	21.49	2.41	25.07
5c	21.61	2.48	26.41
$[Zn(en)][Ni(CN)_4]$ (calculated)	25.18	2.11	29.36
6c	27.67	4.65	32.04
6c $[Zn(en)_2Ni(CN)_4]$ (recalculated)	27.58	4.63	32.17
$[Ni(en)][Ni(CN)_4]$ (calculated)	25.78	2.16	30.06
7c	28.57	6.34	33.16
7c $[Ni(en)_3][Ni(CN)_4]$ (recalculated)	29.90	6.02	34.86
$[Cu(en)][Ni(CN)_4]$ (calculated)	25.34	2.13	29.55
8c	27.69	4.70	32.03
8c $[Cu(en)_2][Ni(CN)_4]$ (recalculated)	27.73	4.65	32.34

3.221 Crystal structure of $[Cu(en)_2][Ni(CN)_4]$ (8)

To further understand the structures of these compounds, single crystal X-ray diffraction was undertaken for suitable crystals. The single crystal of $[Cu(en)_2][Ni(CN)_4]$ (**8**) was found to be triclinic (P1bar) (Figure 7).

Figure 7: Crystal structure of $[Cu(en)_2][Ni(CN)_4]$ (8)

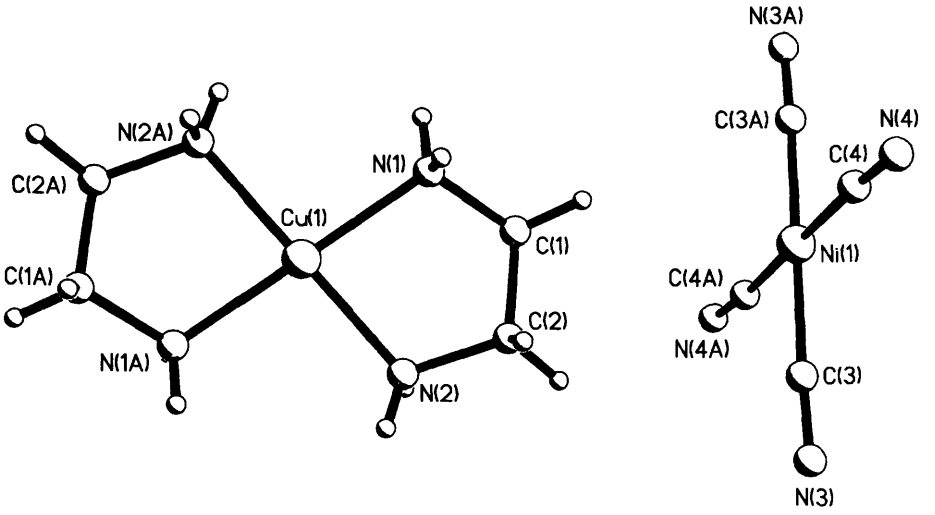

Lokaj *et al.*[53] previously determined the single crystal structure of $[Cu(en)_2][Ni(CN)_4]$ which allowed a comparison to be made between the two structures. Despite their data being collected at room temperature with an R_1 value of 0.056, compared to our data collected at 150 K and R_1 value of 0.0258, there was excellent correlation between the values. The bond lengths on both en ligands were equal as expected and compared well with other $[M(en)_2][Ni(CN)_4]$ complexes [52, 54, 55]. The bond length between the copper centre and the nitrogen atoms of the en ligand were 2.0114(14) Å (Cu(1)–N(1)) compared to the literature value of 2.001(3) Å. The bonds between these nitrogen atoms and the ethylene carbons were 1.480(2) Å (N(1)–C(1)). The distance between the two carbons forming the ethylene fragment of this ligand are 1.510(2) Å (C(1)–C(2)). In the tetracyanonickelate fragment, the crystal structure was almost identical to that in **4b**. The nickel-cyanide bond length of 1.8636(15) Å (Ni(1)–C(3)) in this crystal matched its equivalent in $[Cu(NH_3)_4][Ni(CN)_4]$ (**4b**) at 1.8648(18) Å and the literature value of 1.864(3) Å. The bond length forming the cyanide triple bond was 1.148(2) Å (N(4)–C(4)), typical for cyanides bonds.

This purple rod-like crystal showed a distorted square planar $[Cu(en)_2]^{2+}$ moiety which displayed a pseudo octahedral geometry with the weak interaction to the square planar $[Ni(CN)_4]^{2-}$ anion, above and below the amine plane. This bridging by cyanide groups was unsymmetrical in both our crystal and the literature crystal. The Ni-C bond (Ni(1)-C(3)) was 1.8636(15) Å and Cu-N was 2.531(6) Å (Cu(1)-N(3A)) compared to the literature values of 1.850(4) Å and 2.533(4) Å respectively. The interaction between the cyanides and copper centres create *trans*-bridges forming a chain (Figure 8).

Figure 8: Interaction of the moieties in $[Cu(en)_2][Ni(CN)_4]$ (8)

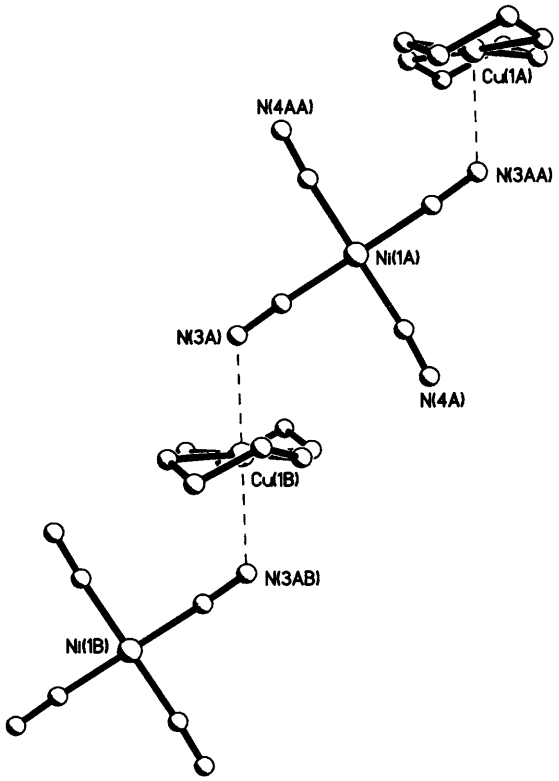

The angles in this structure were all within the expected range for the geometry (Table 3). Both fragments had square planar or distorted square planar geometry.

Table 3: Selected bond angles in the crystal structure of 8

Bonds	Angles (°)
N(1)–Cu(1)–N(2)	84.56 (6)
C(2)–N(2)–Cu(1)	108.78 (10)
N(2)–C(2)–C(1)	107.74 (12)
N(1)–Cu(1)–N(1A)	180.00 (1)
C(3)–Ni(1)–C(4)	88.02 (6)
N(3)–C(3)–Ni(1)	176.82 (13)
C(4)–Ni(1)–C(4B)	180.00 (1)

3.222 Crystal structure of $[Ni(en)_3][Ni(CN)_4].H_2O$ (7)

The second single crystal structure successfully determined with en ligands was $[Ni(en)_3][Ni(CN)_4].H_2O$. An orthorhombic pink plate had the space group (Pbca) and gave good quality data (R_1 = 0.0203) (Figure 9). This crystal confirmed the elemental analysis and the complexing of three bidentate ligands. Although we hoped to form the single en ligand complex, the excess of en ligand present allowed the formation of this stable compound.

Figure 9: Crystal structure of $[Ni(en)_3][Ni(CN)_4].H_2O$ (7)

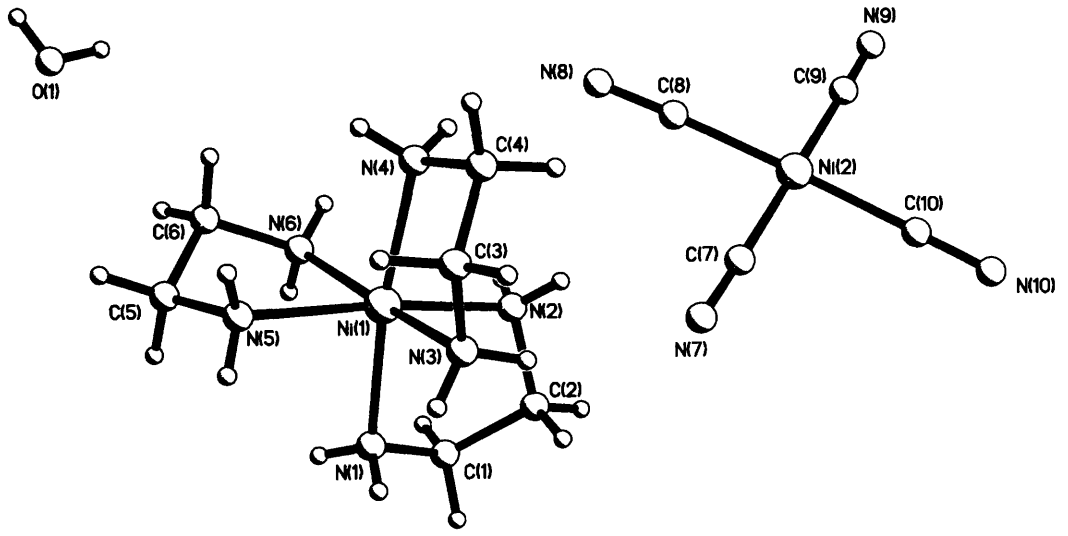

As with the structure of $[Cu(en)_2][Ni(CN)_4]$ (**8**), the en ligands are all equivalent and the $[Ni(CN)_4]^{2-}$ fragment was virtually identical to the values of the previous structure. The

$[Ni(en)_3]^{2+}$ centre is a distorted octahedral (N(3)–Ni(1)–N(6)) 171.34(4)°. This structure was previous determined by another research group [56] and a comparison of the two show excellent correlation, even though their data was collected at room temperature and ours at 150 K.

3.23 Thermal Gravimetric Analysis (TGA) and Differential Scanning Calorimetry (DSC).

Thermal analysis is a common technique used for inclusion compounds such as Hoffmann-type compounds. The two processes used were thermal gravimetric analysis (TGA) and differential scanning calorimetry (DSC). The TGA process involves recording the mass of a sample over a period of time as it is heated in a controlled atmosphere. This allows identification of the phase changes and decomposition of the compound. With good quality samples, fragments lost can be identified and this possibly leads to the determination of decomposition mechanisms. The DSC technique records discrepancies in heat flow into a sample and an inert reference, while they are concurrently heated. This data aids understanding of physical and chemical changes through the change in heat (gained or lost).

All the cyanide complexes were tested using TGA and DSC in order to study the binding of amines and reconcile structural and analytical data. The temperature range used was 25 - 500°C with a ramp range of 10 K/min. The results for the ammonia compounds (**1-4a-b**) showed good correlation between the calculated and observed mass losses. In some cases, due to the gradual sloping of the TGA curve, highly accurate values were more difficult to ascertain but the values were generally within the expected range.

Comparison of the TGA data for compounds $[Cd(NH_3)_2][Ni(CN)_4]$ (**1a** and **1b**) showed good agreement with the calculated loss of 2 NH_3 molecules equalling 11 %. Both traces showed broad curves between 120 – 180°C, equalling 12 % and 15 % respectively. Interestingly, **1b** showed a second loss of 21 % between 320 – 380°C with a large exothermic DSC reading not observed for **1a**. This peak has been attributed to the loss of 3CN ligands from the $[Ni(CN)_4]^{2-}$ fragment of the compound with an enthalpy value of 1025 ± 5 J/g (Graph 1).

Graph 1: TGA (red) and DSC (blue) curves for 1b $[Cd(NH_3)_2][Ni(CN)_4]$

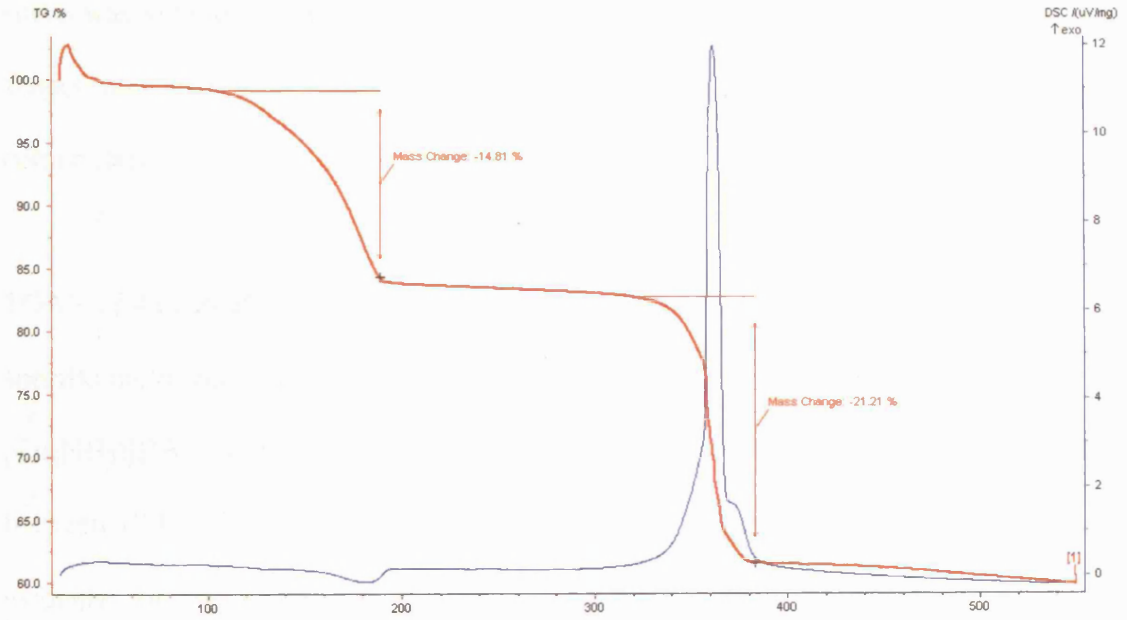

The TGA of **2b**, the zinc compound, whose elemental analysis data did not confirm the expected formulation, did however exhibit the correct loss of 14 % compared to the calculated loss of 13 %. This graph has a broad curve between 200 – 300°C with a considerable endothermic DSC curve valuing –30.42 ± 5 J/g. This would indicate that the proposed complex was formed and that the elemental analysis collected was incorrect.

TGAs' for the complexes $[Ni(NH_3)_2][Ni(CN)_4]$ (**3a** and **3b**) showed very good correlation between the calculated and observed losses. Both compounds were expected to lose 2 NH_3 equalling 13 %. For **3a**, a loss of 13 % was observed over two broad curves with a very small endothermic DSC curve. A second sharp loss of 32 % was observed at 400°C, which accounts for the loss of 3 CN ligands. This loss had a sharp exothermic peak in the DSC curve with an enthalpy value of 1164 ± 5 J/g. Compound **3b** showed the same two-stage curve with a loss of 15 % (2 NH_3) and 32 %, attributed to the loss of 3 CN ligands. The enthalpy value calculated from the DSC curve was similar to **3a**. Overall, there was excellent correlation between the graphs shapes and values extracted from them, confirming the proposed formula of the compounds.

TGA's of **4a** and **4b** were much more complicated and therefore more difficult to assign specific molecular loss. The elemental analysis data for **4a** suggested the formula to be $[Cu(NH_3)][Ni(CN)_4]$, therefore loss of NH_3 would be 7 %. The broad curve observed between 180 – 250°C of 18 % and with two stages suggested a loss of 2 NH_3. Further evidence for this was the endothermic DSC curve with an enthalpy of –13 ± 5 J/g. Based on the elemental analysis results, the expected formula for **4b** is $[Cu(H_2O)][Ni(CN)_4]$. Careful consideration of the TGA suggested a loss of 15 % over two stages between 125 – 350°C. This could possibly represent the loss of H_2O molecule and NH_3 or possibly 2 NH_3 but it is not possible to assign accurate molecular loss.

Most of the TGA data agreed well with the calculated values for the compounds. There were some that differed and the author has provided speculative opinion. One of the

possible reasons behind the discrepancy could be the calculated values were based on elemental analysis data. Elemental analysis samples were exposed to air for a significant period of time in which weakly bound amines could possibly have been lost, therefore giving different elemental percentages. The samples prepared for TGA analysis were taken from solution just before the experiment and atmospheric exposure kept to a minimum, therefore reducing amine loss and maintaining a true composite compound.

The TGA and DSC results for the en compounds (**5-8**) were all as expected with the approximate loss of molecules attributable to specific en ligands. The formula for **5** was proposed to be $[Cd(en)][Ni(CN)_4]$ based on elemental analysis data and therefore calculated a loss of 17 % for the en ligand. The graph displayed solvent loss initially due to a wetter sample followed by a loss of 17 % over the temperature range of 300 - 380 °C representing the en ligand loss with a large endothermic DSC peak of 74 ± 5 J/g (Graph 2).

Graph 2: TGA and DSC curves for 1c $[Cd(en)_2][Ni(CN)_4]$

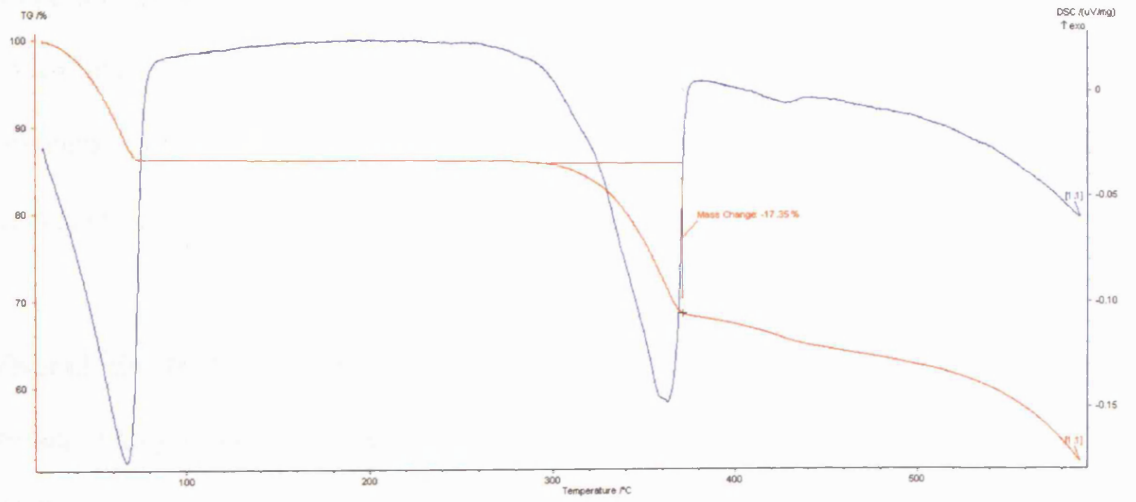

The elemental analysis data correctly identified **6** as $[Zn(en)_2][Ni(CN)_4]$ so the expected percentage loss would be 35 % (2 en ligands). The TGA graph showed a broad loss of 37 % over the temperature range of 200 – 300°C. This accurately accounted for the loss of two ligands with an endothermic DSC curve and an enthalpy value of –610 ± 5 J/g.

Compound **7** had the formula $[Ni(en)_3][Ni(CN)_4]$ so a total loss of 45 % was expected. The TGA graph showed three distinct curves, each approximately 15 %, which equalled 3 en ligands over a temperature period of 100 – 350°C. Each loss was accompanied by an endothermic DSC curve dip with enthalpy values of –15 ± 5 J/g, -15 ± 5 J/g and –93 ± 5 J/g, representing each en ligand, with the last en ligand requiring a larger amount of energy to leave the nickel ion. In addition to this, there was a peak at 375°C with a loss of 25 % and a large exothermic DSC curve. The enthalpy value for this peak equalled 1103 ± 5 J/g and correlated to the loss of 4 CN ligands (26%).

Finally, $[Cu(en)_2][Ni(CN)_4]$ (**8**) had 2 en ligands that accounted for a loss of 16 % each which was observed in the TGA graph in two different stages at 200°C and 280°C. The value for the first stage was 16 % and the second stage was 14 %, which was slightly lower than expected due to the broadest of the curve, therefore making accurate assignment difficult. Both these stages were accompanied with endothermic DSC curves in the range of –28 ± 5 J/g and –30 ± 5 J/g.

Overall, the TGA graphs have showed the expected percentage loss in the compounds tested. Many values recorded were highly accurate with other less so due to the sloping of the curve. It is clear that the losses of ammonia and en ligands are endothermic reactions with an average enthalpy value of –28 ± 5 J/g and in the temperature range

150 – 350°C. Some compounds have displayed the loss of cyanide ligands from the tetracyanonickelate fragment in the higher temperature range of 350 - 450°C with exothermic DSC peaks as expected due to the expected strong nature of M-CN bonds. This was clearly demonstrated by the large enthalpy values approximately 1000 ± 5 J/g.

3.24 Polymerisation Results

All the compounds were tested using the standard procedure as described in experimental section 3.43. An important factor to be considered when testing the catalytic properties of these compounds was the presence of amine (ammonia or ethylenediamine) found in excess as both ligands and solvent in crystal formation. The excess of these basic molecules could potentially polymerise PO *via* a base catalysed mechanism, giving false evidence for the compounds in question. To overcome this, the crystalline compounds were removed from the solution, dried on filter paper, washed with ethyl diether and finally dried in a fumehood. This drying system was to remove any guest molecules of amine so that only the compound was only reacted with PO. Unfortunately, all the compounds tested showed no evidence of polymerisation.

3.3 Conclusions

Following the synthesis outlined for Hoffmann-type compounds, ten compounds were successfully formed with various transition metals with two different amines (ammonia and ethylenediamine). The compounds formed a range of crystals, differing in colour, shape and size and were characterised using elemental analysis, IR, TGA, DSC and X-ray diffraction. Large numbers of the synthesised compounds were the anticipated compound with some variation in the number of ammonia and ethylenediamine ligands.

Three single crystal structures were attained with the characterisation of the new compound, $[Cu(NH_3)_4][Ni(CN)_4]$.

The characterisation of the compounds showed the appropriate peaks in the IR and elemental analysis percentages. The thermal analysis of the compounds by TGA and DSC allowed a greater understanding of the compounds and their constituents. In many cases, the mass loss observed agreed with the calculated loss. The amine losses were accompanied by endothermic DSC curves while the cadmium and nickel compounds displayed cyanide ligand losses at higher temperatures with large exothermic values. In some of the compounds, the TGA graphs have shown the desired number of amines and the appropriate loss, even though the elemental analysis data does not indicate this. It is proposed that some elemental analysis data may not accurately represent the compounds as the data was recorded after atmospheric exposure and potentially loss of weakly bound ligands, therefore offering a plausible explanation for the correct observation of TGA values.

All the compounds were tested for polymerisation using the standard method. Unfortunately, all the compounds were found to be inactive catalysts for the ROP of PO. These compounds have similar networks of DMC compounds but due to their apparent crystalline nature maybe inactive as catalysts. A possible avenue of further research would be to attempt to form these networks with the same glyme products that are used in DMC compounds. These may prepare the metal centres for coordination with the epoxide and polymerisation.

3.4 Experimental

All IR spectra were recorded using a Shimaduz FT-IR 8700 spectrometer, operating in the region of 4000 - 400 cm^{-1}. The IR samples were prepared using KBr powder to make discs or as neat samples between NaCl plates. The Elemental Analysis (elemental analysis) was carried out using Elemental Analyzer (CE-440) (Exeter Analytical Inc). The instrument used for thermal analysis was the Netzsch Jupiter.

3.41 Synthesis of compounds with ammonia.

*3.411 Synthesis of **1-4a** using ammonia solution (Method A)*

Synthesis of **1a**: ammonia solution (35%) (5.00 ml, 30.00 mmol) was added to an aqueous solution (50 ml) of $CdCl_2$ (0.92 g, 5.00 mmol) in a conical flask. An aqueous solution (50 ml) of $K_2Ni(CN)_4.2H_2O$ (1.20 g, 5.00 mmol) was added to the flask and a cork stopper sealed the flask. This was left at room temperature for a period of one to three months to produce shiny yellow fine needle crystals. IR (KBr) *v*: 3630m, 3377br, 3246m, 2139s, 1605m, 1190m cm^{-1}; anal. calc. for $C_4H_6N_6Cd_1Ni_1$: C, 15.54; H, 1.96; N, 27.18. Found C, 15.37; H, 1.62; N, 25.02.

Synthesis of **2a:** failed to form crystals.

Synthesis of **3a**: follow experimental above with ammonia solution (35%) (5.00 ml, 30.00 mmol), $NiCl_2.6H_2O$ (0.74 g, 5.00 mmol) and $K_2Ni(CN)_4.2H_2O$ (1.20 g, 5.00 mmol) to give fluffy purple precipitate. IR (KBr) *v*: 3620m, 3373m, 3300m, 2625br, 2160s, 1609m, 1225br cm^{-1}; anal. calc. for $C_4H_6N_6Ni_2$: C, 18.80; H, 2.37; N, 32.89. Found C, 18.28; H, 2.21; N, 30.46.

Synthesis of **4a**: follow experimental above with ammonia solution (35%) (5.00 ml, 30.00 mmol), $CuCl_2$ (0.85 g, 5.00 mmol) and $K_2Ni(CN)_4.2H_2O$ (1.20 g, 5.00 mmol) to give dark blue small rod-like crystals. IR (KBr) *v*: 3366m, 3287s, 2174s, 2145s, 2122, 1605br, 1238s, 1225s cm^{-1}; anal. calc. for $C_4H_6N_6Cu_1Ni_1$: C, 18.45; H, 2.34; N, 32.28. Found C, 18.96; H, 1.46; N, 28.12. Recalc. $C_4H_3N_5Cu_1Ni_1$: C, 29.46; H, 3.58; N, 33.19.

*3.412 Synthesis of **1-4b** using liquid ammonia (Method B)*

Synthesis of **1b**: liquid ammonia (10.00 ml, 30.00 mmol) was added to an aqueous solution (50 ml) of $CdCl_2$ (0.92 g, 5.00 mmol) in a conical flask. An aqueous solution (50 ml) of $K_2Ni(CN)_4.2H_2O$ (1.20 g, 5.00 mmol) was added to the flask and a cork stopper sealed the flask. This was left at room temperature for a period of a month to produce yellow-orange needle crystals. IR (KBr) *v*: 3379m, 3288s, 2145s, 1593br, 1190m cm^{-1}; anal. calc. for $C_4H_6N_6Cd_1Ni_1$: C, 15.54; H, 1.96; N, 27.18. Found C, 15.56; H, 1.72; N, 25.61.

Synthesis of **2b**: follow experimental above with liquid ammonia (10.00 ml, 30.00 mmol), $ZnCl_2$ (0.92 g, 5.00 mmol) and $K_2Ni(CN)_4.2H_2O$ (1.20 g, 5.00 mmol) to give golden brown feather needles. IR (KBr) *v*: 3273br, 2193s, 1506br, 1394br, 1047m, 953br cm^{-1}; anal. calc. for $C_4H_6N_6Zn_1Ni_1$: C, 18.32; H, 2.31; N, 32.05. Found C, 16.48; H, 0.44; N, 18.02.

Synthesis of **3b**: follow experimental above with liquid ammonia (10.00 ml, 30.00 mmol), $NiCl_2.6H_2O$ (0.74 g, 5.00 mmol) and $K_2Ni(CN)_4.2H_2O$ (1.20 g, 5.00 mmol) to give fine dark blue-green needles. IR (KBr) *v*: 3371m, 3302s, 2160s, 1607m, 1223br

cm^{-1}; anal. calc. for $C_4H_6N_6Ni_2$: C, 18.80; H, 2.37; N, 32.89. Found C, 18.22; H, 2.09; N, 30.06.

Synthesis of **4b**: follow experimental above with liquid ammonia (10.00 ml, 30.00 mmol), $CuCl_2$ (0.85 g, 5.00 mmol) and $K_2Ni(CN)_4.2H_2O$ (1.20 g, 5.00 mmol) to give blue fine needle crystals. IR (KBr) *v*: 3369m, 3277s, 2172s, 2152s, 2127s, 1603br, 1184m cm^{-1}; anal. calc. for $C_4H_6N_6Cu_1Ni_1$: C, 18.45; H, 2.32; N, 32.28. Found C, 18.90; H, 0.73; N, 23.71. Recalc. $C_4H_2N_4O_1Cu_1Ni_1$: C, 18.39; H, 0.69; N, 19.11.

*3.42 Synthesis of **5-8** using ethylenediamine*

Synthesis of **5**: ethylenediamine (0.90 g, 15.00 mmol) was added to an aqueous solution (50 ml) of $CdCl_2$ (0.92 g, 5.00 mmol) in a conical flask. An aqueous solution (50 ml) of potassium tetracyanonickelate dihydrate ($K_2Ni(CN)_4.2H_2O$) (1.20 g, 5.00 mmol) was added to the flask and a cork stopper sealed the flask. This was left at room temperature for a period of one to three months to produce cream precipitate. IR (KBr) *v*: 3371s, 3310s, 2976m, 2916s, 2872s, 2152m, 1591m, 1452s, 1315m, 1115m, 1016m, 993m, 955m cm^{-1}; anal. calc. for $C_6H_6N_6Cd_1Ni_1$: C, 21.49; H, 2.41; N, 25.07. Found C, 21.61; H, 2.48; N, 26.41.

Synthesis of **6**: follow experimental above with ethylenediamine (0.90 g, 15.00 mmol), $ZnCl_2$ (0.68 g, 5.00 mmol) and $K_2Ni(CN)_4.2H_2O$ (1.20 g, 5.00 mmol) to give orange needle crystals. IR (KBr) *v*: 3337m, 3286s, 2959m, 2912m, 2868m, 2139s, 2114s, 1609m, 1589m, 1446m, 1329s, 1277s, 1123m, 1030s, 993m, 962m cm^{-1}; anal. calc. for $C_6H_6N_6Zn_1Ni_1$: C, 25.18; H, 2.11; N, 29.36. Found C, 27.67; H, 4.65; N, 32.04. Recalc. $C_8H_{12}N_8Zn_1Ni_1$ C, 27.74; H, 4.07; N, 32.35.

Synthesis of **7**: follow experimental above with ethylenediamine ((0.90 g, 15.00 mmol), $NiCl_2.6H_2O$ (0.74 g, 5.00 mmol) and $K_2Ni(CN)_4.2H_2O$ (1.20 g, 5.00 mmol) to give dark pink square plate crystals. IR (KBr) *v*: 3344s, 3315s, 3294s, 3267s, 2951m, 2885s, 2120s, 2112s, 1578m, 1456m, 1271m, 1092m, 1016m, 966m cm^{-1}; anal. calc. for $C_6H_6N_6Ni_2$: C, 25.78; H, 2.16; N, 30.06. Found C, 28.57; H, 6.34; N, 33.16. Recalc. $C_8H_{12}N_8Ni_1$: C, 29.46; H, 3.58; N, 33.19.

Synthesis of **8**: follow experimental above with ethylenediamine (0.90 g, 15.00 mmol), $CuCl_2$ (0.85 g, 5.00 mmol) and $K_2Ni(CN)_4.2H_2O$ (1.20 g, 5.00 mmol) to give thick purple rod crystals. IR (KBr) *v*: 3310s, 3279m, 3161m, 2964m, 2878m, 2116s, 1597br, 1450m, 1167m, 1092m, 1034m, 974m cm^{-1}; anal. calc. for $C_6H_6N_6Cu_1Ni_1$: C, 25.34; H, 2.13; N, 29.55. Found C, 27.69; H, 4.70; N, 32.03. Recalc. $C_8H_{12}N_8Cu_1Ni_1$: C, 29.46; H, 3.58; N, 33.19.

3.43 Experimental Procedure for Polymerisation Reactions

Preparation of the cyanide compounds for PO polymerisation involved removing the crystalline compound from the solution, dried on filter paper, washed with ethyl diether and finally dried in a fumehood. This drying system was to remove any guest molecules of ammonia so that only the compound was reacted with PO. The standard testing procedure followed to ensure consistency in testing.

Standard PO testing procedure

Small-scale test tube reactions were undertaken in a fumehood as PO is toxic. The catalyst (approximately 0.01-0.05 g) was placed in a test tube with PO (2 ml), sealed and stirred for 17 h. with a magnetic stirrer. Each catalyst was tested twice, once as

above and the other with EtOH (2 ml) to initiate the reaction. The product was then dissolved in dichloromethane (DCM) (2 ml) and placed on the vacuum line for 10 min. to remove residual PO. The product was characterised using NMR and IR and the degree of polymerisation if any, was recorded. Unfortunately, the results showed there was no evidence that PO was polymerised.

3.5 References

[1] J. S. Miller, *MRS Bulletin* **2000**, *25*, 60.
[2] K. R. Dunbar, R. A. Heintz, in *Progress in Inorganic Chemistry, Vol. 45*, **1997**, pp. 283.
[3] R. Uson, J. Fornies, M. A. Uson, E. Lalinde, *Journal of Organometallic Chemistry* **1980**, *185*, 359.
[4] K. Nakamoto, *Infrared and Raman Spectra of Inorganic and Cordination Compounds*, 3rd ed., Wiley, New York, **1978**.
[5] A. M. Golub, H. K. H. Kohler, V. V. Skopenko, *Chemistry of Pseudo-halide, Vol. 2*, Pergamon, New York, **1987**.
[6] D. F. Shriver, S. A. Shriver, S. E. Anderson, *Inorganic Chemistry* **1965**, *4*, 725.
[7] D. Britton, *Perspectives in Structural Chemistry, Vol. 1*, Wiley, New York, **1967**.
[8] J. L. Hoard, *Zeitschrift fuer Kristallographie* **1933**, *84*, 231.
[9] A. Rosenzweig, D. T. Cromer, *Acta Crystallographica* **1959**, *12*, 709.
[10] G. Thiele, R. Bauer, D. Messer, *Naturwissenschaften* **1974**, *61*, 215.
[11] A. G. Sharpe, *Comprehensive Coordination Chemistry, Vol. 2*, Pergamon, New York, **1987**.
[12] Bertinot.C, Bertinot.A, *Acta Crystallographica Section B-Structural Crystallography and Crystal Chemistry* **1970**, *B 26*, 422.
[13] K. Krogmann, D. Stephan, *Zeitschrift Fur Anorganische Und Allgemeine Chemie* **1968**, *362*, 290.
[14] J. Ledent, *Bulletin de la Societe Royale des Sciences de Liege* **1972**, *41*, 537.
[15] M. Ruegg, A. Ludi, *Theoretica Chimica Acta* **1971**, *20*, 193.
[16] K. N. Raymond, P. W. Corfield, J. A. Ibers, *Inorganic Chemistry* **1968**, *7*, 1362.
[17] A. Terzis, K. N. Raymond, T. G. Spiro, *Inorganic Chemistry* **1970**, *9*, 2415.
[18] L. J. Basile, J. R. Ferraro, M. Choca, K. Nakamoto, *Inorganic Chemistry* **1974**, *13*, 496.
[19] A. Tullberg, Vannerbe.Ng, *Acta Chemica Scandinavica Series A-Physical and Inorganic Chemistry* **1974**, *A 28*, 551.
[20] M. P. Gupta, H. J. Milledge, A. E. McCarthy, *Acta Crystallographica Section B-Structural Science* **1974**, *B 30*, 656.
[21] H. Siebert, A. Siebert, *Zeitschrift Fur Anorganische Und Allgemeine Chemie* **1970**, *378*, 160.
[22] R. W. G. Wyckoff, *Crystal Structures, Vol. 3*, 2nd ed., Interscience, New York, **1965**.

[23] R. L. R. Towns, R. A. Levenson, *Journal of the American Chemical Society* **1972**, *94*, 4345.
[24] R. A. Levenson, R. L. R. Towns, *Inorganic Chemistry* **1974**, *13*, 105.
[25] M. G. B. Drew, P. C. H. Mitchell, C. F. Pygall, *Journal of the Chemical Society-Dalton Transactions* **1977**, 1071.
[26] J. M. Manoli, C. Potvin, J. M. Bregeault, W. P. Griffith, *Journal of the Chemical Society-Dalton Transactions* **1980**, 192.
[27] W. Jacob, Z. Jacob, *Roczniki Chem.* **1962**, *36*, 601.
[28] B. J. Corden, J. A. Cunningh, R. Eisenber, *Inorganic Chemistry* **1970**, *9*, 356.
[29] L. D. C. Bok, J. G. Leipoldt, S. S. Basson, *Acta Crystallographica Section B-Structural Crystallography and Crystal Chemistry* **1970**, *B 26*, 684.
[30] S. S. Basson, J. G. Leipoldt, L. D. C. Bok, J. S. Vanvollenhoven, P. J. Cilliers, *Acta Crystallographica Section B-Structural Science* **1980**, *36*, 1765.
[31] K. A. Hofmann, F. Hoechtlen, *Berichte der Deutschen Chemischen Gesellschaft* **1903**, *36*, 1149.
[32] K. A. Hofmann, H. Arnoldi, *Berichte der Deutschen Chemischen Gesellschaft* **1906**, *39*, 339.
[33] H. M. Powell, J. H. Rayner, *Nature* **1949**, *163*, 566.
[34] J. H. Rayner, H. M. Powell, *Journal of the Chemical Society* **1952**, 319.
[35] J. H. Rayner, H. M. Powell, *Journal of the Chemical Society* **1958**, 3412.
[36] A. Ludi, R. Hugi, *Helvetica Chimica Acta* **1967**, *50*, 1283.
[37] Y. Mathey, C. Mazieres, *Canadian Journal of Chemistry-Revue Canadienne De Chimie* **1974**, *52*, 3637.
[38] R. Baur, G. Schwarzenbach, *Helvetica Chimica Acta* **1960**, *43*, 842.
[39] T. Iwamoto, T. Miyoshi, T. Miyamoto, Y. Sasaki, S. Fujiwara, *Bulletin of the Chemical Society of Japan* **1967**, *40*, 1174.
[40] T. Iwamoto, T. Nakano, M. Morita, T. Miyoshi, T. Miyamoto, Y. Sasaki, *Inorganica Chimica Acta* **1968**, *2*, 313.
[41] T. Iwamoto, *Inclusion Compounds, Vol. 1*, Academic, London, **1984**.
[42] T. Iwamoto, *Inclusion Compounds, Vol. 5*, Oxford University Press, Oxford, **1991**.
[43] M. Hashimoto, T. Iwamoto, *Chemistry Letters* **1990**, 1531.
[44] T. Hasegawa, T. Iwamoto, *Journal of Inclusion Phenomena* **1988**, *6*, 549.
[45] S. I. Nishikiori, T. Iwamoto, *Inorganic Chemistry* **1986**, *25*, 788.
[46] S. I. Nishikiori, T. Iwamoto, Y. Yoshino, *Bulletin of the Chemical Society of Japan* **1980**, *53*, 2236.
[47] M. Hashimoto, T. Hasegawa, H. Ichida, T. Iwamoto, *Chemistry Letters* **1989**, 1387.
[48] T. Iwamoto, M. Kiyoki, Y. Ohtsu, Y. Takeshigekato, *Bulletin of the Chemical Society of Japan* **1978**, *51*, 488.
[49] T. Nakano, T. Miyoshi, T. Iwamoto, Y. Sasaki, *Bulletin of the Chemical Society of Japan* **1967**, *40*, 1297.
[50] K. M. Park, R. Kuroda, T. Iwamoto, *Angewandte Chemie* **1993**, *105*, 939.
[51] C. Janiak, H. P. Wu, P. Klufers, P. Mayer, *Acta Crystallographica Section C-Crystal Structure Communications* **1999**, *55*, 1966.
[52] J. Cernak, K. A. Abboud, *Acta Crystallographica Section C-Crystal Structure Communications* **2002**, *58*, m167.
[53] J. Lokaj, K. Gyerova, A. Sopkova, J. Sivy, V. Kettmann, V. Vrabel, *Acta Crystallographica Section C-Crystal Structure Communications* **1991**, *47*, 2447.

[54] Z. Smekal, Z. Travnicek, J. Mrozinski, J. Marek, *Inorganic Chemistry Communications* **2003**, *6*, 1395.
[55] H. Imai, K. Inoue, M. Ohba, M. Okawa, K. Kikuchi, *Synthetic Metals* **2003**, *137*, 919.
[56] J. Cernak, J. Chomic, D. Baloghova, M. Dunajjurco, *Acta Crystallographica Section C-Crystal Structure Communications* **1988**, *44*, 1902.

Chapter 4

Dithiocarbamates

4.1 Introduction

Sulfur-compounds have been used to form a wealth of useful ligands and complexes. Key examples are thiolate (RS^-) and dithiolate compounds that have electron-rich sulfur atoms able to form bonds with various organic and metallic groups. Thiolates have been used in various reactions due to their ability to bind in a wide range of geometries [1, 2]. The main disadvantage of using thiolates is their propensity to oxidise to the corresponding disulfur compound. This is overcome with the use of hindered thiolates and these stabilise highly reactive, coordinatively unsaturated complexes [3]. When such thiolates are bound to a metal centre, their ability to act as both π-acceptors and π-donors allows a range of metals to be used and results in a stabilising effect on the metal centre.

Potentially chelating 1, 1-dithiolate compounds have been widely investigated and assortments of ligands designed (Figure 1). One of the most versatile ligands of this type is the dithiocarbamate ($R_2NCS_2^-$). First prepared over 100 years ago, they have been the subject of numerous reviews [4, 5] and patents [6-8] due to their utility as ligands and diverse applications.

Figure 1: Selection of 1, 1-dithiolates ligands [3]

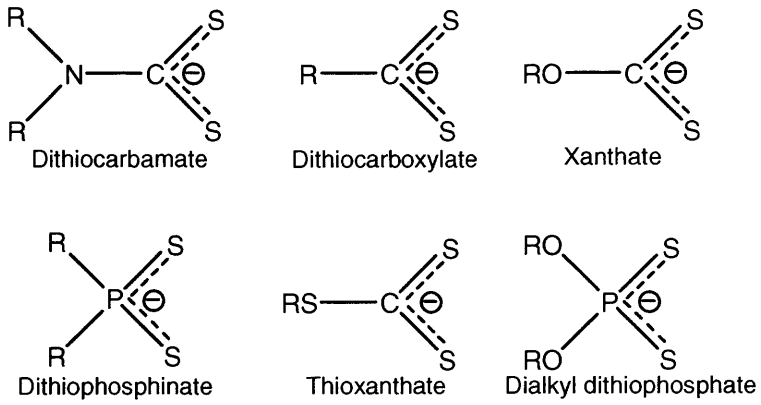

For example, metal dithiocarbamates have been used as agricultural fungicides[9] and pesticides[10] including Ziram™ [$Zn(S_2CNMe_2)_2$], Feram™ [$Fe(S_2CNMe_2)_3$] and Nabam™ [$Na_2[S_2CNHCH_2CH_2NHCS_2]$]. Other uses are as accelerators in the vulcanisation of rubber[11], floatation agents and high-pressure lubricants.

Dithiocarbamates are generally formed by the reaction of primary or secondary amines with carbon disulfide in the presence of a base such as sodium or potassium hydroxide. A wide variety of stable dithiocarbamates can be formed from secondary amines and a number of solvents can be used including water, acetone, methanol and ethanol. The properties and reactivities of dithiocarbamate compounds can be fine-tuned by varying the R groups on the amine to form designer compounds.

Dithiocarbamates can adopt different resonance forms, which allow for monodentate and bidentate modes of linking. However, in by far the majority of complexes are bidentate and three resonance forms can be considered (Figure 2).

Figure 2: Resonance of Dithiocarbamate ligand

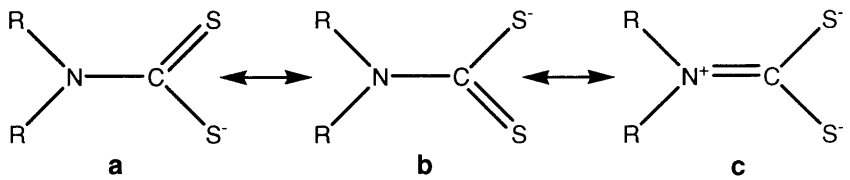

In line with the adoption of thiouride hybrid (resonance form **c**), the backbone nitrogen-carbon bond has double bond character when bound with a metal centre. Early research by Chatt *et al.*[12] showed with the use of IR studies that this C-N stretch is best described as a vibration of a polar $C=N^+$ bond (thiouride)[13].

Dithiocarbamates are often reacted with metal ions to form a variety of compounds with different geometries. This anionic ligand can stabilise a wide host of oxidation states and form a multitude of structures with different coordination geometries. In the solid state, bond lengths of 1.24 – 1.52 Å for C-N(R_2) and 1.52 – 1.82 Å for C-S are typical, with the angle at the central carbon ranging between 110.1 – 128.9°. IR spectroscopy is a useful characterisation tool, stretches for C-N(R_2) moiety coming at about 1500 ± 50 cm^{-1} and for C=S at 980 ± 50 cm^{-1}[14].

Alkali and alkaline earth metals can be used to form water-soluble dithiocarbamate salts. Transition metals, p-block metals and lanthanides can form metal bis- and tris-dithiocarbamates, which are ether and chloroform soluble (Figure 3). Nearly all main-group and transition metal dithiocarbamates are formed in good yields with metal-sulfur bonds in transition metal compounds being approximately equal and due to the stabilising affect of these ligands, high oxidation states are accessible (e.g. Fe^{IV}, Cu^{III}, Ni^{IV})[5].

Figure 3: Bis- and Tris-Metal dithiocarbamates (M = Transition metal; R = alkyl group)

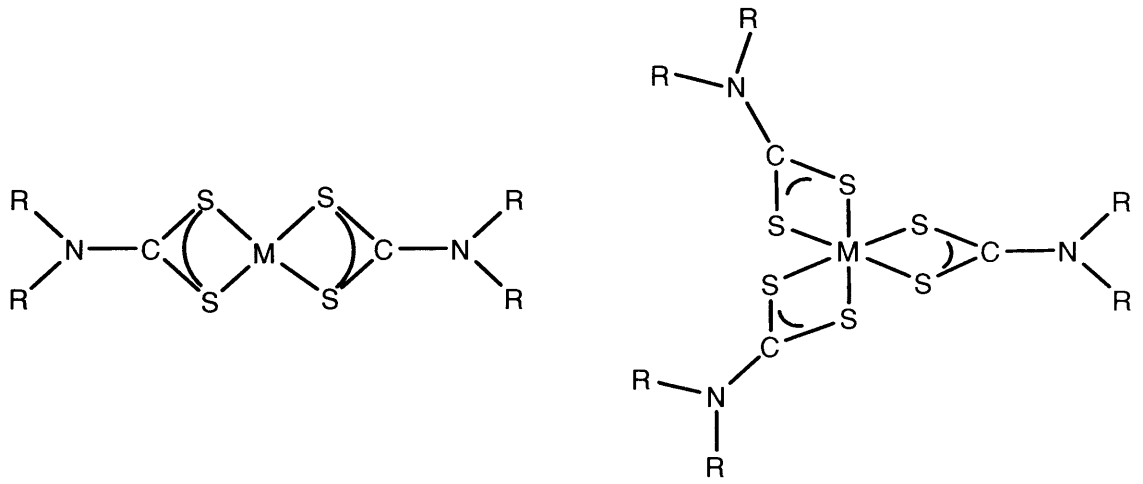

We were interested to see if dithiocarbamate complexes could act as catalysts for the ROP of epoxides. While the free dithiocarbamate ligand itself is expected to be a weak nucleophile (due to the soft sulfur centres and charge delocalisation) and generally bind strongly to the transition metal centre, we felt it important to determine the effect of the free ligand itself before proceeding with its complexes. A search of the literature revealed a short paper published by Cui *et al.*[15]. In their research, they investigated the formation of dithiocarbamates and their ability to ring-open epoxides. A number of epoxides and amines were tested and all were successful with the exception of aniline. The use of a three-membered ring epoxide with varying Y group (Y = Me, CH_2SMe, $CH_2OC_6H_4$-NO_2-*p*) appeared to have no effect on the ring-opening reaction, showing regioselective reactivity (Equation 1).

Equation 1. Reaction of secondary amine with carbon disulfide and epoxide[15]

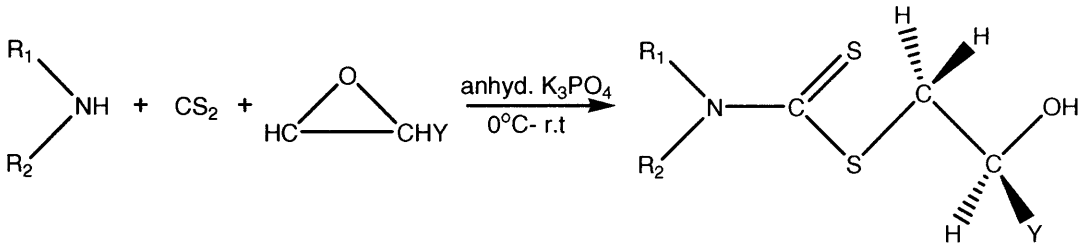

Y
Me
CH_2SMe
$CH_2OC_6H_4$-NO_2-*p*

They devised a one-pot synthesis where the amine was stirred with anhydrous potassium phosphate in acetone. The use of anhydrous potassium phosphate instead of potassium hydroxide allowed base-sensitive compounds to be used. Another reason for not using potassium hydroxide was that this base catalyses the ring-opening of PO, whereas potassium phosphate does not. This solution was stirred for 30 min. at 0°C to

room temperature, followed by the addition of carbon disulfide dropwise. To avoid amines reacting with the epoxides, the epoxide was added only once the dithiocarbamate was formed.

Our research aimed to investigate the ring-opening of epoxides and the formation of polymers. By first testing the free dithiocarbamate ligand with the PO monomer, we hoped to gain a greater understanding of their reactivity and apply this knowledge when considering metal complexes as catalysts. By using a range of amines to form the dithiocarbamates, we also considered the effects of R-groups on dithiocarbamate reactivities. Ultimately, we aspired to form a chain of propylene oxide units on the dithiocarbamate which could be cleaved at a later stage, cleanly synthesising poly(propylene oxide) polymer.

4.2 Results and Discussion

Following the synthetic protocol described by Cui *et al.*[15], numerous dithiocarbamate ligands were prepared by varying the R groups on the amines. The amine was stirred with anhydrous potassium phosphate in acetone at 0°C followed by the addition of carbon disulfide. This was stirred for 30 min. and then propylene oxide was added and stirred overnight at room temperature. The solution was reduced and purified with column chromatography yielding brightly coloured (yellow/orange) oils in moderate to high yields (48 - 91 %). The compounds were characterised using ^{1}H NMR, ^{13}C NMR, MS, IR spectroscopy, some elemental analysis and variable temperature NMR studies.

As previous discussed in Chapter 1, the propylene oxide (PO) epoxide has two different ring carbons, C_α and C_β (Figure 4). The ring-opening cleavage takes place at the least

sterically hindered carbon atom, C_β. Cui *et al.*[15] found that this phenomenon was followed in their reactions, being independent of the size of the Y group on the ring.

Figure 4: Structure of PO

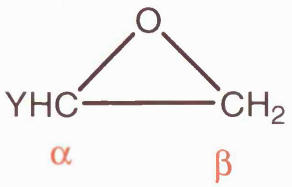

Y = Me

Using NMR speculative software (ChemDraw 8), we considered the possibility of ring-opening at C_α. Figures 5 and 6 showed the predicted ^1H NMR spectra of the product of ring-opening at C_β and at C_α respectively. Each proton environment is colour-coded to aid comprehension. In Figure 5, the methine H proton is downfield to due to its proximity to the more electronegative hydroxyl group whereas the methylene protons (H and H) were at higher field due to the less electronegative sulfur atoms. In contrast, in Figure 6, the methine and methylene protons are in opposite positions.

Figure 5: Speculative proton spectrum of the PO epoxide cleaved at C_β

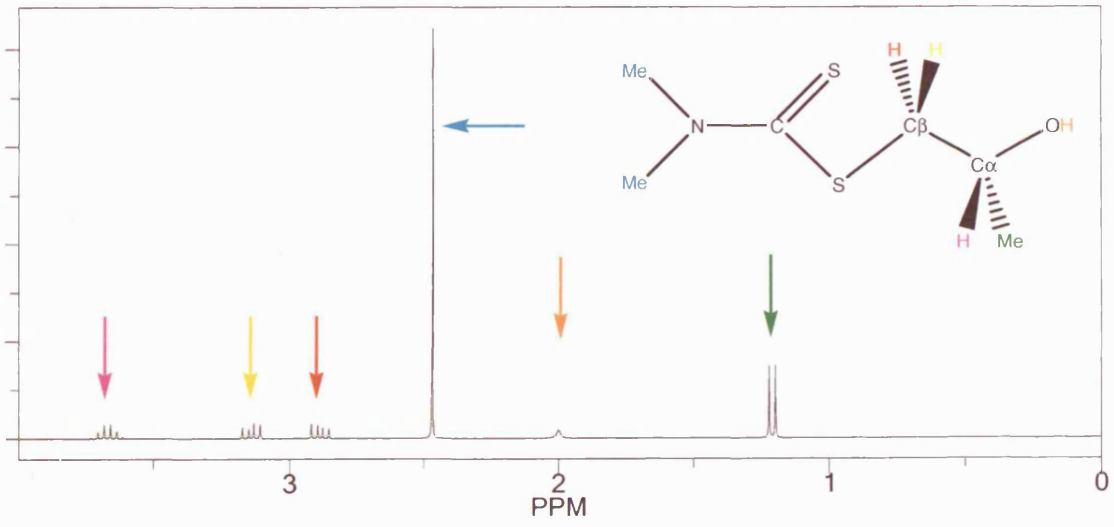

Figure 6: Speculative proton spectrum of the PO epoxide cleaved at C_α

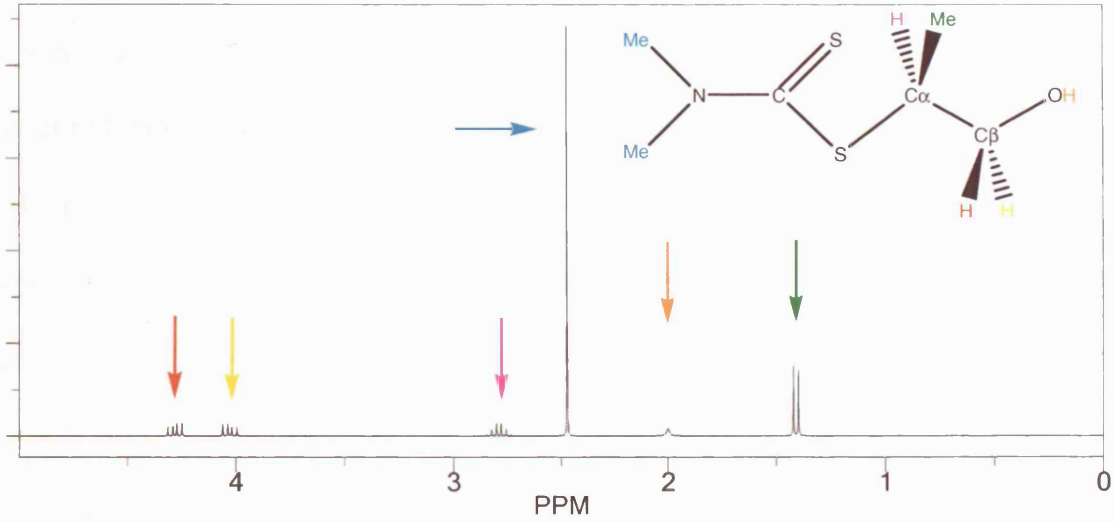

Using these predicted spectra to aid characterisation, we were able to confirm that the PO ring was opened at the C_β as all the spectra for synthesised compounds were similar to that in Figure 5, observing the least-hindered rule.

4.21 Simple Secondary Amines: a wide range of simple secondary amines was used to form dithiocarbamates that further reacted with the PO monomer (Figure 7). The ring-opened compounds (**1a-f**) formed have a chiral centre but as expected no enantioselectivity was observed.

Figure 7: Dithiocarbamates with ring-opened PO monomer attached

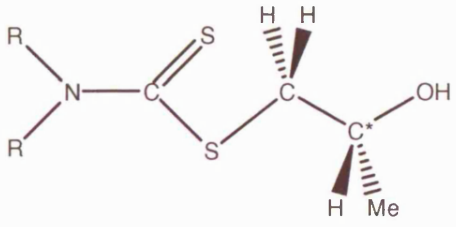

1a	R = Et
1b	Pr
1c	^{i}Pr
1d	Bu
1e	^{i}Bu
1f	CH_2Ph

There was little variation in the 400 MHz ^{1}H NMR spectra of the ring-opened PO group as a function of the R-group on the amine. For example, **1a** (R = Et), as the simplest system, produced a yellow/ orange oil (48 %). Using 400 MHz ^{1}H NMR, the PO fragment showed a clear multiplet at δ 4.13 assigned to the methine proton (Figure 8). The methylene protons appeared as two doublet of doublets at δ 3.36 (J 14.3, 7.2 Hz) and 3.66 (J 14.3, 3.8 Hz). The methyl group from PO was hidden under the methyl groups from the ethyl fragment to form a pseudo sextet at δ 1.27. The methylene groups of the ethyl appeared as two septets at δ 4.03 (J 6.9 Hz) and 3.82 (J 7.2 Hz). There was also a broad singlet at δ 2.64 to represent the proton of the hydroxyl group at the end of PO.

Figure 8: 400 MHz ^{1}H NMR spectrum of compound 1a

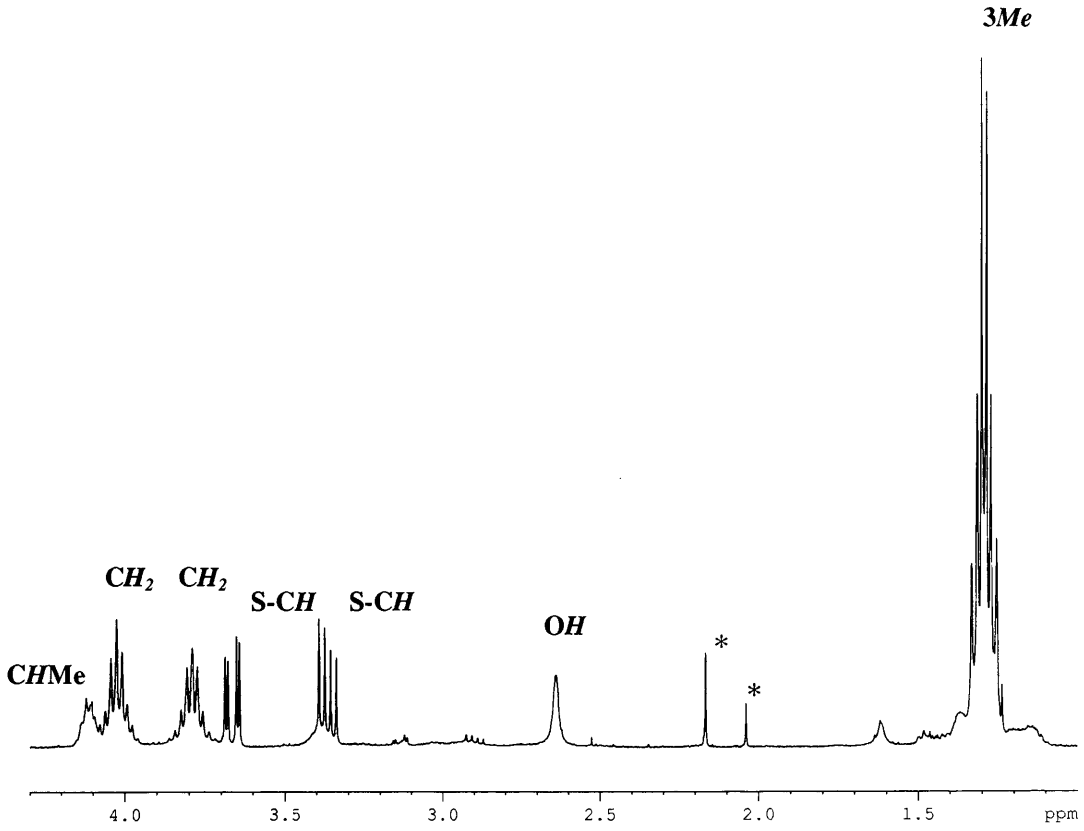

* known impurity

In order to further understand the unexpected pseudo sextet at high-field the sample was also examined at 300 MHz ^{1}H NMR. In this spectrum, the pseudo sextet formed at δ1.27, representing the PO methyl group and the two methyl groups from the ethyl amine, appeared as a sharp doublet (J 5.5 Hz) with broad triplets on either side.

Further, the methylene protons of the ethyl fragment, which appeared as two septets in the 400 MHz ^{1}H NMR spectrum were seen in the 300 MHz spectrum as two broad quartets. The seemingly unusual observation of the septets at 400 MHz is due to second order effects.

The ^{13}C NMR spectrum of **1a** was in accordance with the proposed structure, showing a total of eight separate carbon environments. The quaternary carbon appeared at δ 195.7, a characteristically low-field resonance as expected. For the ring-opened PO fragment, the methine carbon was observed at δ 66.8, the attached methylene carbon at δ 44.8 and the methyl group at δ 22.4. The methyl groups of the dithiocarbamate moiety were observed at δ 12.3 and 13.1 and the methylene carbons at δ 46.9 and 49.8. Other relevant spectroscopic data for this compound include the observation of a parent ion (*m/z* 222 (M^{+})) in the mass spectrum and IR stretches at 985 cm^{-1} and 1505 cm^{-1} assigned to ν(C-S) and ν(C=N) respectively. For the remaining compounds in this series, characterising data showed the distinctive peaks for the ring-opened PO and the respective alkyl groups.

The variation in the room temperature 300 and 400 MHz ^{1}H NMR spectra of **1a** is attributed to restricted rotation about the backbone C-N bond. This is well known for metal complexes but would not necessarily be expected in organic compounds. In order

to investigate the restricted rotation about the carbon-nitrogen bond of the dithiocarbamate moiety, a variable temperature ^{1}H NMR study was undertaken. Changing the temperature under which the proton data is collected changes the rate of proton fluxionality; increasing the temperature, increases the rate of C-N bond rotation. Using Equation 2, the free energy of activation, $\Delta G^{\ddagger}$ was calculated using $\Delta\nu$ and the temperature at which the peaks collapse into one broad peak (coalescence).

Equation 2: Free Energy of Activation ($\Delta G^{\ddagger}$)

$$\Delta G^{\ddagger} = -RT_c \, In\left[\frac{\pi h \Delta \upsilon}{\sqrt{2}kT_c}\right]$$

where $\Delta\upsilon$ = frequency separation (Hz)

and T_c = coalescence temperature of signals

^{1}H NMR spectra were collected in the temperature range 298 – 333 K, allowing an estimate $\Delta G^{\ddagger}$ to be made. At room temperature, rotation about the C-N bond is slow on the NMR timescale, therefore allowing the calculation of $\Delta\nu$. The coalescence temperature was estimated by observing the temperature at which the signals merge.

The stacked plot in Figure 9 shows the spectral changes for **1b** (dipropyldithiocarbamate complex) as a function of temperature. The PO proton environments vary little but the inequivalent N-CH_2 protons at δ 3.65 (partially hidden) and 3.89 collapse into one broad peak upon heating, coalescence occurring at approximately 333 K (Figure 9). The methyl groups of the propyl fragment also varied over this step temperature range from two overlapping triplets to a triplet, showing coalescence of the two end methyl groups at 318 K.

Figure 9: ^{1}H NMR variable temperature stack plot of 1b

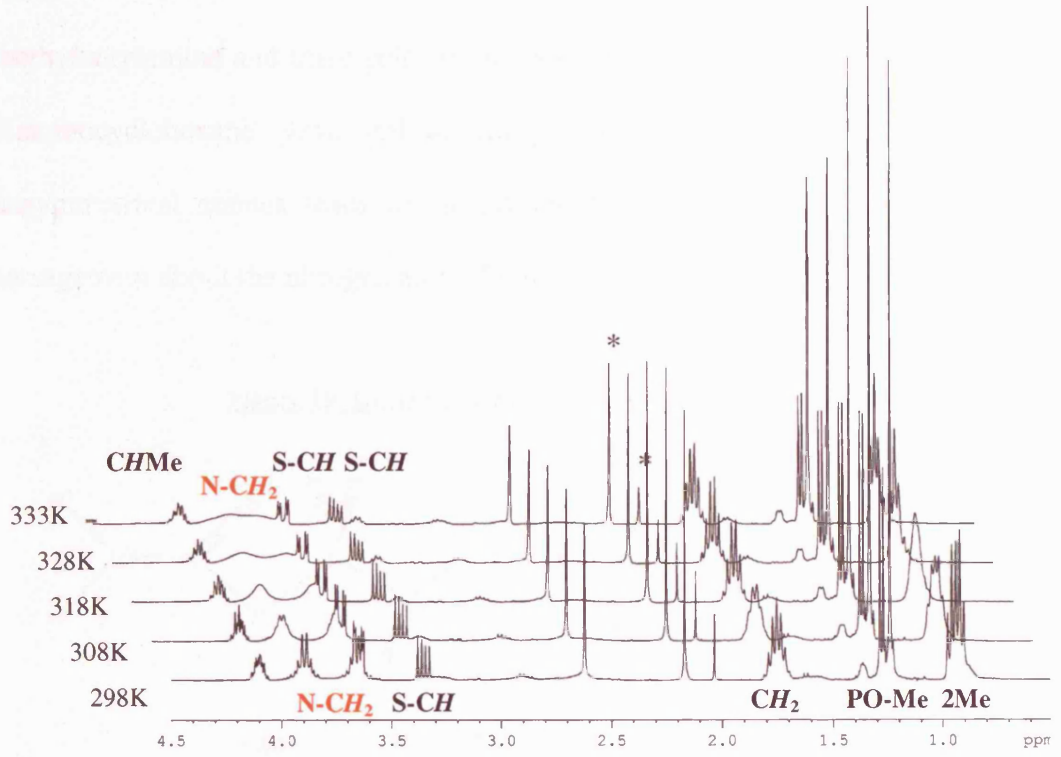

* known impurity

Applying Equation 2, free energies of activation were calculated to be in the range of 66 – 70 kJ mol^{-1} for the compounds in this series (Table 1). As the size of the R-group on the dithiocarbamate increases, the value of $\Delta G^{\ddagger}$ also appeared to increase, suggesting the energy required to facilitate rotation about the C-N was higher with increasing size of R-group.

Table 1: Coalescence temperatures and free energy of activation values

Linear Amine in Dithiocarbamate	Coalescence Temperature (T_c) (K)	$\Delta\nu$ (Hz)	$\Delta G^{\ddagger}$ (kJ mol^{-1}) ($\pm$ 1)
Diethylamine **(1a)**	328	94.66	66.0
Dipropylamine **(1b)**	333	89.43	67.2
Diisobutylamine **(1e)**	318	17.11	68.5

4.22 Unsymmetrical Amines: four unsymmetric amines were used to form dithiocarbamates with the attached PO monomer (**2a-d**). The secondary amine N-methylbutylamine and three primary amines (methylamine, hexylamine and *trans*-1,2-diaminocyclohexane) gave yellow/ orange oils in 20 - 90 % yields. The use of unsymmetrical amines leads to the possibility of a number of isomers due to the arrangement about the nitrogen atom (Figure 10).

Figure 10: Unsymmetric dithiocarbamates with PO (2a-d)

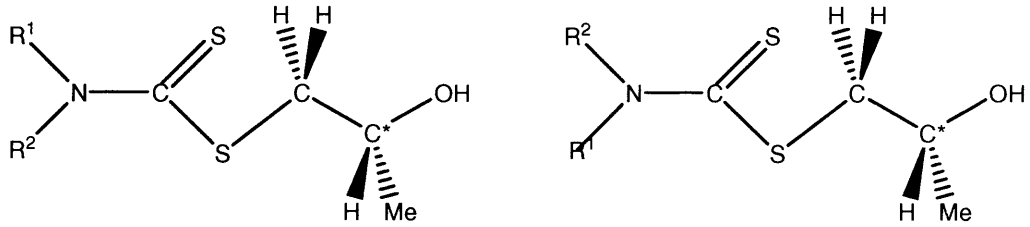

2a R^1 = Me
R^2 = Bu

2b R^1 = Me
R^2 = H

2c R^1 = C_6H_{13}
R^2 = H

2d R_1/ R_2 = *trans*-1, 2-diaminocyclohexane

Compound **2a** was an orange oil formed in high yield (90 %) and was studied using variable temperature ^{1}H NMR experiments, over the range 238 – 333 K. Careful examination of the NMR data confirmed the proposed structure with two conformers in approximately 1:1 ratio. The key ^{1}H NMR peaks, which led to the identification of the conformers, were the overlapping triplets at δ 0.94, which represented two methyl groups of the butyl fragment that turned into a sharp triplet at 333 K. The two N-Me groups of each conformer were singlets at δ 3.34 (hidden) and 3.48, which coalesced to form one peak at 315 K. Another key piece of data was the pseudo triplet at δ 3.73 which actually was two overlapping doublet of doublets representing two individual

methylene protons on the PO fragment. The other peaks in the spectra were considered quite complicated and many peaks overlapped due to the conformers. The complexity of two conformers was best observed at 238 K when the conformers were slowed down on NMR timescale, showing two sets of peaks. Coalescence of the N-Me groups and the end methyl groups of butyl was observed to be 315 K and the free energy of activation was $\Delta G^{\ddagger}$ 68.6 kJ mol^{-1}.

The ^{13}C NMR spectrum further aided characterisation by displaying all the related carbon peaks of the two conformers, particularly by the two CS_2 environments low-field at δ 196.3 and 196.8. Further analyses found IR spectroscopic data and MS parent ion (222 (M^+)) were in accordance with the proposed structure.

Aqueous solutions of methylamine and hexylamine were reacted with CS_2 and PO to form the desired compound (**2b** and **2c** respectively). However, due to the formation of numerous isomers of the complexes, the ^1H NMR spectra were very complicated. In both cases, the peaks of the ring-opened PO were visible, indicting successful epoxide cleavage but elucidation was not possible. The ^{13}C NMR spectra displayed numerous peaks, indicative of conformers further substantiated with additional CS_2 peaks low-field. Both exhibited the expected IR stretches and parent ions in their mass spectra.

In the case of **2d**, this primary amine with a cyclic ring formed a yellow oil. The NMR data collected indicated the formation of conformers leading to the spectra being very complicated and we were unable to fully assign specific peaks. However, the key distinctive peaks of the ring-opened PO were observed in the expected range. In

addition to this, IR spectroscopy and the MS parent ion 237 (M^+) were in accordance to the proposed structure.

4.23 More Complex Amines: As simple secondary and unsymmetric amines were successful in forming the required compounds, the range was expanded to include more complex amines. These were all large amines with some having multiple nitrogen atoms that could act as potential sites for carbon disulfide attachment. These compounds were formed in the same manner as the others, yielding orange oils (**3a-e**) in moderate to high yields (Figure 11).

Figure 11: Complex amine dithiocarbamates with ring-opened PO (3a-e)

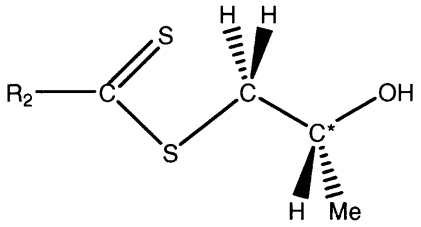

3a *N,N*-di-*tert*-butylethylenediamine

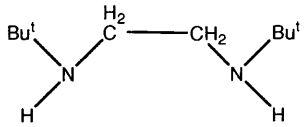

3b *N,N*-dimethylethylenediamine

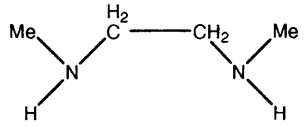

3c 3-dimethylamine-1-propylamine

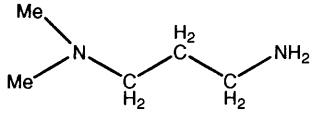

3d Diethylenetriamine

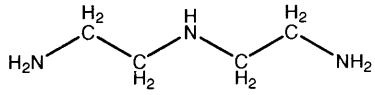

3e Pentaethylenehexamine

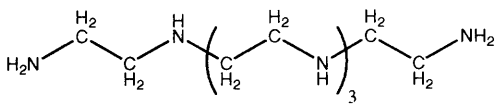

NMR and spectroscopic data showed the addition of CS_2 and the ring-opened PO on one end of the bidentate amine, confirming the structure of **3a**. Conformers were expected due to the unsymmetric nature of the amine once bonded with the CS_2 and PO. However, the NMR data indicated only one conformer was formed which could be due to the steric bulk of the ^{t}Bu. The ^{1}H NMR spectrum displayed the PO fragment clearly with all the relevant peaks, similar to previous complexes. The amine protons were all in the anticipated ranges, such as the ^{t}Bu groups were singlets at δ 1.74 and 2.63 and the ethylene protons were triplets at δ 2.84 and 4.01 both with the coupling constant of 7.9 Hz. The ^{13}C NMR data exhibited the appropriate number of carbon environments for one isomer. In addition, the IR stretches and the MS data correctly display the desired data to confirm complex formation.

As this amine was bidentate with two potential sites for CS_2 and PO addition, two equivalents of CS_2 and PO were added to attempt addition on both ends. However, the NMR and spectroscopic data observed only one addition, which could be due to the steric bulk of ^{t}Bu group hindering addition at the other end.

The *N,N*-dimethylethylenediamine was reacted with CS_2 and PO to form an orange **3b** in 54 % yield. This complex was characterised using the standard techniques but was found to be more complicated that expected. Like the unsymmetric amines, conformers were possible and the ^{1}H NMR spectrum indicted a major and minor product (2:1). Although the spectrum was very complicated, the PO peaks were visible in the accepted range with two methine protons at δ 4.26 (minor) and 4.66 (major) suggesting two conformers. Further evidence to conformer formation was the PO-methyl group appearing as pseudo triplets, which were actually two overlapping doublets of different

sizes. The N-methyl groups of the amine also displayed two peaks at δ 3.44 (minor) and 3.54 (major), which indicted conformers. More detailed assignment of the protons proved difficult due to the overlapping peaks of the minor isomer. The ^{13}C NMR displayed two sets of carbon environments, major and minor peaks that related well to the proposed structure. The key features in confirming the conformers were twice the expected number of carbon atoms and the two CS_2 peaks at δ 197.7 (major) and 199.2 (minor). Infra-red spectroscopic and MS data both indicated the formation of the complex with two conformers. As this amine had two potentially active sites, two equivalents of CS_2 and PO were reacted with this amine but the data indicated only one unit of CS_2 and PO was added.

The ^{1}H NMR spectrum for **3c**, formed from a primary amine, implied the formation of the desired compound as a major product with other conformers, making peak assignment difficult. The key PO peaks were present along with the methyl and methylene protons of the amine in the complicated spectrum. The ^{13}C NMR data also displayed a range of environments suggesting conformers. The IR and MS data indicated the correct values suggesting formation of the compound.

Compounds **3d** and **3e** were formed using amines with both primary and secondary amines, leading to the possibility of various isomers. The ^{1}H and ^{13}C NMR spectra of these compounds were very complicated and were unable to assign individual peaks due to conformers and multiple bonding sites. Spectroscopic and MS data corroborated the proposed complexes but due to the complex nature of these compounds, a definite conclusion is difficult.

4.24 Cyclic Amines: To further investigate the flexibility of the ring-opening of PO, cyclic amines were reacted with CS_2 and PO. The synthesis of compounds (**4a-d, 4f**) was identical to that of the linear amines, producing yellow/orange oils with moderate yields of 50 – 60 % (Figure 12).

Figure 12: Cyclic amine dithiocarbamates with PO (4a-d, f)

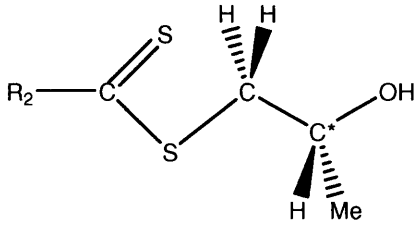

	R_2H		R_2H
4a	Piperdine 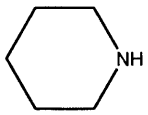	**4d**	Piperazine 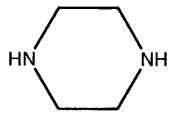
4b	Pyrrolidine 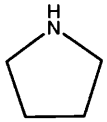	**4f**	Homopiperazine 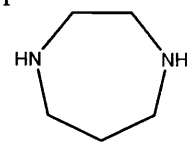
4c	S-2-pyrrolidine methanol 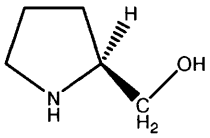		

One of the cleanest reactions was that with piperidine, to give **4a**. This was a bright yellow solid, formed in 58 % yield and characterised by ^1H NMR, ^{13}C NMR, MS and IR spectroscopy. The ^1H NMR spectrum showed the ring-opened PO had protons appearing with similar signals to those from linear dithiocarbamates. The methine proton was seen as a mutliplet at δ 4.09, the methylene protons as doublet of doublets at δ 3.76 (J 19.1, 5.2 Hz) and 3.69 (J 19.1, 9.7 Hz). The methyl group on the PO was a

doublet at δ 1.30 (J 8.3 Hz) and the hydroxyl proton at δ 2.51 was a singlet. The six piperidine protons furthest from the nitrogen atom appeared as broad singlet at δ 1.72 and the two sets of N-CH_2 protons appeared as two broad multiplets at δ 4.28 and 4.02 assigned to the equatorial and axial protons, their broadness suggesting fluxionality at room temperature (Figure 13).

Figure 13: ^{1}H NMR spectrum for 4a

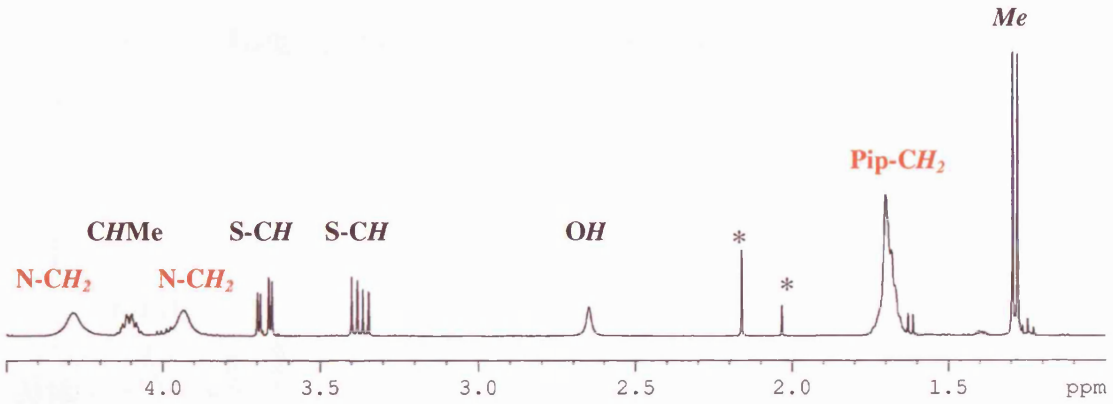

* known impurity

The ^{13}C NMR spectrum of **4a** was in accordance with the proposed structure, showing the expected eight carbon environments (Figure 14). The quaternary carbon appeared at δ 195.8, while the carbon atoms on the PO were seen at δ 67.1 for the methine carbon, δ 44.9 for the methylene carbon and δ 22.5 for the methyl carbon. The C_3 atom on the piperidine ring had a peak at δ 26.0, the two C_2 carbons were equivalent at δ 24.2 and the two C_1 atoms were marginally inequivalent at δ 53.5 and δ 51.6.

Figure 14: Structure of 4a

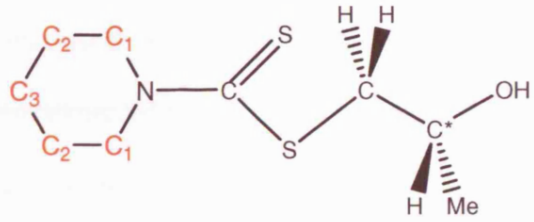

Other spectroscopic data that confirmed the structure of **4a** included MS, which produced the parent ion *m/z* 220 (M^+), elemental analysis data gave the correct percentages and IR data displayed all expected stretches. Variable temperature ^1H NMR spectroscopy was carried out for **4a** in the range of 298 – 333 K, which allowed the coalescence temperature to be observed at 328 K and the free energy of activation to be estimated as 66.0 kJ mol^{-1}, slightly lower than the linear amines values (Figure 15).

Figure 15: Variable temperature ^1H NMR stack plot for 4a

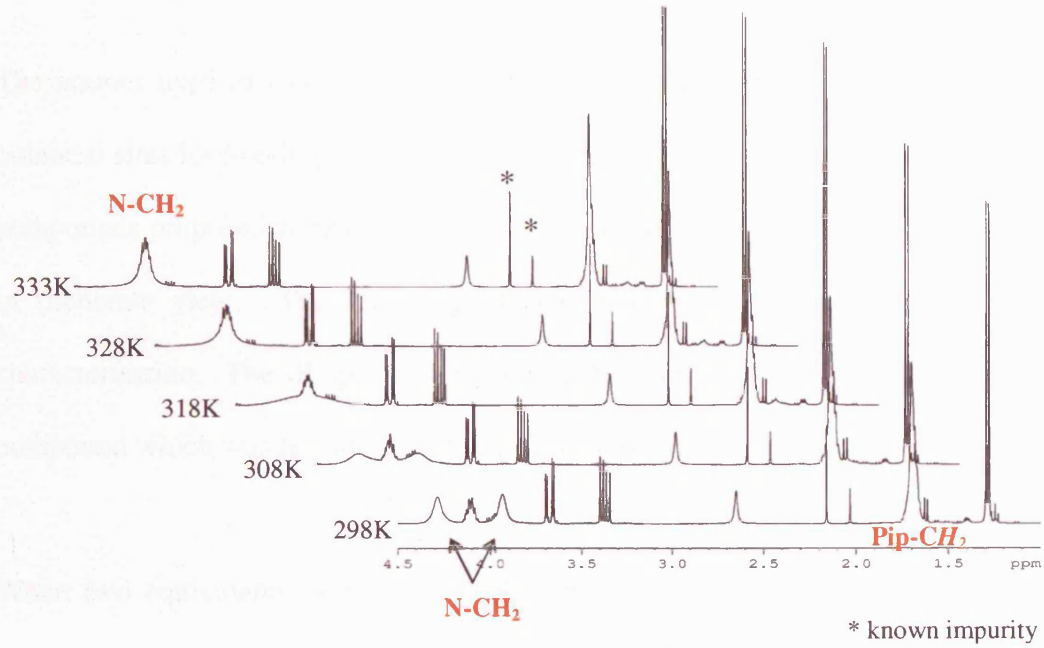

* known impurity

One purpose of this research was to consider the possibility that PO polymers could be formed using free dithiocarbamates as initiators. As it has been established that dithiocarbamates can ring-open one equivalent of PO, a series of reactions were undertaken with piperidine-dithiocarbamate and instead of adding a molar equivalent of PO, 2 - 10-fold excess was used. As one ring was opened onto the dithiocarbamate, the other PO monomers were expected to react, forming a chain. Unfortunately, excess PO did not lead to more than one ring opening of PO.

The other cyclic amines in this series, all successfully formed the desired complexes. Characterisation of **4b** was comprehensive, NMR, MS and IR spectra clearly supporting the proposed structure. The ^{1}H and ^{13}C NMR spectrum of **4c** was very complicated due to the two chiral centres present resulting in doubling of the peaks as diastereoisomers. There was some indication of ring-opened PO peaks, however individual peaks could not be assigned due to the complex nature of the spectra and the overlapping of peaks. The use of MS and IR aided data collection, corroborating the proposed structure but was unable to confirm the structure conclusively.

The amines used to form compounds **4d** and **4f** were bidentate amines, offering two potential sites for bonding. Using one equivalent of base and CS_2, the mono-substituted compounds proposed were achieved. Compound **4d** was formed as a white-cream solid in moderate yield. The solubility of this compound was poor, therefore limiting characterisation. The IR spectrum exhibited the appropriate stretches for the proposed compound which was further corroborated with elemental analysis.

When two equivalents of base and CS_2 were used, the piperazine amine formed the bisubstituted compound (**4e**) (Figure 16).

Figure 16: Bidentate amine with two dithiocarbamate ends (4e)

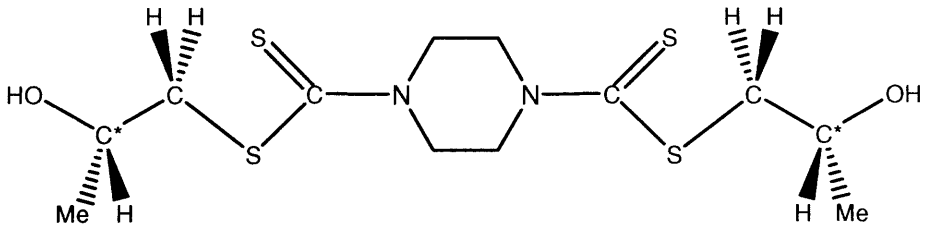

This compound formed a white-cream solid in poor yield, which was characterised using NMR, IR, MS and elemental analysis. The ^{1}H NMR spectrum showed the PO protons were all in the same range as the other successful compounds. The methine proton was a broad multiplet at δ 4.14, the methylene protons were doublet of doublets at δ 3.69 (J 14.1, 7.2 Hz) and δ 3.40 (J 14.1, 7.2 Hz) and the methyl protons were a doublet at δ 1.33. The hydroxyl proton was broad singlet at δ 2.30 and the piperazine protons were a broad multiplet at δ 4.44.

The ^{13}C NMR spectrum identified six different environments. These included the piperazine carbons at δ 48.1 and the C-S peak at δ 198.2. As the numbers of carbons were correct with only one C-S resonance, this indicated only one conformer was formed. The carbons of PO were in the same range as the other compounds, the methine carbon was δ 67.1, methylene carbon was δ 44.9 and the methyl carbon was δ 22.5.

Other characterising data were the MS, which presented a parent ion at 356 (M^{+}) and the IR data showed the respective stretches. Based on the inclusion of ½ $CHCl_3$, the elemental analysis data presented a reasonable fit for the proposed structure. All this spectroscopic data confirmed the formation of the compound.

The data of **4f** indicated two conformers in a 1: 1 ratio as the ^{1}H NMR spectrum shows doubling of the peaks with two methyl groups as overlapping doublets at δ 1.25. The PO peaks were visible but the other protons were too complicated to assigne due the complex nature of the ring protons. Twice as many carbons in the ^{13}C NMR spectrum further substantiated this with two C-S peaks at δ 197.0 and 197.3. In addition to this,

the correct parent ion of 235 (M^+) was identified from the MS spectrum and the IR stretches displayed the appropriate stretches.

When two equivalents of base, CS_2 and PO were used with homopiperazine, the ^1H NMR spectrum of the product was too complicated to assigned peaks. However, the ^{13}C NMR spectrum showed seven different environments equalling the bisubstituted compound, indicting that when two PO units were attached to this compound, there was a preferred conformer. There were smaller peaks, which were attributed to minor conformers. The MS identified the parent ion and the IR stretches exhibited the appropriate stretches.

4.25 Other epoxides: we have illustrated that dithiocarbamates are able to ring-open PO and other epoxides were used to examine the versatility of the process. The piperdine-dithiocarbamate was synthesised by standard techniques followed by the addition of BO (1,2 epoxybutane) and stirred overnight. This gave **5a** (48 %) as a yellow oil being characterised using NMR, IR and MS. Like PO, BO has two different carbons in the epoxide ring, with the least hindered C_α being the point of bond cleavage.

The ^1H NMR spectrum of **5a** agreed with the projected ring-opening. The BO ring was opened *via* the C_α so that the S-CH_2 protons (C_A) were doublet of doublets at δ 3.37 (J 14.3 Hz) and 3.69 (J 14.3 Hz). The methine proton on (C_B) was a multiplet at δ 3.82, the second methylene protons (C_C) were at δ 1.58 as a multiplet and the methyl (C_D) was a triplet δ 0.97 (J 7.6 Hz) with the hydroxyl group at δ 2.62 as a broad singlet. The distant piperidine protons (protons on C_2 and C_3) appeared as a broad multiplet at δ 1.83 and the N-methylene protons as broad singlets at δ 3.93 and 4.30 (Figure 17).

Figure 17: Structure of 5a

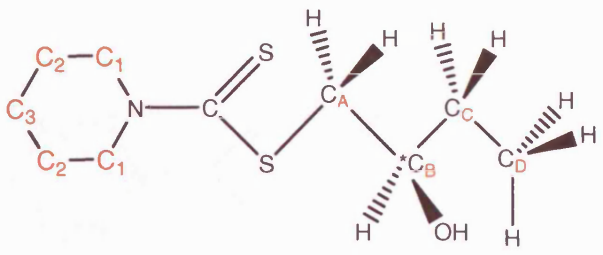

The ^{13}C NMR spectrum of **5a** was similar to that of **4a**, the piperidine carbon atoms appeared at δ 26.6 for C_3 and 25.4 for C_2. The C_1 carbons were inequivalent at δ 51.1 and 52.7. The methylene carbon, closest to the sulfur (C_A) was δ 43.3, methine carbon was δ 72.1 (C_B), the next methylene carbon (C_C) was δ 29.5, methyl (C_D) was δ 9.3 and finally, the quaternary carbon appeared at δ 195.9. In addition to the NMR data, MS spectrum identified the correct parent ion as 234 (M^+) and the IR spectrum showed all the expected vibrations.

As BO was successfully opened with piperidine-dithiocarbamate, the reaction was repeated with styrene oxide. Using the same technique and characterisation, compound **5b** was formed as a yellow/orange oil in low yield. The protons on CH_2 of SO (C_A) which was the site of bond cleavage appeared as doublet of doublets at δ 3.61 (J 14.5, 8.8 Hz) and 3.88 (J 14.5, 3.3 Hz). The methine proton on C_B was a doublet of doublets at δ 5.05 (J 8.8, 3.3 Hz). The phenyl ring appeared as a doublet δ 7.48 (J 7.3 Hz) and triplets δ 7.39 (2H, J 7.3 Hz) and 7.30 (1H, J 7.3 Hz). The piperidines' six protons (protons on C_2 and C_3) were a broad multiplet at δ 2.10, the remaining four protons nearest to the nitrogen (protons on C_1) were broad singlets at δ 3.94 and 4.32 (Figure 18).

Figure 18: Structure of 5b with ring-opened SO

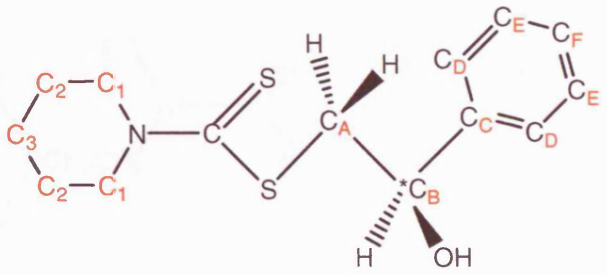

The ^{13}C NMR spectrum of this compound was as expected for this type of compound and fully characterised. In addition to the NMR data, MS data identified the correct parent ion as 282 (M^+) with all the corresponding IR stretches to confirm formation.

As piperidine-dithiocarabamate successfully opened the epoxides BO and SO, a more complicated bidentate amine *N,N*-di-*tert*-butylethylenediamine was used to form the dithiocarbamate. Reaction of this with BO and SO resulted in the formation of orange oils (**5c-d**) in good yield of 60 – 80 % and were characterised using the standard methods (Figure 19). The NMR spectra were complex with some evidence that the desired structures were formed. In the case of **5c,** the ^1H NMR spectrum showed the key peaks for the ring-opened BO. The first set of methylene protons (protons on C_A) were doublet of doublets at δ 3.34 and 3.64. The methine proton on C_B was a multiplet at δ 3.80, the second set of methylene protons (protons on C_C) was a multiplet at δ 1.53 and finally δ 0.95 was the peak for the methyl group (protons on C_D). There are numerous isomers that result in additional peaks, which led to the inability to elucidate the whole ^1H NMR spectrum. The IR data collected shows the relevant peaks to provide further evidence that the compound was formed.

Figure 19: Structure of 5c

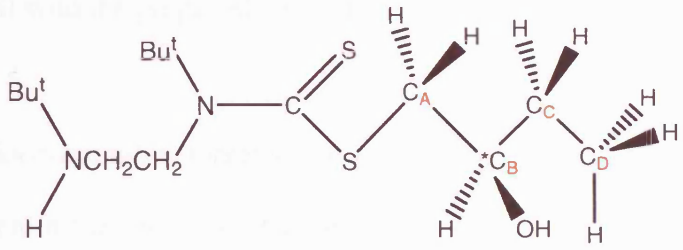

For the compound with SO (**5d**), the ring-opened peaks were also identified correctly which correlated to the other SO compound (**5b**) (Figure 20). In the ^{1}H NMR spectrum, the methylene protons were doublet of doublets at δ 3.84 (protons on C_A) and 5.02 (protons on C_C). The methine proton on C_B was a multiplet at δ 3.59 and the aromatic protons were represented with a multiplet at δ 7.3 (protons on $C_{D\text{-}F}$).

Figure 20: Structure of 5d

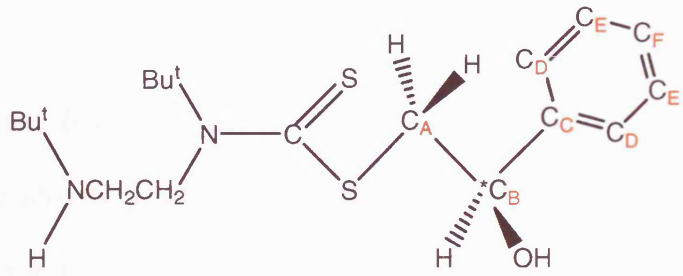

The ^{13}C NMR spectrum exhibited all the relevant peaks to represent the desired compound (**5d**). The end methyl group of the dithiocarbamate moiety was at δ 28.0 with the two methylene carbons from the amine at δ 44.3 and 49.8. The methyl carbon on the second nitrogen was at δ 28.7 followed by the C-S at δ 183.3. The epoxide moiety with the methylene carbon next to the sulfur at δ 42.6 (C_A) followed by the methine carbon at δ 56.7 (C_B). The aromatic carbons of the styrene were at δ 143.5

(C_C), 128.2 (C_D), 127.6 (C_E) and 125.1 (C_F). In addition to this, the IR stretches all corresponded well with the proposed structure.

4.26 Metal Dithiocarbamates: Organic dithiocarbamates can only ring-open only one PO monomer even in the presence of excess PO. As the leading catalysts for ROP of PO are metal-based compounds, metallic bis(dithiocarbamates) were synthesised as potential catalysts. The dimethyl and diethyl dithiocarbamates were reacted with CS_2 and metal chlorides in water. The other amines formed dithiocarbamates by reacting with CS_2 to form the dithiocarbamate followed by the addition of metal acetates in methanol. The compounds formed were of the general formula $[M(S_2CNR_2)_2]$ (M = Zn, Cd, Hg, Cu, Ni; R = Me, Et, Bu, ^{i}Bu). The yields were generally in high (around 60%) and produced solids of various colours. As these compounds have been previously synthesised and characterised, ^{1}H NMR data, IR and sample elemental analysis were collected to confirm their structures.

4.27 Polymerisation Reactions: The metal bis(dithiocarbamate) compounds were tested for their catalytic activity towards the polymerisation of PO. The catalyst (~0.01-0.05 g) was placed in a test tube with ethanol (2 ml) and PO (2 ml), covered and stirred over night. Next, a small quantity of DCM was added to the mixture and pumped dry on the vacuum line. The residue was dissolved in $CDCl_3$ and examined *via* ^{1}H NMR. The data showed no signs of polymerisation for any of the compounds. Therefore, it was concluded that metallic bis(dithiocarbamates) were not active catalysts for the ROP of PO.

4.3 Conclusions

Most preparations attempted in this chapter were successful. The characterisation of some compounds became difficult due to the use of complex amines. With the simple secondary amines, numerous sources of data consistently confirmed the structure of the dithiocarbamate and the attached PO ring. The unsymmetric amines were more complicated due to isomers formed using the primary amines. The N-methylbutylamine system offered an interesting insight into the unsymmetric dithiocarbamate and yet, there appeared to be no effect on the resonance values of the opened epoxide.

Extending the range of compounds to more complicated amines resulted in the limited characterisation with NMR spectroscopy. Here, other spectroscopic methods proved very useful. Using an excess of PO with piperidine-dithiocarbamate, it was found that only one unit of PO monomer was ring-opened onto the dithiocarbamate. Bidentate amines were investigated to consider the addition of CS_2 and PO units on either end of the bidenate amine. The compounds with the dithiocarbamate units on either side of the amine were formed with the bidentate amines; piperazine and homopiperazine.

Other epoxides such as BO and SO were investigated to confirm that this mechanism of ring-opening was not specific to PO. These epoxides were opened *via* bond cleavage at the least hindered carbon of the ring and bound to the dithiocarbamate. Finally, a range of metallic bis(dithiocarbamates) were synthesised and tested for RO polymerisation. Unfortunately, these reactions were unsuccessful in polymerising PO.

4.4 Experimental

All ^{1}H and ^{13}C NMR spectra were obtained on a Bruker AMX300 and AMX400 spectrometer, operating at 299.87 MHz and 400.12 MHz respectively. The same instrument was used for variable temperature work, using the range 233 – 333 K unless otherwise stated. All spectra were recorded using $CDCl_3$ solutions unless otherwise specified and were referenced against internal standards. All IR spectra were recorded using a Shimaduz FT-IR 8700 spectrometer, operating in the region of 4000 - 400 cm^{-1}. The IR samples were prepared using KBr powder to make discs or as neat samples between NaCl plates. The mass spectra were obtained using a Micromass 70-SE magnetic sector mass spectrometer. Three different procedures were used to maximise accuracy of the data for individual samples. These were Electron Impact (EI) Mode with ionisation at 70 eV, Chemical Ionisation (CI) with methane reagent gas and Fast Atom Bombardment (FAB^{+}) using a caesium ion gun. The Elemental Analysis (elemental analysis) was carried out using Elemental Analyzer (CE-440) (Exeter Analytical Inc).

The general experimental procedure[15] followed for the synthesis of all compounds was as followed:

Amine (14.30 mmol) and K_3PO_4 (3.04 g, 14.30 mmol) were stirred in acetone (40 ml) for 30 min. followed by the dropwise addition of carbon disulfide (CS_2) (1.09 g, 14.30 mmol) at 0°C. This solution was stirred for a further 30 min. and then propylene oxide (PO) (0.83 g, 14.30 mmol) was added and stirred overnight at room temperature. The solvent was removed from the coloured solution on the rotatory evaporator to produce a orange/yellow oil. Column chromatography was undertaken on the oil using ethyl

acetate/ petroleum spirit (40 - 60°C). The extract from this was then reduced using the rotatory evaporator and coloured oil was triturated with hexane (15 ml) and ether (15 ml) to attain the product.

4.41 Synthesis using Simple Secondary Amines

Synthesis of compound **1a:** diethylamine (1.05 g, 14.30 mmol), K_3PO_4 (3.04 g, 14.30 mmol), CS_2 (1.09 g, 14.30 mmol) and PO (0.83 g, 14.30 mmol) to give yellow/ orange oil (0.96 g, 48 %). IR (neat) ν: 3416br, 2973s, 2932s, 2873s, 1705s, 1643m, 1630s, 1488m, 1417m, 1379s, 1356s, 1301s, 1270s, 1207s, 1143s, 1124m, 1074m, 1008s, 985m, 936m cm^{-1}; variable temperature experiments undertaken between 298 – 333K, ^1H NMR ($CDCl_3$) (298 K): δ 4.13 (m, 1H, C*H*MeOH), 4.03 (sept, 2H, J 6.9, CH_2), 3.82 (sept, 2H, J 7.2, CH_2), 3.66 (dd, 1H, J 14.3, 3.8, S-CH_2), 3.36 (dd, 1H, J 14.3, 7.2, S-CH_2), 2.64 (brs, 1H, O*H*), 1.33 (t, 3H, J 7.0, Bu-*Me*), 1.26 (d, 3H, J 7.1, CH*Me*), 1.15 (t, 3H, J 7.0, Bu-*Me*); ^{13}C NMR ($CDCl_3$) δ 195.7, 67.4, 49.8, 46.9, 44.8, 22.4, 13.1, 12.3; mass spectrum (CI): *m/z* 222 (M^+).

Synthesis of compound **1b:** dipropylamine (1.45 g, 14.30 mmol), K_3PO_4 (3.04 g, 14.30 mmol), CS_2 (1.09 g, 14.30 mmol) and PO (0.84 g, 14.30 mmol) to give yellow/ orange oil (2.30 g, 68 %). IR (neat) ν: 3416br, 2966s, 2930s, 2874s, 1707s, 1694m, 1644m, 1483m, 1464m, 1414m, 1367m, 1306m, 1272m, 1237m, 1198m, 1147m, 1125m, 1090m, 1032m, 990m, 935m cm^{-1}; variable temperature experiments undertaken between 298 – 333K, ^1H NMR ($CDCl_3$) (298 K): δ 4.10 (m, 1H, C*H*MeOH), 3.89 (sex, 2H, J 7.5, N-CH_2), 3.65 (m, 3H, 2H N-CH_2, 1H S-CH_2), 3.35 (dd, 1H, J 7.2, S-CH_2), 2.62 (s, 1H, O*H*), 1.75 (sept, 4H, J 14.6, 7.2, CH_2), 1.28 (d, 3H, J 6.3, CH*Me*OH), 0.96 (t, 3H, J 7.4, CH_2*Me*), 0.92 (t, 3H, J 7.4, CH_2*Me*); ^{13}C NMR ($CDCl_3$) δ 196.2, 69.5,

67.3, 66.7, 57.0, 54.0, 45.0, 22.0, 21.5, 20.5, 11.1 ; mass spectrum (FAB): *m/z* 236 (M^+); anal. calc. for $C_{10}H_{21}ONS_2$: C, 51.02; H, 8.99; N, 5.95. Found C, 51.35; H, 9.20; N, 4.34.

Synthesis of compound **1c:** diisopropylamine (1.45 g, 14.30 mmol), K_3PO_4 (3.04 g, 14.30 mmol), CS_2 (1.09 g, 14.30 mmol) and PO (0.83 g, 14.30 mmol) to give yellow/ orange oil (1.65 g, 49 %). IR (neat) ν: 3415br, 2971s, 2929s, 2873s, 1705m, 1476s, 1442m, 1370m, 1314m cm^{-1}; variable temperature experiments undertaken between 238 – 333K, ^1H NMR ($CDCl_3$) (298 K): δ 4.91 (brs, 2H, C*H*), 4.12 (m, 1H, C*H*MeOH), 3.66 (dd, 1H, J 14.2, 4.0, S-CH_2), 3.40 (q, 1H, J 14.2, 7.1, S-CH_2), 2.49 (brs, 1H, O*H*), 1.46 (brd, 12H, J 4.0, *Me*), 1.29 (d, 3H, J 6.2, CH*Me*OH), ^{13}C NMR ($CDCl_3$) δ 210.8, 69.6, 66.8, 53.9, 54.7, 44.3, 31.7, 29.2, 22.6, 19.8; mass spectrum (EI): *m/z* 236 (M^+).

Synthesis of compound **1d:** dibutylamine (2.41 ml, 14.30 mmol), K_3PO_4 (3.04 g, 14.30 mmol), CS_2 (1.09 g, 14.30 mmol) and PO (0.84 g, 14.30 mmol) to give orange oil (3.02 g, 81 %). IR (neat) ν: 3418br, 2961s, 2931s, 2873s, 1705m, 1646m, 1484m, 1456m, 1414m, 1369m, 1290m, 1254m, 1218m, 1185m, 1126m, 1043m, 1011m, 983m, 944m cm^{-1}; ^1H NMR ($CDCl_3$): δ 3.70 (m, 4H, N-CH_2), 3.39 (sex, 1H, J 8.6, C*H*MeOH), 3.21(dd, 1H, J 13.8, 4.6, S-CH_2), 3.05 (dd, 1H, S-CH_2), 2.31 (s, 1H, O*H*), 1.85 (d, 3H, J 8.6, CH*Me*OH), 1.39 (q, 4H, J 15.1, 7.5, CH_2), 1.04 (m, 4H, J 14.4, 7.5, CH_2), 0.65 (t, 3H, J 7.4, CH_2*Me*), 0.61 (t, 3H, J 7.4, CH_2*Me*); ^{13}C NMR ($CDCl_3$) δ 213.2, 195.7, 69.4, 66.2, 54.9, 44.8, 31.4, 29.0, 28.0, 22.2, 19.7, 13.5; mass spectrum (CI): *m/z* 264 (M^+).

Synthesis of compound **1e:** diisobutylamine (1.85 g, 14.30 mmol), K_3PO_4 (3.04 g, 14.30 mmol), CS_2 (1.09 g, 14.30 mmol) and PO (0.84 g, 14.30 mmol) to give yellow/ orange

oil (3.38 g, 90 %). IR (neat) ν: 3419br, 2963s, 2931s, 2871s, 1703m, 1631m, 1467m, 1409m, 1386m, 1360m, 1291m, 1242m, 1198m, 1148m, 1124m, 1093m, 1043m, 996m, 938m cm^{-1}; variable temperature experiments undertaken between 298 – 333K, ^1H NMR ($CDCl_3$) (298 K): δ 4.09 (m, 1H, C*H*MeOH), 3.85 (brm, 2H, N-CH_2), 3.65 (dd, 1H, J 14.3, 3.9, S-CH_2), 3.60 (brm, 2H, N-CH_2), 3.37 (dd, 1H, J 14.2, 7.1, S-CH_2), 2.62 (s, 1H, O*H*), 2.44 (brsept, 1H, J 6.8, C*H*), 2.32 (brsept, 1H, J 6.7, C*H*), 1.28 (d, 3H, J 6.3, CH*Me*OH), 0.93 (d, 6H, J 6.6, *Me*), 0.89 (d, 6H, J 6.7, *Me*); ^{13}C NMR ($CDCl_3$) δ 197.4, 69.5, 66.7, 63.1, 60.8, 54.0, 45.1, 31.7, 27.4, 26.1, 22.5, 14.1; mass spectrum (CI): *m/z* 264 (M^+); anal. calc. for $C_{12}H_{25}ONS_2$: C, 54.70; H, 9.56; N, 5.31. Found C, 54.47; H, 9.78; N, 5.00.

Synthesis of compound **1f:** dibenzylamine (2.82 g, 14.30 mmol), K_3PO_4 (3.04 g, 14.30 mmol), CS_2 (1.09 g, 14.30 mmol) and PO (0.84 g, 14.30 mmol) to give yellow oil (2.44 g, 52 %). Variable temperature experiments undertaken between 298 – 333K, ^1H NMR ($CDCl_3$) (298 K): δ 7.27 (m, 10H, Ph), 5.34 (brq, 2H, N-CH_2), 4.97 (brs, 2H, N-CH_2), 4.16 (m, 1H, C*H*MeOH), 3.73 (dd, 1H, J 14.1, 10.2, S-CH_2), 3.46 (dd, 1H, J 14.1, 6.9, S-CH_2), 2.63 (s, 1H, O*H*), 1.32 (d, 3H, J 6.3, CH*Me*OH); mass spectrum (FAB): *m/z* 338 (M^+).

4.42 Synthesis using Unsymmetric Amines

Synthesis of compound **2a:** N-methylbutylamine (1.25 g, 14.30 mmol), K_3PO_4 (3.04 g, 14.30 mmol), CS_2 (1.09 g, 14.30 mmol) and PO (0.84 g, 14.30 mmol) to give orange oil (2.86 g, 90 %). IR (neat) ν: 3417br 2963s, 2930s, 2872, 1705m, 1632m, 1489m, 1456m, 1390m, 1297m, 1254m, 1213m, 1125m, 1076m, 983s, 938m cm^{-1}; variable temperature experiments undertaken between 238 – 333K, ^1H NMR ($CDCl_3$) (298 K):

4.03 (brt, 1H, C*H*MeOH), 3.76 (brm, 2H, S-C*H*$_2$), 3.64 (brdt, 1H, N-C*H*$_2$), 3.48 (s, 3H, N-*Me*), 3.35 (brq, 2H, J 7.9, 1H N-C*H*$_2$ 1H S-C*H*$_2$), 2.61 (s, 1H, O*H*), 1.67 (m, 2H, Bu-C*H*$_2$), 1.39 (brm, 2H, Bu-C*H*$_2$), 1.28 (d, 3H, J 6.2, CH*Me*OH), 0.96 (t, 3H, J 7.4, CH$_2$*Me*), 0.94 (t, 3H, J 7.4, CH$_2$*Me*); ^{13}C NMR ($CDCl_3$) 196.8, 196.3, 77.5, 77.4, 57.0, 55.2, 54.4, 45.1, 43.8, 41.0, 31.7, 29.1, 28.7, 22.4, 19.7, 13.6; mass spectrum (FAB): *m/z* 222 (M^+); anal. calc. for $C_9H_{19}ONS_2$: C, 48.83; H, 8.65; N, 6.33. Found C, 50.59; H, 9.08; N, 4.79.

Synthesis of compound **2b:** aqueous solution of methylamine (1.11 g, 14.30 mmol), K_3PO_4 (3.04 g, 14.30 mmol), CS_2 (0.86 g, 14.30 mmol) and PO (1.00 ml, 14.30 mmol) to give yellow oil (0.71 g, 34 %). IR (neat) ν: 3358br, 2967s, 2924m, 2872s, 2284m, 1709s, 1663m, 1600m, 1530m, 1449m, 1371m, 1345m, 1313m, 1263m, 1181m, 1125m, 1079m, 1037m, 1002m, 936m cm^{-1}; ^{1}H and ^{13}C NMR ($CDCl_3$) data too complex to identify individual peaks; mass spectrum (CI): *m/z* 172 (M^+).

Synthesis of compound **2c:** hexylamine (1.45 g, 14.30 mmol), K_3PO_4 (3.04 g, 14.30 mmol), CS_2 (1.09 g, 14.30 mmol) and PO (0.84 g, 14.30 mmol) to give orange oil (2.03 g, 21 %). IR (neat) ν: 3255br, 2958s, 2929s, 2857s, 2104m, 1700m, 1660m, 1518m, 1455m, 1375m, 1338m, 1303m, 1256m, 1125m, 1043m, 963m, 934m cm^{-1}; ^{1}H and ^{13}C NMR ($CDCl_3$) data too complex to identify individual peaks; mass spectrum (CI): *m/z* 236 (M^+).

Synthesis of compound **2d:** *trans*-1, 2-diaminocyclohexane (1.17 g, 14.30 mmol), K_3PO_4 (3.04 g, 14.30 mmol), CS_2 (1.09 g, 14.30 mmol) and PO (0.84 g, 14.30 mmol) to give yellow oil (2.28 g, 59 %). IR (neat) ν: 3254br, 2933m, 2861s, 2098m, 1709s,

1692s, 1644m, 1499m, 1371m, 1351m, 1255m, 1156m, 1080m, 1038m, 1006m, 978s, 939m cm^{-1}; ^{1}H NMR and ^{13}C NMR ($CDCl_3$): data too complex to identify individual peaks; mass spectrum (CI): *m/z* 237 (M^+).

4.43 Synthesis using Complex Amines

Synthesis of compound **3a:** *N,N'*-di-tert-butylethylenediamine (2.46 g, 14.30 mmol), K_3PO_4 (3.04 g, 14.30 mmol), CS_2 (1.09 g, 14.30 mmol) and PO (0.84 g, 14.30 mmol) to give pink oil (0.28 g, 5 %). IR (neat) ν: 3991br, 2926m, 2877m, 2787m, 1700s, 1627m, 1474m, 1456m, 1408m, 1329m, 1265m, 1204m, 1124m, 1076m, 1035m, 937m cm^{-1}; variable temperature experiments undertaken between 238 – 333 K, ^{1}H NMR ($CDCl_3$) (298 K): δ 4.08 (m, 1H, C*H*MeOH), 4.01 (t, 2H, J 7.9, N-CH_2), 3.60 (dd, 1H, J 14.2, 4.1, S-CH_2), 3.32 (dd, 1H, S-CH_2), 2.84 (t, 2H, J 7.9, N-CH_2), 2.63 (s, 9H, ^{t}*Bu*), 1.74 (s, 9H, ^{t}*Bu*), 1.24 (d, 3H, J 6.2, CH*Me*OH); ^{13}C NMR ($CDCl_3$) δ 183.6, 65.9, 56.6, 50.3, 48.01, 44.4, 28.9, 28.1, 22.1; mass spectrum (CI): *m/z* 305 (M^+).

Synthesis of compound **3b:** N,N'-dimethylethylene diamine (1.26 g, 14.30 mmol), K_3PO_4 (3.04 g, 14.30 mmol), CS_2 (1.09 g, 14.30 mmol) and PO (0.84 g, 14.30 mmol) to give yellow/ orange oil (1.71 g, 54 %). IR (KBr) ν: 3427br, 2925m, 2851m, 2764m, 1700s, 1653s, 1618m, 1511m, 1483m, 1445m, 1325m, 1286m, 1219m, 1113s, 1067s, 999s, 958s cm^{-1}; ^{1}H NMR ($CDCl_3$): data too complex to identify individual peaks; ^{13}C NMR ($CDCl_3$) δ 199.2, 197.7, 66.6, 66.6, 53.9, 52.7, 50.6, 48.2, 45.2, 44.9, 44.2, 40.8, 35.0, 31.4, 22.6, 22.3; mass spectrum (CI): *m/z* 223 (M^+).

Synthesis of compound **3c:** 3-dimethylamine-1-propylamine (1.46 g, 14.30 mmol), K_3PO_4 (3.04 g, 14.30 mmol), CS_2 (1.09 g, 14.30 mmol) and PO (1.09 g, 14.30 mmol) to give yellow oil (1.29 g, 38 %). IR (neat) ν: 3240br, 2967m, 2928m, 2865s, 2823s,

2781m, 1695m, 1646m, 1595m, 1516m, 1463m, 1372s, 1341m, 1305m, 1262m, 1174m, 1126m, 1074m, 1039m, 1003m, 938m cm^{-1}; ^{1}H and ^{13}C NMR ($CDCl_3$): data too complex to identify individual peaks; mass spectrum (CI): *m/z* 237 (M^+).

Synthesis of compound **3d:** diethylenetriamine (1.48 g, 14.30 mmol), K_3PO_4 (3.04 g, 14.30 mmol), CS_2 (1.09 g, 14.30 mmol) and PO (0.84 g, 14.30 mmol) to give brown oil (2.65 g, 78 %). IR (neat) ν: 1263m, 1238m, 1069m, 1129m, 1077m, 1050m, 1008s, 938s; ^{1}H and ^{13}C NMR ($CDCl_3$): data too complex to identify individual peaks; mass spectrum (CI): m/z 237 (M^+).

Synthesis of compound **3e:** pentaethylenehexamine (3.32 g, 14.30 mmol), K_3PO_4 (3.04 g, 14.30 mmol), CS_2 (1.09 g, 14.30 mmol) and PO (0.84 g, 14.30 mmol) to give brown oil (4.56 g, 87 %). Variable temperature experiments undertaken between 298 – 333 K, ^{1}H NMR and ^{13}C NMR ($CDCl_3$) data too complex to identify individual peaks; mass spectrum (CI): m/z 366 (M^+).

4.44 Synthesis using Cyclic Amines

Synthesis of compound **4a:** piperidine (1.22 g, 14.30 mmol), K_3PO_4 (3.04 g, 14.30 mmol), CS_2 (1.09 g, 14.30 mmol) and PO (0.84 g, 14.30 mmol) to give yellow oil/ precipitate (1.94 g, 58 %). IR (KBr) ν: 3142br, 2855s, 2345s, 1647s, 1585s, 1474m, 1425m, 1373s, 1344m, 1238s, 1105m, 1061m, 978s cm^{-1}; variable temperature experiments undertaken between 298 – 333 K, ^{1}H NMR ($CDCl_3$) (298 K): δ 4.28 (brm, 2H, N-C*H*$_2$), 4.09 (m, 1H, C*H*MeOH), 4.02 (brm, 2H, N-C*H*$_2$), 3.76 (dd, 1H, J 19.1, 5.2, S-C*H*$_2$), 3.69 (dd, 1H, J 19.1, 9.7 S-C*H*$_2$), 2.51 (s, 1H, O*H*), 1.72 (brs, 6H, C*H*$_2$), 1.30 (d, 3H, J 8.3, CH*Me*OH); ^{13}C NMR ($CDCl_3$) δ 195.8, 67.1, 53.5, 51.6, 44.9, 26.0, 25.5,

24.2, 22.5; mass spectrum (FAB): *m/z* 220 (M^+); anal. calc. for $C_9H_{17}ONS_2$: C, 49.28; H, 7.75; N, 6.39. Found C, 48.93; H, 7.82; N, 6.27.

Using the standard synthesis for **4a**, the amount of PO added varied from 1.66 g (28.6 mmol), 4.15 g (71.50 mmol) and 8.30 g (143.00 mmol) to give orange oil. The ^1H NMR spectra showed peaks resembling compound **4a** for all three reactions, showing the addition of one PO to the piperidine-dithiocarbamate. There was no evidence in the ^1H NMR to suggest the addition of more PO units after the reaction with the initial PO unit.

Synthesis of compound **4b:** pyrrolidine (1.02 g, 14.30 mmol), K_3PO_4 (3.04 g, 14.30 mmol), CS_2 (1.09 g, 14.30 mmol) and PO (0.84 g, 14.30 mmol) to give orange oil (1.64 g, 56 %). IR (neat) ν: 3406br, 2969m, 2925m, 2872s, 1709m, 1692s, 1645m, 1630m, 1553m, 1434m, 1378m, 1333m, 1251m, 1161s, 1125m, 1076m, 1039m, 1006s, 956s cm^{-1}; variable temperature experiments undertaken between 238 – 333 K, ^1H NMR ($CDCl_3$) (298 K): δ 4.11 (m, 1H, C*H*MeOH), 3.93 (t, 2H, Ar), 3.68 (m, 3H, 2H Ar, 1H S-CH_2), 3.36 (dd, 1H, J 19.1, 9.5, S-CH_2), 2.62 (s, 1H, O*H*), 1.28 (d, 3H, J 8.3, CH*Me*OH); ^{13}C NMR ($CDCl_3$) δ 193.0, 67.0, 55.9, 50.9, 44.2, 26.0, 24.3, 22.4; mass spectrum (FAB): *m/z* 206 (M^+).

Synthesis of compound **4c:** S-2-pyrrolidine methanol (1.45 g, 14.30 mmol), K_3PO_4 (3.04 g, 14.30 mmol), CS_2 (1.09 g, 14.30 mmol) and PO (0.84 g, 14.30 mmol) to give red/ brown oil (3.35 g, 99 %). IR (neat) ν: 3379br, 2966s, 2925s, 2875s, 1710s, 1643m, 1416m, 1369m, 1340m, 1311m, 1245m, 1177m, 1152m, 1124m, 1042m, 973m, 936m

cm^{-1}; ^1H NMR and ^{13}C ($CDCl_3$) data too complex to identify individual peaks; mass spectrum (CI): *m/z* 236 (M^+).

Synthesis of compound **4d:** piperazine (1.23 g, 14.30 mmol), K_3PO_4 (3.04 g, 14.30 mmol), CS_2 (1.09 g, 14.30 mmol) and PO (0.84 g, 14.30 mmol) to give white-cream solid (2.11 g, 67 %). IR (neat) ν: 3420br, 2937m, 2857s, 1702m, 1645m, 1475m, 1428m, 1367m, 1281m, 1275s, 1211m, 1161m, 1123m, 1072m, 1039s, 996s, 914m cm^{-1}; anal. calc. for $C_8H_{16}N_2S_2O_1$: C, 43.62; H, 7.33; N, 12.73. Found C, 37.31; H, 6.44; N, 12.13. Recalc. for $C_8H_{16}N_2S_2O_1.½CH_2Cl_2$: C, 37.31; H, 6.44; N, 12.13.

Synthesis of compound **4e:** piperazine (1.23 g, 14.30 mmol), K_3PO_4 (3.04 g, 28.60 mmol), CS_2 (1.72 ml, 28.60 mmol) and PO (2.00 ml, 28.60 mmol) to give white-cream solid (0.28 g, 6 %). IR (KBr) ν: 3314br, 2963s, 2920m, 2868m, 1701m, 1625m, 1448m, 1417m, 1275s, 1256m, 1229m, 1130m, 1116m, 1072m, 1041m, 1005m, 978m, 937m cm^{-1}; ^1H NMR ($CDCl_3$): δ 4.44 (brm, 8H, N*H*$_2$); 4.14 (brm, 2H, C*H*MeOH); 3.69 (dd, 2H, J 14.1, 7.2, S-C*H*$_2$), 3.40 (dd, 2H, J 14.2, 7.2, S-C*H*$_2$), 2.30 (brs, 2H, O*H*); 1.33 (d, 6H, J 6.2, CH*Me*OH); ^{13}C NMR ($CDCl_3$) δ 198.2, 67.1, 44.9, 22.5, 20.0, 13.6; mass spectrum (CI): *m/z* 309; anal. calc. for $C_{12}H_{22}O_2N_2S_4$: C, 40.65; H, 6.25; N, 7.90. Found C, 37.53; H, 5.84; N, 7.14. Recalc. for formula $C_{12}H_{22}O_2N_2S_4.½CHCl_3$: C, 36.24; H, 5.47; N, 6.76.

Synthesis of compound **4f:** homopiperazine (1.43 g, 14.30 mmol), K_3PO_4 (3.04 g, 14.30 mmol), CS_2 (1.09 g, 14.30 mmol) and PO (0.84 g, 14.30 mmol) to give yellow oil (2.78 g, 83 %). IR (neat) ν: 3329br, 2926m, 2867m, 2755m, 1708s, 1645m, 1483m, 1412m, 1361m, 1332m, 1291m, 1175m, 1127m, 1073m, 982m, 921m cm^{-1}; ^1H NMR ($CDCl_3$):

δ 4.28 (m, 2H, C*H*Me), 4.04 (m, 4H, N-C*H*$_2$), 3.60 (dd, 2H, S-C*H*$_2$), 3.56 (dd, 2H, 2H, S-C*H*$_2$), 3.04 (m, 2H, N-C*H*$_2$), 2.83 (brt, 2H, N-C*H*$_2$), 1.91 (quint, 2H, C*H*$_2$), 1.26 (d, 3H, *Me*), 1.25 (d, 3H, *Me*); ^{13}C NMR ($CDCl_3$): δ 197.3, 197.0, 66.7, 66.6, 58.4, 55.6, 54.6, 54.6, 51.9, 50.9, 48.2, 47.9, 47.5, 47.3, 45.1, 30.9, 28.7, 27.7, 22.6; mass spectrum (CI): *m/z* 235 (M^+).

Synthesis of compound **4g:** homopiperazine (1.43 g, 14.30 mmol), K_3PO_4 (3.04 g, 28.60 mmol), CS_2 (1.72 ml, 28.60 mmol) and PO (2.00 ml, 28.60 mmol) to give yellow oil (4.51 g, 80 %). ^{1}H NMR ($CDCl_3$): data too complex to identify individual peaks; ^{13}C NMR ($CDCl_3$): δ 210.7, 69.7, 66.5, 53.8, 31.7, 29.2; mass spectrum (CI): *m/z* 367 (M^+).

4.45 Other Epoxides

Synthesis of compound **5a:** piperidine (1.22 g, 14.30 mmol), K_3PO_4 (3.04 g, 14.30 mmol), CS_2 (1.09 g, 14.30 mmol) and butylene oxide (BO) (1.03 g, 14.30 mmol) to give yellow oil (1.59 g, 48 %). IR (neat) ν: 3414br, 2935m, 2856m, 2666m, 1692s, 1645s, 1627m, 1475m, 1425m, 1356m, 1281m, 1228m, 1130m, 1115m, 1073m, 1005m, 977m, 937s cm^{-1}; ^{1}H NMR ($CDCl_3$): δ 4.30 (brs, 2H, N-C*H*$_2$), 3.93 (brs, 2H, N-C*H*$_2$), 3.82 (m, 1H, J 3.6, C*H*OH), 3.69 (dd, 1H, J 14.3, 3.6, S-C*H*), 3.37 (dd, 1H, J 14.3, 7.6, S-C*H*), 2.62 (s, 1H, O*H*), 1.83 (brm, 6H, Pip-C*H*$_2$), 1.58 (m, 2H, C*H*$_2$Me), 0.97 (t, 3H, J 7.6, CH$_2$*Me*); ^{13}C NMR ($CDCl_3$) δ 195.9, 72.1, 52.7, 51.1, 43.3, 29.5, 26.6, 25.4, 22.9, 9.26; mass spectrum (CI): *m/z* 234 (M^+).

Synthesis of compound **5b:** piperidine (1.22 g, 14.30 mmol), K_3PO_4 (3.04 g, 14.30 mmol), CS_2 (1.09 g, 14.30 mmol) and styrene oxide (SO) (1.72 g, 14.30 mmol) to give yellow/ orange oil (0.68 g, 17 %). IR (KBr) ν: 3393br, 2932m, 2855s, 2361m, 1699s,

1626m, 1478s, 1434s, 1380m, 1279s, 1241m, 1159m, 1130m, 1113s, 1051s, 1005s, 975s cm^{-1}; ^1H NMR ($CDCl_3$): δ 7.48 (d, 2H, J 7.3, Ar), 7.39 (t, 2H, J 7.3, Ar), 7.30 (t, 1H, J 7.3, Ar), 5.04 (dd, 1H, J 8.8, 3.3, S-C*H*), 4.32 (brs, 2H, N-CH_2), 3.94 (brs, 2H, N-CH_2), 3.88 (dd, 1H, J 14.5, 3.3, CH_2OH), 3.61 (dd, 1H, J 14.5, 8.8, CH_2OH), 2.01 (brm, 6H, N-CH_2); ^{13}C NMR ($CDCl_3$) δ 195.7, 143.0, 128.4, 127.6, 125.8, 73.1, 51.9, 45.4, 24.4; mass spectrum (CI): *m/z* 282 (M^+).

Synthesis of compound **5c:** *N, N'*-di-*tert*-butylethylene diamine (3.07 ml, 14.30 mmol), K_3PO_4 (3.04 g, 14.30 mmol), CS_2 (1.09 g, 14.30 mmol) and BO (1.23 ml, 14.30 mmol) to give yellow oil (3.11 g, 68 %). IR (KBr) ν: 3422br, 2964s, 2929m, 2875s, 2478m, 1700s, 1651m, 1560s, 1458m, 1400m, 1362s, 1317s, 1265m, 1206m, 1110m, 1050m, 1014m, 997m, 978m cm^{-1}; ^1H NMR ($CDCl_3$): δ 3.80 (m, 1H, C*H*OH), 3.64 (dd, 1H, J 3.7, S-CH_2), 3.34 (dd, 1H, J 7.5, S-CH_2), 1.53 (m, 2H, CH_2Me), 0.95 (m, 3H, CH_2*Me*).

Synthesis of compound **5d:** *N, N'*di-*tert*-butylethylene diamine (3.07 ml, 14.30 mmol), K_3PO_4 (3.04 g, 14.30 mmol), CS_2 (0.84 ml, 14.30 mmol) and SO (1.63 ml, 14.30 mmol) to give orange oil (3.89 g, 81 %). IR (neat) ν: 3252br, 2966m, 2922m, 2870m, 2479m, 1631m, 1600m, 1475m, 1451m, 1400m, 1362m, 1317m, 1264m, 1204m, 1160m, 1104m, 1084m, 1061m, 1014m, 997s cm^{-1}; ^1H NMR ($CDCl_3$): 7.35 (m, 5H, Ar), 5.02 (dd, 1H, S-CH_2), 3.84 (dd, 1H, S-CH_2), 3.59 (m, 1H, C*H*OHAr); ^{13}C NMR ($CDCl_3$) δ 183.3, 143.5, 128.2, 125.1, 56.7, 49.8, 42.6, 28.7, 28.0.

4.46 Synthesis of Metal Dithiocarbamates

Metal Bis(dimethyldithiocarbamate)

Synthesis of compound **7a:** zinc chloride (1.00 g, 7.34 mmol) and $NaS_2CNMe_2.3H_2O$ (2.10 g, 14.67 mmol) were placed in a round bottom flask with distilled water (100 ml) and stirred for 30 min. The white precipitate formed was collected by filtration, washed successively with distilled water and air-dried to give white solid (1.66 g, 74 %), $ZnC_6H_{12}N_2S_4$. ^1H NMR ($CDCl_3$): δ 3.47 (s, 12H, *Me*); anal. calc. for $Zn_1C_6H_{12}N_2S_4$: C, 23.56; H, 3.95; N, 9.16. Found C, 23.51; H, 3.99; N, 8.95.

Synthesis of compound **7b**: follow experimental as above with cadmium chloride (0.68 g, 3.67 mmol), and $NaS_2CNMe_2.3H_2O$ (1.05 g, 7.34 mmol) to give white solid (0.98 g, 76 %) $CdC_6H_{12}N_2S_4$. ^1H NMR ($CDCl_3$): δ 3.51 (s, 12H, *Me*).

Synthesis of compound **7c:** follow experimental as above with mercury chloride (0.99 g, 3.67 mmol), and $NaS_2CNMe_2.3H_2O$ (1.05 g, 7.34 mmol) to give brown solid (0.92 g, 57 %). $HgC_6H_{12}N_2S_4$. ^1H NMR ($CDCl_3$): δ 3.53 (s, 12H, *Me*).

Synthesis of compound **7d:** follow experimental as above with copper chloride dihydrate (0.63 g, 3.67 mmol), and $NaS_2CNMe_2.3H_2O$ (1.05 g, 7.34 mmol) to give grey solid (0.42 g, 38 %). $CuC_6H_{12}N_2S_4$. Paramagnetic solid.

Metal Bis(diethyldithiocarbamate)

Synthesis of compound **8a:** follow experimental as above with zinc chloride (1.00 g, 7.34 mmol) and $NaS_2CNEt_2.3H_2O$ (3.31 g, 14.67 mmol) were placed in a round bottom flask with distilled water (100 ml) and stirred for 30 min. The white precipitate was collected by filtration, washed successively with distilled water and air-dried to give a

white solid (2.22 g, 84 %), $ZnC_{10}H_{20}N_2S_4$. ^1H NMR ($CDCl_3$): δ 3.86 (q, J 7.1, 8H, CH_2), 1.32 (t, J 7.1, 12H, *Me*).

Synthesis of compound **8b:** follow experimental as above with cadmium chloride (0.67 g, 3.67 mmol), and $NaS_2CNEt_2.3H_2O$ (1.66 g, 7.34 mmol) to give white solid (1.34 g, 89 %). $CdC_{10}H_{20}N_2S_4$. ^1H NMR ($CDCl_3$): δ 3.93 (q, J 7.1, 8H, CH_2), 1.33 (t, J 7.1, 12H, *Me*).

Synthesis of compound **8c:** follow experimental as above with mercury chloride (0.99 g, 3.67 mmol), and $NaS_2CNEt_2.3H_2O$ (1.66 g, 7.34 mmol) to give grey solid (0.92 g, 51 %). $HgC_{10}H_{20}N_2S_4$ ^1H NMR ($CDCl_3$): δ 3.80 (q, J 7.1, 8H, CH_2), 1.34 (t, J 7.1, 12H, *Me*).

Synthesis of compound **8d:** follow experimental as above with copper chloride dihydrate (0.63 g, 3.67 mmol), and $NaS_2CNEt_2.3H_2O$ (1.66 g, 7.34 mmol) to give brown solid (1.23 g, 93 %). $CuC_{10}H_{20}N_2S_4$. Paramagnetic.

Metal Bis(dibutyldithiocarbamate)

Synthesis of compound **9a:** dibutylamine (1.08 g, 14.67 mmol) and KOH (0.82 g, 14.67 mmol) were stirred in distilled water (100 ml) for 30 min. followed by the dropwise addition of CS_2 (1.12 g, 14.67 mmol). This solution was stirred for a further 30 min. zinc chloride (1.00 g, 7.34 mmol) was added and stirred for 30 min. The white precipitate was collected by filtration, washed successively with distilled water and air-dried to give white solid (2.44 g, 70 %), $Zn_1C_{18}H_{36}N_2S_4$. ^1H NMR ($CDCl_3$): δ 3.78 (brt,

8H, N-C*H*$_2$), 1.71 (m, 8H, J 7.4, C*H*$_2$), 1.34 (sex, 8H, J 7.4, C*H*$_2$), 0.95 (t, 12H, J 7.4, *Me*).

Synthesis of compound **9b:** follow experimental as above with dibutylamine (0.54 g, 7.34 mmol), KOH (0.41 g, 7.34 mmol), CS_2 (0.56 g, 7.34 mmol) and nickel acetate (0.91 g, 3.67 mmol) to give green solid (2.26 g, 66 %), $Ni_1C_{18}H_{36}N_2S_4$. ^{1}H NMR ($CDCl_3$): δ 3.51 (t, 8H, J 7.1, N-C*H*$_2$), 1.59 (brm, 8H, C*H*$_2$), 1.31 (brq, 8H, J 7.1, C*H*$_2$), 0.92 (t, 12H, J 7.1, *Me*).

Synthesis of compound **9c:** follow experimental as above with dibutylamine (1.08 g, 14.67 mmol), KOH (0.82 g, 14.67 mmol), CS_2 (1.12 g, 14.67 mmol) and mercury acetate (2.34 g, 7.34 mmol) to give grey solid (0.61 g, 13 %), $Hg_1C_{18}H_{36}N_2S_4$. ^{1}H NMR ($CDCl_3$): δ 3.71 (brt, 8H, N-C*H*$_2$), 1.77 (brm, 8H, C*H*$_2$), 1.33 (brm, 8H, C*H*$_2$), 0.95 (t, 12H, J 7.4, *Me*).

Synthesis of compound **9d:** follow experimental as above with dibutylamine (1.07 g, 14.67 mmol), KOH (0.83 g, 14.67 mmol), CS_2 (1.12 g, 14.67 mmol) and cadmium chloride (1.35 g, 7.34 mmol) in distilled water (50 ml) to give cream solid (2.49 g, 71 %), $Cd_1C_{18}H_{36}N_2S_4$. ^{1}H NMR ($CDCl_3$): δ 3.83 (brt, 8H, J 7.5, N-C*H*$_2$), 1.74 (brm, 8H, J 7.5, C*H*$_2$), 1.32 (sex, 8H, J 7.5, C*H*$_2$), 0.94 (t, 12H, J 7.5, *Me*).

Metal Bis(diisobutyldithiocarbamate)

Synthesis of compound **10a:** diisobutylamine (1.07 g, 14.67 mmol) and KOH (0.83 g, 14.67 mmol) were stirred in methanol (100 ml) for 30 min. followed by the dropwise addition of CS_2 (1.12g, 14.67 mmol). This solution was stirred for 30 min., zinc acetate

(1.61 g, 7.34 mmol) was added and stirred for a further 30 min. The white precipitate was collected by filtration, washed successively with distilled water and air-dried to give white solid (0.98 g, 28 %), $Zn_1C_{18}H_{36}N_2S_4$. ^{1}H NMR ($CDCl_3$): δ 3.67 (d, 8H, N-C*H*$_2$), 2.39 (sept, 4H, J 6.7, C*H*), 0.96 (d, 24H, J 6.7, *Me*).

Synthesis of compound **10b:** follow experimental as above with diisobutylamine (1.07 g, 14.67 mmol), KOH (0.83 g, 14.67 mmol), CS_2 (1.12g, 14.67 mmol) and cadmium chloride (1.34 g, 7.34 mmol) in distilled water (50 ml) to give cream solid (1.11 g, 32%), $Cd_1C_{18}H_{36}N_2S_4$. ^{1}H NMR ($CDCl_3$): δ 3.71 (d, 8H, J 7.5, N-C*H*$_2$), 2.47 (sept, 4H, J 6.8, C*H*), 0.95 (d, 24H, J 6.8, *Me*).

Synthesis of compound **10c:** follow experimental as above with diisobutylamine (1.90 g, 14.67 mmol), KOH (083 g, 14.67 mmol), CS_2 (1.12 g, 14.67 mmol) and mercury chloride (1.99 g, 7.34 mmol) in distilled water (50 ml) to give grey solid (1.79 g, 40%), $Hg_1C_{18}H_{36}N_2S_4$. ^{1}H NMR ($CDCl_3$): δ 3.60 (d, 8H, J 7.5, N-C*H*$_2$), 2.42 (sept, 4H, J 6.9, C*H*), 0.96 (d, 24H, J 6.9, *Me*).

Synthesis of compound **10d:** follow experimental as above with diisobutylamine (1.90 g, 14.67 mmol), KOH (083 g, 14.67 mmol), CS_2 (1.12 g, 14.67 mmol) and copper chloride dihydrate (1.25 g, 7.34 mmol) in distilled water (50 ml) to give brown solid (2.25 g, 64%), $Cu_1C_{18}H_{36}N_2S_4$. ^{1}H NMR ($CDCl_3$): δ 3.60 (d, 8H, J 7.5, N-C*H*$_2$), 2.42 (sept, 4H, J 6.9, C*H*), 0.96 (d, 24H, J 6.9, *Me*).

Synthesis of compound **10e:** follow experimental as above with diisobutylamine (1.90 g, 14.67 mmol), KOH (083 g, 14.67 mmol), CS_2 (1.12 g, 14.67 mmol) and nickel

chloride hexahydrate (3.49 g, 14.67 mmol) in distilled water (50 ml) to give green solid (2.44 g, 71%), $Ni_1C_{18}H_{36}N_2S_4$. ^1H NMR ($CDCl_3$): δ 3.40 (d, 8H, J 7.6, N-C*H*$_2$), 2.17 (sept, 4H, J 6.8, C*H*), 0.91 (d, 24H, J 6.8, *Me*).

4.47 Experimental Procedure for Polymerisation Reactions.

Small-scale test tube reactions were undertaken in a fumehood as PO is toxic. The catalyst (approximately 0.01-0.05 g) was placed in a test tube with PO (2 ml), sealed and stirred for 17 h. with a magnetic stirrer. Each catalyst was tested twice, once as above and the other with EtOH (2 ml) to initiate the reaction. The product was then dissolved in dichloromethane (DCM) (2 ml) and pumped dry on the vacuum line for 10 min. to remove residual PO. The product was characterised using NMR and IR and the degree of polymerisation if any, was recorded.

4.5 References

[1] V. F. Plyusnin, V. P. Grivin, S. V. Larionov, *Coordination Chemistry Reviews* **1997**, *159*, 121.
[2] L. I. Victoriano, *Coordination Chemistry Reviews* **2000**, *196*, 383.
[3] R. B. King, *Encyclopedia of Inorganic Chemistry* 2ed., Wiley, New York, **2005**.
[4] G. Hogarth, *Prog. Inorg. Chem.* **2005**, *53*, 71.
[5] D. Coucouvanis, *Prog. Inorg. Chem.* **1977**, *11*, 233.
[6] M. Zhou, J. Wang, H. Li, CN A 20050817, **2005**.
[7] J. Speakman, R. Stierl, S. Strathmann, P. Dombo, M. Niedenbrueck, V. Egon, **2006**,
[8] H. Koehle, R. Stierl, E. Randall, F. Goerth, WO A1 20060601 **2006**.
[9] D. A. Cauzzi, G. Mori, G. Predieri, A. Tiripicchio, F. Cavatorta, *Inorganica Chimica Acta* **1993**, *204*, 181.
[10] M. F. Perpinan, L. Ballester, M. E. Gonzalez-Casso, A. Santos, *Journal of the Chemical Society, Dalton Transactions,* **1987**, 281.
[11] W. Braune, J. Okuda, *Angewandte Chemie-International Edition* **2003**, *42*, 64.
[12] J. Chatt, L. A. Duncanson, L. M. Venanzi, *Nature* **1956**, *177*, 1042.
[13] A. I. El-Said, A. S. A. Zidan, M. S. El-Meligy, A. A. M. Aly, O. F. Mohammed, *Transition Metal Chemistry* **2001**, *26*, 13.
[14] P. J. Heard, *Prog. Inorg. Chem.* **2005**, *53*, 1.
[15] J. L. Cui, Z. M. Ge, T. M. Cheng, R. T. Li, *Synthetic Communications* **2003**, *33*, 1969.

Chapter 5

Arenes with Dithiocarbamates

5.1 Introduction

In the last chapter, we saw how the dithiocarbamates ring-opened epoxides to form organic dithiocarbamates. A second route to these compounds would be through the simple nucleophilic substitution of organic halides. In this context, benzyl halides have attracted attention to the role products can play in living polymerisation reactions.

Recent work has involved hyperbranched polymer systems with diethyldithiocarbamate compounds. Various mechanisms of living polymerisation have been used, including living cationic polymerisation[1], group-transfer polymerisation[2] and atom transfer radical polymerisation[3, 4]. These systems have been used to polymerise an assortment of monomers e.g. styrene[5], vinyl chloride[6], *para*-phenylene vinylene[7] and ethyl methacrylate[8] using both thermal treatment and photolysis to form radicals and initiate reactions.

One leading research group considered using designer polymers for gene delivery[9]. They synthesised hyperbranched star polymers from multi-dithiocarbamate substituted benzene rings. Based on pioneering work by Ostu *et al.*[10-12], compounds were formed by iniferter (*ini*tiator-trans*fer* agent-*ter*minator) based photo-living polymerisation. For example, the iniferter in this case, benzyl *N,N*-diethyldithiocarbamate was irradiated with UV light to dissociate the weak bonds, forming the benzyl radical and the diethyldithiocarbamyl radical. The monomer units were inserted by propagation *via* the benzyl radical, which was responsible for polymer formation by reacting with the vinyl (i.e. 3-(*N,N*-diemthylamino)propyl acrylamide). The polymer chain could continue growing in the presence of monomers and irradiation or undergo chain transfer. The dithiocarbamyl radical does not favour reacting with the vinyl but instead prefers chain

termination[9]. As this polymerisation required irradiation to proceed, the length of the polymer chains were controlled by the time of irradiation, the intensity of irradiation and the composition of solution. The end polymer product had iniferter bonds at the chain ends, which could further react in the presence of monomer units and irradiation (Scheme 1).

Scheme 1: Iniferter-based photo-living polymerisation using benzyl *N,N*-diethyldithiocarbamate[9]

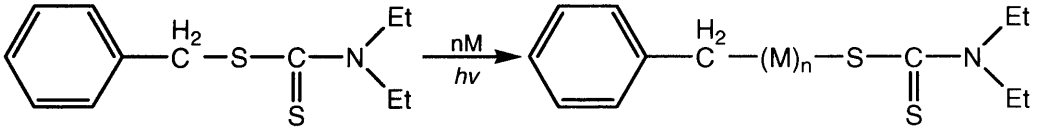

There are many other attractive applications of dithiocarbamate compounds such as their uses in forming liquid crystals[13], precursors for organometallic compounds[14] as well as displaying complexing abilities[15, 16]. These potential applications have led to academic research in organic arene systems with multi-arms extending from the core structure (typically a benzene ring)[16-21]. These "arms" normally consist of alkyl groups or modifications of an alkyl group with a heteroatom end. Researchers have used various types of arms to investigate the stereochemistry of the structures. In a typical system with a planar benzene ring and six ethyl arms, there are many possible conformations: eclipsed (**a**), staggered (**b** and **c**) and perpendicular (**d**)[22] (Figure 1 and note that only one ethyl unit is displayed for clarity).

Figure 1: Four possible conformations of an arene system[23]

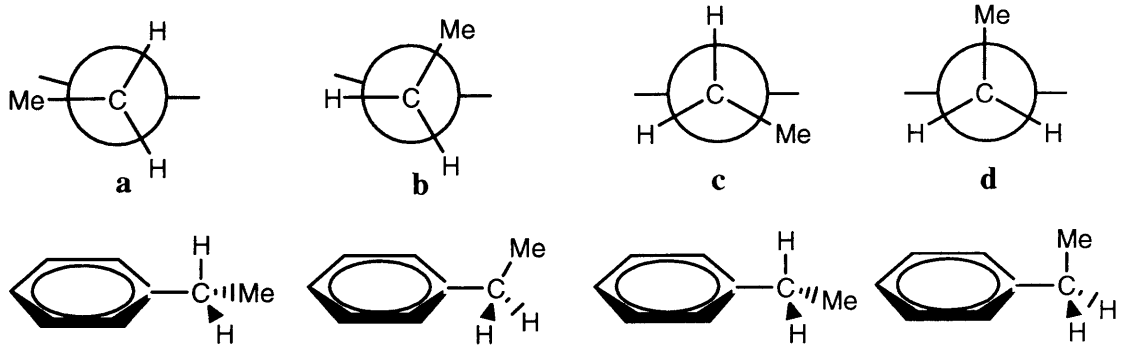

Conformations **a-c** are energetically unfavourable due to steric repulsion between the CH_3 moiety of the ethyl groups relative to its neighbouring methyl groups from the ethyl arms. Therefore the prevailing conformation would be the perpendicular structure (**d**)[17]. To further reduce the repulsion between the ethyl arms, they organise themselves in an alternate "up-down" arrangement related to the plane. This arrangement is favoured by many similar compounds such as hexa-*n*-propylbenzene[18], hexakis(bromomethyl)benzene[19] and all *trans*-1,2,3,4,5,6-hexaethylcyclohexane[23].

Hexakis(bromomethyl)benzene has been favoured in this type of work as the sidearms are analogous to the ethyl groups while the bromide can be readily displaced by a range of nucleophiles[23]. Substitutions of bromide has led to a whole host of compounds such as **1**[24] and **2**[25] in Figure 2.

Figure 2: Examples of multi-armed benzene rings 1-2[24, 25]

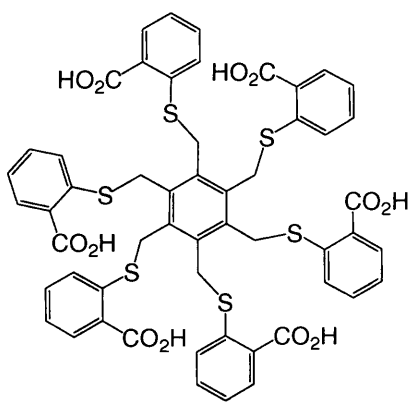

1

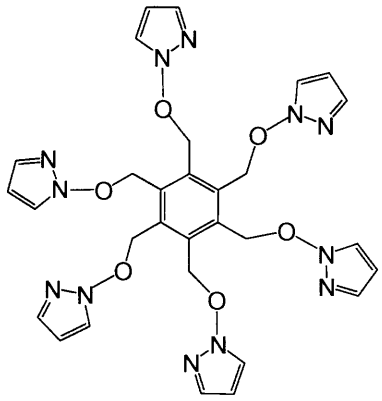

2

An interesting observation was that the conformation of the arms is dictated by the bulk of the transition metal core. For example, Hunter *et al.*[21] found that hexaethylbenzene coordinated to $Cr(CO)_3$ and the "up-down" orientation of the ethyl arms was maintained (**1** in Figure 3). However, when the arene was bound to $Cr(CO)_2PPh_3$ (**2**), the ethyl arms arranged themselves to point away from the metal centre.

Figure 3: Hexaethylbenzene coordinated to $Cr(CO)_3$ (1) with "up-down" orientation of the ethyl arms verses the orientation of $Cr(CO)_2PPh_3$ (2)[21]

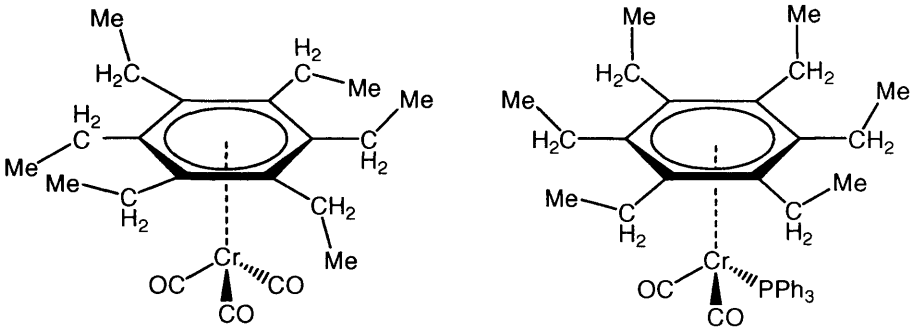

1 2

Another arene, 1,3,5 tris(bromomethyl)-2,4,6-triethyl benzene was used to form ligands that could be used to coordinate with metal ions (Figure 4). When reacted with various copper compounds, crystalline complexes of the type $[(CuI)_3L]$ and $[(CuNCMe)_3L][PF_6]_3$ were formed[26]. Binding of the aromatic methylene arms with the copper compounds resulted in their positioning on one side of the plane of the benzene ring with the three ethyl arms on the other side. This showed that the original "up-down" orientations of the arms were retained. This tridentate ligand formed metal complexes where the donor metal core was bound to one side of the ring thereby retaining the preferred 'up-down' stereochemistry.

Figure 4: Structure of ligand (L) derived from 1,3,5 tris(bromomethyl)-2,4,6-triethyl benzene[26]

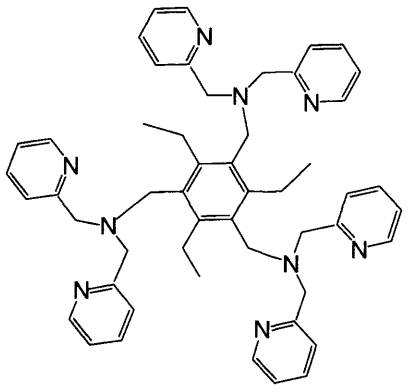

L

Following on from the dithiocarbamate compounds of Chapter 3, we have considered reacting various arene rings with dithiocarbamates to form multi-substituted arenes with multifunctional arms. By varying the R-groups of the dithiocarbamates, we hoped to form a range of compounds and study the orientation of the arms in relation to the size of the R-group. Other possibilities included having charged R-groups, which would facilitate further addition onto the multifunctional arms. Once these compounds were formed, we hoped to use photolysis to insert monomers into the chains *via* living polymerisation to generate novel polymers.

5.2 Results and Discussion

Both purchased and synthesised dithiocarbamate salts were reacted with four different arene rings with bromomethyl moieties. These had two (1, 4-di-α,α-(bromomethyl)benzene) (**1**), three (1,3,5-tris(bromomethyl)-2,4,6-trimethylbenzene) (**2**), four (1,2,4,5-tetrakis(bromomethyl)benzene) (**3**) and six (hexakis(bromomethyl)benzene) (**4**) bromomethyl substituents (Figure 5).

Figure 5: Structure of the four arene systems investigated.

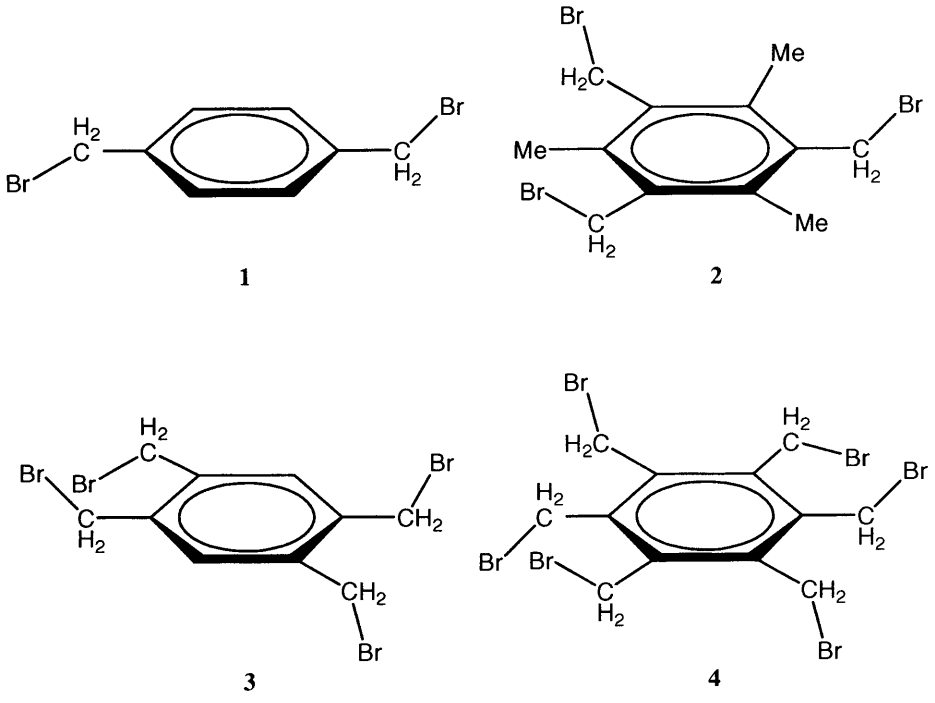

All gave cream-white solids, which were collected and characterised using NMR, IR, MS and elemental analysis. The results for these systems will be discussed in two sections, firstly in terms of classes of arene rings and secondly, exploring the effects of the R-groups on the dithiocarbamates.

5.21 1,4-α,α-di(bromomethyl)benzene

1,4-α,α-di(bromomethyl)benzene (**1**) was reacted with different dithiocarbamate ligands and a selection of compounds were formed in moderate to high yields (**1a-e**) (Figure 6). Utilising numerous spectroscopic techniques, these compounds were characterised and parallels were identified.

Figure 6: 1,4-α,α-di(bromomethyl)benzene system with various dithiocarbamate ligands (displayed in the proposed up-down orientation)

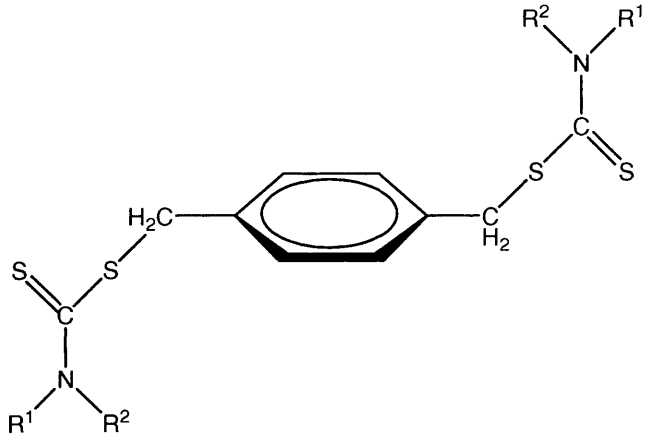

1a	$R^1 = R^2 = Me$
1b	$R^1 = R^2 = Et$
1c	$R^1 = R^2 = {}^iBu$
1d	$R^1 = Me$, $R^2 = Bu$
1e	$R_2 = C_5H_{10}$

Using ^1H NMR spectroscopy, the formations of the desired compounds were confirmed and peaks clearly identified. For example, the ^1H NMR spectrum for **1a** showed a symmetrical structure, the aromatic protons appearing as a singlet at δ 7.33. While the

methylene groups appeared as a singlet at δ 4.52. Two singlets at δ 3.35 and 3.51 were assigned to the inequivalent methyl environments, the higher δ value due to their adjacent nitrogen atom of the dithiocarbamate fragment.

The proposed structure was confirmed by the corroborative data provided by IR stretches ν(C-N) at 1250 - 1020 cm^{-1}, ν(C-S) at 1575 - 1450 cm^{-1}, ν(C-H) at 2980 - 2850 cm^{-1}, ν(CH_2-N) 2820 - 2760 and 1475 - 1445 cm^{-1} and finally the aromatic ν(C-C) at 1600 - 1400 and ν(C-H) at 3100 - 3000 cm^{-1}. The MS spectrum identified the correct parent ion of 345 (M^+). The elemental analysis values for compound **1a** showed excellent correlation between the calculated (C, 48.80; H, 5.85; N, 8.13) and found (C, 48.68; H, 5.98; N, 8.03) values for carbon, hydrogen and nitrogen.

The other compounds in this series were analysed in the same manner and the information collated. The data for each compound in this series confirmed the proposed structure and was fully characterised. As observed in Chapter 3, the N-methylbutyl R-group formed rotational conformers, which were observed in **1d** in a 1: 1 ratio. Two individual N-methyl groups confirmed this with singlets at δ 3.28 and 3.49 as well as the overlapping two triplets at δ 0.95, which appears as pseudo quartet, representing the butyl's end methyl groups. Although the elemental analysis of **1d** was poor, the abundant NMR, IR and accurate parent ion from MS confirmed the proposed structure. The characterisation data for **1e** also showed sufficient evidence to substantiate the proposed structures.

In this section, the core structure of di-substituted benzene ring (benzene ring protons and the two methylene protons arms) is discussed. The proton NMR peaks for the core

structure of all the compounds (**1a-e**) were compared to investigate any electronic effects of differing R-groups on the dithiocarbamates. The aromatic protons on all these compounds (**1a-e**) were virtually identical in the range δ 7.32 – 7.33, which was typical for these types of aromatic protons. All the methylene protons attached to the benzene ring also exhibited peaks practically identical between δ 4.51 - 4.53. Although the R-groups on the dithiocarbamate ligands vary considerably in size and electronic properties, the four bonds between the R-groups and methylene protons appeared to be a sufficient distance to have no effect on the core protons peaks.

From this work, we were able to confirm the formation of the desired compounds and characterise them. However, the orientation of the arms could not be determined from this data and so attempted to grow single crystals for X-ray diffraction. Unfortunately, we were unable to grow X-ray quality crystals and therefore, unable to determine if the multifunctional arms were orientated *syn* or *anti* in relation to the benzene ring.

5.22 1,3,5-tris(bromomethyl)-2,4,6-trimethylbenzene (2)

In the case of the compounds **2a-e**, a mesitylene-type benzene ring was used as the core structure on which to build dithiocarbamate fragments (Figure 7). As these aromatic rings lacked protons, the three methyl groups positioned at 2, 4, 6- on the benzene ring allowed a comparison between standard substituted benzene rings (**1, 3, 4**) with a mesitylene ring (**2**). Compounds **2a-e** were formed using the standard procedure with 1,3,5-tris(bromomethyl)-2,4,6-trimethylbenzene[27]. The white-cream solids were formed in yields of 55 – 92 % and were characterised using the standard techniques.

Figure 7: 1,3,5-tris(bromomethyl)-2,4,6-trimethylbenzene system with various dithiocarbamates

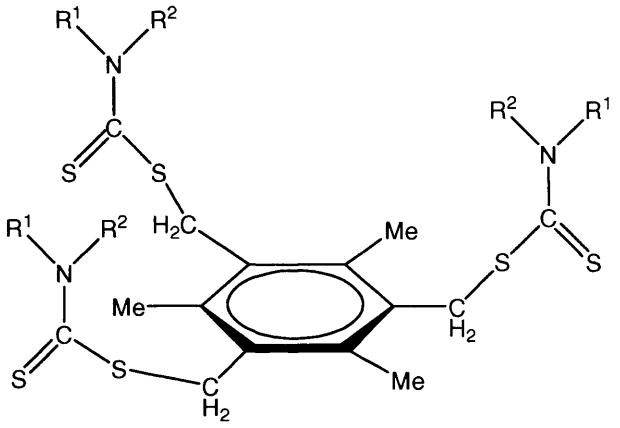

2a	$R^1 = R^2 = Me$
2b	$R^1 = R^2 = Et$
2c	$R^1 = R^2 = {}^iBu$
2d	$R^1 = Me$
	$R^2 = Bu$
2e	$R_2 = C_5H_{10}$

As a representative example, the ^1H NMR spectrum for **2a** showed the aromatic methyl groups at the 2, 4 and 6 positions as a singlet at δ 2.40. The aromatic methylene protons were at δ 4.44 as a singlet with the dithiocarbamate methyl groups inequivalent at δ 3.33 and 3.57. The ^{13}C NMR and IR data were in agreement with the proposed structure with the MS parent ion at 515 (M^+). The elemental analysis displayed excellent correlation to the calculated values of C, 48.51; H, 6.40; N, 8.08 and found C, 48.49; H, 6.43; N, 7.93. The other compounds (**2b-e**) in this series were analysed in the same manner and the data collated. The data for each compound in this series confirmed the structure and was fully characterised despite the poor elemental analysis results of **2d**.

The core structure in this series consisted of the aromatic methyl groups and the aromatic methylene fragments. When comparing the values for the methyl proton peaks down the series, a consistent value of δ 2.40 was observed. The aromatic methylene protons were also found to be within the range δ 4.35 - 4.47. These values were almost

0.6 ppm lower than that of the other systems, which had values in the range of δ 4.51 – 4.53. This difference was attributed to the three methyl groups donating electrons into the aromatic ring which increased shielding on the aromatic methylene protons, therefore reducing the chemical shift value.

Figure 8 represents a collection of ^{1}H NMR spectra of compounds **2a** at different temperatures in the range of 298 – 373 K. This stack plot clearly identified the aromatic methylene group at δ 4.50 and the inequivalent methyl groups at δ 3.34 and 3.52 at 298 K. As the temperature increases, these two peaks collapse into one (coalesce) at 333 K. As the temperature continues to rise to 373 K, these methyl groups fluctuate faster to form one sharp peak showing equivalency in NMR timescale for both methyl groups.

Figure 8: Variable temperature ^{1}H NMR stack plot of 2a (298-373 K)

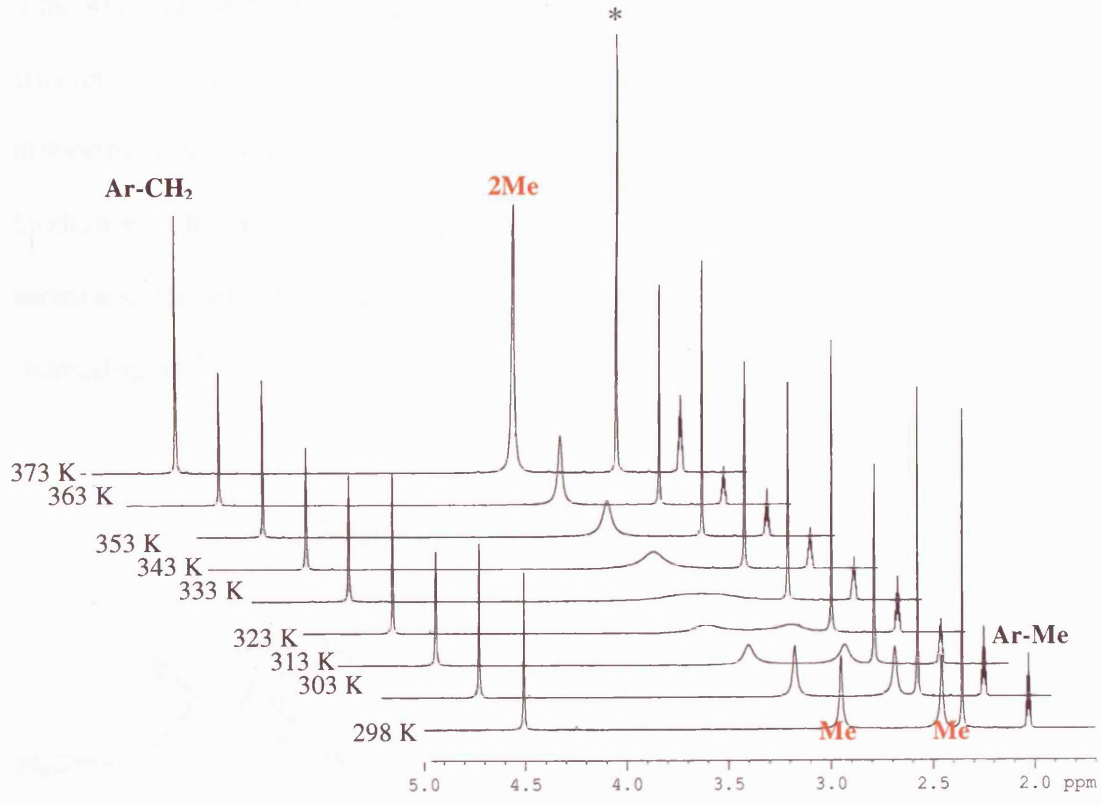

* - known impurity

Variable temperature ^1H NMR studies were undertaken on this series to collate the coalescence temperature and the free energies of activation (Table 1). The activation energy values for **2b** and **2d** were in the range of approximately $\Delta G^{\ddagger} \approx 65$ kJ mol^{-1}. Compound **2e** with a ring amine had a lower value of 62.1 kJ mol^{-1} compared to the linear R-groups.

Table 1: Coalescence temperatures and free energies of activation for arene system 2 compounds

Tri-substituted benzene compounds		Coalescence Temperature (K)	Δν (Hz)	ΔG‡ (kJ mol^{-1}) (± 1)
Dimethyl	**(2a)**	333	197.62	65.0
Diethyl	**(2b)**	328	135.13	65.1
N-Methylbutyl	**(2d)**	333	143.08	65.9
Piperidine	**(2e)**	318	188.90	62.1

Using molecular mechanic calculations, the angle between C=N-R was predicted for the dimethyl compound **2a** and piperidine **2e** (see below). It could be plausible that the smaller $\Delta G^{\ddagger}$ for compound **2e** is due to the larger angle between the amine part of the dithiocarbamate and the bulk of the rest of the molecule. This could result in less steric hindrance, allowing easier rotation about the C-N bond. As the size of R-groups increases, the energy required to rotate about the bond also increases, leading to increasing $\Delta G^{\ddagger}$.

Figure 9: Comparison of the angles of C=N-R

To investigate the orientation of the arms relative to the arene ring, single crystal X-ray diffraction of **2a** and **2b** were completed. The quasi-cubic single-crystal structure of **2a** was crystallised in the monoclinic space group ($P_{21/n}$). This colourless crystal structure had all three of the dithiocarbamate arms on one side of the plane, which was assumed to be the conformational ground state (Figure 10).

Figure 10: Crystal structure of 1,3,5-tris(bromomethyl)-2,4,6-trimethylbenzene with dimethyldithiocarbamate (2a)

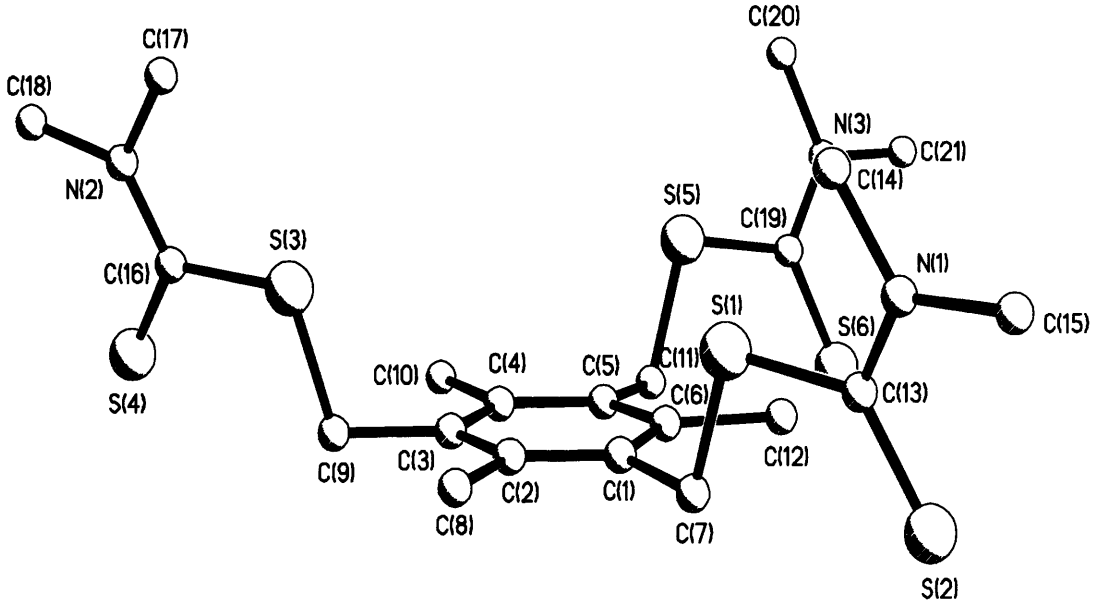

The stacking arrangement of **2a** showed the benzene rings lying parallel to each other with the arms facing away from the rings. This allowed optimal packing of the compound with the lowest energy. The R_1 values of 0.0437 showed excellent correlation between the proposed structure and the observed crystal structure (Figure 11).

Figure 11: Stacking arrangement of 1,3,5-tris(bromomethyl)-2,4,6-trimethylbenzene with dimethyldithiocarbamate (2a)

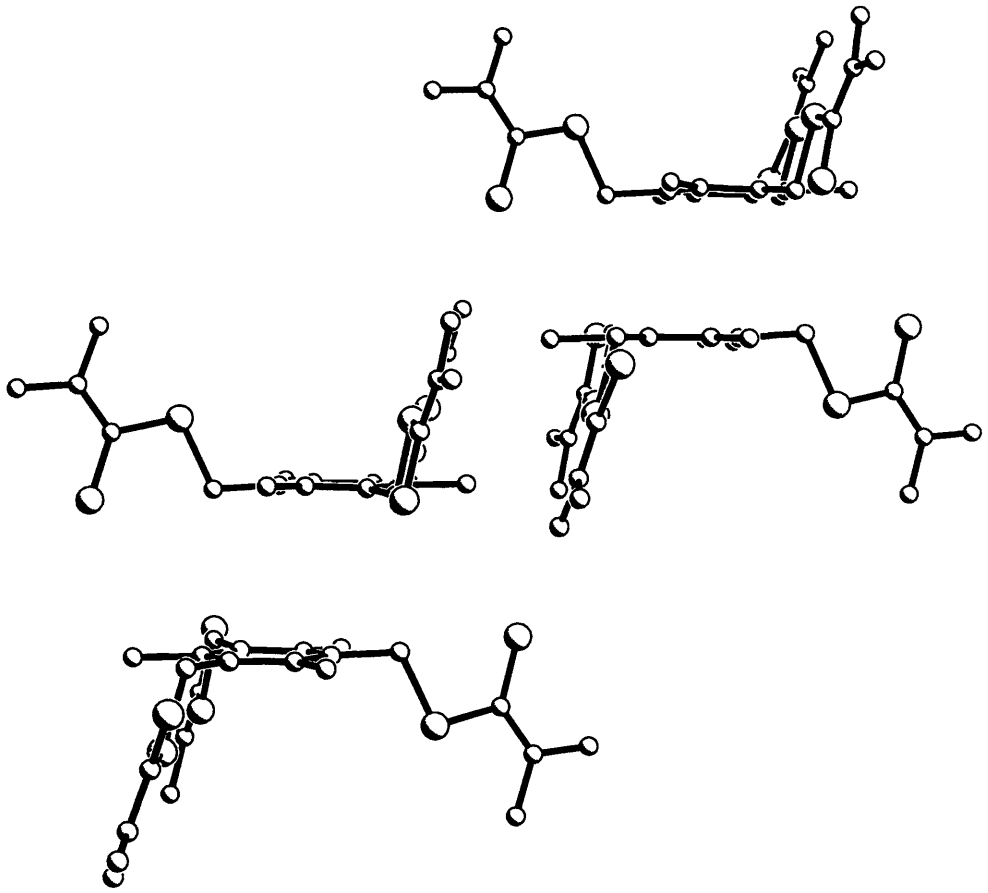

On close examination of the crystal, the bond lengths of the benzene ring were consistent with the expected length. Comparison of all three dithiocarbamate arms showed agreement in bond lengths of each arm. The other bonds off the benzene ring to the methyl groups and the aromatic methylene were within the anticipated range. Table 2 demonstrates the average bond length of the various dithiocarbamate arms.

Table 2: Selected bond lengths of 1,3,5-tris(bromomethyl)-2,4,6-trimethylbenzene with dimethyldithiocarbamate (2a)

	Bond	Length (Å)
Aromatic Ring carbon	Average bond	1.400(3)
Aromatic Ring carbon-Me	C(2)–C(8)	1.516(3)
Aromatic Ring carbon-CH_2	C(1)–C(7)	1.509(3)
CH_2-SCS	S(1)–C(7)	1.817(2)
S-CS	S(1)–C(13)	1.770(2)
SC=S	S(2)–C(13)	1.674(2)
N-CS_2	N(1)–C(13)	1.333(3)
N-Me	N(1)–C(15)	1.458(3)

The crystal structure showed a range of bond angles, all consistent with the predicted values (Table 3). The benzene ring holds the carbons close to 120° to maximise separation between them. The other angles all compare well with the expected geometry.

Table 3: Bond angles of 1,3,5-tris(bromomethyl)-2,4,6-trimethylbenzene with dimethyldithiocarbamate (2a)

	Bond	Angle (°)
Aromatic Ring carbon	C(1)–C(2)–C(3)	119.10(18)
Aromatic Ring carbon-Me	C(1)–C(2)–C(8)	119.29(18)
Aromatic Ring carbon-CH_2	C(2)–C(1)–C(7)	120.19(18)
Aromatic Ring carbon-CH_2-S	C(1)–C(7)–S(1)	108.54(13)
CH_2-S-CS	C(13)–S(1)–C(7)	103.41(9)
S-C=S	S(2)–C(13)–S(1)	122.76(11)
N-C=S	N(1)–C(13)–S(1)	112.94(14)
N-C-S	N(1)–C(13)–S(2)	124.30(15)
S_2C-N-Me	C(13)–N(1)–C(15)	121.62(18)
Me-N-Me	C(15)–N(1)–C(14)	115.42(17)

The single crystal of **2b** was a colourless rectangle with a co-crystallised molecule of $CHCl_3$. The interesting observation in this crystal structure was the arrangement of the three diethyldithiocarbamate arms. In compound **2a** with the dimethyldithiocarbamate arms, all the arms were on one side of the benzene ring whereas with the diethyl

equivalent, two arms were on one side and the third arm was on the other side (Figure 12).

Figure 12: Crystal structure of 1,3,5-tris(bromomethyl)-2,4,6-trimethylbenzene with diethyldithiocarbamate (2b)

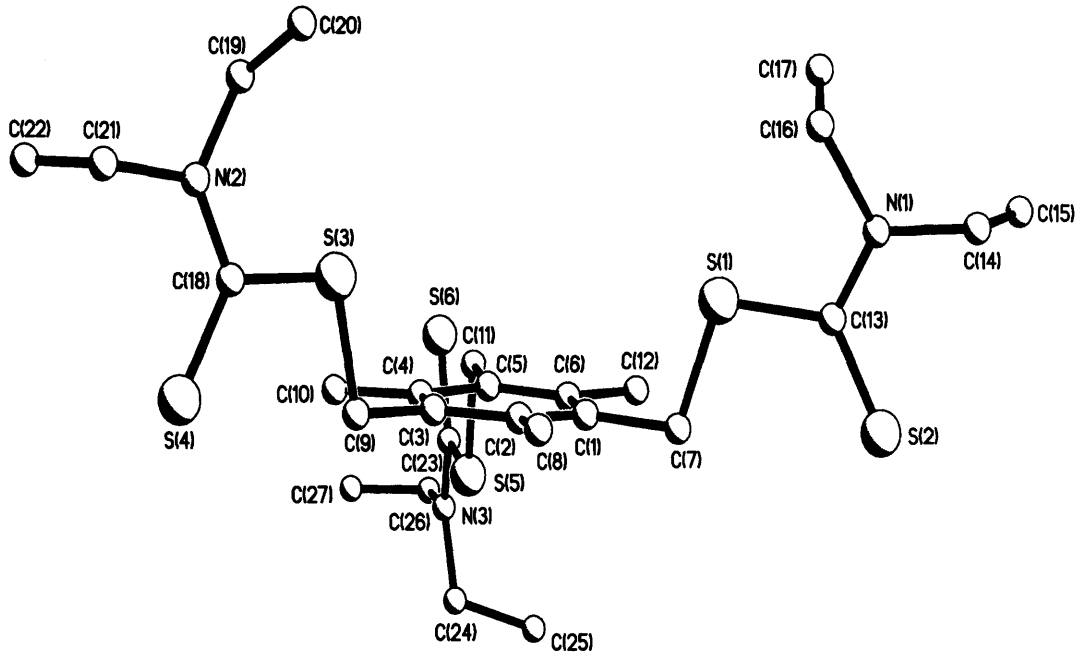

The stacking arrangement in this crystal was interesting as due to steric repulsion, the likely structure would involve the benzene rings parallel to each other with the one dithiocarbamate arm pointing downward and the two arms pointing away from the ring. However, the actual structure attained was the opposite, the benzene rings were parallel to each other but both arene rings arranged the two arms downwards, facing each other and the single arm on the other side pointing away as displayed in Figure 13.

Figure 13: Stacking arrangement of two units of 2b.

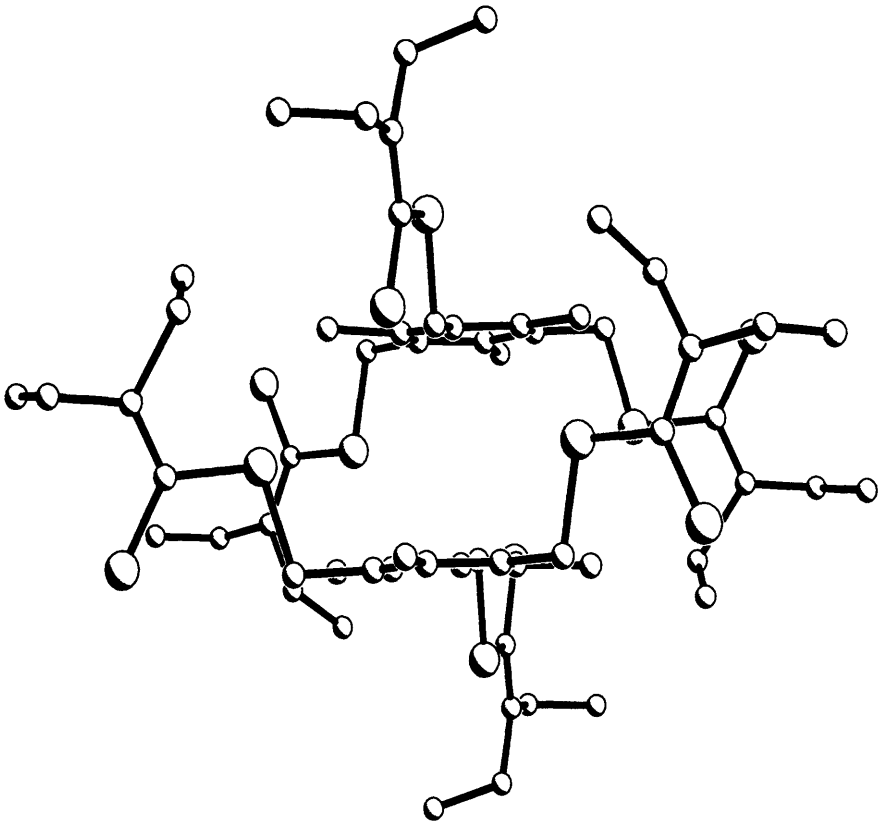

A comparison of the bond lengths of the two dithiocarbamate arms on the same side showed agreement in the values. Comparison of an upward dithiocarbamate arm and a downward arm followed below showed good agreement (Table 4). The bond lengths all followed the expected values and compared well with the similar compound **2a** with the dimethyl groups. Both dithiocarbamate arm bond length values were in good agreement with two small exceptions. The upward dithiocarbamate arm had two inconsistent values for N-CH_2 and CH_2-Me with high errors. The reason for this discrepancy was probably due to the solvent in the crystal structure and the high R_1 value of 0.1076.

Table 4: Bond lengths for the crystal structure of 1,3,5-tris(bromomethyl)-2,4,6-trimethylbenzene with diethyldithiocarbamate (2b)

	Bond	Length (Å)
Aromatic Ring carbon	Average Bond	1.386(7)
Aromatic Ring carbon-Me	C(2)–C(8)	1.509(7)
Aromatic Ring carbon-CH_2	C(1)–C(7)	1.515(7)
CH_2-S	S(1)–C(7)	1.806(5)
S-C	S(1)–C(13)	1.745(6)
C=S	S(2)–C(13)	1.639(7)
N-C	C(13)–N(1)	1.316(10)
N-CH_2	C(16)–N(1)	1.777(18)
CH_2-Me	C(14)–C(15)	1.583(19)

The bond angles in this crystal were consistent with the expected values of the different arms as well as with **2a**. The only inconsistent angle was between N-CH_2-Me. The applicable bond lengths forming this angle were already incoherent values leading to a smaller angle than anticipated (Table 5).

Table 5: Bond angles of 1,3,5-tris(bromomethyl)-2,4,6-trimethylbenzene with diethyldithiocarbamate (2b)

	Bond	Angle (°)
Aromatic Ring carbon	C(1)–C(2)–C(3)	119.5(4)
Aromatic Ring carbon-Me	C(1)–C(2)–C(8)	120.5(5)
Aromatic Ring carbon-CH_2	C(2)–C(1)–C(7)	119.0(4)
CH_2-S-CS	C(13)–S(1)–C(7)	104.2(3)
S-C=S	S(2)–C(13)–S(1)	123.3(4)
N-C=S	N(1)–C(13)–S(2)	123.0(5)
N-C-S	N(1)–C(13)–S(1)	113.7(5)
S_2C-N-CH_2	C(13)–N(1)–C(14)	121.7(8)
N-CH_2-Me	N(1)–C(14)–C(15)	113.9(13)
CH_2-N-CH_2	C(14)–N(1)–C(16)	115.0(9)

Two single-crystal structures were determined with the expected geometry attained. With the exception of compound **2b**, the lowest conformational geometry prevailed. The structure of **2b** was unusual with the lack of symmetry but the inclusion of a solvent molecule could explain the unexpected geometry.

This section of work using the series **2** showed that all the compounds were formed successfully and well characterised. From the single crystal data, we were able to examine any effects of the methyl groups at the 2, 4 and 6 positions on the orientation of the arms. In **2a**, we observed all the dithiocarbamate arms were arranged on one side of the arene ring and this allowed effective stacking of the rings. In the case of **2b**, the inclusion of the $CHCl_3$ molecule could explain why this orientation was not observed.

5.23 1,2,4,5-tetrakis(bromomethyl)benzene (3)

The compounds **3a-e** (Figure 14) were formed as white-yellow solid in yields of 50 – 70 % following the standard procedure.

Figure 14: 1,2,4,5 tetrakis(bromomethyl)benzene system with various dithiocarbamate ligands (displayed in the proposed up-down orientation)

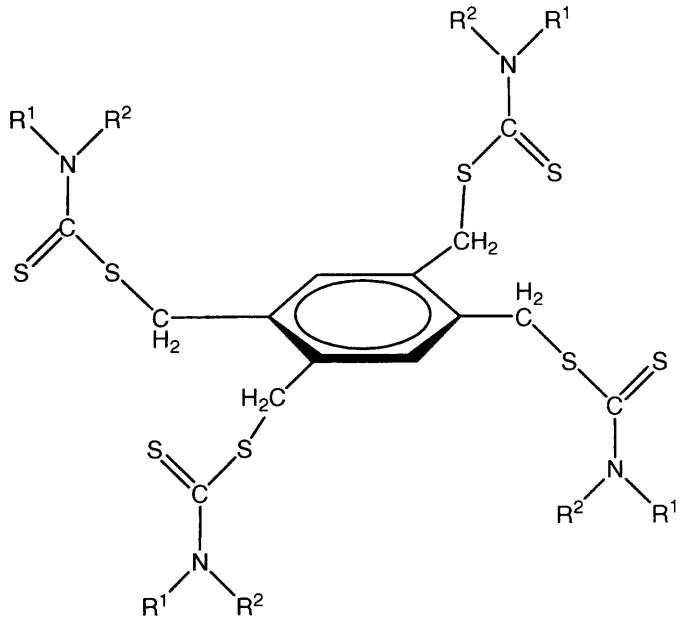

3a	$R^1 = R^2 = Me$
3b	$R^1 = R^2 = Et$
3c	$R^1 = R^2 = {}^iBu$
3d	$R^1 = Me$, $R^2 = Bu$
3e	$R_2 = C_5H_{10}$

The ^{1}H NMR spectra of these compounds were similar to compounds **1a-e.** For example, in **3a,** the aromatic protons appeared as a singlet at δ 7.46 and the aromatic methylene protons at δ 4.56. The inequivalent methyl groups were singlets at δ 3.35 and 3.51. Other characteristic data collected corroborated the desired structure *via* ^{13}C NMR, IR and MS with a parent ion of 634 (M^{+}). The elemental analysis data exhibited good agreement with the calculated and found values for the structure; calculated C, 43.24; H, 5.61; N, 9.17 and found C, 42.16; H, 5.53; N, 8.48.

The other compounds (**3b-e**) in this series were analysed in the same manner and the information collated. The data for each compound in this series confirmed the structure and was fully characterised despite the poor elemental analysis results of **3b-d**.

The core arene structures of these tetra-substituted compounds were similar to the di-substituted benzene ring system. The ^{1}H NMR spectral peaks of the core structure in this series were almost identical to the di-substituted compounds (**1a-e**). The aromatic protons peaks of the tetra-substituted compounds were slightly higher than the di-substituted between δ 7.46 - 7.48 which were typically in the range of aromatic protons. The methylene protons attached to the benzene ring were also similar despite the varying R-groups at δ 4.56 - 4.59. These peaks were higher than the equivalent peaks in the di-substituted benzene ring by approximately 0.5 ppm.

This study of tetra-substituted compounds showed that a variety of dithiocarbamates could be bonded with the arene system to form multifunctional arms. Attempts to grow single crystals for X-ray diffraction were unsuccessful and therefore the orientation of the arms could not determined.

5.24 Hexakis(bromomethyl)benzene (4)

Compounds **4a-e** were formed using the established procedure to give white solids in high yields (Figure 15).

Figure 15: Hexakis(bromomethyl)benzene systems with various dithiocarbamate ligands

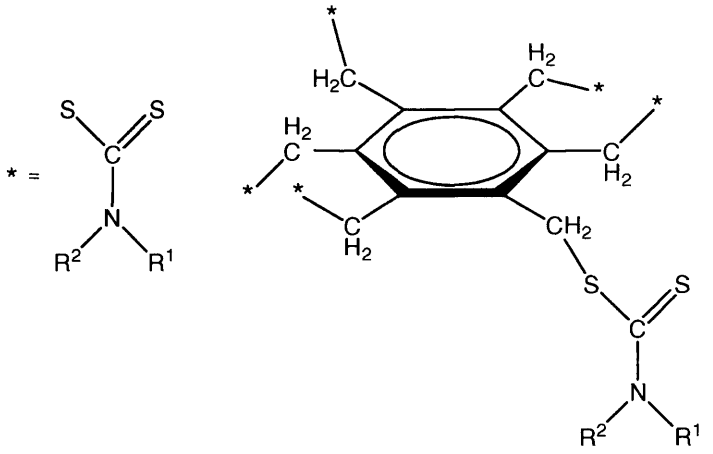

4a	$R^1 = R^2 = Me$
4b	$R^1 = R^2 = Et$
4c	$R^1 = R^2 = {}^iBu$
4d	$R^1 = Me$, $R^2 = Bu$
4e	$R_2 = C_5H_{10}$

These compounds were characterised using the standard techniques as well as *via* variable temperature NMR studies in the temperature range of 298 – 333 K. Although ^1H NMR spectral data confirmed the proposed formulation, other spectroscopic data were limited due to their reduced solubility.

As there were no aromatic protons on this benzene ring, the core structure was assessed based on the aromatic methylene proton fragment. These peaks for this system were similar to the di- and tetra-substituted methylene protons in the range of δ 4.51 - 4.57. The peaks observed in the ^1H NMR spectra were broad which led to the possibility of rotamers in the solution in the temperature range of 298 – 333 K.

As the temperature increased, the rotation about the C-N bond increased, allowing the proton units nearest to the nitrogen atom to interchange on the NMR timescale so that coalescence was observed. Using the spectral data and Equation 2 from Chapter 3 (p. 109), the coalescence temperatures and the free energy of activation values were approximated (Table 6).

Table 6: Coalescence temperatures and free energies of activation for compounds 4a-e.

Hexa-substituted benzene compounds			Coalescence Temperature (K)	Δν (Hz)	$\Delta G^{\ddagger}$ (kJ mol^{-1}) (± 1)
Dimethyl	**(4a)**		318	72.90	64.6
Diethyl	**(4b)**		323	114.10	64.5
Diisobutyl	**(4c)**		328	103.78	65.8
N-Methylbutyl	**(4d)**	N-Me	323	72.03	65.7
		$N-CH_2$	330	121.92	65.7
Piperidine	**(4e)**		308	152.86	60.6

The ^1H NMR spectra of **4d** clearly displayed the appropriate resonances to confirm that this compound formed rotational conformers in a ratio of 1: 1. The stacked plot of spectra in Figure 16 represents a collection of ^1H NMR spectra of **4d** at different temperatures in the range of 233 – 373 K. The stack plot clearly identified the aromatic methylene group at δ 4.54. It also clearly showed the inequivalent methylene protons (δ 3.69 and 4.01) of the butyl, nearest to the nitrogen and the N-methyl group at δ 3.28 and 3.45. As the temperature increases, the N-methyl singlets begin to merge and collapse to mark coalescence at 323 K and the $N-CH_2$ of the butyl coalescence at 330K, both with $\Delta G^{\ddagger}$ 65.7 kJ mol^{-1}. Another observation is that the broad peaks of the other methyl and methylene protons of the butyl fragments begin to sharpen with temperature, producing better resolved peaks.

Figure 16: Variable temperature ^{1}H NMR stack plot of 4d (233 - 333 K)

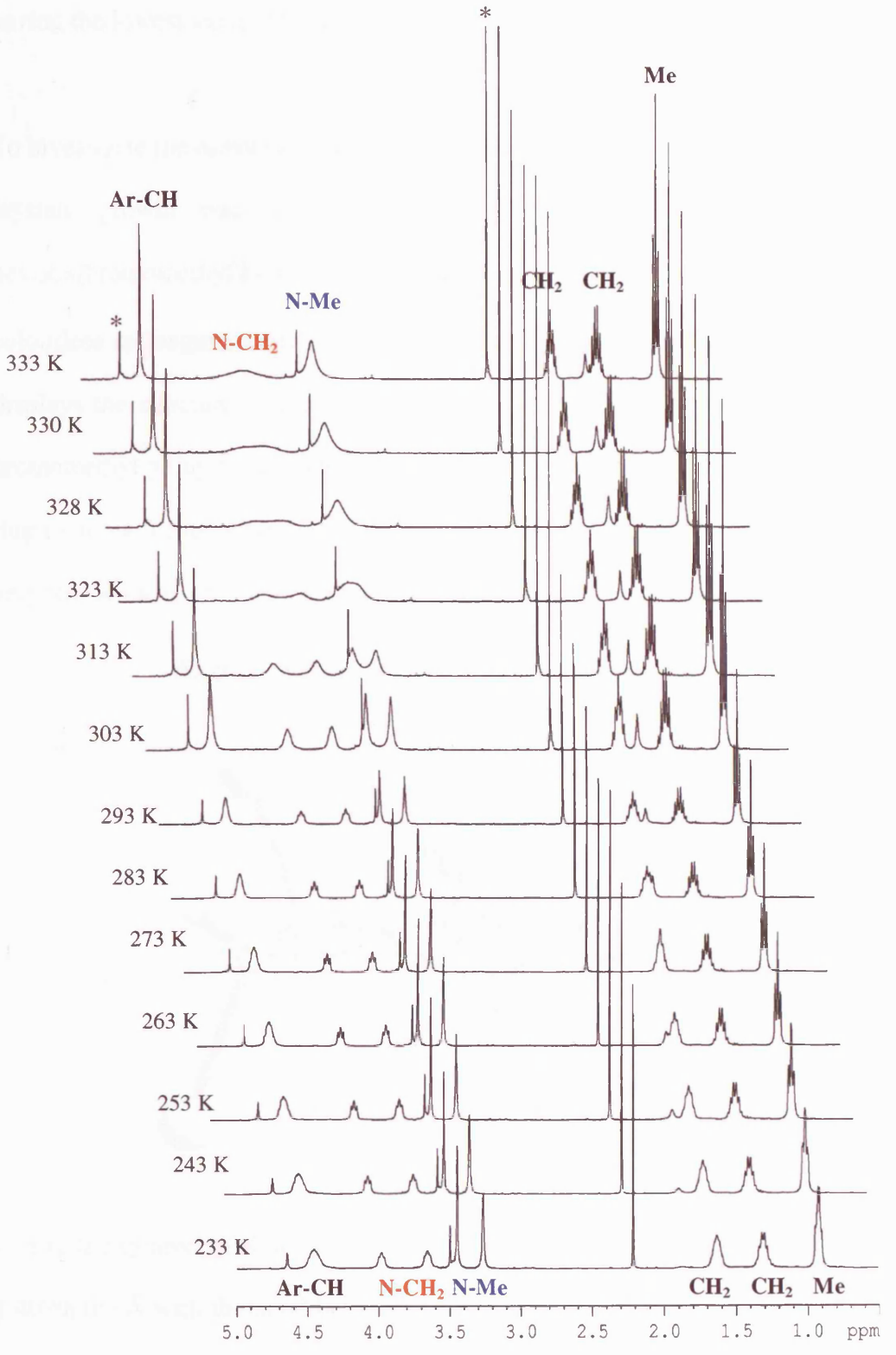

* = known impurity

The $\Delta G^{\ddagger}$ values for compounds **4a-e** were in the range of 60.6 – 67.2 kJ mol^{-1} with **4e** having the lowest value (60.6 kJ mol^{-1}).

To investigate the orientation of the multifunctional arms in relation to the arene, single-crystals growth was attempted. During this process, the starting material, hexakis(bromomethyl)benzene was crystallised from chloroform/ethanol to form colourless rectangular crystals with a hexagonal space group ($R\bar{3}$). Figure 17 clearly displays the structure of the starting material with the alternative arrangement of the bromomethyl group on the benzene ring. The bromine atom is orientated away from the ring to allow for its bulky size and electronegativity. The crystal data is reliable with a very low R-value of 0.0150 and was consistent with the expected structure.

Figure 17: Crystal structure of hexakis(bromomethyl)benzene

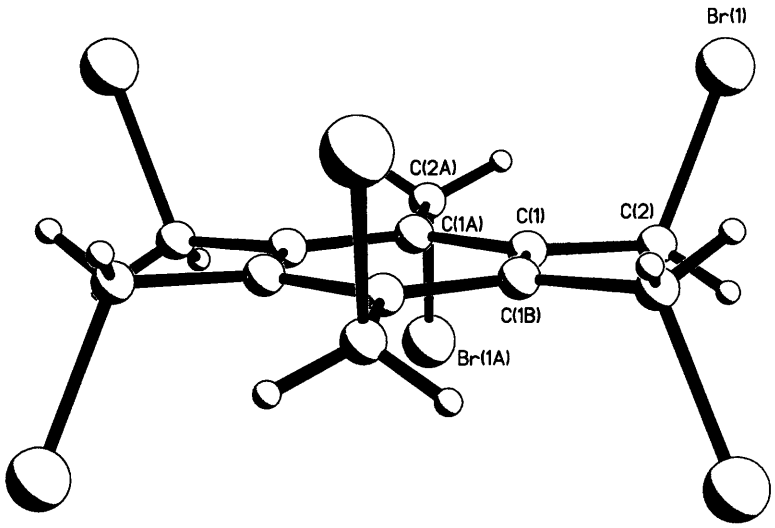

Due to the symmetry of this structure, the bond length of aromatic ring were all equal at 1.4079(16) Å with the bond between the aromatic carbon and the bromomethyl carbon {C(1)–C(2)} being slightly longer at 1.490(2) Å. The longest bond in this structure was the Br(1)–C(2) which was 1.9747(17) Å. The angles between the carbons within the ring {C(1A)–C(1)–C(1B)} were as expected 119.979(7)°. The external angles between the ring

and the methylene carbon {C(1A)–C(1)–C(2)} were 120.13(15)° and 119.87(15)° {C(1B)–C(1)–C(2)}. Finally, the angle between the C(1)–C(2)–Br(1) was 111.24(12)° which was smaller than the average 120° due to the size and electronegativity of the bromine atom.

The single-crystal structure of **4c** was also resolved as a monoclinic space group ($P_{21/c}$). This colourless needle crystal mimicked the starting material arrangement of the dithiocarbamate arms with alternating up-down arms to adopt the conformational ground state (Figure 18).

Figure 18: Crystal structure of hexakis(bromomethyl)benzene with diisobutyldithiocarbamate (4c)

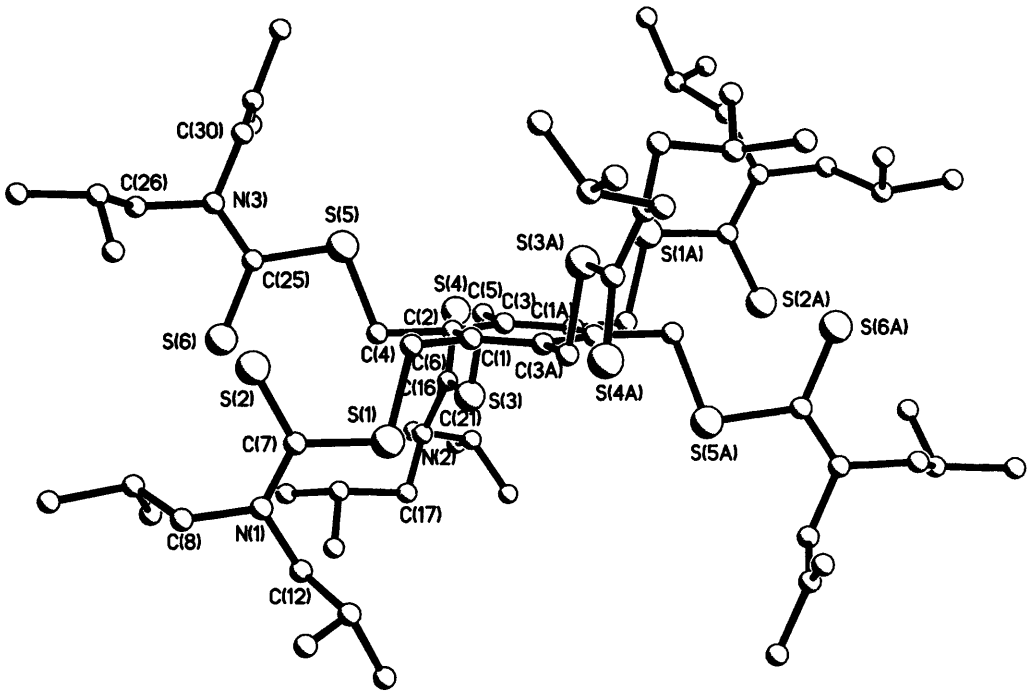

A comparison of bond lengths of an upward and downward facing dithiocarbamate arm showed concurrent values, all within the expected range for those typical bonds. Table 7 shows a selection of bond lengths and Table 8 shows the key angles in the structure.

Table 7: Bond lengths of crystal structure 4c

	Bond	Length (Å)
Aromatic Ring carbon	C(36)–C(39)	1.514 (11)
CH_2-S	S(9)–C(49)	1.770 (9)
S-C	S(11)–C(58)	1.762 (9)
C=S	S(10)–C(49)	1.664 (9)
N-C	N(5)–C(49)	1.340 (11)
N-CH_2	N(5)–C(50)	1.477(12)
CH-Me	C(51)–C(52)	1.560 (2)

Table 8: Bond angles of crystal structure 4c

	Bond	Angle (°)
Aromatic Ring carbon	C(36)–C(35)–C(34)	120.6 (7)
Aromatic C-CH_2-S	C(36)–C(39)–S(9)	105.1 (6)
CH_2-S-CS	C(49)–S(9)–C(39)	103.2 (4)
S-C=S	S(10)–C(49)–S(9)	121.7 (5)
N-C=S	N(5)–C(49)–S(10)	125.1(7)
N-C-S	N(5)–C(49)–S(9)	113.1(6)
S_2C-N-CH_2	C(49)–N(5)–C(54)	123.0(7)
N-CH_2-CMe_2	N(5)–C(50)–C(51)	111.6(10)
CH_2-CH-Me	C(57)–C(55)–C(54)	111.4(8)
Me-CH-Me	C(53)–C(51)–C(52)	109.4(13)

Therefore, in this section of work, we were successful in forming the proposed structures which were well characterised. Further to this, we attained single crystal data that allowed us to consider the orientation of the six arms attached to the arene ring. According to the literature[23], we would expect the up-down arrangement of the arms to be observed, which indeed was observed in both compounds. This indicated that the lowest energy state (ground state) was occupied, in which the steric interactions of the arms were minimised by this specific orientation.

5.25 R-groups in different core environments

Following the discussion of different core structures of the benzene rings, comparisons of R-groups on the different arene rings was undertaken. Tabulation of the ^1H NMR

chemical shifts for each type of R-group allowed comparison (Table 9). The data clearly showed excellent correlation between the R-group proton peaks in the different arene systems. This suggests that substitution of the different benzene ring does affect the R-groups as there are four bonds between the arene ring and the R-groups.

Table 9: Tabulation of all the chemical shifts of all the compounds

	Complex	N-CH_2	N-CH_2	N-Me	N-Me	CH_2	CH_2	Me	$CHMe_2$	$CHMe_2$
Me	**1a**			3.51	3.35					
	2a			3.57	3.33					
	3a			3.51	3.35					
	4a			3.52	3.34					
Et	**1b**	4.04	3.71					1.27		
	2b	4.04	3.70					1.27		
	3b	4.03	3.72					1.28		
	4b	3.99	3.71					1.28		
^{t}Bu	**1c**	3.87	3.57					0.92	2.47	2.29
	2c	3.87	3.54					0.93	2.45	2.27
	3c	3.85	3.55					0.93	2.47	2.30
	4c	3.81	3.55					0.92	2.47	2.31
NMeBu	**1d**	4.05	3.70	3.28		1.66	1.34	0.95		
	2d	4.05	3.70	3.26		1.66	1.34	0.93		
	3d	4.03	3.71	3.29		1.69	1.23	0.95		
	4d	4.01	3.69	3.28		1.66	1.34	0.95		
NC_5H_{10}	**1e**	4.29	3.85					1.70		
	2e	4.30	3.83					1.71		
	3e	4.28	3.86					1.70		
	4e	4.24	3.86					1.70		

5.3 Conclusions

A range of compounds were attempted and successfully formed using four different arene systems. The five standard dithiocarbamates used reacted with the aromatic system forming white solids in moderate to high yields. These compounds were fully

characterised with some extended work using variable temperature NMR. A temperature range of 233 – 333 K was used to monitor the fluxionality of various proton environments and observe coalescence of peaks. This allowed the collection of coalescence temperatures and free energy of activation values all within a similar range of 60 – 67 kJ mol^{-1}.

Crystals were attained for the starting material hexakis(bromomethyl)benzene as well as compounds **4c**, **2a** and **2b**. Examination of these structures allowed the observation of the "up-down" arrangement of the arms. The only structure to defer from this arrangement was compound **2b**, 1,3,5-tris(bromomethyl)-2,4,6-trimethylbenzene with diethyldithiocarbamate. This structure displayed two arms on one side of the benzene plane and the third on the other side. As there was a molecule of solvent ($CHCl_3$) in the crystal, this could explain the unexpected orientation of arms.

Further work in this area involves using zwitterions to form dithiocarbamates, which are then reacted with the arene rings. A zwitterion ion such as $H_2N^+C_4H_8CS_2^-$ could form a dithiocarbamate and bind with the arene ring. The end of the zwitterion has NH_2^+ that could be further reacted with base and CS_2 to form an active species, ready to react further, increasing the chain (see Chapter 6). The di-substituted arene could form linear chains as the arm length increases where as the tri-substituted arene could form cylinders above or below the arene ring.

Other work planned involves using these arene systems to form radicals *via* thermolysis and photolysis. Once the radical is formed, a range of monomers could be polymerised *via* living polymerisation of each arm of the arene, forming organised and uniformed

linear chains. When the polymer chain is completed, cleaving it from the dithiocarbamate can retrieve the polymer.

5.4 Experimental

All ^{1}H and ^{13}C NMR spectra were obtained on a Bruker AMX300 and AMX400 spectrometer, operating at 299.87 MHz and 400.12 MHz respectively. The same instrument was used for variable temperature work, using the range 233 – 333 K unless otherwise stated. All spectra were recorded using $CDCl_3$ solutions unless otherwise specified and were referenced against internal standards. All IR spectra were recorded using a Shimaduz FT-IR 8700 spectrometer, operating in the region of 4000 - 400 cm^{-1}. The IR samples were prepared using KBr powder to make discs or as neat samples between NaCl plates. The mass spectra were obtained using a Micromass 70-SE magnetic sector mass spectrometer. Three different procedures were used to maximise accuracy of the data for individual samples. These were Electron Impact (EI) Mode with ionisation at 70 eV, Chemical Ionisation (CI) with methane reagent gas and Fast Atom Bombardment (FAB^{+}) using a caesium ion gun. The Elemental Analysis was carried out using Elemental Analyzer (CE-440) (Exeter Analytical Inc).

*5.41 Synthesis of **1a-e** using 1, 4-di-α,α-(bromomethyl)benzene*

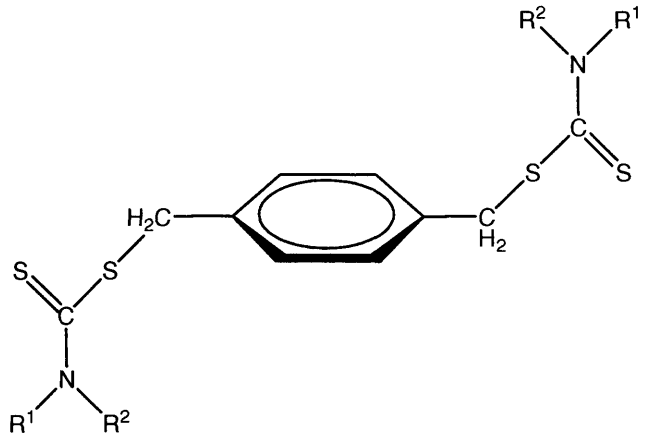

Synthesis of **1a:** 1, 4-di-α,α-(bromomethyl)benzene (0.50 g, 1.89 mmol) and $NaS_2CNMe_2.3H_2O$ (0.81 g, 5.68 mmol) were placed in a round bottom flask with methanol (100 ml) and refluxed overnight. The cream coloured precipitate was collected by filtration, washed successively with methanol and diethylether and air-dried to give a cream-white solid (0.61 g, 93 %). IR (KBr) ν: 2952s, 2968s, 1508m, 1421s, 1379m cm^{-1}; ^1H NMR ($CDCl_3$): δ 7.33 (s, 4H, Ar), 4.52 (s, 4H, CH_2), 3.51 (s, 6H, *Me*), 3.35 (s, 6H, *Me*); anal. calc. for $C_{14}H_{20}S_4N_2$: C, 48.80; H, 5.85; N, 8.13. Found C, 48.68; H, 5.98; N, 8.03.

Synthesis of **1b:** followed the experimental as above using 1, 4-di-α,α (bromomethyl)benzene (0.50 g, 1.89 mmol) and $NaS_2CNEt_2.3H_2O$ (1.28 g, 5.68 mmol) to give a cream-white solid (0.41g, 55 %). IR (KBr) ν: 2974s, 2923s, 2907s, 2868s, 1927m, 1489s, 1456s, 1439s, 1352s, 1377s cm^{-1}; ^1H NMR ($CDCl_3$): δ 7.33 (s, 4H, Ar), 4.51 (s, 4H, CH_2), 4.04 (q, 8H, J 7.0, CH_2), 3.71 (q, 8H, J 7.0, CH_2), 1.28 (t, 6H, J 7.0, *Me*), 1.27 (t, 6H, J 7.0, *Me*); ^{13}C NMR ($CDCl_3$): δ 135.22, 129.51, 49.40, 46.64, 41.73,

12.39, 11.50; anal. calc. for $C_{18}H_{28}S_4N_2$: C, 53.95; H, 7.04; N, 6.19. Found C, 53.13; H, 7.26; N, 6.77.

Synthesis of **1c:** diisobutylamine (0.73 g, 5.68 mmol) and KOH (0.32 g, 5.68 mmol) were stirred in methanol (100 ml) for 30 min. followed by the dropwise addition of CS_2 (0.43 g, 5.68 mmol). This solution was stirred for a further 30 min. and 1, 4-di-α,α (bromomethyl)benzene (0.50 g, 1.89 mmol) was added and the mixture refluxed overnight. The cream coloured precipitate was collected by filtration, washed successively with methanol and diethylether and air-dried to give a cream-white solid (0.23 g, 23 %). IR (KBr) ν: 2963m, 2930s, 2866s, 1651m, 1508m, 1479s, 1464s, 1400s, 1385s, 1354s cm^{-1}; ^1H NMR ($CDCl_3$): δ 7.32 (s, 4H, Ar), 4.51 (s, 4H, C*H*$_2$), 3.87 (d, 4H, J 7.3, C*H*$_2$), 3.57 (d, 4H, J 6.6, C*H*$_2$), 2.47 (m, 2H, J 5.4, C*H*), 2.29 (m, 2H, J 5.5, C*H*), 0.92 (d, 24H, J 6.7, *Me*); ^{13}C NMR ($CDCl_3$): δ 196.81, 135.10, 129.52, 62.92, 60.79, 42.09, 27.41, 26.16, 20.15.

Synthesis of **1d:** followed the experimental as above using N-methylbutylamine (0.50 g, 5.68 mmol), KOH (0.32 g, 5.68 mmol), CS_2 (0.43 g, 5.68 mmol) and 1, 4-di-α,α (bromomethyl)benzene (0.50 g, 1.89 mmol) to give cream-white solid (0.37 g, 46 %). IR (KBr) ν: 2957s, 2924s, 2862s, 1487s, 1450m, 1421s, 1369m cm^{-1}; ^1H NMR ($CDCl_3$): δ 7.33 (s, 4H, Ar), 4.52 (s, 4H, S-C*H*$_2$), 4.05 (t, 2H, J 7.6, N-C*H*$_2$), 3.70 (t, 2H, J 7.8, N-C*H*$_2$), 3.14 (s, 6H, N-*Me*), 1.53-1.69 (m, 4H, C*H*$_2$), 0.91-0.97 (m, 4H, C*H*$_2$Me), 0.96 (t, 6H, J 8.1, *Me*), 0.94 (t, 6H, J 8.1, *Me*); mass spectrum (FAB): *m/z* 429 (M^+).

Synthesis of **1e**: followed experimental above with piperidine (0.48 g, 5.68 mmol), KOH (0.32 g, 5.68 mmol), CS_2 (0.43 g, 5.68mmol) and 1, 4-di-α,α

(bromomethyl)benzene (0.50 g, 1.89 mmol) to give cream-white solid (0.79 g, 99 %). IR (KBr) ν 3047s, 2939s, 2922s, 2851s, 2787s, 1512s, 1477s, 1427m, 1400s, 1358s cm^{-1}; ^1H NMR ($CDCl_3$): δ 7.33 (s, 4H, Ar), 4.53 (s, 4H, S-CH_2), 4.18 (brm, 4H, N-CH_2), 3.85 (brm, 4H, N-CH_2), 1.70 (brs, 6H, Pip CH_2); ^{13}C NMR ($CDCl_3$): δ 195.02, 135.27, 129.51, 53.76, 51.50, 24.18; mass spectrum (FAB): *m/z* 599 (M^+); anal. calc. for $C_{20}H_{28}S_4N_2$: C, 56.56; H, 6.65; N, 6.60. Found C, 39.01; H, 4.66; N, 4.40. Recalc. formula $C_{20}H_{28}S_4N_2.2CHCl_3$ C, 39.83; H, 4.55; N, 4.22.

Formation of 1,3,5-tris(bromomethyl)-2,4,6-trimethylbenzene[27]

A solution of 33 % hydrogen bromide in acetic acid (149 ml, 833 mmol) was rapidly added to a mixture of mesitylene (25.04 g, 208 mmol), paraformaldehyde (25.00 g, 833 mmol) and glacial acetic acid (430 ml). A white precipitate formed, which was removed by filtration, dissolved in dichloromethane (2 L) and washed with sodium carbonate (1M, 2 x 2 L), distilled water, brine (2 L) and dried over anhydrous magnesium sulfate. The drying agent was removed by filtration and the filtrate was concentrated *in vacuo*. Recrystallisation from warm dichloromethane/petroleum ether (40 - 60) yielded the product as white needles (43.93 g, 53 %).

5.42 Synthesis of ***2a-e*** *using 1,3,5-tris(bromomethyl)-2,4,6-trimethylbenzene*

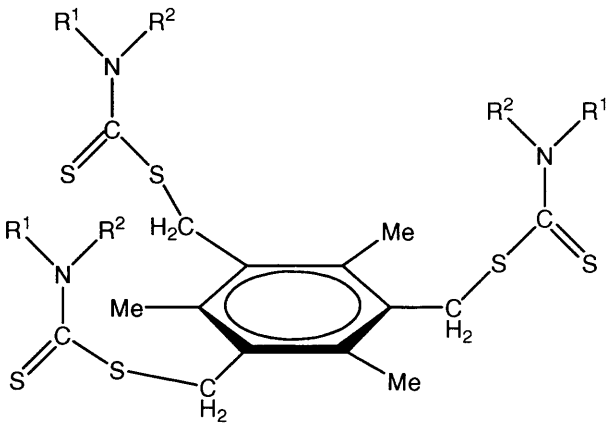

Synthesis of **2a:** 1,3,5-tris(bromomethyl)-2,4,6-trimethylbenzene (0.50 g, 1.26 mmol) and $NaS_2CNMe_2.3H_2O$ (0.54 g, 3.78 mmol) were placed in a round bottom flask with methanol (100 ml) and refluxed overnight. The white precipitate was collected by filtration, washed successively with methanol and diethylether and air-dried to give a white solid (0.42 g, 65 %). IR (KBr) ν: 2920s, 2843s, 2392s, 1948s, 1497m, 1437s, 1375s cm^{-1}; ^1H NMR ($CDCl_3$): δ 4.44 (s, 6H, CH_2), 3.57 (s, 9H, N-*Me*), 3.33 (s, 9H, N-*Me*), 2.40 (s, 9H, Ar-*Me*); ^{13}C NMR ($CDCl_3$): δ 196.54, 137.45, 130.54, 40.14, 32.03, 23.09, 16.36; anal. calc. for $C_{21}H_{33}S_6N_3$: C, 48.51; H, 6.40; N, 8.08. Found C, 48.49; H, 6.43; N, 7.93.

Synthesis of **2b:** follow experimental above with 1,3,5-tris(bromomethyl)-2,4,6-trimethylbenzene (0.50 g, 1.26 mmol) and $NaS_2CNEt_2.3H_2O$ (0.85 g, 3.78 mmol) to give white solid (4.18 g, 92 %). IR (KBr) ν: 3447br, 2974s, 2930s, 2870s, 2359s, 2341s, 1500, 1485s, 1437s, 1379s cm^{-1}; variable temperature experiments undertaken ranging 298 – 333K, ^1H NMR ($CDCl_3$) (298 K): δ 4.44 (s, 6H, CH_2), 4.04 (q, 6H, J 7.2, CH_2), 3.70 (q, 6H, J 7.2, CH_2), 2.41 (s, 9H, Ar-*Me*), 1.29 (t, 9H, J 7.2, *Me*), 1.25 (t, 9H, J 7.2, *Me*); ^{13}C NMR ($CDCl_3$): δ 195.45, 138.05, 129.82, 49.08, 46.67, 39.00, 16.31, 12.37 cm^{-1}; anal. calc. for $C_{27}H_{45}S_6N_3$: C, 53.73; H, 7.46; N, 6.97. Found $C_{27}H_{45}S_6N_3.CHCl_3$ C, 47.73; H, 6.66; N, 5.92. Recalc. formula $C_{27}H_{45}S_6N_3.CHCl_3$ C, 46.50; H, 6.41; N, 5.81.

Synthesis of **2c:** diisobutylamine (0.73 g, 5.68 mmol) and KOH (0.32 g, 5.68 mmol) were stirred in methanol (100 ml) for 30 min. followed by the dropwise addition of CS_2 (0.43 g, 5.68 mmol). This solution was stirred for a further 30 min. and 1,3,5-tris(bromomethyl)-2,4,6-trimethylbenzene (0.50 g, 1.89 mmol) added and refluxed

overnight. The white precipitate was collected by filtration, washed successively with methanol and diethylether and air-dried to give a white solid (0.59 g, 59 %). IR (KBr) ν: 2957s, 2934s, 2868s, 1477m, 1464m, 1435s, 1385m, 1356m cm^{-1}; ^1H NMR ($CDCl_3$): δ 4.35 (s, 6H, C*H*$_2$), 3.87 (d, 6H, J 7.1 C*H*$_2$), 3.54 (d, 6H, J 7.1 C*H*$_2$), 2.43-2.47 (brm, 3H, C*H*), 2.40 (s, 9H, Ar-*Me*), 2.25-2.28 (brm, 3H, J 6.2, C*H*), 0.93 (d, 36H, J 6.5, *Me*); ^{13}C NMR ($CDCl_3$): δ 197.27, 138.12, 129.97, 62.33, 60.58, 39.31, 27.34, 26.19, 20.13, 16.30; anal. calc. for $C_{39}H_{69}S_6N_3$: C, 60.65; H, 9.00; N, 5.44. Found C, 59.77; H, 8.89; N, 5.13.

Synthesis of **2d:** follow experimental above with N-methylbutylamine (0.50 g, 5.68 mmol), KOH (0.32 g, 5.68 mmol), CS_2 (0.43 g, 5.68 mmol) and 1,3,5-tris(bromomethyl)-2,4,6-trimethylbenzene (0.50 g, 1.89 mmol) to give yellow solid (0.78 g, 64 %). Variable temperature experiments undertaken ranging 298 – 333 K, ^1H NMR ($CDCl_3$) (298 K): δ 4.43 (s, 6H, C*H*$_2$), 4.04 (brt, 3H, N-C*H*$_2$), 3.70 (brt, 3H, N-C*H*$_2$), 3.49 (s, 9H, N-*Me*), 2.40 (s, 9H, Ar-*Me*), 1.66 (brm, 6H, C*H*$_2$), 1.34 (brm, 6H, C*H*$_2$), 0.96 (t, 9H, *Me*), 0.92 (t, 9H, *Me*).

Synthesis of **2e:** follow experimental above with piperidine (0.54 g, 6.30 mmol), KOH (0.35 g, 6.30 mmol), CS_2 (0.48 g, 6.30 mmol) and 1,3,5-tris(bromomethyl)-2,4,6-trimethylbenzene (0.50 g, 1.26 mmol) to give cream-white solid (0.46 g, 56 %). IR (KBr) ν: 2988s, 2937s, 1474s, 1425s, 1358s cm^{-1}; variable temperature experiments undertaken ranging 298 – 333 K, ^1H NMR ($CDCl_3$) (298 K): δ 4.47 (s, 6H, C*H*$_2$), 4.30 (brs, 6H, N-C*H*$_2$), 3.83 (brs, 6H, N-C*H*$_2$), 2.41 (s, 12H, Ar-*Me*), 1.71 (brs, 18H, Pip-C*H*$_2$); ^{13}C NMR ($CDCl_3$): δ 195.45, 137.95, 129.80, 52.32, 51.14, 39.07, 25.87, 24.17,

16.32; anal. calc. for $C_{30}H_{45}S_6N_3$: C, 56.29; H, 7.09; N, 6.56. Found C, 55.63; H, 7.10; N, 6.13.

*5.43 Synthesis of **3a-e** using 1,2,4,5-tetrakis(bromomethyl)benzene*

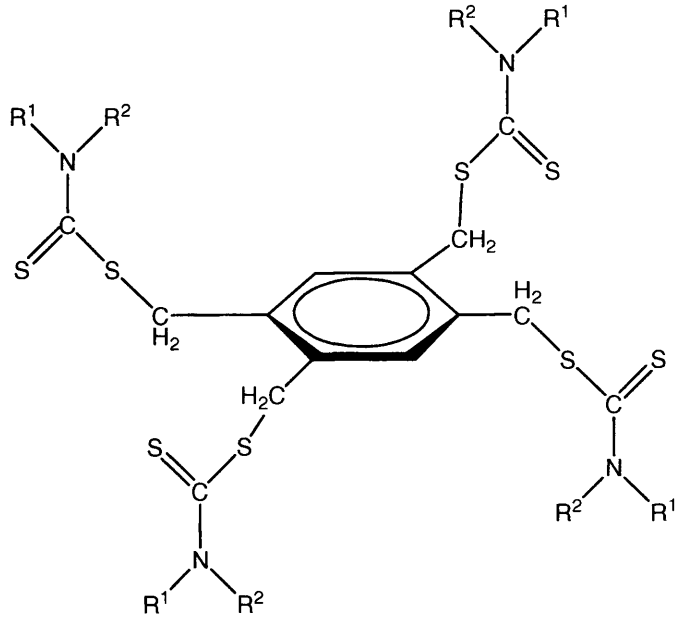

Synthesis of **3a:** 1,2,4,5-tetrakis(bromomethyl)benzene (0.50 g, 1.10 mmol) and $NaS_2CNMe_2.3H_2O$ (0.96 g, 6.60 mmol) were placed in a round bottom flask with methanol (100 ml) and refluxed overnight. The white precipitate was collected by filtration, washed successively with methanol and diethylether and air-dried to give a white solid (0.36 g, 54 %). IR (KBr) ν: 3416m, 2922s, 2837s, 2800s, 2640m, 1499m, 1448m, 1406s, 1375m cm^{-1}; ^1H NMR ($CDCl_3$): δ 7.46 (s, 2H, Ar), 4.57 (s, 8H, CH_2), 3.51 (s, 12H, *Me*), 3.35 (s, 12H, *Me*); ^{13}C NMR ($CDCl_3$): δ 196.24, 134.60, 133.17, 45.29, 41.40, 39.66; anal. calc. for $C_{22}H_{34}S_8N_4$: C, 43.24; H, 5.61; N, 9.17. Found C, 42.16; H, 5.53; N, 8.48.

Synthesis of **3b:** followed the same experimental as above with 1,2,4,5-tetrakis(bromomethyl)benzene (0.50 g, 1.10 mmol) and $NaS_2CNEt_2.3H_2O$ (1.49 g, 6.60 mmol) to give yellow solid (0.49 g, 61 %). IR (KBr) ν: 2972s, 2932s, 2899s, 2870s, 2814m, 1487s, 1456s, 1418s, 1439s, 1375s, 1354s cm^{-1}; ^1H NMR ($CDCl_3$): δ 7.46 (s, 2H, Ar), 4.57 (s, 8H, CH_2), 4.03 (q, 16H, J 7.0, CH_2), 3.72 (q, 16H, J 7.0, CH_2), 1.28 (t, 24H, J 7.0, *Me*), 1.28 (t, 24H, J 7.0, *Me*); ^{13}C NMR ($CDCl_3$): δ 194.68, 134.66, 133.36, 49.42, 46.69, 39.23, 12.47, 1152.

Synthesis of **3c:** diisobutylamine (0.85 g, 6.60 mmol) and KOH (0.37 g, 6.60 mmol) were stirred in methanol (100 ml) for 30 min. followed by the dropwise addition of CS_2 (0.50 g, 6.60 mmol). This solution was stirred for a further 30 min. and 1,2,4,5-tetrakis(bromomethyl)benzene (0.50 g, 1.10 mmol) was added and the mixture refluxed overnight. The cream precipitate was collected by filtration, washed successively with methanol and diethylether and air-dried to give a cream-white solid (0.62 g, 59 %). ^1H NMR ($CDCl_3$): δ 7.45 (s, 2H, Ar), 4.56 (s, 8H, CH_2), 3.85 (d, 8H, J 6.7, CH_2), 3.55 (d, 8H, J 6.7, CH_2), 2.47 (m, 4H, J 6.7, *CH*), 2.30 (m, 4H, J 6.7, *CH*), 0.93 (d, 48H, J 6.7, *Me*); ^{13}C NMR ($CDCl_3$): δ 196.38, 134.62, 133.34, 62.93, 60.83, 39.53, 27.46, 26.14, 20.21.

Synthesis of **3d:** follow experimental above with N-methylbutylamine (0.58 g, 6.60 mmol), KOH (0.37 g, 6.60mmol), CS_2 (0.50 g, 6.60 mmol) and 1,2,4,5-tetrakis(bromomethyl)benzene (0.50 g, 1.10 mmol) to give yellow solid (0.62 g, 53 %). IR (KBr) ν: 2957m, 2623br, 1647m, 1556m, 1487m, 1393m cm^{-1}; ^1H NMR ($CDCl_3$): δ 7.48 (s, 2H, Ar), 4.57 (s, 8H, CH_2), 4.03 (q, 4H, J 7.6, N-*CH*), 3.71 (q, 4H, J 7.1, N-

CH), 3.45 (s, 12H, N-*Me*), 3.29 (s, 12H, N-*Me*), 1.69 (m, 8H, J 7.6, C*H*$_2$), 1.23 (m, 8H, J 7.1, C*H*$_2$), 0.96 (t, 12H, *Me*), 0.94 (t, 12H, *Me*).

Synthesis of **3e:** follow experimental above with piperidine (0.56 g, 6.60 mmol), KOH (0.37 g, 6.60 mmol), CS_2 (0.50 g, 6.60 mmol) and 1,2,4,5-tetrakis(bromomethyl)benzene (0.50 g, 1.10 mmol) to give white solid (0.57 g, 67 %). ^{1}H NMR ($CDCl_3$): δ 7.47 (s, 2H, Ar), 4.62 (s, 8H, C*H*$_2$), 4.28 (brs, 8H, N-C*H*$_2$), 3.86 (brs, 8H, N-C*H*$_2$), 1.70 (brs, 24H, Pip-C*H*$_2$); ^{13}C NMR ($CDCl_3$): δ 194.67, 134.67, 133.28, 53.42, 51.56, 39.28, 24.21; anal. calc. for $C_{34}H_{50}S_8N_4$: C, 52.94; H, 6.53; N, 7.26. Found C, 50.94; H, 6.33; N, 6.36.

*5.44 Synthesis of **4a-e** using hexakis(bromomethyl)benzene*

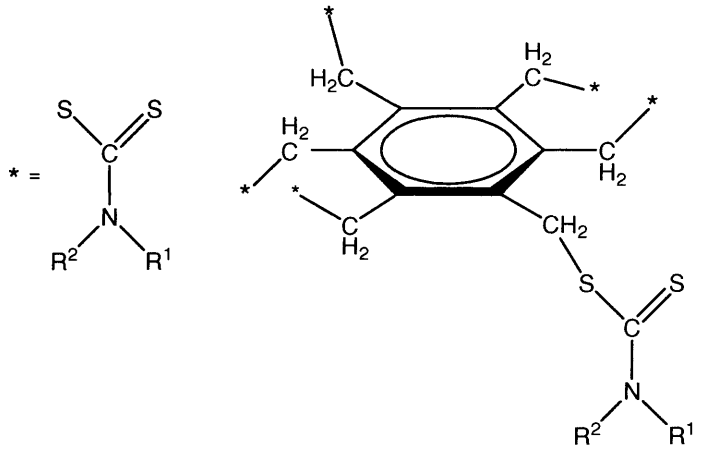

Synthesis of **4a:** hexakis(bromomethyl)benzene (1.00 g, 1.57 mmol) and $NaS_2CNMe_2.3H_2O$ (1.80 g, 12.60 mmol) were placed in a round bottom flask with methanol (100 ml) and refluxed overnight. The white precipitate was collected by filtration, washed successively with methanol and diethylether and air-dried to give a white solid (1.07 g, 78 %). IR (KBr) ν: 2922s, 2883s, 2839s, 2297br, 1657br, 1497m,

1445m, 1406s, 1373m cm^{-1}; variable temperature experiments undertaken ranging 298 – 333 K, ^1H NMR ($CDCl_3$) (298 K): δ 4.57 (s, 12H, S-CH_2), 3.34 (brs, 36H, N-*Me*); mass spectrum (FAB): *m/z* 902 (M^+ + Na); anal. calc. for $C_{30}H_{48}S_{12}N_6$: C, 41.06; H, 5.51; N, 9.58. Found C, 34.25; H, 4.17; N, 5.66. Recalc. formula $C_{30}H_{48}S_{12}N_6.3CHCl_3$ C, 32.08; H, 4.16; N, 6.80.

Synthesis of **4b:** follow experimental above with hexakis(bromomethyl)benzene (1.00 g, 1.57 mmol) and $NaS_2CNEt_2.3H_2O$ (2.84 g, 12.60 mmol) to give cream-white solid (1.17 g, 71 %). IR (KBr) ν: 3028s, 2974s, 2833s, 2399s, 1647m, 1489s, 1443s, 1377s cm^{-1}; variable temperature experiments undertaken ranging 298 – 333K, ^1H NMR ($CDCl_3$) (298 K): δ 4.56 (s, 12H, CH_2), 3.99 (brd, 24H, N-CH_2), 3.71 (brd, 24H, N-CH_2), 1.28 (brs, 36H, *Me*); ^{13}C NMR ($CDCl_3$): δ 194.02, 136.25, 46.75, 37.33, 12.62, 11.59.

Synthesis of **4c:** diisobutylamine (1.63 g, 12.60 mmol) and KOH (0.71 g, 12.60 mmol) were stirred in methanol (100 ml) for 30 min followed by the dropwise addition of CS_2 (0.96 g, 12.60 mmol). This solution was stirred for a further 30 min. and hexakis(bromomethyl)benzene (1.00 g, 1.57 mmol) added and refluxed overnight. The white precipitate was collected by filtration, washed successively with methanol and diethylether, and air dried to give a white solid (1.22 g, 56 %). IR (KBr) ν: 3414m, 2959s, 2932s, 2810s, 1483s, 1466s, 1439s, 1498s, 1385s, 1354s cm^{-1}; variable temperature experiments undertaken ranging 298 – 333K, ^1H NMR ($CDCl_3$) (298 K): δ 3.81 (brd, 12H, S-CH_2), 3.54 (brd, 12H, S-CH_2), 2.48 (brs, 12H, N-CH_2), 2.31 (brs, 12H, N-CH_2), 1.79 (sept, 12H, $CHMe_2$), 0.92 (brd, 60H, *Me*); anal. calc. for

$C_{66}H_{120}S_{12}N_6$: C, 57.34; H, 8.75; N, 6.08. Found C, 55.68; H, 8.65; N, 5.62. Recalc. formula $C_{66}H_{120}S_{12}N_6.0.5CHCl_3$ C, 55.38; H, 8.42; N, 5.83.

Synthesis of **4d:** follow experimental above with N-methylbutylamine (1.10 g, 12.60 mmol), KOH (0.71 g, 12.60 mmol), CS_2 (0.96 g, 12.60 mmol) and hexakis(bromomethyl)benzene (1.00 g, 1.57 mmol) to give yellow solid (1.82 g, 74 %). IR ν(KBr) 3028s, 2955s, 2928s, 2866s, 1645br, 1487m, 1443m, 1387m cm^{-1}; variable temperature experiments undertaken ranging 298 – 333K, (298 K) ^1H NMR ($CDCl_3$): δ 4.54 (brs, 12H, CH_2), 4.01 (brt, 6H, J 7.1, N-CH_2), 3.69 (brt, 6H, J 7.2, N-CH_2), 3.45 (s, 18H, N-*Me*), 3.28 (s, 18H, N-*Me*), 1.66 (sex, 12H, J 7.5, CH_2), 1.34 (sex, 12H, J 7.4, CH_2), 0.95 (t, 36H, J 7.4, *Me*); ^{13}C NMR ($CDCl_3$): δ 194.69, 136.17, 56.73, 54.60, 43.39, 39.48, 29.37, 19.95, 13.81.

Synthesis of **4e:** follow experimental above with piperidine (1.07 g, 12.60 mmol), KOH (0.71 g, 12.60 mmol), CS_2 (0.96 g, 12.60 mmol) and hexakis(bromomethyl)benzene (1.00 g, 1.57 mmol) to give cream-white solid (0.93 g, 53 %). IR (KBr) ν: 3028s, 2914m, 2853m, 2347m, 1474m, 1443m, 1423m, 1356s cm^{-1}; variable temperature experiments undertaken ranging 298 – 333 K, ^1H NMR ($CDCl_3$) (298K): δ 4.56 (s, 12H, CH_2), 4.19 (brs, 12H, N-C*H*), 3.86 (brs, 12H, N-C*H*), 1.70 (brs, 36H, Pip-CH_2); anal. calc. for $C_{48}H_{72}S_{12}N_6$: C, 51.57; H, 6.49; N, 7.52. Found C, 42.38; H, 5.18; N, 5.35. Recalc. formula $C_{48}H_{72}S_{12}N_6.3CHCl_3$ C, 43.05; H, 5.31; N, 5.91.

5.5 References

[1] K. Ishizu, Y. Ohta, S. Kawauchi, *Macromolecules* **2002**, *35*, 3781.
[2] J. M. J. Frechet, S. Aoshima, Application: WO, 9614346, **1996**.
[3] S. G. Gaynor, S. Edelman, K. Matyjaszewski, *Macromolecules* **1996**, *29*, 1079.

[4] M. W. Weimer, J. M. J. Frechet, I. Gitsov, *Journal of Polymer Science Part A-Polymer Chemistry* **1998**, *36*, 955.
[5] K. Ishizu, A. Mori, *Polymer International* **2001**, *50*, 906.
[6] M. D. Cho, Y. Tsuji, T. Hiiro, Application: JP, 2002363217, **2002**.
[7] Y. Zhao, T. Higashihara, K. Sugiyama, A. Hirao, *Journal of the American Chemical Society* **2005**, *127*, 14158.
[8] K. Ishizu, T. Shibuya, J. Park, S. Uchida, *Polymer International* **2004**, *53*, 259.
[9] Y. Nakayama, T. Masuda, M. Nagaishi, M. Hayashi, M. Ohira, M. Harada-Shiba, *Current Drug Delivery* **2005**, *2*, 53.
[10] T. Otsu, T. Matsunaga, T. Doi, A. Matsumoto, *European Polymer Journal* **1995**, *31*, 67.
[11] T. Otsu, M. Yoshida, T. Tazaki, *Makromolekulare Chemie-Rapid Communications* **1982**, *3*, 133.
[12] S. DiMari, W. Funke, M. A. Haralson, D. Hunkeler, B. Joos-Muller, A. Matsumoto, O. Okay, T. Otsu, A. C. Powers, A. Prokop, T. G. Wang, R. R. Whitesell, *Advances in Polymer Science, Volume 136: Microencapsulation, Microgels, Iniferters*, **1998**.
[13] K. Praefcke, B. Kohne, W. Stephan, P. Marquardt, *Chimia* **1989**, *43*, 380.
[14] F. Moulines, D. Astruc, *Angewandte Chemie-International Edition* **1988**, *27*, 1347.
[15] F. Vogtle, E. Weber, *Angewandte Chemie-International Edition* **1974**, *13*, 814.
[16] F. Vogtle, W. M. Muller, E. Buhleier, W. Wehner, *Chemische Berichte-Recueil* **1979**, *112*, 899.
[17] D. J. Iverson, G. Hunter, J. F. Blount, J. R. Damewood, K. Mislow, *Journal of the American Chemical Society* **1981**, *103*, 6073.
[18] G. Hunter, T. J. R. Weakley, W. Weissensteiner, *Journal of the Chemical Society-Perkin Transactions 2* **1987**, 1633.
[19] M. P. Marsau, *Acta Crystallographica* **1965**, *18*, 851.
[20] A. Immirzi, E. Torti, *Atti Della Accademia Nazionale Dei Lincei Rendiconti-Classe Di Scienze Fisiche-Matematiche & Naturali* **1968**, *44*, 98.
[21] G. Hunter, D. J. Iverson, K. Mislow, J. F. Blount, *Journal of the American Chemical Society* **1980**, *102*, 5942.
[22] U. Berg, J. Sandstrom, *Advances in Physical Organic Chemistry* **1989**, *25*, 1.
[23] N. Zuaretz, O. Golan, S. E. Biali, *Journal of Organic Chemistry* **1991**, *56*, 2444.
[24] C. Yang, W.-T. Wong, *Journal of Materials Chemistry* **2001**, *11*, 2898.
[25] D. Sanz, J. A. Jimenez, R. M. Claramunta, J. Elguero, *ARKIVOC* **2004**, 100.
[26] C. Walsdorff, S. Park, J. Kim, J. Heo, K.-M. Park, J. Oh, K. Kim, *Journal of the Chemical Society, Dalton Transactions* **1999**, 923.
[27] A. W. Van der Made, R. H. Van der Made, *Journal of Organic Chemistry* **1993**, *58*, 1262.

Chapter 6

Metal Dithiocarbamates

6.1 Introduction

Transition metal dithiocarbamates are an exciting class of compounds with several applications. Following on from the dithiocarbamate compounds in Chapters 4 and 5, we focused our attention on metal dithiocarbamates. All transition metal ions are known to combine with dithiocarbamates to form stable complexes and some have found uses in the formation of nanoparticles[1] with semiconducting properties[2, 3]. However, the most commonly used metals are those of groups 8 to 10 due to their potential redox reactivity[4-7].

Other potential uses of these types of compounds were in supramolecular chemistry. Recent work by Beer *et al.*[8] has utilised the well-defined architecture of these compounds to prepare a range of exciting new supramolecular structures based on multifunctional dithiocarbamates[8, 9]. These complexes included dinuclear zinc(II) dithiocarbamate macrocyclic receptors with a range of aryl spacers (Figure 1).

Figure 1: Zinc dithiocarbamate macrocyclic receptors with aryl spacers [9, 10]

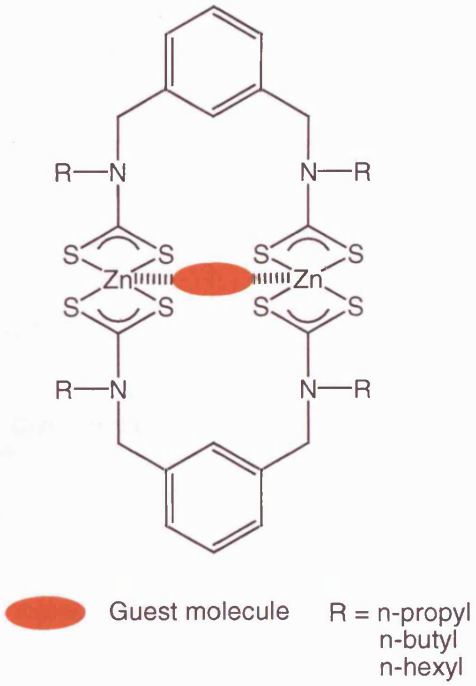

The zinc centre was able to bind to a bidentate guest molecule such as 4,4'-bipyridine, DABCO and pyrazine in the centre of the ring or link two ring systems parallel to each other. Other examples of these cyclic systems with aryl spacer groups included the transition metals copper[9, 11], gold [9], iron and cobalt[8].

Reacting imidazolium moieties with (bromomethyl)aryl systems allowed chains to be extended forming aryl rings[9]. These were then reacted with base, carbon disulfide and metal acetate (M = Ni(II), Cu(II), Zn(II)) to form bridges between the chains (**1**) (Figure 2). Other examples have used multi-armed arene systems previous seen in Chapter 5. This complex used 1,3,5 tris(chloromethyl)-2,4,6-triethyl benzene with the imidazolium ligands to form multifunctional arms and then added base, CS_2 and $CoCl_2$ (**2**) (see below)[12].

Figure 2: Imidazolium arms linked with metal dithiocarbamates[12]

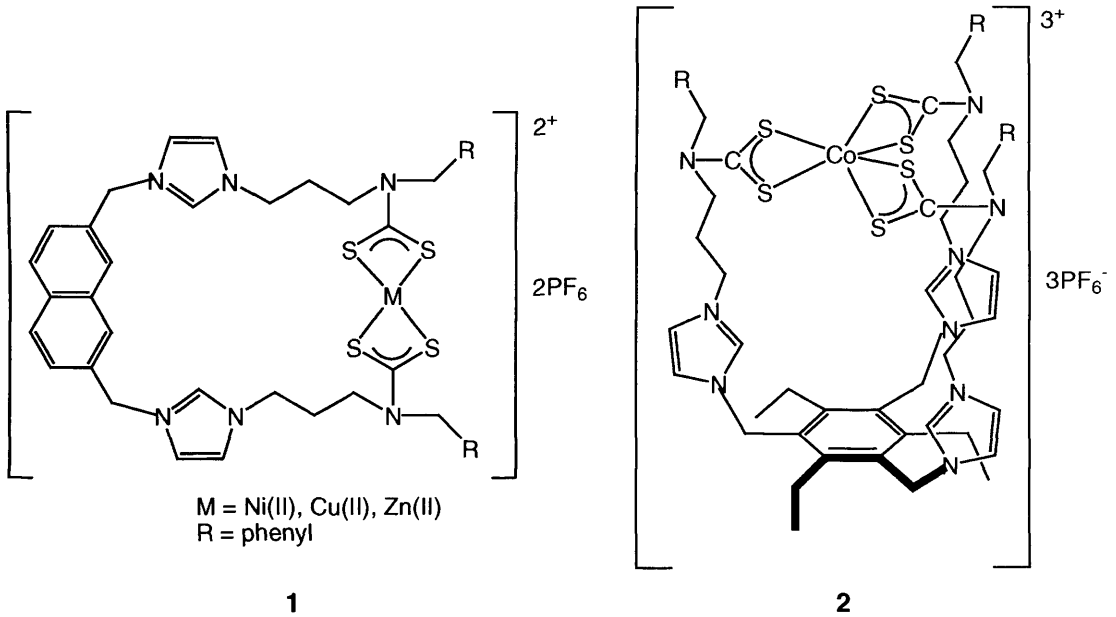

1 **2**

Pratt and Beer[13] formed ruthenium(II) bipyridyl-transition metal macrocycles which allowed the formation of a range of complexes, binding different transition metals to the dithiocarbamate fragments. These complexes were formed *via* metal directed self-assembly process and displayed anion recognition. Other examples of metal directed self-assembly with dithiocarbamates were nano-sized resorcarene-based assemblies[14, 15], catenanes[11], assorted macrocycles[10] and cyptands[16].

In spite of the increasing number of cyclic systems with bridging dithiocarbamtes, there are very few examples of linear arrays of metal centres with dithiocarbamates[17, 18]. We wished to address this by creating range of starting materials, which bridged various metal centres in a linear fashion, forming networks of multimetallic arrays. We chose piperazinedithiocarbamates as the spacer units as they had two secondary amine centres (*para*), which could be reacted with CS_2 to form active dithiocarbamates on either one or both ends of the ring, allowing controlled addition to the ring and increase the chain length. For example, the reaction of piperazine (**1**) with CS_2 formed the zwitterion (**2**) which could be reacted with a metal centre to form a metal dithiocarbamate complex (**3**) (Scheme 1). This complex could potentially be reacted with base and CS_2 to form an active dithiocarbamate at the other end of the piperazine ring which could be reacted with the same metal or indeed another metal centre, forming a bimetallic-bridged dithiocarbamate (**4**). This stepwise addition permits great control of complex formation and structural architecture.

Scheme 1: Process of building bimetallic complexes using piperazine ligands

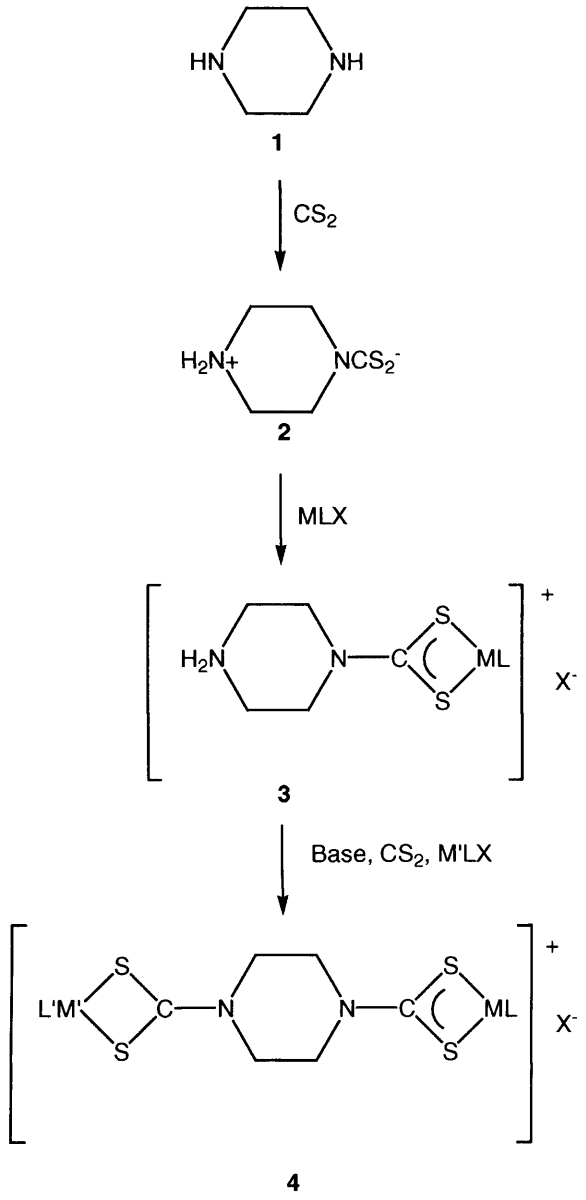

To form linking units, two equivalents of the zwitterion could be reacted with one equivalent of metal source (i.e. metal acetate) to form the bis(dithiocarbamate) complex (**5**) (Scheme 2). This complex could then be extended by the addition of CS_2 to form the metallic zwitterion (**6**) or two equivalents of base and CS_2 formed active dithiocarbamates on each end of the linear chain (**7**). By controlling the addition of base and CS_2, the desired end of the piperazine could be activated and the other end protected by NH_2 group. The chain length of complexes **5** - **7** could be further increased

by the controlled addition of linking dithiocarbamates and metal complexes to design multimetallic arrays using dithiocarbamates.

Scheme 2: Process of building multimetallic arrays using piperazine ligands

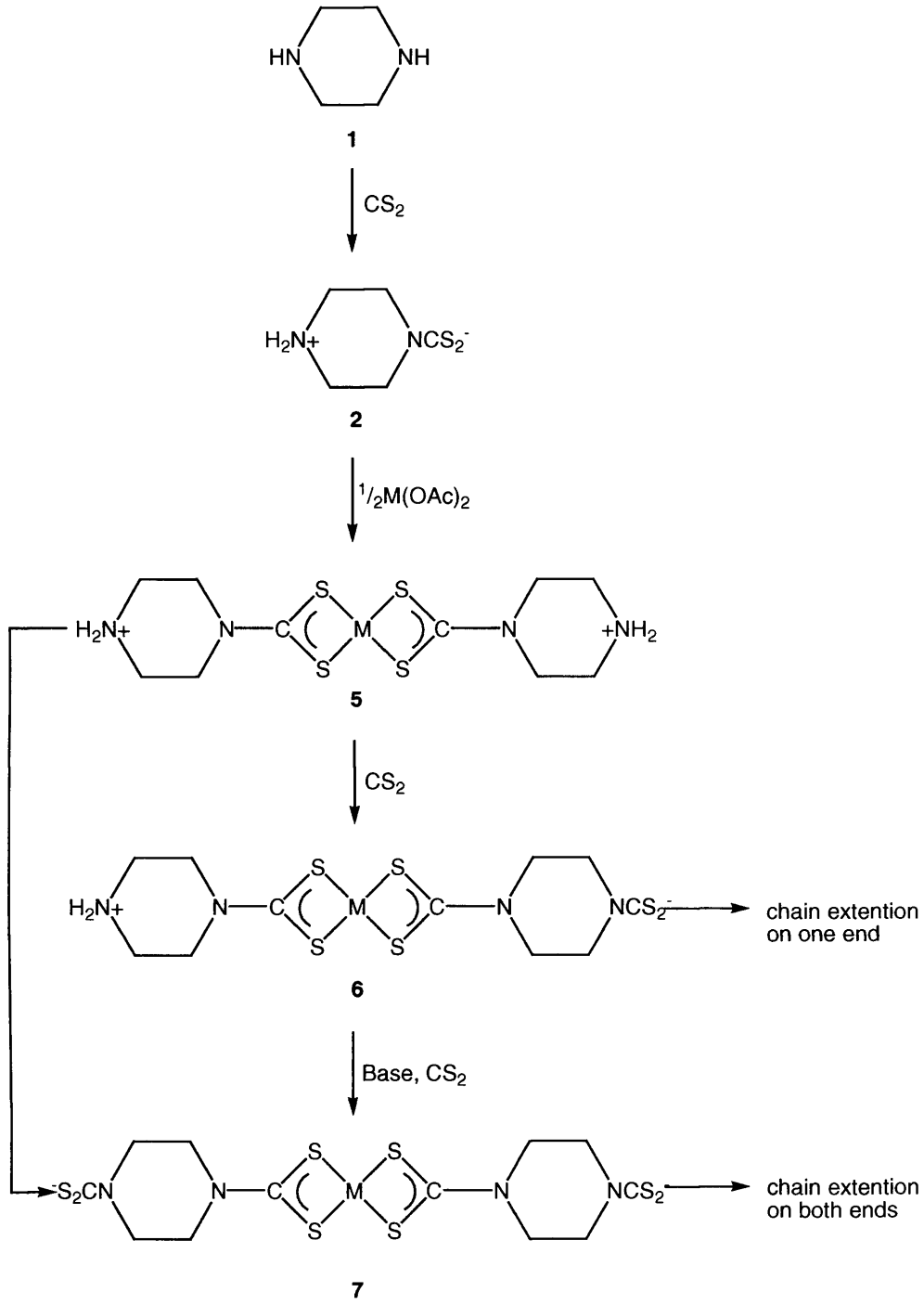

Our work investigated piperazine and substituted piperazine with different metal centres and formed linear arrays of metal dithiocarbamates as well as some star-based structures.

6.2 Results and Discussion

The aim of the work described in this chapter was to form a range of compounds that formed multimetallic units to potentially form chains. Synthesis of piperazine-based dithiocarbamates and metallodithiocarbamates compounds was undertaken, linking various transition metals. The work attempted to display the controlled, stepwise manner in which these dithiocarbamates were formed.

6.21 Starting Materials

In order to synthesise linear multimetallic complexes bridged by dithiocarbamates, a number of starting materials were made. Piperazine and substituted piperazines (2,6-dimethylpiperazine, *trans*-2,5-dimethylpiperazine and 2-methylpiperazine) were most commonly used as they have nitrogen atoms at the 1 and 4 positions (*para*). This facilitates the addition of CS_2 onto either one or both ends allowing further bonding and linking of units. Each type of piperazine ring was used to form complexes in order to allow comparisons between the compounds at a later stage when reacted with different metal ions.

The three sets of starting materials were zwitterions (**1**), disalts (**2**) and monosalts (**3**) (Figure 3). Synthesis of **1** involved the reaction between the piperazine and CS_2 in distilled water whereas **2** and **3** were formed using same method with the addition of base (KOH) in a methanol solution. Many of these compounds displayed poor solubility in distilled water and common organic solvents, limiting characterisation. The techniques used were elemental analysis, IR and where possible ^{1}H NMR, ^{13}C NMR and MS.

Figure 3: Starting Material compounds 1-3

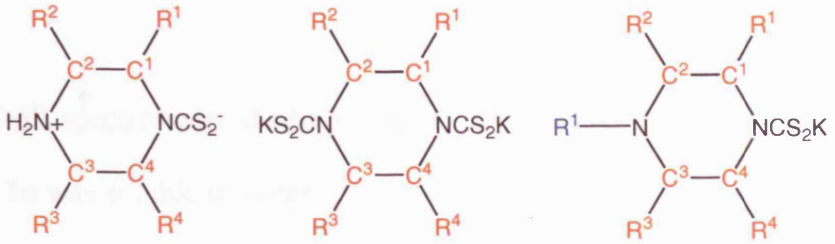

Zwitterions (**1**) were formed using a range of substituted piperazines. These compounds were synthesised by stirring the desired piperazine system in distilled water and carefully adding CS_2 dropwise, forming the zwitterion as a pale green/white precipitate in good yields (Figure 4). These were collected and characterised using the standard methods.

Figure 4: Zwitterion compounds with various substituted piperazine rings

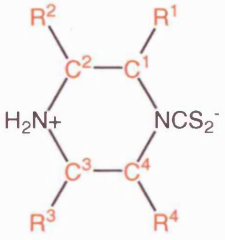

Compound	Substituents on C atom
1a	All protons
1b	R^1 = Me, R^3 = Me
1c	R^1 = Me, R^3 = Me or R^4 = Me, R^2 = Me
1d	R^3 = Me or R^4 = Me

Depending on which end the CS_2 attacked, different compounds could be formed. However, due to steric effects, it was expected that the CS_2 would attack the less hindered end of the ring, so positioned away from the methyl substituents, where

possible, which was generally observed with only a small proportion of products where the CS_2 attacked the more hindered site.

Using ^1H NMR spectroscopy, the formation of the proposed compounds was confirmed. Compound **1a** was soluble in water. The ^1H NMR (D_2O) spectrum showed a multiplet at δ 4.31, representing the two sets of CH_2 nearest to CS_2. This is upfield due to the nitrogen atom and the electron withdrawing CS_2^- group. The other four protons of the piperazine ring, nearer to the NH_2^+ also appeared as multiplet at δ 2.88 and finally, the singlet at δ 4.30 clearly represented the two protons from NH_2^+. The mass spectrum identified the parent ion as 162 (M^+) and the IR peaks corroborated the proposed structure at 966 cm^{-1} for ν(C-S) and 3230 cm^{-1} for ν(N-H). The elemental analysis data showed excellent correlation between the calculated and found values: calculated: C, 37.00; H, 6.20; N, 17.30, found: C, 37.70; H, 6.50; N, 17.50.

Compound **1b** was formed from 2, 6-dimethylpiperazine and was modernately soluble. The ^1H NMR spectrum indicated four distinct environments for the protons on the piperazine ring due to the axial and equatorial orientation of the substituents (Figure 5). As the methyl substituents would be expected to take the equatorial positions on the ring as the most energically favoured, the axial protons on C_2 and C_3 would be multiplets, coupled to the methyl at δ 3.00. The most upfield protons were the CH_{eq} doublet at δ 5.57 (J 14.1 Hz) as they were antiperiplanar to the methyl groups and closest to the CS_2 fragment. The two axial proton on C_1 and C_4 were triplets at δ 2.76 (J 13.5 Hz) and the two methyl groups appeared as a doublet at δ 1.07 (J 6.5 Hz). The ^{13}C NMR data and the IR spectrum both showed the expected peaks for the required compound, as did the elemental analysis.

Figure 5: The 2, 6-dimethylpiperazine dithiocarbamate zwitterion (1b)

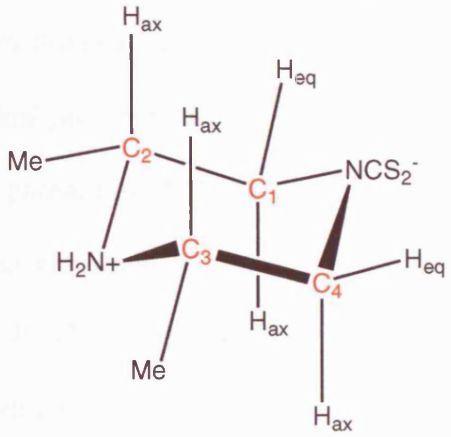

For **1c**, the amine *trans*-2, 5-dimethylpiperazine was used and a white solid was formed in 67 % yield. Although the trans-configuration had been fixed, the methyl substituents were still expected to take equatorial positions on the piperazine ring, resulting in four types of proton environments as (**1b**) (Figure 6).

Figure 6: The 2, 5-dimethylpiperazine dithiocarbamate zwitterion (1c)

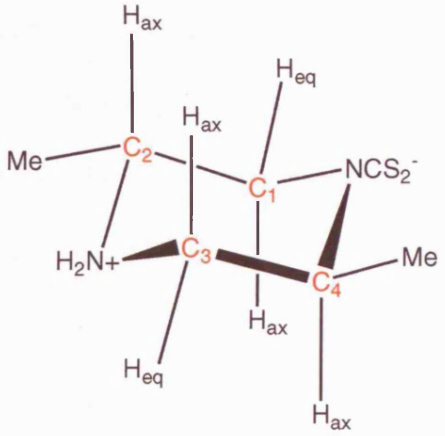

Unfortunately, this compound was poorly soluble in common solvents and therefore all the standard data were not collected. The IR data exhibited all the expected peaks for the compound and compared well with the IR spectrum of **1b**. The elemental analysis percentages further confirmed the compound's formula with excellent agreement.

Compound **1d** was formed in low yield and characterised using the standard techniques. However, peaks observed in the ^{1}H NMR spectrum showed a mixture of isomers were

formed. This was due to the possibility of the CS_2 attacking either ends of the substituted piperazine (2-methylpiperazine) (Figure 7). This resulted in a complicated spectrum in which individual proton environments could not be assigned. Despite this, MS identified the correct parent ion (173 (M^+)) and IR stretches also agreed with the predicted compound. The elemental analysis showed exceptional agreement in the calculated percentages: C, 40.87; H, 6.86; N, 15.89 and found percentages: C, 40.40; H, 6.97; N, 15.52 to confirm structure.

Figure 7: Two forms of 2-methylpiperazine dithiocarbamate zwitterion

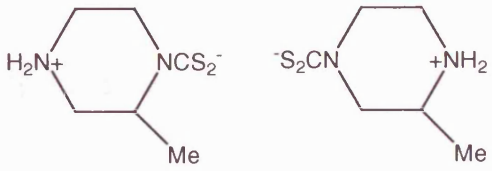

The last compound in this set was $[S_2CNC_5H_{10}][H_2NC_5H_{10}]$ (**1e**), formed from piperidine (Figure 8). The ^1H NMR spectrum showed a broad singlet at δ 8.89, which represented the NH_2^+ protons. Following this were the four protons on C_{2a} and C_{6a} closest to the N-CS_2 were a triplet at δ 4.32 (J 5.0 Hz). The four protons closest to the NH_2^+ (protons on C_{2b} and C_{6b}) were also triplets at δ 3.26 (J 5.7 Hz). Finally, the twelve protons furthest from both the CS_2 (protons on C_{3a} – C_{5a}) and NH_2^+ (protons on C_{3b} – C_{5b}) piperdines appeared as a multiplet at δ 1.56.

Figure 8: Structure of piperidine compound 1e

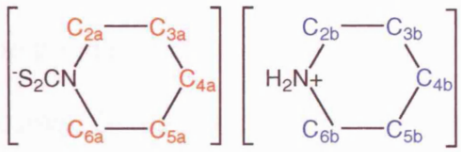

The ^{13}C NMR data identified the expected peaks that were typical for these types of compounds. The IR and MS data correctly displayed the desired peaks and stretches with excellent elemental analysis data confirming structure.

Disalts (**2**): Compounds **2a-d** were all formed in a similar fashion to compounds in set **1.** The desired piperazine was stirred in distilled water with two equivalents of base (KOH) and CS_2 to form a white precipitate. The general structure of these compounds is outlined below, including some compounds with substituents on the ring (Figure 9).

Figure 9: Structure of disalt dithiocarbamate compounds 2a-d

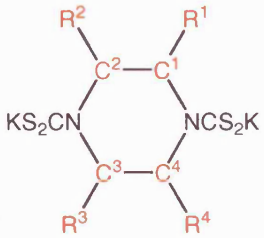

Compound	Substituents on C atom
2a	All protons
2b	R^1 = Me, R^3 = Me
2c	R^1 = Me, R^3 = Me or R^4 = Me, R^2 = Me
2d	R^3 = Me or R^4 = Me

Characterisation was carried out in order to confirm the formation of the proposed compounds. The ^1H NMR spectrum for **2a** had two sets of triplets at δ 3.82 and 5.18 representing the piperazine protons. The elemental analysis values for the calculated and found percentages of carbon, hydrogen and nitrogen were found to be accurate.

The other compounds in this set, namely **2b** and **2c** showed excellent correlation with the anticipated data. Both ^{1}H NMR spectra had four individual proton environments for the ring proton, very similar to their counterparts in set **1.** Further to this, the elemental analysis data showed good agreement, confirming the successful synthesis. As with **1d**, **2d** formed a mixture of isomers, therefore making peak assignment very difficult. However, IR and elemental analysis data confirmed the formation of the desired compound.

Monosalts (**3**): The synthesis of these compounds were identical to the compounds in set **2** but only one equivalent of base and CS_2 was used to attempt monosalt formation. In the case of **3a** and **3b**, the piperazines used (for **3a** 1-methylpiperazine and for **3b** for 1-ethylpiperazine) were primary amines on one nitrogen with the other nitrogen atom had a R group. The third amine used for **3c**, 2-methylpiperazine, had two primary amines. On examination of the characterisation data undertaken on these compounds, it was found that the monosalt was not formed but a type of zwitterion instead (Figure 10).

Figure 10: Zwitterions formed instead of the monosalts (3a-c)

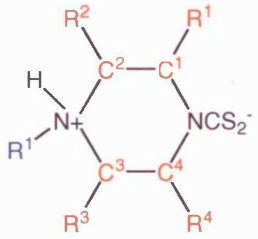

Compound	Substituents on R atom
3a	R^1 = Me, R^1 - R^4 = H
3b	R^1 = Et, R^1 - R^4 = H
3c	R^4 = Me, R^1 = R^1 – R^3 = H or
	R^3 = Me, R^1 = R^1 – R^2 = R^4 = H

Compound **3a** was found to be insoluble therefore limiting characterisation data. The IR spectrum identified the correct stretches expected for this compound and the elemental analysis data confirmed the formation of the zwitterion with exceptional agreement. Compound **3b** was also found to be an insoluble zwitterion with good IR data and excellent elemental analysis values confirming the formation of zwitterion and not monosalts (calculated: C, 44.17; H, 7.41; N, 14.72; found C, 44.03; H, 7.64; N, 14.54).

The final compound (**3c**) in this set was formed from 2-methylpiperazine and like its predecessors, also formed a mixture of isomers. This compound was more soluble and NMR data was collected but due to the numerous isomers, the spectrum was too complicated to elucidate. However, the compound formula was been confirmed with elemental analysis data showing excellent corroboration.

6.22 Nickel compounds

After successful formation and characterisation of the various starting materials, the zwitterions **1a-d** were reacted with $Ni(OAc)_2$ in distilled water followed by base to form complexes **4a-d** in high yields (88 - 92%) (Figure 11).

Figure 11: Nickel compounds with piperazine rings (4a-d)

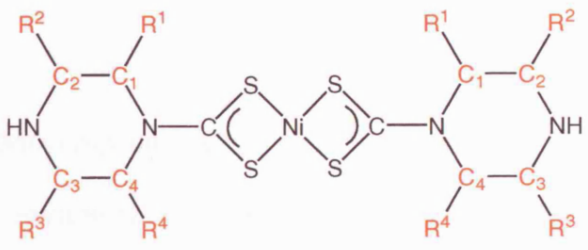

Compound	Substituents on C atom
4a	All protons
4b	R^2 = Me, R^3 = Me
	R^1 = Me, R^4 = Me
4c	R^1 = Me, R^3 = Me or
	R^4 = Me, R^2 = Me
4d	R^3 = Me

Compound **4a** was found to be poorly soluble and elemental analysis was used to confirm the structure. The elemental percentages showed the calculated values as C, 31.50; H, 4.72; N, 14.70; S, 33.60 and the found values were C, 31.13; H, 4.67; N, 14.53; S, 33.20.

Characterisation of **4b** using ^{1}H NMR spectroscopy showed four individual proton environments including the substituent methyl groups in compound **4b**. The spectrum showed the axial protons were represented as a triplet at δ 2.53 (J 11.6 Hz) and a broad singlet at δ 2.85, which were the protons coupled to the methyl group on the same carbon. The four equatorial protons antiperiplanar to the methyl groups on both rings appeared as a doublet at δ 4.41 (J 12.7 Hz). The two methyl groups were equivalent as a doublet at δ 1.10 (J 5.9 Hz) as expected. The ^{13}C NMR data identified the correct number of carbon peaks in the expected ranges. Despite the elemental analysis data being poor, the MS data identified the correct parent ion 437 (M^+) to further substantiate the structure.

The data collected from compound **4c** was different to **4b**. The ^{1}H NMR data displayed a multitude of proton environments. Due to the complex nature of the compound, there was some difficulty in identifying the axial and equatorial protons. However, we

identified the appropriate number of protons at δ 2.59 (d, 2H, J 13.3 Hz), 3.23 – 3.32 (m, 6H), 4.12 (d, 2H, J 11.8 Hz) and 4.97 (brm, 2H) with two different sets of methyl groups as doublets at δ 1.18 and 1.32 (both have J 6.8 Hz). The MS data identified the parent ion as 437 (M^+) and the IR data also displayed the correct stretches. The elemental analysis percentages calculated as C, 38.45; H, 5.99; N, 12.81 and values found were C, 37.08; H, 5.57; N, 11.52, showing good agreement.

With compound **4d**, the starting material zwitterion was a mixture but on reaction with the nickel source, formed one product with the methyl groups pointing away from the nickel centre (Me on C_3). This indicated the isomers of **1d** were in equilibrium and that addition of a nickel source shifted the equilibrium to favour one isomer and therefore one product. The ^{1}H NMR spectrum assigned four equatorial protons as a multiplet at δ 2.82 (J 9.5 Hz) and the other two equatorial protons triplet at δ 2.63 (J 10.7 Hz). The two sets of axial protons at δ 3.02 and 4.41 were a multiplet and quartet respectively with δ 1.10 as a doublet for four methyl groups (J 6.3 Hz). The ^{13}C NMR spectrum peaks were in the expected range for this compound. The MS parent ion was 409 (M^+) with corroborating IR stretches, verifying structure.

6.23 Copper compounds

As the nickel compounds were successfully made, copper acetate was reacted with the zwitterions (**1a-d**) to form brown solids in high yields (Figure 12). Due to the paramagnetic nature of these compounds, NMR analysis was problematic. Therefore, IR spectra and elemental analysis data was used to characterise structure formation. The calculated percentages of **5a** were C, 29.74; H, 4.96; N, 13.87; S, 31.72 and the

observed values were 29.52; H, 4.40; N, 13.37; S, 31.72 showing excellent agreement along with appropriate IR stretches.

Figure 12: Copper compounds with piperazine rings (5a-d)

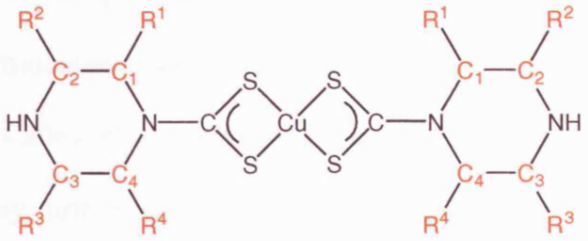

Compound	Substituents on C atom
5a	All protons
5b	R^2 = Me, R^3 = Me
	R^1 = Me, R^4 = Me
5c	R^1 = Me, R^3 = Me or
	R^4 = Me, R^2 = Me
5d	R^3 = Me or R^4 = Me

Compound **5b** was characterised by establishing the parent ion as 442 (M^+) and the use of IR data. The elemental analysis data for this compound was calculated as C, 31.40; H, 4.94; N, 9.15 and the observed values were C, 30.37; H, 5.31; N, 9.93, substantiating the compound. Compounds **5c** and **5d** were characterised with parent ions of 442 (M^+) and 414 (M^+) respectively. The elemental analysis data for both compounds also showed good agreement.

As the nickel and copper complexes had limited solubility and the paramagnetism of copper centre complicated characterisation, further addition of units would be problematic. Therefore, we considered alternative metal centre from which to build networks of dithiocarbamate compounds. The metal compounds were required to have well-defined geometry and highly soluble.

6.24 Ruthenium compounds

The complex, *cis*-$[Ru(dppm)_2Cl_2]$[19] was the key metal compound in our investigation of dithiocarbamates. This complex was chosen as it reacted cleanly with a range of dithiocarbamate salts forming $[Ru(dppm)_2(S_2CNR_2)]^+$[20] in high yields. By varying the R-groups of the dithiocarbamates, numerous complexes could be formed. Using piperazine zwitterions allowed one end of the ring to be fixed with a capping metal unit, therefore directing any further reactions to the other end of the compound. The *para*-piperazine system forced any joining units to be added at the vacant site in a linear fashion.

Following the synthesis outlined by Menon *et al.*[20] the starting material, *cis*-$[Ru(dppm)_2Cl_2]$ (**6**) was formed and characterised. The ^1H NMR spectrum confirmed the formation of the structure. The expected phenyl protons from the (diphenylphosphino)methane (dppm) fragment were represented by numerous multiplets in the region δ 6.56 – 8.21, equalling forty protons. The two methylene protons of the dppm units bridging PPh_2 were two multiplets at δ 4.65 and 4.91. The ^{31}P NMR spectrum identified the two phosphorus peaks as mulitplets at δ -25.9 and -6.6. Further to this NMR data, the MS showed the parent ion 905 (M^+ - Cl) and the IR stretches concurred with the expected values. The elemental analysis data showed excellent correlation between the calculated (C, 63.84; H, 4.71) and observed (C, 63.66; H, 4.86) values, confirming the structure.

Once this compound was fully characterised, it was used to synthesis the other compounds in this chapter. To first test the versatility of this compound, it was reacted with standard dithiocarbamates, such as commercially available NaS_2CNMe_2 and

NaS_2CNEt_2 as well as piperidine dithiocarbamate. The reactants were stirred in a methanol solution with an aqueous solution of $NaBF_4$ for a period of 1 h. This was then reduced to dryness and recrystallised from DCM and ethanol to form pale white-yellow solids in excellent yields (**6a-c** respectively). The compounds were characterised using the standard techniques, which confirmed the formation of the required compounds (Figure 13).

Figure 13: Ruthenium dithiocarbamate compounds with different amine groups (7a-c)

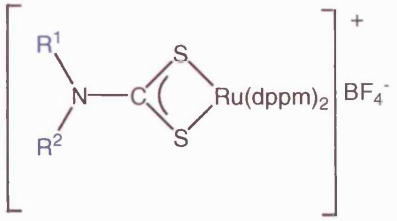

Compound	Substituents on N atom
7a	$R^1 = R^2 = Me$
7b	$R^1 = R^2 = Et$
7c	R_2 = Piperidine

Compound **7a** showed the expected ^1H NMR peaks for the phenyl groups equalling the forty protons in the range δ 6.45 - 7.59. The dppm-CH_2 protons were also mulitplets at δ 4.46 and 4.88. The amine fragment of the dithiocarbamate had two methyl groups as singlets at δ 3.31 and 3.51, which were expected to be at higher field due to the attached nitrogen atom. The ^{31}P NMR showed two triplets at δ -3.80 and δ -17.38 with J coupling of 34.2 Hz. Other data agreed with the proposed structure as MS and IR exhibited the expected values, as did the elemental analysis data (calculated: C, 57.40; H, 4.60; N, 1.30 and found: C, 57.60; H, 4.70; N, 1.30).

Compounds **7b** and **7c** displayed very similar NMR data for the core structure of the compounds. The ^{1}H NMR data for **7b** included the additional two CH_2 group at δ 3.48 as a multiplet from the ethyl fragment on the dithiocarbamate. The ^{31}P NMR data was similar to **7a** as triplets at δ -4.4 and -17.0 (both J 34.1 Hz). The ^{1}H NMR spectrum for **7c** showed the core structural peaks of the dppm with the appropriate number of protons. The peaks identified the correct piperdine protons as multiplets at δ 1.46 (6H) and 3.58 (4H). The ^{31}P NMR data was again similar to **7a-b** as triplets at δ -4.2 and -17.8 with J 34.0 Hz. The other characterisation data from IR, MS and elemental analysis all substantiated the proposed structure for **7b** and **7c**.

6.241 Ruthenium compounds with various piperazines

All the dithiocarbamate ligands attached to the starting ruthenium compound **6** were based on piperazine due to the nitrogen at either end on the ring (1, 4 positions). These zwitterions allowed the active CS_2 end to bond with the ruthenium metal centre to form a metallodithiocarbamate with an ammonium end, which was free to react further with the addition of base and CS_2. Figure 14 shows compounds **8a-d** with the various substituents on the piperazine ring.

Figure 14: Structure of ruthenium dithiocarbamate compounds with substituted piperazine rings

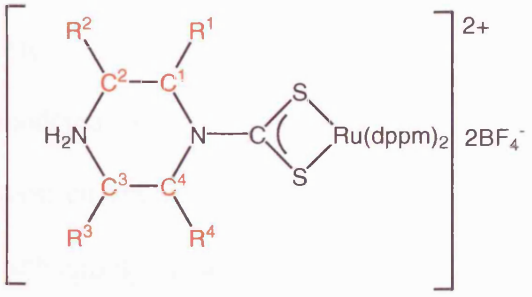

Compound	Substituents on C atom
8a	All protons
8b	R^1 = Me, R^3 = Me
8c	R^1 = Me, R^3 = Me or
	R^4 = Me, R^2 = Me
8d	R^3 = Me or R^4 = Me

All these compounds were formed using the standard method and produced moderate - good yields. Characterisation of **8a** showed the ^{1}H NMR data correctly identify the protons from the phenyl groups as well as the dppm-CH_2 protons in the previously established range. The piperazine protons were represented in two sets, four protons as a multiplet at δ 3.04 and the other four at δ 3.88. The last set of protons on this ring was the NH_2 protons, which appeared as a broad singlet at δ 2.35. The ^{31}P NMR had two triplets at δ -3.8 and -17.3 (J 34.4 Hz), which were similar to the other compounds. The MS identified the parent ion 1030 (M^+) and the IR stretches agreed with the expected compounds. The elemental analysis data further confirmed the proposed structure as the calculated values: C, 57.50; H, 4.70; N, 2.40 and found values: C, 57.80; H, 4.60; N, 2.50 were in excellent agreement.

Both **8b** and **8c** showed similar peaks in the ^{1}H NMR spectra of the core structure with different peaks for the substituted piperazine protons. The ^{1}H NMR spectra for these compounds proved to be more complicated than expected. It showed that all the protons on the ring were inequivalent, unlike in the starting materials. To further understand this, we considered the conformation of the ring as a free ring, adopting a chair conformation (lowest energy conformer). It is proposed that the reaction of the zwitterion with the ruthenium metal centre forces the piperazine to alter its conformation to meet the constraints of the bonding. It is well known that the C-N bond

of the S_2C-N group has double bond character and therefore has planar geometry that extends to the sulfur atoms (see below).

Figure 15: Planar nature of S_2C-N bond exhibiting double bond character

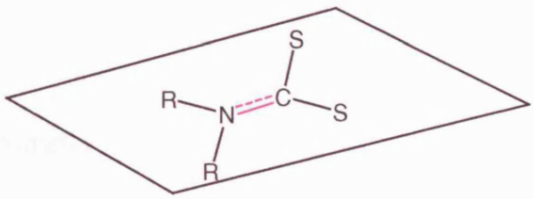

Once the CS_2 end of the dithiocarbamate binds to the ruthenium centre, it forces the piperazine ring to twist so that the S_2C-N bond can have a planar geometry, resulting in a twisted-boat conformation. If this conformation is adopted, all the protons on the ring become inequivalent, giving six proton environments in addition to the methyl protons (Figure 16).

Figure 16: Twisted-boat conformation of 8a

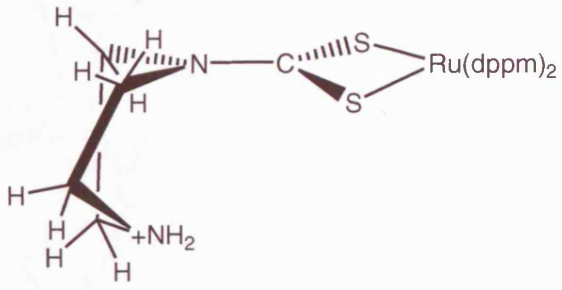

We proposed that there is equilibrium between the chair conformation and the twisted-boat conformation, resulting in the inequivalent proton environments. Aliev *et al.* [21] provided evidence to substantiate this equilibrium through their work on 2, 5 –dimethyl

–4-piperidinone. They conducted detailed NMR studies that investigated the various protons on this complex. The oxygen bound at the fourth carbon *via* double bond constrained the O=C-N to a planar geometry. This constraint was found to contort the ring from a chair conformer to twisted-boat, therefore rendering all the protons inequivalent.

Applying the planar geometry of the C-N bond with a ring system and a metal centre, the crystal structure of [Ni(dppp)($S_2CNC_4H_8NH$)] was determined (Figure 17). This structure was similar to the ruthenium complexes and parallels were made between them. The nickel centre binds with the piperazine dithiocarbamate in which S_2C-N maintains its planar geometry and clearly contorts the ring[22].

Figure 17: Crystal structure of [Ni(dppp)($S_2CNC_4H_8NH$)][22]

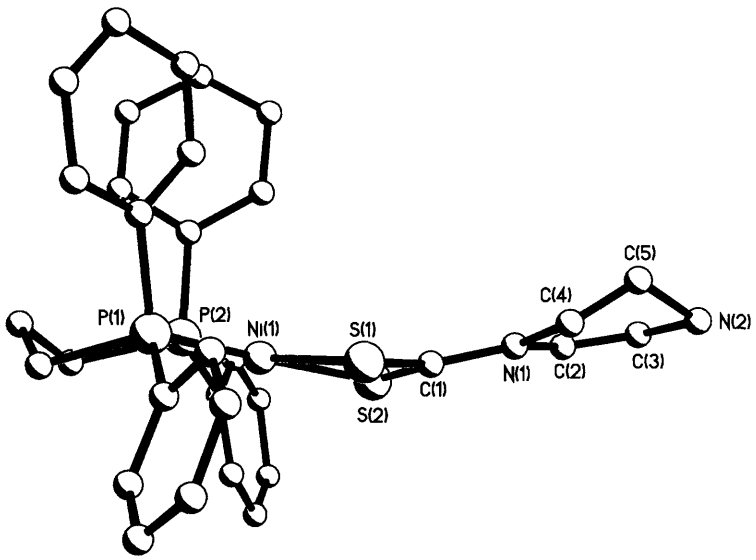

The twisted-boat conformer of the ring can be seen clear in Figure 18 when the S_2C-N bond is exhibited as planar. This crystal confirms the contortion of the ring and the inequivalency of the protons.

Figure 18: Crystal structure of [Ni(dppp)($S_2CNC_4H_8NH$)][22], displays the planar nature of S_2C-N.

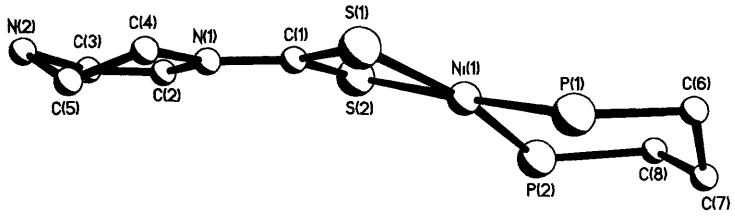

This equilibrium effect in the ruthenium complexes were less pronounced in **8a** due to all the substituents being protons. The substituted rings in compound **8b** and **8c** clearly show this effect. The ^1H NMR spectrum for **8b** has the standard peaks for the phenyl and dppm-CH_2 protons. Two of the equatorial protons were a broad triplet at δ 4.38 (J 14.5 Hz). Next, the two protons on the same carbon as the methyl substituents were multiplets at δ 2.56 – 2.61 and 2.76 – 2.81 and the two axial protons were triplets at δ 2.25 (J 11.6 Hz) and 2.45 (J 11.6 Hz). The methyl groups from the ring were represented by a broad triplet, which suggested slightly different environments (Figure 19). The ^{31}P NMR data showed two multiplets at δ -3.9 and -17.9 with MS and IR data in agreement of the structure. The elemental analysis values of the proposed compounds were accurate with calculated percentages: C, 55.49; H, 4.74; N, 2.27 and found percentages: C, 56.58; H, 4.81; N, 2.22.

Figure 19: Twisted-boat conformation of 8b and 8c.

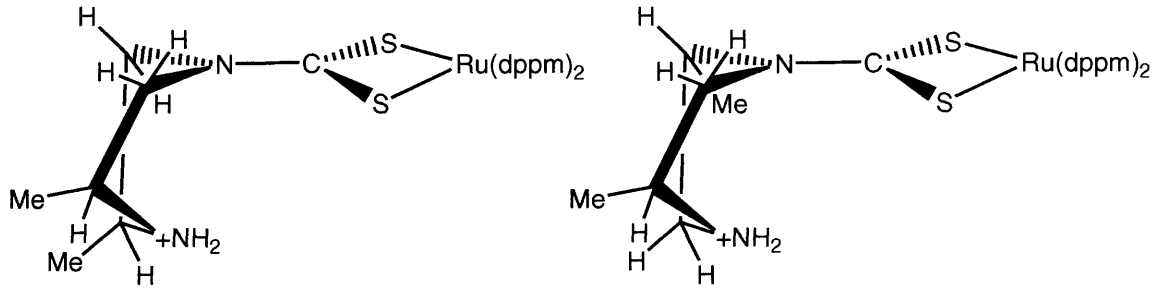

8b **8c**

In compound **8c,** all the data corroborated the structure proposed. The protons in this spectrum exhibited the expected phenyl and dppm-CH_2 protons as well as individual proton environment of the substituted ring. In addition, MS, IR and elemental analysis data also confirmed compound with the *trans*-2, 5-dimethyl substituents (Figure 19).

In this set of compounds, **8d** was formed using the zwitterion **1d.** The zwitterion was found to be a mixture of isomers however, when reacted with *cis*-[$Ru(dppm)_2Cl_2$] (**6**), only one form of the zwitterion reacted with the compound, enabling characterisation of the compound *via* ^1H NMR. This would indicate that the isomers were in equilibrium and that reaction with the ruthenium complex shifted the equilibrium to form one major isomer and therefore one product. The spectrum showed phenyl and dppm-CH_2 protons in the expected range like the other compounds. The CH proton of the substituted piperazine was part of a multiplet at δ 2.51 – 2.62 including the NH_2 protons. The other CH_2 protons were also multiplets at δ 2.81 – 2.89, δ 3.07 – 3.48 and δ 4.23 – 4.46 and the methyl protons appeared as a two overlapping doublets at δ 1.18 (J 6.0 Hz) and 1.21 (J 6.0 Hz). It was difficult to assign all the inequivalent proton environments in this compound due to the complex multiplets. The ^{31}P NMR spectrum peaks were in the same range as the other compounds and the MS/IR data with the elemental analysis data corroborated the proposed structure.

To investigate the possibility of adding units to both ends of the piperazine ring, compounds **9a-c** were first formed using the one equivalent of *cis*-[$Ru(dppm)_2Cl_2$] and the disalt starting materials (**2a-d**) to consider the control of the process. The ruthenium dithiocarbamate salts were successfully formed and had an active dithiocarbamate end that could further react (Figure 20).

Figure 20: Structure of ruthenium dithiocarbamate salts (9a-c)

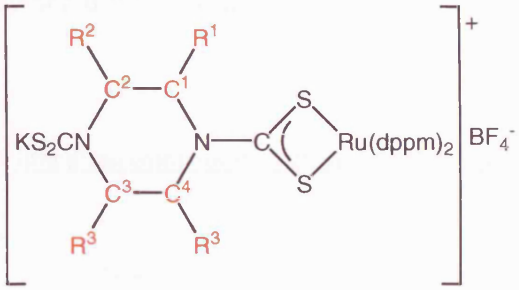

Compound	Substituents on C atom
9a	All protons
9b	R^2 = Me, R^3 = Me
9c	R^1 = Me, R^3 = Me or
	R^4 = Me, R^2 = Me

These compounds were formed in low-medium yields and fully characterised using the standard techniques. The ^{1}H NMR spectrum of **9a** displayed the phenyl and dppm-CH_2 protons in the expected range with the piperazine protons appearing as two multiplets at δ 3.53 and 3.62. Other data that corroborated the structure were the ^{31}P NMR, IR and elemental analysis percentages.

Compounds **9b** and **9c** were similar to compound **8b** and **8c**. As the dithiocarbamate disalt reacted with **6**, the ring interchanged between the chair and twisted-boat conformation. Hence, all protons on the ring were inequivalent, giving different peaks in ^{1}H NMR spectra. Further to this, ^{31}P NMR, IR, MS and elemental analysis data identified the correct values to confirm the structures.

To consider the possibility of having a non-metallic end group such as a substituted piperazine ring, complexes **10a-b** were formed from 1-methylpiperazine (**3a**) and 1-

ethylpiperazine (**3b**) zwitterions respectively (Figure 21). The yields of these yellow compounds were high (80 %) and fully characterised to confirm the structure desired.

Figure 21: Structure of ruthenium compounds with methyl (10a) and ethyl substituents (10b)

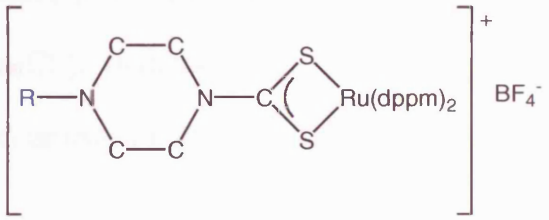

Compound	R group
10a	Me
10b	Et

The ^{1}H NMR data for **10a** showed the related peaks for the phenyl and dppm-CH_2 protons alongside the respective protons for the substituted piperazines. There were four different proton environments on the ring. All were multiplets, representing two ring protons each at δ 2.59, 2.67, 3.62 and 3.72. The methyl substituent was seen as a singlet at δ 2.54. The ^{31}P NMR showed triplets at δ -3.9 and -17.5 and in the MS, a parent ion was identified at 1059 (M^+ - BF_4). The IR and elemental analysis data also confirmed the formula.

The data for compound **10b** with the ethyl substituent was very similar to **10a**, the methyl group appearing as a triplet at δ 1.11 (J 7.1 Hz) and the methylene protons as a quartet at δ 2.47 (J 7.1 Hz). The ^{31}P NMR, MS and IR data were all in accordance to the expected compound. The elemental analysis data showed the calculated percentages as C, 59.74; H, 5.01; N, 2.44 and observed value as C, 58.15; H, 5.03; N, 2.39, therefore further proving the structure.

As we were able to add various piperazine units onto the ruthenium compound (**6**), we attempted and succeeded in forming binuclear compounds consisting of two ruthenium unit on either end of the piperazine by using the appropriate disalt compounds (**11a-c**). To test the limits of this reaction, this binuclear piperazine compound was also prepared by forming the ruthenium piperazine dithiocarbamate (**8a**) compound, then adding base, CS_2 and *cis*-$[Ru(dppm)_2Cl_2]$. Both methods successfully formed the desired compound as a pale yellow solid in generally high yields and was characterised (Figure 22).

Figure 22: Binuclear ruthenium complexes using various substituted piperazine rings

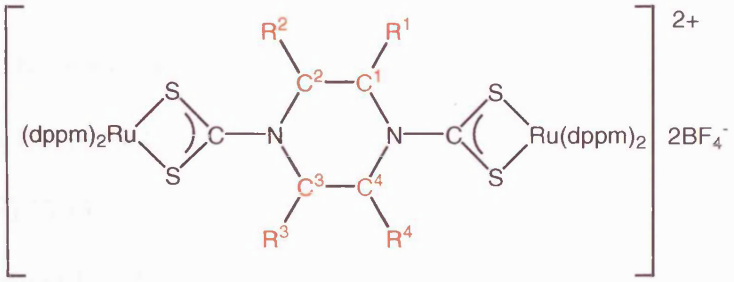

Compound	Substituents on C atom
11a	All protons
11b	R^2 = Me, R^3 = Me
	R^1 = Me, R^4 = Me
11c	R^1 = Me, R^3 = Me or
	R^4 = Me, R^2 = Me

Analysis of **11a** showed that the ^1H NMR spectrum displayed the phenyl and dppm-CH_2 protons along with two multiplets at δ 3.51 and 3.62 for the piperazine protons. The ^{31}P NMR displayed two triplets at δ -4.1 and -16.8 (both J 34.2 Hz). The MS identified the parent ion at 1976 (M^+) with relevant IR stretches. The elemental analysis data further

corroborated the compound as the calculated values were C, 57.50; H, 4.40; N, 1.30 and found values were C, 57.30; H, 4.60; N, 1.30.

The single crystal structure of **11a** was determined to reveal a unique structure. The pale yellow monoclinic crystal (space group $P_{21/c}$) displayed a bridging dithiocarbamate mode in this complex which is rare with only a few examples in the literature such as $[Cp(PPh_3)Ru(S_2CNC_6H_4NCS_2)Ru(PPh_3)Cp]$[23] and dinuclear tin complexes[24].

The bond lengths in the ruthenium dppm fragment were in the expected range. The Ru-P bonds were all approximately the same at 2.322(2) Å (Ru(1)-P(1)) and the distances between the P-CH_2 of the dppm fragment were in the region of 1.829(8) Å (P(1)-C(11)). The bond from the phosphorus to the aromatic phenyl groups were relatively long at 1.825(8) Å (P(3)-C(35)) and were all approximately the same. The carbon bond lengths were all as expected for phenyl rings between 1.370(11) – 1.404(11) Å. Comparison of the Ru-S bonds found good agreement in and around 2.452(2) Å (Ru(1)-S(1)) for both metal centres. The S-C bonds on both ruthenium centres measured 1.701(8) – 1.730(8) Å. Both C-N bonds were a similar length at 1.340(9) Å (C(1)-N(1)) which confirmed partial double bond character as the values were between a single C-N bond was 1.47(7) Å and a double bond C=N was1.29(8) Å[25]. Finally, within the piperazine ring, the N-C bonds was measured to be 1.483(9) Å (N(1)-C(2)). The piperazine ring was in a chair conformation and the C-C bonds were in the range 1.493(9) Å (C(2)-C(3)) to 1.503(11) Å (C(4)-C(5)), as expected for this conformation (Figure 23).

Figure 23: Crystal structure of binuclear compound 11a

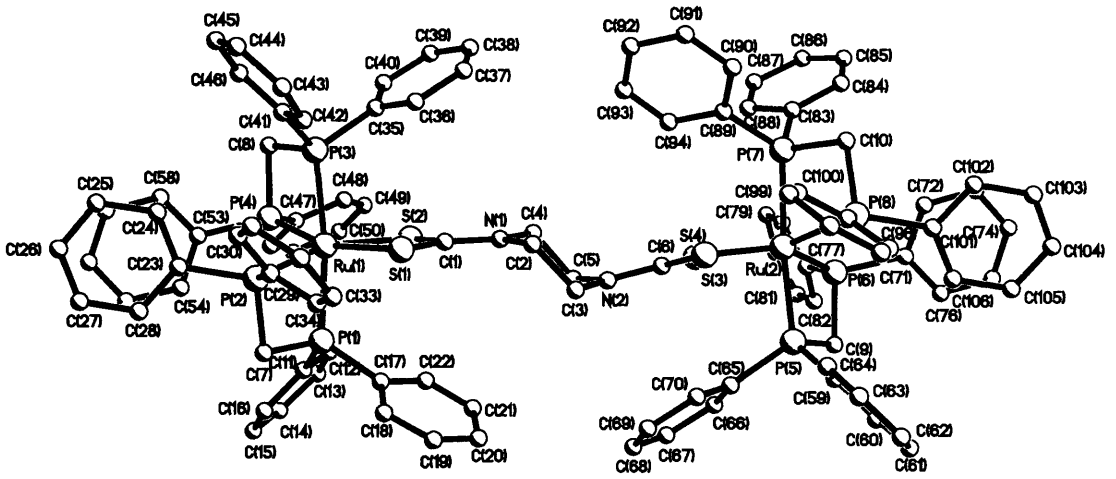

The angles in both sections of this complex displayed the ruthenium metal centres as distorted octahedral centres at 172.98° (P(1)-Ru(1)-P(3)) and 162.20° (P(4)-Ru(1)-S(1)). The phosphine bite-angles P-Ru-P were 73.34° (P(3)-Ru(1)-P(4)) for both centres. The angle between P-CH_2-P in the dppm moiety was measured to be 97.30° (P(4)-C(10)-P(3)). The phenyl rings in the dppm moiety exhibited the expected angles to confirm the structure of phenyl ring. A key angle in this complex was the bite angle, S-Ru-S angle, which was nearly equal on both centres at 71.40° (S(2)-Ru(1)-S(1)) and 71.97° (S(3)-Ru(2)-S(4)). The S-C-S angle was measured to be 112.30° (S(1)-C(1)-S(2)). The final key angle in this structure was the piperazine ring C-N-C that was approximately the same at 113.90° (C(4)-N(1)-C(2)).

Compounds **11b** and **11c** were similar **11a**. The interesting pattern observed was that the ^{1}H NMR data show four proton environments, suggesting that the ring was no longer in equilibrium with a twisted-boat confirmation but had reverted back to the more stable chair conformation. It is proposed that the addition of one ruthenium

compound **6** contorts the ring into the twisted-boat conformer but having the ruthenium centre on each end fixes the geometry of the ring and does not allow flipping. This forms the most stable conformer with the piperazine in the chair conformation. For example, the ^{1}H NMR data for **11b** showed the two axial protons as a multiplet at δ 3.15, the two equatorial protons were also multiplets at δ 4.35 and the axial protons on the carbon with the methyl group at δ 3.31. The two methyl groups were triplets at δ 1.21 (J 7.0 Hz). Further to this, the ^{31}P NMR, IR and elemental analysis data also confirmed the anticipated compound. The data for **11c** was, as anticipated, similar to **11b** corroborating the structure from NMR, IR and elemental analysis data.

6.242 Ruthenium compounds with various metal compounds

After the successful formation of ruthenium compounds with various substituted piperazine dithiocarbamates and bimetallic bridging-dithiocarbamates, we expanded the range of end groups to different metals. The first set of compounds (**12a-c**) prepared was with gold triphenylphosphine ($AuPPh_3$). These were formed in moderate yields as yellow-brown solids (Figure 24).

Figure 24: Dithiocarbamate-bridged bimetallic complexes with different substituted piperazine rings.

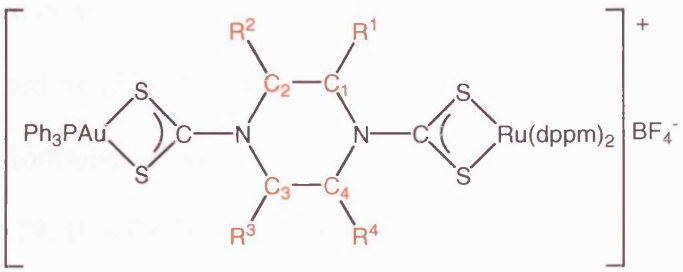

Compound	Substituents on C atom
12a	All protons
12b	R^2 = Me, R^3 = Me
	R^1 = Me, R^4 = Me
12c	R^1 = Me, R^3 = Me or
	R^4 = Me, R^2 = Me

In **12a**, the ^{1}H NMR spectrum showed the eleven different phenyl protons, eight from the dppm fragment and three from the $AuPPh_3$ moiety as numerous multiplet of multiplets in the range δ 6.69 – 7.63 (55H). The methylene protons from dppm fragment were multiplets at δ 4.75 and 5.36. The other protons in this compound were the piperazine protons, all multiplets, representing two protons each at δ 3.73, 3.92, 4.14 and 4.23. In the ^{31}P NMR spectrum, a broad singlet at δ 37.5 was assigned to $AuPPh_3$ and two triplets at δ -3.0 and δ -18.0 (both J 34.5 Hz) to the dppm. The MS gave a parent ion at 1566 (M^+) and all the IR stretches present were as expected. The elemental analysis values for the calculated: C, 53.80; H, 4.10; N, 1.70 and found: C, 54.00; H, 4.00; N, 1.60 showed excellent agreement.

The same reaction was carried out with the substituted piperazines to form **12b** and **12c**. The data for these compounds compared well with **12a** with the relevant peaks for the corresponding substituents. Unfortunately, they were only partially soluble and the NMR data was too complex to identify individual peaks. However, in the MS parent ions were confirmed as 1528 (M^+) for **12b** and 1566 (M^+) for **12c**. The key data for confirming their formulation was elemental analysis data. For **12b**, the calculated percentages C, 53.79; H, 4.09; N, 1.70 and the found C, 52.07; H, 4.76; N, 1.78 were in outstanding agreement. The elemental analysis data for **12c** was also in excellent

agreement as the calculated percentages were C, 53.79; H, 4.09; N, 1.70 and the found percentages were C, 54.74; H, 5.25; N, 1.57.

Continuing to expand the range of compounds formed with linking piperazine units, bis and tris compounds were prepared using piperazine and a range of metal centres (Figure 25) to form complexes **13**. These were formed in a range of colours and good yields. The syntheses involved using compound **8a** and adding base and CS_2 to form the active metallodithiocarbamate followed by the addition of the required metal source and $NaBF_4$ to balance the charges. The trimetallic units were formed based on two ruthenium dithiocarbamate ligands with CS_2 ends reacting with nickel and copper acetate to form compounds **13a** and **13b** respectively. The tetranuclear compounds were formed in a similar method to that of **13a** and **13b** with cobalt acetylacetone (**13c**) and lanthanide trichloride (**13d**).

Figure 25: Tri- and tetranuclear metal complexes with ruthenium dithiocarbamate complexes

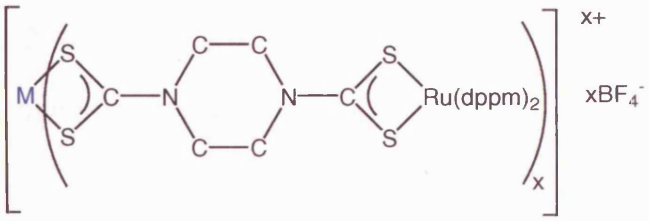

Compound	M	x
13a	Ni	2
13b	Cu	2
13c	Co	3
13d	La	3

Compound **13a** contains a diamagnetic nickel metal centre. This brown solid was fully characterised using the standard techniques. As the standard unsubstituted piperazine was used, the ^{1}H NMR data was less complicated than the substituted piperazines. The eighty phenyl protons were represented as a group of multiplets in the range δ 6.52 – 7.61. The two sets of dppm-CH_2 from the two ruthenium centres appeared as multiplets at δ 4.64 and 4.98, a further multiplet equalling sixteen protons corresponding to the two piperazine rings. The ^{31}P NMR spectrum showed triplets in the standard range of δ -4.2 and -16.8 (both J 34.5 Hz). The MS correctly identified the parent ion 2271 (M^+) and the elemental analysis percentages confirmed the formula (calculated: C, 55.00; H, 4.30; N, 2.30 and found: C, 55.40; H, 4.20; N, 2.20).

Compound **13b** formed a similar bis-compound to **13a** with a copper centre with the data showing good agreement with the proposed structure. The ^{1}H NMR data identified the phenyl and dppm-CH_2 protons in the correct region but the piperazine protons were not observed due to the paramagnetism of the copper (II) centre. The ^{31}P NMR peaks were almost identical to that of **13a** and the IR data also showed the correct stretches. The MS parent ion 2276 (M^+) and the calculated elemental percentages: C, 53.60; H, 4.20; N, 2.20 and found percentages: C, 53.40; H, 4.20; N, 2.20 were in excellent agreement.

The other two compounds in this set were tris-compounds (tetranuclear) with cobalt (**13c**) and lanthanum (**13d**). Both displayed the correct phenyl and dppm-CH_2 protons in the appropriate range. There were two sets of protons corresponding to the piperazine environments as multiplets at δ 3.66 and 3.79 for **13c**, δ 3.64 and 3.79 for **13d**. The ^{31}P NMR for both compounds were similar to that of **13a-b** and the individual

MS parent ions were identified. The IR and elemental analysis values for both compounds were in agreement of the proposed compounds.

It was established that a range of dithiocarbamate-bridged binuclear and trinuclear metal complexes could be formed using suitable reagents. The compounds [Os(CH=CHR)Cl(CO)(BTD)] (BTD = 2, 1, 3-benzothiadiazole), $[Pd(C_6H_4CH_2NMe_2)(\mu\text{-}Cl)_2]$ and $[Ni(dppp)Cl_2]$ (dppm = bis(diphenylphosphino)propane) were reacted with the ruthenium dithiocarbamate compound to form **14a-c** (Figure 26).

Figure 26: Dithiocarbamate-bridged bimetallic complexes using osmium, palladium and nickel centres

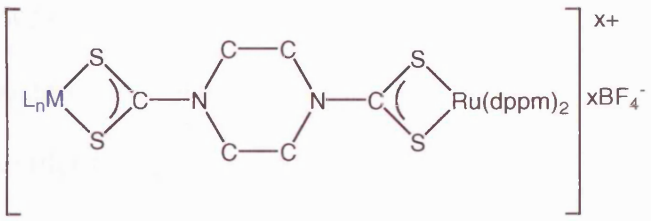

Compound	L_nM Group	x
14a	$Os(CH{=}CHC_6H_4Me\text{-}4)(CO)(PPh_3)_2$	1
14b	$Pd(C,N\text{-}C_6H_4CH_2NMe_2)$	1
14c	Ni(dppp)	2

The characterisation of **14a** showed the formation of the desired compound. The ^1H NMR spectrum identified the phenyl and dppm-CH_2 protons in the anticipated range. The H_α and H_β protons were at δ 8.28 and 5.59 respectively. The aromatic protons on the alkene group were at δ 6.36 and 6.81. The piperazine protons appeared as a broad multiplet between δ 2.78 – 3.33 and the methyl was represented as a singlet at δ 2.21.

The ^{31}P NMR spectrum displayed three peaks for the phosphorous, a singlet at δ 9.3 for the PPh_3 and two triplets at δ –4.4 and –17.1, both with coupling constants of 34.4 Hz. The parent ion 1967 (M^+) was identified and the elemental analysis showed excellent agreement in percentages (calculated: C, 57.90; H, 4.40; N, 1.30, found: C, 57.70; H, 4.50; N, 1.30) to confirm the structure.

Compound **14b** formed a white solid in excellent yield (89 %) and was characterised using the standard techniques. The ^1H NMR data exhibited the forty protons for the phenyls and the four protons of C_6H_4 from the palladium fragment. The dppm-CH_2 protons were multiplets at δ 4.64 and 4.96. The eight piperazine protons were multiplets at δ 3.71 and 3.79 and the CH_2 was a singlet at δ 4.01 for the two protons. The two methyl groups of the substituted piperazine appeared as a singlet at δ 2.92. The ^{31}P NMR peaks quoted two triplets in the standard range, confirming the ruthenium compounds were similar to the other compounds. The IR spectrum had corroborating data as did the MS and elemental analysis data.

The formation of compound **14c** used a different bidentate phosphine, di(phenylphosphino)propane (dppp). The ^1H NMR spectrum correctly identified the appropriate phenyl and dppm-CH_2 protons for the ruthenium and nickel centres. In addition, the three dppp-CH_2 protons appeared at δ 1.80 – 2.60 as a multiplet. Further to these, the piperazine protons were multiplets at δ 3.47 and 3.65. The ^{31}P NMR peaks identified δ 13.7 as a singlet of the dppp phosphorus and two triplets at δ -4.1 and -16.8 with J = 34.9 Hz. The MS, IR and elemental analysis data all corroborate the proposed compound.

Overall, the zwitterionic starting materials reacted with the ruthenium compound (**6**) to form the proposed compounds in variable yields. Many were soluble and characterised using standard techniques. Successful formation of the ruthenium compounds with the piperazines (**9a-c**) and detailed characterisation showed that when one ruthenium centre is co-ordinated with a piperazine dithiocarbamate, the planar nature of the S_2C-N bond contorts the ring to form an equilibrium between the stable chair and the twisted-boat conformers. Interestingly, when bimetallic ruthenium complexes were formed, this equilibrium was not observed, confirmed by the ^1H NMR data and crystal structure, exhibiting a chair conformer for the piperazine.

Various other metals centres (Au, Os, Pd, Co, Ni, La) were reacted with the ruthenium dithiocarbamate complex to form bi-, tri and tetrametallic compounds. These were all fully characterised and showed the versatility of the dithiocarbamate binding.

6.25 Palladium allyl compounds

The success of the ruthenium compounds led us to consider another metal system that still displayed good solubility and well-defined structure that could be reacted with the zwitterionic starting materials to form a new range of complexes. Palladium allyl dimer compounds, namely $[Pd(\eta^3\text{-}C_3H_5)(\mu\text{-}Cl))]_2$ and $[Pd(\eta^3\text{-}C_4H_7)(\mu\text{-}Cl))]_2$ were reacted with the piperazine dithiocarbamate zwitterions to form chains of units.

6.251 Protonic allyl compounds

Using $[Pd(\eta^3\text{-}C_3H_5)(\mu\text{-}Cl))]_2$ (see experimental section), compounds **17a-c** were formed using the synthesised zwitterions (**1a-c**). The compounds formed were yellow solids, which were characterised using the standard techniques (Figure 27).

Figure 27: Pallaldium protonic allyl complexes 17a-c

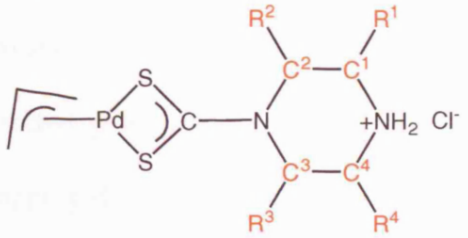

Compound	Substituents on C atom
17a	All protons
17b	R^2 = Me, R^3 = Me
	R^1 = Me, R^4 = Me
17c	R^1 = Me, R^3 = Me or
	R^4 = Me, R^2 = Me

Compound **17a** was found to have poor solubility and therefore, ^{1}H and ^{13}C NMR data collection was difficult. However, IR data showed stretches that correspond to the appropriate compounds. The elemental analysis percentages of the calculated and found values were as expected (calculated: C, 25.25; H, 3.53; N, 6.54, found C, 26.04; H, 3.52; N, 6.07) substantiating the formula.

Compound **17b** showed better solubility and ^{1}H NMR data was collected to confirm the structure. The five allyl protons were identified as a quartet at δ 2.78 (J 9.9 Hz), a doublet at δ 4.04 (J 6.7 Hz) and a multiplet at δ 5.12. The substituted piperazine axial protons appeared as a multiplet at δ 3.26 - 3.42 for four axial protons and the two other equatorial protons were a doublet at δ 4.54 (J 13.1 Hz). The methyl groups on the piperazine appeared as a pseudo quartet at δ 1.19, which were overlapping doublets. The IR stretches and MS parent ion 338 (M^+) confirm the expected structure, despite poor elemental analysis results.

Finally, compound **17c** had very similar ^{1}H NMR allyl peaks to that of **17b**. The piperazine peaks were two sets of multiplets at δ 2.59 and 4.81. The axial protons on the same carbon as the methyl group were a multiplet at δ 2.87 with the two methyl groups at δ 1.12 as overlapping doublet of doublets. The IR stretches matched that of **17c** and MS identified the parent ion 431 (M^+). Therefore, compound **17a-c** were successfully formed and characterised.

6.252 Methyl allyl compounds

As compounds **17a-c** had limited solublity, the reactions of $[Pd(\eta^3\text{-}C_4H_7)(\mu\text{-}Cl))]_2$ dimers with the zwitterions (**1a-d**) were attempted to increase solubility of the products and the possibility of further reactions and chain growth. These compounds were formed in good-moderate yields as pale yellow solids (Figure 28).

Figure 28: Palladium methyl allyl complexes 18b-d

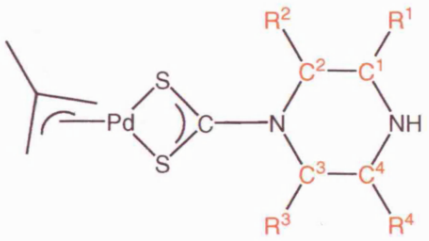

Compound	Substituents on C atom
18b	All protons
18c	R^2 = Me, R^3 = Me
	R^1 = Me, R^4 = Me
18d	R^1 = Me, R^3 = Me or
	R^4 = Me, R^2 = Me

The characterisations of these compounds were completed using the standard techniques. In this set of compounds, η^3-2-methylallyl had three distinctive peaks in ^1H NMR spectra. Compound **18a** was the same as **18b** but was charged with a NH_2^+ at the end of the piperazine ring with Cl^- anion. The two sets of allyl CH_2 in **18a** were singlets at δ 2.61 and 3.84 with a singlet for the methyl group at δ 1.77. The protons on the piperazine were represented by the singlet δ 3.12 (2H), broad doublet δ 3.25 (4H), a triplet at δ 4.03 (2H) and the broad singlet δ 4.14 (2H) for the NH_2. The other data that verified the compound was the parent ion at 288 (M^+ - Cl) and the elemental analysis. Compound **18b** exhibited the same data as **18a** but the uncharged neutral compound. The ^1H NMR, MS, IR and elemental analysis data all confirmed the formation of the neutral compound.

The ^1H NMR data of **18c** appeared to be similar to **18b**, identifying all the allyl peaks in the same range. The substituted piperazine protons offered four different environments including the methyl substituents as doublets at δ 1.13. The equatorial protons antiperiplanar to the methyl groups were doublets at δ 4.84 (J 10.8 Hz). The four axial protons were multiplets at δ 2.56 and 2.89. The MS parent ion, IR stretches and the elemental analysis values verified the compound formation.

In the case of **18d**, due to limited solubility and complex peaks, elucidation of individual peaks was difficult. However, the IR stretches exhibited all the relevant peaks to indicate the structure of the compound. The elemental analysis data displayed the correct percentages of carbon, hydrogen and nitrogen to confirm the empirical formula and structure of compound.

An interesting observation in these compounds was noted when comparing these to ruthenium compounds equivalents. There appeared to be no indication of an equilibrium between chair and twisted-boat conformers in the palladium compounds, which were observed in the ruthenium compounds. There was no inequivalency in the proton environments in these palladium compounds, which suggested the geometry around the palladium to be flexible to allow the piperazine ring to flip between its chair conformations.

As with the ruthenium compounds, one equivalent the palladium allyl dimer were reacted with two equivalents of the piperazine disalts to form three compounds (**19a-c**) (Figure 29). This led to the addition of the palladium allyl complex to one end of the piperazine, allowing the other dithiocarbamate end to be available for further reaction.

Figure 29: Complexes 19a-c with palladium allyl

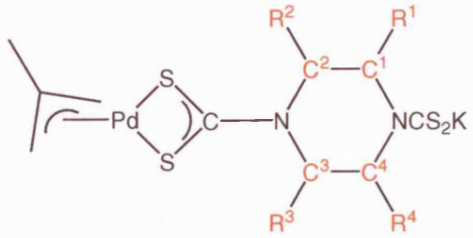

Compound	Substituents on C atom
19a	All protons
19b	R^2 = Me, R^3 = Me
	R^1 = Me, R^4 = Me
19c	R^1 = Me, R^3 = Me or
	R^4 = Me, R^2 = Me

The compounds in this set were formed as white-yellow solids in high yields. Characterisation of **19a** was difficult, as it appeared that the unsubstituted piperazine compound had limited solubility. However, the IR and elemental analysis data provided the desired peaks and values to validate the structure proposed.

However, **19b** and **19c** were more soluble and these compounds were characterised using ^{1}H NMR. The allyl protons were the same for both compounds, with the appropriate piperazine protons being very similar to each other and that of the corresponding **18c** and **18d**. The MS correctly identified the parent ion for **19b** as 425 (M^{+} - K). The final source of data that established the formation of these compounds was elemental analysis, which showed good conformity between the calculated and found percentages.

Next the zwitterions with the methyl and ethyl substituents (**3a-b**) were reacted with the palladium allyl dimers to attempt the formation of **20a-b** (Figure 30).

Figure 30: Attempted formation of palladium complexes 20a and 20b

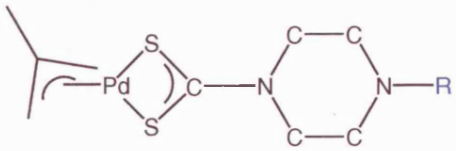

Compound	R group
20a	Me
20b	Et

Interestingly, we found that the data did not verify the formation of the compounds attempted. Due to the poor solubility of these compounds, only IR and elemental analysis data was collected. IR data showed the relevant peaks and the elemental

analysis data percentages indicated the allyl ligand was displaced and the bis-compound was formed instead (Figure 31). A possible explanation for the formation of the bis-compound could be due to the presence of a base (:NR) which destabilises the allyl unit and allow the bis-formation.

Figure 31: Actual structure of compounds 20a and 20b

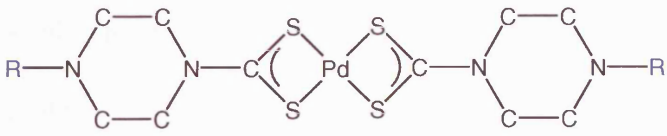

Compound	R group
20a	Me
20b	Et

The next stage of developing this section of work was to attempt forming a binuclear compound with a palladium allyl group on either side of the piperazine ring. Compounds **21a-c** were attempted using disalt piperazine starting materials (Figure 32).

Figure 32: Attempted formation of the bimetallic piperazine dithiocarbamate complexes.

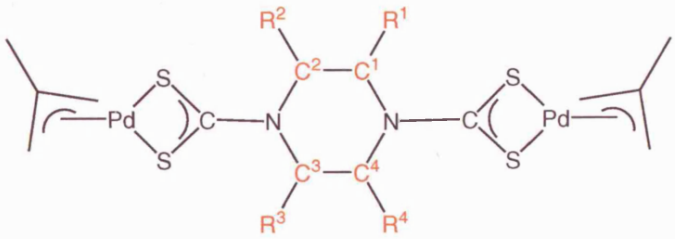

Compound	Substituents on C atom
21a	All protons
21b	R^2 = Me, R^3 = Me
	R^1 = Me, R^4 = Me
21c	R^1 = Me, R^3 = Me or
	R^4 = Me, R^2 = Me

The only successful formation of the desired compound was **21a**. Characterisation of this compound was limited due to poor solubility therefore IR and elemental analysis data was used to verify structure. The IR stretches were examined to pinpoint the required stretches and the elemental analysis data showed the required percentages of carbon, hydrogen and nitrogen.

Compound **21b** was also poorly soluble and relied on IR and elemental analysis data to identify the compound. The elemental analysis percentages indicated that the compound formed was actually the substituted piperazine ring with only one palladium allyl group (same as **18c**) and not the binuclear complex. The calculated percentages for the single palladium-substituted piperazine were C, 29.34; H, 4.61; N, 8.55 and the found values for **21b** were C, 29.34; H, 4.78; N, 7.86, therefore confirming this compound

The data for **21c** allowed for the use of NMR as this compound was found to be soluble. Examining the ^{1}H NMR spectrum, the allyl peaks were in the expected range, like the previous compounds. These peaks were singlets at δ 2.76 and 3.91 with the allyl methyl group also a singlet at δ 1.85. The equatorial protons antiperiplanar to the methyl groups in the ring were doublets at δ 5.06 (J 11.6 Hz), four axial protons appeared as a multiplet at δ 3.42 and the two methyl groups a doublet at δ 1.64 (J 6.0 Hz). The IR stretches and MS data (419 (M^{+})) correctly identified the key features to aid classification. The elemental analysis values found that in this compound (same as **21b**), only one palladium-allyl unit was bonded to the substituted piperazine. It is proposed that these allyl groups are sensitive to reaction conditions and experimental

technique[26] and found that the allyl ligands are loosely bound and can be readily displaced.

We wanted to form hetero-bimetallic compounds with the palladium allyl dimers. This was achieved by reacting the palladium dithiocarbamate compound with *cis*-$[Ru(dppm)_2Cl_2]$ to form **22a-c** in good-high yields (Figure 33).

Figure 33: Structure of compounds 22a-c

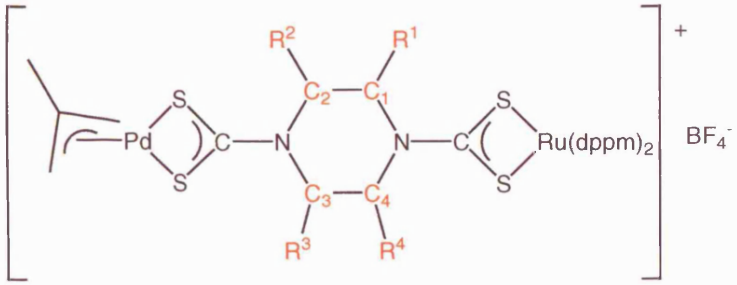

Compound	Substituents on C atom
22a	All protons
22b	R^2 = Me, R^3 = Me
	R^1 = Me, R^4 = Me
22c	R^1 = Me, R^3 = Me or
	R^4 = Me, R^2 = Me

The characterisation of these compounds confirmed the structure using IR and elemental analysis data as other techniques were not viable due to poor solubility. The IR stretches highlighted the key features of the compounds and the elemental analysis percentages were all in good agreement, for example, analysis for **22b**; calculated; C, 49.51; H, 4.35; N, 1.80, found; C, 49.43; H, 4.44; N, 1.87.

The final compound in the palladium section was **23a** that was formed in 70 % yield. This was made by initially synthesising the nickel bis-substituted piperazine compound (see compound **4b**), then adding one equivalent of base and CS_2 to form the zwitterion. This was followed by the addition of the palladium dimer to form **23a** (Figure 34).

Figure 34: Structure of compound 23a

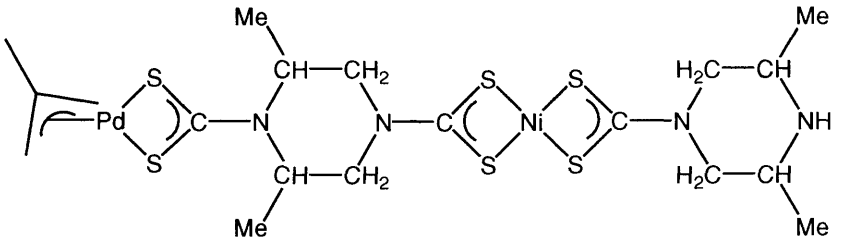

This compound was partially soluble so accurate assignment of peaks were difficult but the allyl and substituted piperazine peaks were observed. The MS showed a parent ion at 676 (M^+). The IR spectrum showed the key feature of the structure as expected. The main source of corroborating data for this structure was the elemental analysis percentages showing good agreement.

In summary, a large number of palladium complexes in this section generally formed the proposed complexes. Some reactions led to the displacement of the allyl ligands and resulted in the formation of bis-compounds. It was also found that the solubility of these compounds varied considerably, limiting characterisation data. Only one binuclear complex with piperazine was formed compared to all three binuclear complexes with *cis*-$[Ru(dppm)_2Cl_2]$ (**11a-c**).

6.3 Conclusions

In this chapter, we considered the formation of multimetallic arrays formed by dithiocarbamates. The use of piperazine-based dithiocarbamates allowed the addition of CS_2 at the 1 and 4 (*para*) positions to link different metal centres. Diamagnetic nickel and paramagnetic copper ions were reacted with the piperazine starting materials to form a range of compounds but displayed limited solubility, therefore we considered other metal centres.

We were successfully able to form a wide range of ruthenium dppm-based complexes with various substituted piperazines and further add CS_2 to increase the chain of units. We found the double bond character of the C-N bond maintained a planar geometry and when reacted with the $[Ru(dppm)_2Cl_2]$, forced the piperazine ring to contort, creating an equilibrium between the stable chair and the twisted-boat conformations.

Bimetallic ruthenium complexes were formed, one of which was crystallised to attain a single crystal structure with the piperazine linking the two metal centres. The contortion of the piperazine was not observed in the bimetallic complexes, suggesting the two metal centres forces the ring back into a chair conformation. Further to this, other metal centres such as Au, Os, Pd, Ni, Co and La were reacted with the ruthenium dithiocarbamate to form tri- and tetrametallic complexes.

As the formations of various ruthenium dithiocarbamate complexes were successful, palladium allyl compounds were reacted with the substituted piperazines to form many analogues of the ruthenium compounds. Interestingly, bonding to the palladium did not cause interconversion between conformers, suggesting the palladium bite angle offered

greater flexibility. These palladium complexes were considered less robust as in some instances, the allyl group appeared to be displaced by the zwitterions to form bis(dithiocarbamate) metal complexes. Further work is being undertaken to increase the number of metal centres linked together with piperazine rings.

6.4 Experimental

All ^{1}H, ^{13}C and ^{31}P NMR spectra were obtained on a Bruker AMX300 (^{1}H 299.87 MHz, ^{31}P 121.39 MHz) and AMX400 (^{1}H 400.14 MHz, ^{31}P 161.97 MHz) spectrometer respectively. The same instrument was used for variable temperature work, using the range 233 – 333 K unless otherwise stated. All spectra were recorded using $CDCl_3$ solutions unless otherwise specified and were referenced against internal standards. All IR spectra were recorded using a Shimaduz FT-IR 8700 spectrometer, operating in the region of 4000 - 400 cm^{-1}. The IR samples were prepared using KBr powder to make discs or as neat samples between NaCl plates. The mass spectra were obtained using a Micromass 70-SE magnetic sector mass spectrometer. Three different procedures were used to maximise accuracy of the data for individual samples. These were Electron Impact (EI) Mode with ionisation at 70 eV, Chemical Ionisation (CI) with methane reagent gas and Fast Atom Bombardment (FAB^{+}) using a caesium ion gun. The Elemental Analysis (elemental analysis) was carried out using Elemental Analyzer (CE-440) (Exeter Analytical Inc).

6.41 Synthesis of Starting materials

Synthesis of **1a**: piperazine (2.00 g, 0.023 mol) was stirred in distilled water (30 ml) with the dropwise addition of CS_2 (1.75 g, 0.023 mmol). This was stirred for 1 h. and the pale green precipitate was filtered, washed with cold distilled water (5 ml) and dried under vacuum (2.18 g, 58 %). IR (KBr) *v*: 1601m, 1580m, 1265m, 1227m, 1207m,

1134m, 1119m, 1015m, 966s, 897s cm^{-1}; ^1H NMR ($CDCl_3$): 4.31 (m, 4H, $H_2CN(CS_2)CH_2$), 4.30 (s, 2H, NH_2), 2.88 (m, 4H, $H_2CNH_2CH_2$); mass spectrum (EI): *m/z* 162 (M^+); anal. calc. for $C_5H_{10}N_2S_2$: C, 37.0; H, 6.2; N, 17.3. Found: C, 37.7; H, 6.5; N, 17.5.

Synthesis of **1b:** follow experimental above with 2, 6-dimethylpiperazine (0.50 g, 4.38 mmol) and CS_2 (0.33 g, 4.38 mmol) to give a white solid (0.43 g, 51 %). IR (KBr) *v*: 2956s, 2799m, 2696m, 2403 m, 1549m, 1450s, 1394s, 1367s, 1232m, 1097m, 989m, 947m cm^{-1}; ^1H NMR (D_2O): δ 5.57 (d, 2H, J 14.1, CH_{eq}), 3.00 (m, 2H, CH_{ax}-Me), 2.76 (t, 2H, J 12.3, CH_{ax}), 1.07 (d, 6H, J 6.5, 2*Me*); ^{13}C NMR ($CDCl_3$): δ 51.29, 48.25, 16.29; anal. calc. for $C_7H_{14}N_2S_2$: C, 44.17; H, 7.41; N,14.72. Found C, 46.46; H, 8.38; N, 16.09.

Synthesis of **1c:** follow experimental above with 2, 5-dimethylpiperazine (0.50 g, 4.38 mmol) and CS_2 (0.33 g, 4.38 mmol) to give a white solid (0.55 g, 67 %). IR (KBr) *v*: 2974s, 2936s, 2878m, 2496m, 2415m, 2195s, 1583s, 1566s, 1512s, 1406s, 1393m, 1344s, 1232m, 1128m, 1099s, 1059s, 1047s, 1026m, 989m, 935m cm^{-1}; ^1H NMR and ^{13}C NMR (D_2O): poor solubility; mass spectrum (CI): *m/z* 115 (M^+ - CS_2); anal. calc. for $C_5H_{10}N_2S_2$: C, 44.17; H, 7.41; N, 14.72. Found C, 44.17; H, 7.61; N, 14.65.

Synthesis of **1d:** 2-methylpiperazine (1.00 g, 9.96 mmol) was stirred in distilled water (60 ml) for 30 min. followed by the dropwise addition of CS_2 (0.38 g, 4.99 mmol) to give a light yellow solution. Solution was stirred overnight and reduced on rotatory evaporator. The white-yellow precipitate was washed successively with distilled water and methanol then air-dried to give a white solid (0.62 g, 35 %). IR (KBr) *v*: 2856br,

2725br, 2471m, 1576m, 1398m, 1223m, 1134m, 1113m, 1034m, 989m, 949m cm^{-1}; ^{1}H NMR and ^{13}C NMR (D_2O): data too complex to identify individual peaks due to a mixture of compounds; mass spectrum (CI): *m/z* 173 (M^+); anal. calc. for $C_6H_{12}N_2S_2$: C, 40.87; H, 6.86; N, 15.89. Found C, 40.40; H, 6.97; N, 15.52.

Synthesis of **1e:** piperidine (1.00 g, 0.012 mol) was stirred in distilled water (15 ml) and CS_2 was added dropwise (0.90 g, 0.02 mmol) and stirred for 2 h. Chloroform (50 ml) was added and after vigorous stirring, the aqueous layer discarded. Reduction in solvent volume led to precipitation of an off-white product, which was dried under vacuum (0.91 g, 62 %). IR (KBr) *v*: 1583m, 1277m, 1240m, 1219m, 1157m, 1124m, 1022m, 1001m, 972m, 949m, 883m, cm^{-1}; ^{1}H NMR ($CDCl_3$): 8.89 (brs, 2H, N*H*$_2$), 4.32 (t, 4H, J 4.97, S_2CNCH_2), 3.26 (t, 4H, J 5.66, H_2NCH_2), 1.56 (m, 12H, C*H*$_2$); ^{13}C NMR ($CDCl_3$): 208.5, 51.9, 45.0, 22.7, 26.1, 22.5, 24.4; mass spectrum (FAB): *m/z* 247 (M^+); anal. calc. for $C_{11}H_{22}N_2S_2$: C, 53.60; H, 9.00; N, 11.40. Found: C, 53.40; H, 9.10; N, 11.20.

Synthesis of **2a:** piperazine (0.05 g, 5.80 mmol) and KOH (0.75 g, 13.40 mmol) was stirred in methanol (20 ml) for 30 min. followed by the dropwise addition of CS_2 (1.02 g, 13.40 mmol) and stirred overnight to give a yellow solution. The precipitate formed was collected by vacuum filtration, washed with methanol and a small solution of chloroform then dried (0.64 g, 35 %). IR (KBr) *v*: 3307br, 2988s, 2864m, 2486m, 2486m, 2104m, 1456s, 1408m, 1358s, 1269s, 1209m, 1148s, 1119m, 997m cm^{-1}; anal. calc. for $C_6H_8N_2S_4K_2$: C, 22.19; H, 2.56; N, 8.90. Found C, 21.15; H, 3.59; N, 8.28.

Synthesis of **2b:** follow experimental above with 2, 6-dimethylpiperazine (0.50 g, 4.38 mmol), KOH (0.57 g, 10.00 mmol), CS_2 (0.77 g, 10.00 mmol) to give a white solid (0.60 g, 40 %). IR (KBr) *v*: 2970s, 2880s, 2557m, 2504s 2411s, 1549m, 1450s, 1429s, 1393s, 1367s, 1285s, 1232m, 1180s, 1144m, 1097m, 1045m, 991m, 945m cm^{-1}; ^1H NMR (D_2O): δ 5.62 (d, 2H, J 13.8, C*H*$_{eq}$), 3.12 (brm, 2H, C*H*$_{ax}$-Me), 2.83 (t, 2H, J 12.2, C*H*$_{ax}$), 1.10 (d, 6H, J 6.5, 2*Me*); anal. calc. for $C_8H_{12}N_2S_4K_2$: C, 28.04; H, 3.53; N, 8.18. Found C, 42.95; H, 7.23; N, 14.23. Recalc. for $C_7H_{14}N_2S_2$: C, 44.17; H, 7.61; N, 14.65.

Synthesis of **2c:** follow experimental above with 2, 5-dimethylpiperazine (0.50 g, 4.38 mmol), KOH (0.57 g, 10.71 mmol) and CS_2 (0.77 g, 10.07 mmol) to give a white solid (0.27 g, 18 %). IR (KBr) *v*: 3441br, 2970s, 2870s, 1597s, 1454s, 1433s, 1408s, 1367s, 1333s, 1258s, 1173m, 1096s, 176s, 1057m, 972s, 939s cm^{-1}; ^1H NMR ($CDCl_3$): δ 5.94 (m, 2H, C*H*$_{ax}$-Me), 5.36 (d, 2H, J 13.9, C*H*$_{eq}$), 3.31 (dd, 2H, J 10.1, C*H*$_{ax}$), 1.05 (d, 6H, J 6.9, 2*Me*); anal. calc. for $C_8H_{12}N_2S_4K_2$: C, 28.04; H, 3.53; N, 8.18. Found C, 25.09; H, 4.20; N, 7.25. Recalc. for $C_8H_{12}N_2S_4K_2.CHCl_3$: C, 25.37; H, 3.13; N, 6.96.

Synthesis of **2d:** follow experimental above with 2-methylpiperazine (0.50 g, 4.99 mmol), KOH (0.64 g, 11.50 mmol) and CS_2 (0.88 g, 11.50 mmol) to give a yellow solid (0.18 g, 11 %). IR (KBr) *v*: 3327br, 2986m, 2880m, 2110br, 1466m, 1408m, 1375s, 1290m, 1265s, 1227s, 1198s, 1157m, 1096m, 1038s, 1012m, 939m cm^{-1}; ^1H and ^{13}C NMR (D_2O): data too complex to identify individual peaks; anal. calc. for $C_7H_{10}N_2S_4K_2$: C, 25.58; H, 3.07; N, 8.52. Found C, 23.30; H, 3.93; N, 7.86.

Synthesis of **3a:** 1-methylpiperazine (1.00 g, 9.97 mmol) was stirred in methanol (60 ml) with KOH (0.56 g, 9.97 mmol) for 30 min. followed by dropwise addition of CS_2

(0.76 g, 9.97 mmol) to give a yellow solution. The solution was stirred overnight and the precipitate formed was collected by vacuum filtration, washed with distilled water and methanol then dried to give yellow solid (0.50 g, 23 %). IR (KBr) *v*: 2986m, 2856s, 2367br, 1470s, 1555m, 1413s, 1367m, 1356s, 1307s, 1263s, 1188m, 1139m, 1093s, 1070s, 1029m, 970m, 912s cm^{-1}; anal. calc. for $C_6H_{11}N_2S_2K_1$: C, 33.61; H, 5.17; N, 13.07. Found C, 40.84; H, 6.99; N, 15.68. Recalc. for $C_6H_{12}N_2S_2$: C, 40.87; H, 6.86; N, 15.89.

Synthesis of **3b:** follow experimental above with 1-ethylpiperazine (1.00 g, 8.74 mmol), KOH (0.49 g, 8.74 mmol) and CS_2 (0.66 g, 8.74 mmol) to give a white solid (0.53 g, 25 %). IR (KBr) *v*: 2976m, 2922m, 2848m, 2397m, 1445m, 1375m, 1313m, 1263m, 1205m, 1182s, 1139s, 1122m, 1085s, 1029s, 984m, 918s cm^{-1}; anal. calc. for $C_7H_{13}N_2S_2K_1$: C, 36.81; H, 5.74; N, 12.26. Found C, 44.03; H, 7.64; N, 14.54. Recalc. for $C_7H_{14}N_2S_2$: C, 44.17; H, 7.41; N, 14.72.

Synthesis of **3c:** follow experimental above with 2-methylpiperazine (0.50 g, 4.99 mmol), KOH (0.28 g, 4.99 mmol) and CS_2 (0.38 g, 4.99 mmol) to give white solid (0.36 g, 33 %). IR (KBr) *v*: 2860m, 2725m, 2473m, 1578m, 1437m, 1389m, 1294m, 1261s, 1225m, 1193s, 1134s, 1113s, 1067s, 1035m, 989s, 949s, 922m cm^{-1}; ^1H NMR ($CDCl_3$): data too complex to identify individual peaks due to a mixture of compounds; anal. calc. for $C_6H_{11}N_2S_2K_1$: C, 33.61; H, 5.17; N, 13.07. Found C, 39.72; H, 6.86; N, 15.22. Recalc. for $C_6H_{12}N_2S_2$: C, 40.57; H, 6.86; N, 15.89.

6.42 Synthesis of Nickel compounds

Synthesis for **4a**: compound **1a** (0.81 g, 5.00 mmol) and nickel acetate tetrahydrate (0.62 g, 2.50 mmol) were stirred in distilled water (50 ml) for 30 min. followed by the addition of NaOH (0.10 g, 2.50 mmol). The green solution was stirred for a further 30 min. and the precipitate collected by filtration, washed successively with distilled water and air-dried to give a green solid (0.76 g, 80 %). ^{1}H and ^{13}C NMR ($CDCl_3$): poor solubility; anal. calc. for $C_{10}H_{18}N_4S_4Ni_1$: C, 31.50; H, 4.72; N, 14.70; S, 33.60. Found C, 31.13; H, 4.67; N, 14.53; S, 33.20.

Synthesis for **4b**: follow experimental above with **1b** (0.10 g, 0.53 mmol), nickel acetate tetrahydrate (0.07 g, 0.26 mmol) and KOH (0.03 g, 0.79 mmol) to give a brown solid (1.11 g, 93 %). IR (KBr) *v*: 3250s, 2966s, 2885m, 2812m, 1524m, 1474s, 1373s, 1317s, 1244m, 1190s, 1153m, 1107m, 962m cm^{-1}; ^{1}H NMR ($CDCl_3$): δ 4.41 (d, 4H, J 12.7, CH_{eq}), 2.85 (brs, 4H, CH_{ax}-Me), 2.53 (t, 4H, J 11.6, CH_{ax}), 1.10 (d, 12H, J 5.9, 2Me; ^{13}C NMR ($CDCl_3$): δ 205.37, 52.64, 50.30, 19.06; mass spectrum (FAB): *m/z* 437 (M^+).

Synthesis for **4c**: follow experimental above with **1c** (0.10 g, 0.53 mmol), nickel acetate tetrahydrate (0.05 g, 0.26 mmol) and KOH (0.03 g, 0.79 mmol) to give a green solid (0.11 g, 92 %). IR (KBr) *v*: 2972s, 2885m, 2820m, 1483m, 1429s, 1381s, 1329s, 1306m, 1242m, 1167m, 1103s, 1049m, 941m cm^{-1}; ^{1}H NMR ($CDCl_3$): δ 4.97 (brm, 2H, CH_{ax}-Me), 4.12 (d, 2H, J 11.8, CH_{ax}), 3.23 - 3.32 (m, 6H, 4C$H_{ax/eq}$, 2CH_{ax}-Me), 2.59 (d, 2H, J 13.3, CH_{eq}), 1.32 (d, 6H, J 6.8, 2*Me*), 1.18 (d, 6H J 6.8, 2*Me*); ^{13}C NMR ($CDCl_3$): δ 50.58, 47.46, 46.12, 43.06, 16.65, 14.85; mass spectrum (FAB): *m/z* 437 (M^+); anal. calc. for $C_{14}H_{26}N_4S_4Ni_1$: C, 38.45; H, 5.99; N, 12.81. Found C, 36.08; H, 5.57; N, 11.52.

Synthesis for **4d**: follow experimental above with **1d** (0.10 g, 0.57 mmol) and nickel acetate tetrahydrate (0.07 g, 0.28 mmol) were stirred in distilled water (50 ml) for 30 min. followed by the addition of NaOH (0.03 g, 0.85 mmol). The brown solution was stirred for a further 30 min. and the precipitate collected by filtration, washed successively with distilled water and air-dried to give a green solid (0.10 g, 88 %). IR (KBr) *v*: 2974s, 2885m, 2814br, 2340s, 1506m, 1429m, 1244m, 1207m, 1074m, 1034m, 943m cm^{-1}; ^1H NMR ($CDCl_3$): δ 4.41 (q, 4H, J 13.8, CH_{ax}), 3.02 (m, 4H, J 11.9, CH_{ax}), 2.82 (m, 4H, J 9.5, CH_{eq}), 2.63 (t, 2H, J 10.7, CH_{eq}), 1.10 (d, 12H, J 6.3, 2*Me*); ^{13}C NMR ($CDCl_3$): δ 54.32, 50.14, 46.99, 44.95, 19.09; mass spectrum (FAB): *m/z* 409 (M^+).

6.43 Synthesis of Copper compounds

Synthesis of **5a:** compound **1a** (0.10 g, 0.57 mmol) and copper acetate (0.05 g, 0.28 mmol) were stirred in distilled water (50 ml) for 30 min. followed by the addition of NaOH (0.03 g, 0.85 mmol). The brown solution was stirred for a further 30 min. and the precipitate collected by vacuum filtration, washed successively with distilled water and air-dried to give a brown solid (0.60 g, 63 %). Anal. calc. for $C_{10}H_{18}N_4S_4Cu_1$: C, 31.13; H, 4.67; N, 14.53; S, 33.20. Found C, 29.52; H, 4.40; N, 13.37. Recalc. for $C_{10}H_{18}N_4S_4Cu.H_2O$: C, 29.74; H, 4.96; N, 13.87; S, 31.72. Paramagnetic.

Synthesis of **5b:** follow experimental above with compound **1b** (0.10 g, 0.53 mmol), copper acetate (0.05 g, 0.28 mmol) and KOH (0.03 g, 0.79 mmol) to give a brown solid (0.12 g, 93 %). IR (KBr) *v*: 3152br, 2964s, 2883m, 2831br, 1657br, 1491m, 1435s, 1375m, 1319m 1242m, 1190m, 1148m, 1105m, 1084m, 989m, 961m cm^{-1}; mass spectrum (FAB): *m/z* 441 (M^+); anal. calc. for $C_{14}H_{26}N_4S_4Cu_1$: C, 38.03; H, 5.93; N,

12.67. Found C, 30.37; H, 5.31; N, 9.93. Recalc. for $C_{14}H_{26}N_4S_4Cu_1.2CH_2Cl_2$: C, 31.40; H, 4.94; N, 9.15. Paramagnetic.

Synthesis of **5c:** follow experimental above with compound **1c** (0.10 g, 0.53 mmol), copper acetate (0.05 g, 0.26 mmol) and KOH (0.03 g, 0.79 mmol) to give a brown solid (0.09 g, 75 %). IR (KBr) *v*: 2972s, 2878s, 2820s, 1475m, 1425s, 1379s, 1325s, 1242m, 1167m, 1103s, 1049s, 976m, 939m cm^{-1}; mass spectrum (FAB): *m/z* 442 (M^+); anal. calc. for $C_{14}H_{26}N_4S_4Cu_1$: C, 38.03; H, 5.93; N, 12.67. Found C, 32.22; H, 4.95; N, 10.03. Recalc. for $C_{14}H_{26}N_4S_4Cu_1.CHCl_3$ C, 32.08; H, 4.85; N, 9.98. Paramagnetic.

Synthesis of **5d:** follow experimental above with compound **1d** (0.10 g, 0.57 mmol), copper acetate (0.05 g, 0.28 mmol) and KOH (0.03 g, 0.85 mmol) to give a brown solid (0.11 g, 93 %). IR (KBr) *v*: 2882m, 1491m, 1425s, 1298s 1242m, 1072m, 1032m, 941m cm^{-1}; mass spectrum (FAB): *m/z* 414 (M^+); anal. calc. for $C_{12}H_{22}N_4S_4Cu_1$: C, 34.80; H, 5.35; N, 13.53. Found C, 28.03; H, 4.27; N, 10.30. Recalc. for $C_{12}H_{22}N_4S_4Cu_1.2CH_2Cl_2$: C, 28.79; H, 4.49; N, 9.59. Paramagnetic.

6.44 Synthesis of Ruthenium compounds

Synthesis of **6:** synthesis for *cis*-$[Ru(dppm)_2Cl_2]$ from Keller *et al.*[27]: $RuCl_3 \cdot H_2O$ (0.316 g, 1.52 mmol), dppm (1.22 g, 3.17 mmol), PPh_3 (1.12 g, 4.27 mmol) and 50 ml of amyl alcohol was added together. The mixture was refluxed under N_2 for at least 3 h. The yellow precipitate was filtered off, washed with amyl alcohol (5 ml), MeOH/ether (3 × 5 ml) and ether (3 × 5 ml) and next dried *in vacuo*. The product was recrystallised from DCM and pentane (1.42 g, 85 %). IR (KBr) *v*: 3416br, 3044s, 2365m, 2340m, 1612m, 1570m, 1478s, 1431m, 1096m cm^{-1}; ^1H NMR ($CDCl_3$): δ 8.21 (m, 4H, *Ph*),

7.93 (m, 4H, *Ph*), 7.42 (m, 6H, *Ph*), 7.16 (q, 6H, *Ph*), 7.01 (t, 6H, *Ph*), 6.95 (t, 6H, Ph), 6.77 (t, 4H, Ph), 6.56 (m, 4H, Ph), 4.91 (m, 2H, dppm-CH_2), 4.65 (m, 2H, dppm-CH_2); ^{31}P NMR ($CDCl_3$): δ -25.9 m, -6.6 m; mass spectrum (FAB): *m/z* 905 (M^+ - Cl); anal. calc. for $C_{50}H_{44}P_4Cl_2Ru_1$: C, 63.84; H, 4.71. Found C, 63.66; H, 4.86.

Synthesis for **7a**: *cis*-[Ru(dppm)$_2$Cl$_2$] (0.01 g, 0.11 mmol) and $NaS_2CNMe_2.xH_2O$ (0.02 g, 0.16 mmol) were suspended in methanol (20 ml) and an aqueous solution (5 ml) of $NaBF_4$ (0.02 g, 0.21 mmol) added. The reaction was stirred for 1 h. and then all solvent was removed *via* rotatory evaporator. The residue was dissolved in a minimum volume of DCM and filtered through diatomaceous earth. Ethanol (20 ml) was added and the solvent volume reduced until precipitation was complete. The product was filtered and washed with distilled water (5 ml), ethanol (10 ml) and hexane (10 ml) to give a white solid (0.09 g, 78 %). IR (KBr) *v*: 1616m, 1310m, 1281m, 1258m, 1051m, 999m cm^{-1}; ^{1}H NMR ($CDCl_3$): δ 6.45 - 7.59 (mm, 40H, *Ph*), 4.88 (m, 2H, dppm-*C*H_2), 4.46 (m, 2H, dppm-*C*H_2), 3.51 (s, 3H, N-*Me*), 3.31 (s, 3H, N-*Me*); ^{31}P NMR ($CDCl_3$): δ-3.80 (t, 2H, J 34.2, *P*Ph$_2$), -17.38 (t, 2H, J 34.2, *P*Ph$_2$); mass spectrum (FAB): *m/z* 990 (M^+); anal. calc. for $C_{53}H_{50}B_1F_4N_1P_4RuS_2.0.5CH_2Cl_2$: C, 57.40; H, 4.60; N, 1.30. Found: C, 57.60; H, 4.70; N, 1.30.

Synthesis for **7b**: follow experimental above with *cis*-[Ru(dppm)$_2$Cl$_2$] (0.01 g, 0.11 mmol), $NaS_2CNEt_2.3H_2O$ (0.04 g, 0.16 mmol) and $NaBF_4$ (0.02 g, 0.21 mmol) to give a pale yellow solid (0.08 g, 71 %). IR (KBr) *v*: 1587m, 1574m, 1306m, 1279m, 1211m, 1192m, 1059m, 914m, 849m cm^{-1}; ^{1}H NMR ($CDCl_3$): δ 5.47 - 7.62 (mm, 40H, *Ph*), 4.97 (m, 2H, dppm-*C*H_2), 4.52 (m, 2H, dppm-*C*H_2), 3.48 (m, 4H, J 7.1, N-*C*H_2CH$_3$), 1.06 (t, 6H, J 7.1, 2*Me*); ^{31}P NMR ($CDCl_3$): δ -4.4 (t, 2H, J 34.1, *P*Ph$_2$), -17.0 (t, 2H, J

34.1, PPh_2); mass spectrum (FAB): *m/z* 1018 (M^+); anal. calc. for $C_{55}H_{54}B_1F_4N_1P_4RuS_2$: C, 59.80; H, 4.90; N, 1.30. Found: C, 59.40; H, 5.00; N, 1.20.

Synthesis for **7c**: follow experimental above with *cis*-$[Ru(dppm)_2Cl_2]$ (0.10 g, 0.11 mmol), compound **1e** (0.04 mg, 0.16 mmol) and $NaBF_4$ (0.02 g, 0.21 mmol) to give a pale yellow solid (0.10 g, 86 %). IR (KBr) *v*: 1574m, 1321m, 1246m, 1192m, 1057m cm^{-1}; ^1H NMR ($CDCl_3$): δ 6.52 - 7.61 (mm, 40H, *Ph*), 4.95 (m, 2H, dppm-CH_2), 4.61 (m, 2H, dppm-CH_2), 3.58 (m, 4H, CH_2), 1.46 (m, 6H, CH_2); ^{31}P NMR ($CDCl_3$): δ -4.2 (t, 2H, J 34.0, PPh_2), -17.8 (t, 2H, J 34.0, PPh_2); mass spectrum (FAB): *m/z* 1031 (M^+); anal. calc. for $C_{56}H_{54}BF_4NP_4RuS_2$: C, 60.20; H, 4.90; N, 1.30. Found: C, 59.50; H, 4.90; N, 1.20.

6.441 Ruthenium compounds with various piperazines

Synthesis for **8a**: compound **1a** (0.03 g, 0.16 mmol) and $NaBF_4$ (0.02 g, 0.21 mmol) were suspended in methanol (20 ml) and *cis*-$[Ru(dppm)_2Cl_2]$ (0.10 g, 0.11 mmol) added as a DCM (10 ml) solution. The reaction was heated to reflux for 10 min. and then stirred for 2 h. All the solvent was removed and the residue was taken up in a minimum amount of DCM and filtered through diatomaceous earth. Addition of ethanol (30 ml) and reduction of solvent volume by rotary evaporation yielded the pale yellow solid (0.09 g, 73 %). IR (KBr) *v*: 1585m, 1574m, 1312m, 1269m, 1236m, 1190m, 1161m, 1057m, 918m cm^{-1}; ^1H NMR ($CDCl_3$): δ 6.48 - 7.57 (mm, 40H, *Ph*), 4.91 (m, 2H, dppm-CH_2), 4.53 (m, 2H, dppm-CH_2), 3.88 (m, 4H, N-CH_2), 3.04 (m, 4H, N-CH_2), 2.35 (brs, 2H, NH_2); ^{31}P NMR ($CDCl_3$): δ -3.8 (t, 2H, J 34.4, PPh_2), -17.3 (t, 2H, J 34.4, PPh_2); mass spectrum (FAB): *m/z* 1030 (M^+); anal. calc. for $C_{55}H_{53}BF_4N_2P_4RuS_2$: C,

59.09; H, 4.78; N, 2.50 Found: C, 57.80; H, 4.60; N, 2.50. Recalc. For $C_{55}H_{53}BF_4N_2P_4RuS_2.½CH_2Cl_2$: C, 57.50; H, 4.70; N, 2.40

Synthesis for **8b**: follow experimental above with *cis*-[Ru(dppm)$_2$Cl$_2$] (0.10 g, 0.11 mmol), compound **1b** (0.04 g, 0.21 mmol) and $NaBF_4$ (0.01 g, 0.43 mmol) to give a yellow solid (0.09 g, 68 %). IR (KBr) *v*: 3051s, 2979m, 2880m, 1483m, 1435s, 1319m, 1242m, 1190s, 1159s, 1097m, 1059m, 999m cm^{-1}; ^{1}H NMR ($CDCl_3$): δ 6.91 – 7.61 (mm, 46H, *Ph*), 6.53 (q, 4H, J 8.5, *Ph*), 4.92 – 4.99 (m, 2H, dppm-C*H*$_2$), 4.55 – 4.64 (m, 2H, dppm-C*H*$_2$), 4.38 (brt, 2H, J 14.5, 2C*H*$_{eq}$), 2.76 – 2.81 (m, 1H, C*H*$_{ax}$-Me), 2.56 – 2.61 (m, 1H, C*H*$_{ax}$-Me), 2.45 (t, 1H, J 11.6, C*H*$_{ax}$), 2.25 (t, 1H, J 11.6, C*H*$_{ax}$), 1.14 (t, 6H, J 6.3, 2*Me*); ^{31}P NMR ($CDCl_3$): δ -3.9 (m, 2P, *P*Ph$_2$), -17.9 (m, 2P, *P*Ph$_2$); mass spectrum (FAB): *m/z* 1059 (M^+ - 2BF_4); anal. calc. for $C_{57}H_{58}N_2S_2P_4B_2F_8Ru_1$: C, 55.49; H, 4.74; N, 2.27. Found C, 56.58; H, 4.81; N, 2.22.

Synthesis for **8c**: follow experimental above with *cis*-[Ru(dppm)$_2$Cl$_2$] (0.10 g, 0.11 mmol), **1c** (0.04 g, 0.21 mmol), $NaBF_4$ (0.01 g, 0.43 mmol) to give a yellow solid (0.05 g, 36 %). IR (KBr) *v*: 3051m, 2924s, 2853s, 2284m, 1458m, 1435s, 1326m 1261m, 1190m, 1159m, 1097m, 1053m, 999s cm^{-1}; ^{1}H NMR ($CDCl_3$): δ 7.62 (d, 4H, *Ph*), 6.69 – 7.38 (s, 32H, *Ph*), 6.43 (d, 4H, *Ph*), 4.85 (m, 3H, 2H = dppm-C*H*$_2$, 1H = C*H*$_{eq}$-Me), 4.50 (m, 2H, dppm C*H*$_2$), 4.19 (dd, 1H, J 14.3, C*H*$_{ax/eq}$), 3.77 (brs, 1H, *CH*$_{ax/eq}$), 3.48 (m, 1H, C*H*$_{ax/eq}$), 3.32 (brt, 1H, C*H*$_{eq}$), 3.11 (brt, 1H, C*H*$_{eq}$), 1.43 (d, 3H, J 6.8, *Me*), 1.32 (d, 3H, J 6.2, *Me*); ^{31}P NMR ($CDCl_3$): δ -5.0 (t, 2P, J 34.2, *P*Ph$_2$), -16.9 (t, 2P, J 34.2, *P*Ph$_2$); anal. calc. for $C_{57}H_{58}N_2S_2P_4B_2F_8Ru_1$: C, 55.49; H, 4.74; N, 2.27. Found C, 58.41; H, 5.46; N, 1.85.

Synthesis for **8d**: follow experimental above with *cis*-[Ru(dppm)$_2$Cl$_2$] (0.10 g, 0.11 mmol), **1d** (0.04 g, 0.21 mmol) and $NaBF_4$ (0.01 g, 0.43 mmol) to give a yellow solid (0.09 g, 52 %). IR (KBr) *v*: 3526m, 3447m, 3273br, 3051s, 2957m, 2916m, 2847m, 1628m, 1574m, 1483s, 1433s, 1244m, 1059m, 999m cm^{-1}; ^{1}H NMR ($CDCl_3$): δ 6.89 – 7.59 (mm, 36H, *Ph*), 6.51 (q, 4H, J 8.5, *Ph*), 4.94 (brm, 2H, dppm-C*H*$_2$), 4.67 (brm, 2H, dppm-C*H*$_2$), 4.43 (m, 2H, C*H*$_2$), 3.07 – 3.48 (m, 2H, C*H*$_2$), 2.81 – 2.89 (m, 2H, C*H*$_2$), 2.51 – 2.62 (m, 3H, 1H = C*H*-Me, 2H = N*H*$_2$), 1.18 (d, 3H, *Me*), 1.21 (d, 3H, *Me*); ^{31}P NMR ($CDCl_3$): δ -3.9 (q, 2P, J 34.5, *P*Ph$_2$), -17.7 (t, 2P, J 34.5, *P*Ph$_2$); mass spectrum (FAB): *m/z* 1045 (M^+ - 2BF_4); anal. calc. for $C_{57}H_{58}N_2S_2P_4B_2F_8Ru_1$: C, 55.32; H, 4.31; N, 2.30. Found C, 56.98; H, 4.84; N, 2.40.

Synthesis for **9a**: compound **2a** (0.02 g, 0.50 mmol) and $NaBF_4$ (0.01 g, 0.43 mmol) were suspended in methanol (20 ml) and *cis*-[Ru(dppm)$_2$Cl$_2$] (0. 50 g, 0.50 mmol) added as a DCM (10 ml) solution. The reaction was heated to reflux for 10 min. and then stirred for 2 h. All solvent was removed and the residue was taken up in a minimum amount of DCM and filtered through diatomaceous earth. Addition of ethanol (30 ml) and reduction of solvent volume by rotary evaporation yielded the pale yellow solid (0.23 g, 48 %). IR (KBr) *v*: 3051m, 2962m, 2910m, 2858m, 1481m, 1433s, 1358m, 1309m, 1278s, 1217s, 1096m, 1030m, 997m, 920m cm^{-1}; ^{1}H NMR ($CDCl_3$): δ 7.63 (m, 4H, *Ph*), 7.05 (mm, 32H, *Ph*), 6.48 (m, 4H, *Ph*), 4.92 (m, 2H, dppm-C*H*$_2$), 4.530 (m, 2H, dppm-C*H*$_2$), 3.62 (m, 4H, N-C*H*$_2$), 3.53 (m, 4H, N-C*H*$_2$); ^{31}P NMR ($CDCl_3$): δ -4.05 (m, 2P, *P*Ph$_2$), -16.58 (m, 2P, *P*Ph$_2$); anal. calc. for $C_{56}H_{52}N_2S_2P_4Ru_1B_1F_4$: C, 54.54; H, 4.25; N, 2.27. Found C, 51.41; H, 4.11; N, 1.68. Recalc. for $C_{56}H_{52}N_2S_2P_4Ru_1B_1F_4.2CH_2Cl_2$: C, 51.10; H, 4.11; N, 2.06.

Synthesis for **9b**: follow experimental above with *cis*-[Ru(dppm)$_2$Cl$_2$] (0. 50 g, 0.50 mmol), compound **2b** (0.02 g, 0.50 mmol), NaBF$_4$ (0.01 g, 0.43 mmol) to give a yellow solid (0.02 g, 28 %). IR (KBr) *v*: 3416br, 3051s, 2964m, 2926m, 2847m, 1616m, 1487m, 1433s, 1340m, 1250m, 1198m, 1104m, 1064m, 999m cm^{-1}; ^{1}H NMR (CD_2Cl_2): δ 7.67 (m, 4H, *Ph*), 7.05 (m, 32H, *Ph*), 6.95 (m, 4H, *Ph*), 4.95 (m, 2H, dppm-C*H*$_2$), 4.50 (m, 2H, dppm-C*H*$_2$), 4.38 (brt, 2H, J 12.3, C*H*$_{eq}$), 2.76 (m, 1H, C*H*$_{ax}$), 2.54 (m, 1H, C*H*$_{ax}$), 2.39 (t, 1H, J 11.1, C*H*$_{ax}$), 2.19 (t, 1H, J 11.1, C*H*$_{ax}$), 1.10 (d, 3H, J 6.3, *Me*), 1.07 (d, 3H, J 6.3, *Me*); ^{31}P NMR (CD_2Cl_2): δ -1.75 (m, 2P, *P*Ph$_2$), -15.73 (m, 2P, *P*Ph$_2$); mass spectrum (FAB): *m/z* 1060 (M$^+$ - CS$_2$, K); anal. calc. for $C_{58}H_{56}N_2S_4P_4K_1Ru_1B_1F_4$: C, 55.28; H, 4.48; N, 2.22. Found C, 55.16; H, 4.51; N, 1.90.

Synthesis for **9c**: follow experimental above with *cis*-[Ru(dppm)$_2$Cl$_2$] (0. 50 g, 0.05 mmol), **2c** (0.02 g, 0.5 mmol), NaBF$_4$ (0.01 g, 0.43 mmol) to give a yellow solid (0.03 g, 41 %). IR (KBr) *v*: 3051m, 2974m, 2924m, 2855m, 1472m, 1452m, 1435m, 1383m, 1327m, 1261m, 1175m, 1099m, 1051s, 999s cm^{-1}; ^{1}H NMR (CD_2Cl_2): δ 7.56 (d, 4H, *Ph*), 6.86 – 7.34 (mm, 32H, *Ph*), 6.38 (m, 4H, *Ph*), 4.85 (m, 2H, dppm-C*H*$_2$), 4.41 (m, 2H, dppm-C*H*$_2$), 4.29 (brt, 2H, J 12.0, C*H*$_{eq}$), 2.65 (m, 1H, C*H*$_{ax}$-Me), 2.43 (m, 1H, C*H*$_{ax}$-Me), 2.26 (t, 1H, J 11.7, C*H*$_{ax}$), 2.05 (t, 1H, J 11.7, C*H*$_{ax}$), 0.98 (t, 6H, J 6.6, *Me*); ^{31}P NMR (CD_2Cl_2): δ -2.76 (m, 2P, *P*Ph$_2$), -14.7 (m, 2P, *P*Ph$_2$); mass spectrum (FAB): *m/z* 1059 (M$^+$ - BF4, CS$_2$, K); anal. calc. for $C_{58}H_{56}N_2S_4P_4K_1Ru_1B_1F_4$: C, 55.28; H, 4.48; N, 2.22. Found C, 57.61; H, 4.92; N, 2.30.

Synthesis for **10a**: 1-methylpiperazine (0.02 g, 0.21 mmol) and KOH (0.01 g, 0.21 mmol) were stirred in methanol (60 ml) for 30 min. followed by the dropwise addition of CS$_2$ (0.02 g, 0.21 mmol). This solution was stirred for 1 h. and then added to a DCM

solution (20 ml) of *cis*-[Ru(dppm)$_2$Cl$_2$] (0.10 g, 0.11 mmol) to give a murky solution which turned yellow. An excess of $NaBF_4$ (0.70 g, 6.4 mmol) was dissolved in a distilled water/methanol solution (v/v) (10 ml) and added to the solution. Stirred for 30 min. and reduced *via* the rotary evaporator to give a grey-white solid (0.11 g, 93 %). IR (KBr) *v*: 3439br, 3051s, 2926m, 2854s, 2806m, 2365m, 2332m, 1574m, 1485m, 1435s, 1242m, 1103m, 1057m, 998m cm^{-1}; ^{1}H NMR ($CDCl_3$): δ 7.59 (m, 4H, *Ph*), 7.23-7.36 (m, 22H, *Ph*), 7.22 (t, 4H, *Ph*), 7.00 (t, 2H, *Ph*), 6.94 (t, 4H, *Ph*), 6.51 (t, 4H, *Ph*), 4.92-5.09 (m, 2H, dppm-C*H*$_2$), 4.54 - 4.62 (m, 2H, dppm-C*H*$_2$), 3.72 (m, 2H, C*H*$_2$-CNCS$_2$), 3.62 (m, 2H, C*H*$_2$-CNCS$_2$), 2.67 (m, 2H, C*H*$_2$-CNMe), 2.59 (m, 2H, C*H*$_2$- CNMe), 2.54 (s, 3H, *Me*), ^{31}P NMR ($CDCl_3$): δ -3.9 (t, 2P, J 34.5, *P*Ph$_2$), -17.5 (t, 2P, J 34.2, *P*Ph$_2$); mass spectrum (FAB): *m/z* 1059 (M^+ - BF_4); anal. calc. for $C_{56}H_{55}N_2S_2P_4B_1F_4Ru_1$: C, 59.74; H, 4.90; N, 2.47. Found C, 57.87; H, 4.83; N, 2.20.

Synthesis for **10b**: follow experimental above with 1-ethylpiperazine (0.02 g, 0.21 mmol), KOH (0.01 g, 0.21 mmol), CS_2 (0.02 g, 0.21 mmol), *cis*-[Ru(dppm)$_2$Cl$_2$] (0.10 g, 0.11 mmol) and $NaBF_4$ (0.70 g, 6.4 mmol) to give a grey-white solid (0.15 g, 84 %). IR (KBr) *v*: 3439m, 3051s, 2926m, 2854s, 2799s, 2355m, 1969m, 1905m, 1823m, 1574m, 1483m, 1433s, 1238m, 1057m cm^{-1}; ^{1}H NMR ($CDCl_3$): δ 7.60 (q, 4H, *Ph*), 6.92 - 7.38 (m, 32H, *Ph*), 6.53 (q, 4H, *Ph*), 4.99 (m, 2H, dppm-C*H*$_2$), 4.61 (m, 2H, dppm-C*H*$_2$), 3.67 (m, 2H, C*H*$_2$-CNCS$_2$), 3.58 (m, 2H, C*H*$_2$-CNCS$_2$), 2.47 (q, 2H, J 7.1, C*H*$_2$CH$_3$), 2.40 (m, 2H, C*H*$_2$-CNMe), 2.33 (m, 2H, C*H*$_2$-CNMe), 1.11 (t, 3H, J 7.1, CH$_2$C*H*$_3$); ^{31}P NMR ($CDCl_3$): δ -4.01 (t, 2P, J 34.5, *P*Ph$_2$), -17.7 (t, 2P, J 34.5, *P*Ph$_2$); mass spectrum (FAB): *m/z* 1045 (M^+ - BF_4); anal. calc. for $C_{57}H_{57}N_2S_2P_4B_1F_4Ru_1$: C, 59.74; H, 5.01; N, 2.44. Found C, 58.15; H, 5.03; N, 2.39.

Synthesis for **11a** (a): *cis*-[Ru(dppm)$_2$Cl$_2$] (0.05 g, 0.04 mmol) was dissolved in DCM (10 ml) and methanol (5 ml) with **2a** (0.006, 0.02 mmol). Stirring was continued for 1 h. after which all solvent was removed. The residue was dissolved in a minimum volume of DCM and filtered through diatomaceous earth. Diethyl ether (30 ml) was added to precipitate the product. This was filtered and washed with distilled water (5 ml), diethylether (10 ml) and hexane (10 ml) to give a pale yellow solid (0.03 g, 72 %).

Synthesis for **11a** (b): compound **8a** (0.05 g, 0.04 mmol) was dissolved in DCM (10 ml) and methanol (5 ml) and NEt$_3$ (3 drops, excess) added. The reaction was stirred for 10 min. and then CS_2 (2 drops, excess) added. A DCM solution (10 ml) of *cis*-[Ru(dppm)$_2$Cl$_2$] (0.04 g, 0.04 mmol) was added followed by a solution of $NaBF_4$ (0.009 g, 0.08 mmol) in distilled water (1 m) and methanol (5 ml). Stirring was continued for 1 h. after which all solvent was removed. The residue was dissolved in a minimum volume of DCM and filtered through diatomaceous earth. Diethyl ether (30 ml) was added to precipitate the product. This was filtered and washed with distilled water (5 ml), diethylether (10 ml) and hexane (10 ml) to give a pale yellow solid (0.07 g, 76 %). IR (KBr) *v*: 1614m, 1574m, 1310m, 1278m, 1219m, 1057m, 918m cm^{-1}; ^{1}H NMR ($CDCl_3$): δ 6.50 - 7.63 (mm, 80H, *Ph*), 4.91 (m, 2H, dppm-C*H*$_2$), 4.56 (m, 2H, dppm-C*H*$_2$), 3.62 (m, 4H, J 9.5, N-C*H*$_2$), 3.51 (m, 4H, J 9.5, N-C*H*$_2$); ^{31}P NMR ($CDCl_3$): δ -4.1 (t, 2P, J 34.2, *P*Ph$_2$), -16.8 (t, 2P, J 34.2, *P*Ph$_2$); mass spectrum (FAB): *m/z* 1976 (M^+); anal. calc. for $C_{106}H_{96}B_2F_8N_2P_8Ru_2S_4$: C, 59.22; H, 4.50; N, 1.30. Found: C, 57.30; H, 4.60; N, 1.30. Recalc. for $C_{106}H_{96}B_2F_8N_2P_8Ru_2S_4.CH_2Cl_2$: C, 57.50; H, 4.40; N, 1.30.

Synthesis for **11b**: compound **2b** (0.02 g, 0.05 mmol) and $NaBF_4$ (0.14 g, 0.43 mmol) were suspended in methanol (20 ml) and *cis*-$[Ru(dppm)_2Cl_2]$ (0.10 g, 0.11 mmol) added as a DCM (10 ml) solution. The reaction was heated to reflux for 10 min. and then stirred for 2 h. All solvent was removed and the residue was dissolved in a minimum amount of DCM and filtered through diatomaceous earth. Addition of ethanol (30 ml) and reduction of solvent volume by rotary evaporation yielded the pale yellow solid (0.11 g, 96 %). IR (KBr) *v*: 3416br, 3051s, 2980m, 2916m, 2704br, 2467br, 2355m, 1620br, 1483s, 1435s, 1387m, 1261m, 1097br, 1001m cm^{-1}; ^1H NMR ($CDCl_3$): δ 7.59 (m, 4H, *Ph*), 6.92 - 7.52 (m, 72H, *Ph*), 6.49 (m, 4H, *Ph*), 4.88 (m, 2H, dppm-CH_2), 4.35 (m, 4H, 2H = dppm-CH_2, 2H = CH_{eq}), 3.31 (m, 2H, CH_{ax}), 3.15 (m, 2H, CH_{ax}), 1.21 (t, 6H, J 7.0, 2*Me*); anal. calc. for $C_{108}H_{100}N_2S_4Ru_2B_2F_8P_8$: C, 59.56; H, 4.63; N, 1.29. Found C, 54.11; H, 5.02; N, 2.01. Recalc. for $C_{108}H_{100}N_2S_4Ru_2B_2F_8P_8.2CHCl_3$: C, 54.67; H, 4.25; N, 1.16.

Synthesis for **11c**: follow experimental above with *cis*-$[Ru(dppm)_2Cl_2]$ (0.10 g, 0.11 mmol), compound **2c** (0.02 g, 0.05 mmol), $NaBF_4$ (0.14 g, 0.43 mmol) to give a pale yellow solid (0.03 g, 28 %). IR (KBr) *v*: 3049m, 2988m, 2881m, 1433s, 1327m, 1261m, 1051m, 999m cm^{-1}; ^1H NMR (d^6-acteone): δ 7.89 (m, 8H, *Ph*), 7.17 - 7.58 (m, 56H, *Ph*), 7.01 (d, 8H, *Ph*), 6.63 (t, 8H, *Ph*), 5.32 (m, 4H, dppm-CH_2), 5.02 (m, 2H, CH_{eq}), 4.71 (m, 4H, dppm-CH_2), 4.91 - 5.14 (m, 2H, CH_{eq}), 4.46 - 4.74 (m, 2H, CH_{ax}-Me), 2.98 - 3.13 (m, 2H, CH_{ax}), 1.04 (d, 3H, J 6.7, *Me*), 0.88 (d, 3H, J 6.8, *Me*); ^{31}P NMR (d^6-acteone): δ 1.59 (m, 2P, PPh_2), -12.5 (m, 2P, PPh_2); anal. calc. for $C_{108}H_{100}N_2S_4P_8B_2F_8Ru_2$: C, 59.56; H, 4.63; N, 1.29. Found C, 56.58; H, 4.67; N, 1.10. Recalc. $C_{108}H_{100}N_2S_4P_8B_2F_8Ru_2.CH_2Cl_2$ C, 56.22; H, 4.43; N, 1.19.

6.442 Ruthenium compounds with various metal compounds

Synthesis for **12a**: compound **8a** (0.10 g, 0.08 mmol) was dissolved in DCM (10 ml) and treated with NEt_3 (5 drops, excess) and stirred for 5 min. Carbon disulfide (3 drops, excess) was added and the reaction stirred for 5 min. $AuCl(PPh_3)$ (0.04 g, 0.08 mmol) was added as a solid and the reaction was stirred for 1 h. All solvent was removed and the residue was dissolved in a minimum amount of DCM and filtered through diatomaceous earth. The crude product was redissolved in DCM (5 ml) and diethylether (30 ml) added to precipitate the product. This was washed with diethylether (10 ml) and dried to give a grey-white (0.09 g, 63 %). IR (KBr) *v*: 1585m, 1572m, 1310m, 1277m, 1207m, 1155m, 1055m, 912m cm^{-1}; ^1H NMR (d^6-acetone): δ 6.69 - 7.63 (m, 55H, *Ph*), 5.36 (m, 2H, dppm-CH_2), 4.75 (m, 2H, dppm-CH_2), 4.23 (m, 2H, N-CH_2), 4.14 (m, 2H, N-CH_2), 3.92 (m, 2H, N-CH_2), 3.73 (m, 2H, N-CH_2); ^{31}P NMR (d^6-acetone): δ 37.5 (brs, 1P, PPh_3), -3.0 (t, 2H, J_{PP} 34.5, PPh_2), -18.0 (t, 2H, J_{PP} 34.5, PPh_2); mass spectrum (FAB): *m/z* 1566 (M^+); anal. calc. for $C_{74}H_{67}AuBF_4N_2P_5RuS_4$: C, 53.80; H, 4.10; N, 1.70. Found: C, 54.00; H, 4.00; N, 1.60.

Synthesis for **12b**: compound **1b** (0.04 g, 0.21 mmol) and $NaBF_4$ (0.01 g, 0.43 mmol) were suspended in methanol (20 ml) and *cis*-$[Ru(dppm)_2Cl_2]$ (0.10 g, 0.11 mmol) added as a DCM (10 ml) solution. The reaction was heated to reflux for 10 min. and then stirred for 1 h. Next, NEt_3 (3 drops) was added to the mixture, stirred for 10 min. followed CS_2 (3 drops, excess). $AuCl(PPh_3)$ (0.02 g, 0.03 mmol) was added to this solution, stirred for 15 min. then reduced to dryness and recrystallised using DCM/hexane to give a yellow solid (0.05 g, 89 %). IR (KBr) *v*: 3051br, 2922m, 2851br, 1433m, 1325m, 1261m, 1099m, 1084m, 1051m, 997m cm^{-1}; ^1H and ^{13}C NMR ($CDCl_3$): data too complex to identify individual peaks; ^{31}P NMR ($CDCl_3$): δ 34.27 (brs,

1P, PPh_3), -4.8 (t, 2H, J 34.5, PPh_2), -16.9 (t, 2H, J 34.5, PPh_2); mass spectrum (FAB): *m/z* 1528 (M^+); anal. calc. for $C_{74}H_{67}N_2S_4P_5Ru_1Au_1B_1F_4$: C, 53.79; H, 4.09; N, 1.70. Found C, 52.07; H, 4.76; N, 1.78.

Synthesis for **12c**: follow experimental above with *cis*-$[Ru(dppm)_2Cl_2]$ (0.10 g, 0.11 mmol), compound **1c** (0.04 g, 0.21 mmol), $NaBF_4$ (0.01 g, 0.43 mmol) and $AuCl(PPh_3)$ (0.02 g, 0.05 mmol) to give a yellow solid (0.02 g, 24 %). IR (KBr) *v*: 3050m, 2922m, 2853s, 1585s, 1585s, 1458m, 1435s, 1261s, 1173m, 1099m, 1051m, 997s cm^{-1}; ^1H and ^{13}C NMR ($CDCl_3$): data too complex to identify individual peaks; ^{31}P NMR ($CDCl_3$): δ 34.27 (brs, 1P, PPh_3), -4.8 (t, 2H, J 34.5, PPh_2), -16.9 (t, 2H, J 34.5, PPh_2); mass spectrum (FAB): *m/z* 1566 (M^+); anal. calc. for $C_{74}H_{67}N_2S_4P_5Ru_1Au_1B_1F_4$: C, 53.79; H, 4.09; N, 1.70. Found C, 54.74; H, 5.25; N, 1.57.

Synthesis for **13a**: compound **8a** (0.01 g, 0.08 mmol) was dissolved in DCM (15 ml) and methanol (10 ml) added. This solution was treated with NEt_3 (5 drops, excess) and stirred for 5 min. Carbon disulfide (3 drops, excess) was added and the reaction stirred for a further 5 min. Nickel acetate (0.007 g, 0.04 mmol) was added as a solid and the reaction was stirred for 1 h. All solvent was removed and the residue was dissolved in a minimum amount of DCM and filtered through diatomaceous earth. The crude product was redissolved in DCM (5 ml) and diethylether (30 ml) added to precipitate the brown product. This was washed with diethylether (10 ml) and dried (0.07 g, 69 %). IR (KBr) *v*: 1614m, 1559m, 1308m, 1279m, 1221m, 1192m, 1057m, 910m, 849m cm^{-1}; ^1H NMR ($CDCl_3$): δ 6.52 – 7.61 (mm, 80H, *Ph*), 4.98 (m, 4H, dppm-CH_2), 4.64 (m, 4H, dppm-CH_2), 3.58 (m, 16H, N-CH_2); ^{31}P NMR ($CDCl_3$): δ -4.2 (t, 2P, J 34.5, PPh_2), -16.8 (t, 2P, J 34.5, PPh_2); mass spectrum (FAB): *m/z* 2271 (M^+); anal. calc. for

$C_{112}H_{104}B_2F_8N_4NiP_8Ru_2S_8$: C, 55.00; H, 4.30; N, 2.30. Found: C, 55.40; H, 4.20; N, 2.20.

Synthesis for **13b**: compound **8a** (0.10 g, 0.08 mmol) was dissolved in DCM (10 ml) and methanol (10 ml) added. This solution was treated with NEt_3 (5 drops, excess) and stirred for 5 min. Carbon disulfide (3 drops, excess) was added and the reaction stirred for a further 5 min. Copper acetate (0.008 g, 0.04 mmol) was added as a solid and the reaction was stirred for 1 h. All solvent was removed and the residue was dissolved in a minimum amount of DCM and filtered through diatomaceous earth. Ethanol (30 ml) was added to and the solvent volume concentrated under reduced pressure to precipitate the brown product. This was washed with ethanol (10 ml) and hexane (20 ml) and dried (0.06 g, 62 %). IR (KBr) *v*: 1585m, 1572m, 1310m, 1279m, 1221m, 1157m, 1057m, 910m cm^{-1}; ^1H NMR ($CDCl_3$): δ 6.52 – 7.62 (brm, 80H, *Ph*), 4.96 (brs, 2H, dppm-CH_2), 4.61 (brs, 2H, dppm-CH_2), (NC_4H_8N not observed due to effect of paramagnetism); ^{31}P NMR ($CDCl_3$): δ -4.2 (t, 2P, J 34.3, PPh_2), -16.8 (t, 2P, J 34.5, PPh_2); mass spectrum (FAB): *m/z* 2276 (M^+); anal. calc. for $C_{112}H_{104}B_2CuF_8N_4P_8Ru_2S_8.CH_2Cl_2$: C, 53.60; H, 4.20; N, 2.20. Found: C, 53.40; H, 4.20; N, 2.20.

Synthesis for **13c**: compound **8a** (0.10 g, 0.08 mmol) was dissolved in DCM (15 ml) and methanol (10 ml) added. This solution was treated with NEt_3 (5 drops, excess) and stirred for 5 min. Carbon disulfide (3 drops, excess) was added and the reaction stirred for a further 5 min. Cobalt triacetylacetone (0.01 g, 0.03 mmol) was added as a solid and the reaction was stirred for 1 h. All solvent was removed and the residue was dissolved in a minimum amount of DCM and filtered through diatomaceous earth. The crude product was redissolved in DCM (5 ml) and diethylether (30 ml) added to

precipitate the green product. This was washed with diethylether (10 ml) and dried (0.007 g, 71 %). IR (KBr) *v*: 1640m, 1310m, 1279m, 1221m, 1159m, 1058m, 999m, 914m cm^{-1}; ^{1}H NMR ($CDCl_3$): δ 6.47 – 7.64 (mm, 80H, *Ph*), 4.92 (m, 2H, dppm-CH_2), 4.52 (m, 2H, dppm-CH_2), 3.79 (m, 12H, N-CH_2), 3.66 (m, 12H, N-CH_2); ^{31}P NMR ($CDCl_3$): δ-3.9 (t, 2P, J 34.3, PPh_2), 16.8 (t, 2P, J 34.3, PPh_2); mass spectrum (FAB): *m/z* 2272 $(M\text{-}S_2CNC_4H_8NCS_2Ru(dppm)_2)^+$; anal. calc. for $C_{168}H_{156}B_3CoF_{12}N_6P_{12}Ru_3S_{12}.2CH_2Cl_2$: C, 53.80; H, 4.50; N, 2.20. Found: C, 53.60; H, 4.20; N, 2.20.

Synthesis for **13c**: follow experimental above with compound **8a** (0.10 g, 0.08 mmol), NEt_3 (5 drops, excess), CS_2 (3 drops, excess) and $LaCl_3$ (6.8 mg, 0.028 mmol) to give an off-white solid (0.06 g, 57 %). IR (KBr) *v*: 1622m, 1310m, 1279m, 1215m, 1155m, 1057m, 999m, 918m cm^{-1}; ^{1}H NMR ($CDCl_3$): δ 6.49 – 7.59 (mm, 129H, *Ph*), 4.93 (m, 2H, dppm-CH_2), 4.57 (m, 2H, dppm-CH_2), 3.79 (m, 12H, N-CH_2), 3.64 (m, 12H, N-CH_2); ^{31}P NMR ($CDCl_3$): δ-4.0 (m, 2P, PPh_2), -16.9 (m, 2P, PPh_2); mass spectrum (FAB): *m/z* 2353 $(M\text{-}S_2CNC_4H_8NCS_2Ru(dppm)_2)^+$; anal. calc. for $C_{168}H_{156}B_3F_{12}LaN_6P_{12}Ru_3S_{12}$: C, 54.30; H, 4.20; N, 2.30. Found: C, 53.70; H, 4.40; N, 2.20.

Synthesis for **14a**: Compound **8a** (0.10 g, 0.083 mmol) was dissolved in DCM (10 ml) and treated with NEt_3 (5 drops, excess) and stirred for 5 min. Carbon disulfide (3 drops, excess) was added and the reaction stirred for 5 min. to generate $[Ru(S_2CNC_4H_8NCS_2)(dppm)_2]$ *in situ*. $[Os(CH{=}CHC_6H_4Me\text{-}4)Cl(CO)(BTD)(PPh_3)_2]$ (0.09 g, 0.08 mmol) was added as a DCM solution (10 ml) and the reaction was stirred for 1 h. All solvent was removed and the residue was dissolved in a minimum amount

of DCM and filtered through diatomaceous earth. Addition of ethanol (30 ml) and reduction of solvent volume by rotary evaporation yielded the product, which was washed with ethanol (10 ml) and hexane (10 ml) to give pale orange solid (0.12 g, 71 %). IR (KBr) *v*: 1898m, 1614m, 1310m, 1217m, 1188m, 1057m, 918m, 847m cm^{-1}; ^1H NMR ($CDCl_3$): δ 8.28 [dt, 1H, J_{HH} = 17.1 Hz, J_{HP} = 2.6, Hα), 6.52 - 7.61 (mm, 70H, *Ph*), 6.36, 6.81 ($(AB)_2$, 4H, J_{AB} = 8.0, C_6H_4), 5.59 (d, 1H, J17.1, Hβ), 4.64 (m, 2H, dppm-CH_2), 4.97 (m, 2H, dppm-CH_2), 2.78 - 3.33 (brm, 8H, N-CH_2), 2.21 (s, 3H, *Me*); ^{31}P NMR ($CDCl_3$): δ 9.3 (s, 1P, PPh_3), -4.4 (t, 2P, J 34.4, PPh_2), -17.1 (t, 2P, J 34.4, PPh_2); mass spectrum (FAB): *m/z* 1967 (M^+); anal. calc. for $C_{102}H_{91}BF_4N_2OOsP_6RuS_4.CH_2Cl_2$: C, 57.90; H, 4.40; N, 1.30. Found: C, 57.70; H, 4.50; N, 1.30.

Synthesis for **14b**: Compound **8a** (0.10 g, 0.08 mmol) was dissolved in DCM (10 ml) and treated with NEt_3 (5 drops, excess) and stirred for 5 min. Carbon disulfide (3 drops, excess) was added and the reaction stirred for 5 min. $[PdCl(C,N\text{-}C_6H_4CH_2NMe_2)]_2$ (0.02 g, 0.04 mmol) was added as a solution in DCM (5 ml) and the reaction was stirred for 1 h. All solvent was removed and the residue was dissolved in a minimum amount of DCM and filtered through diatomaceous earth. The crude product was redissolved in DCM (5 ml) and diethylether (30 ml) added to precipitate the colourless product. This was washed with diethylether (10 ml) and dried (0.11 g, 89 %). IR (KBr) *v*: 1574m, 1308m, 1278m, 1219m, 1157m, 1055m, 907m, 849m cm^{-1}; ^1H NMR ($CDCl_3$): δ 6.53 - 7.62 (mm, 44H, *Ph*, C_6H_4), 4.96 (m, 2H, dppm-CH_2), 4.64 (m, 2H, dppm-CH_2), 4.01 (s, 2H, CCH_2), 3.79 (m, 4H, N-CH_2), 3.71 (m, 4H, N-CH_2), 2.92 (s, 6H, N*Me*); ^{31}P NMR ($CDCl_3$): δ -4.2 (t, 2P, J 34.2, PPh_2), -16.9 (t, 2P, J 34.2, PPh_2); mass spectrum (FAB):

m/z 1346 (M^+); anal. calc. for $C_{65}H_{64}BF_4N_3P_4PdRuS_4.½CH_2Cl_2$: C, 53.30; H, 4.40; N, 2.90. Found: C, 53.10; H, 5.00; N, 3.20.

Synthesis for **14c** (a): compound **8a** (0.10 mg, 0.08 mmol) was dissolved in DCM (10 ml) and treated with NEt_3 (5 drops, excess) and stirred for 5 min. Carbon disulfide (3 drops, excess) was added and the reaction stirred for 5 min. $[Ni(dppp)Cl_2]$ (0.05 g, 0.08 mmol) was added as a solution in DCM (5 ml) and the reaction was stirred for 1 h. All solvent was removed and the residue was dissolved in a minimum amount of DCM and filtered through diatomaceous earth. The crude product was redissolved in DCM (5 ml) and diethylether (30 ml) added to precipitate the brown product. This was washed with diethylether (10 ml) and dried (0.08 g, 58 %).

Synthesis for **14c** (b): $[Ni(S_2CNC_4H_8NH_2)(dppp)][BF_4]_2$ (0.03 g, 0.04 mmol) was dissolved in DCM (10 ml) and treated with NEt_3 (3 drops, excess) and stirred for 5 min. Carbon disulfide (2 drops, excess) was added and the reaction stirred for 5 min. *Cis*-$[Ru(dppm)_2Cl_2]$ (0.04 g, 0.04 mmol) was added as a solution in DCM (5 ml) and the reaction was stirred for 1 h. All solvent was removed and the residue was dissolved in a minimum amount of DCM and filtered through diatomaceous earth. The crude product was redissolved in dichloromethane (5 ml) and diethylether (30 ml) added to precipitate the brown product. This was washed with diethylether (10 ml) and dried (0.04 g, 59 %). IR (KBr) *v*: 1662m, 1312m, 1279m, 1229m, 1053m cm^{-1}; ^1H NMR ($CDCl_3$): δ 6.46 - 7.59 (mm, 60H, *Ph*), 4.90 (m, 2H, dppm-CH_2), 4.51 (m, 2H, dppm-CH_2), 3.65 (m, 4H, N-CH_2), 3.47 (m, 4H, N-CH_2), 1.80 - 2.60 (m, 6H, dppp-(CH_2)$_3$); ^{31}P NMR ($CDCl_3$): δ 13.7 (s, 1P, dppp), -4.1 (t, 2P, J 34.9, PPh_2), -16.8 (t, 2P, J 34.9, PPh_2); mass spectrum (FAB): *m/z* 1576 (M^+).

6.45 Synthesis of Palladium allyl compounds

Exp from UCL Chemistry Department, Module 5-6 "Synthesis, reaction and applications of η^3-allyl palladium complexes"

Synthesis for bis(η^3-allyl)dichlorodipalladium(II) $[Pd(\eta^3\text{-}C_3H_5)(\mu\text{-}Cl))]_2$: sodium chloropalladate(II) (1.00 g, 3.40 mmol), methanol (60 ml), distilled water (5 ml) and allyl chloride (1 cm^3) were placed in a two-necked round-bottom flask and stirred for 10 min. A rubber balloon filled with CO was fitted to the flask and CO was passed slowly over the solution for 1 h. The colour changed to yellow to signal the end of the reaction. The mixture was cooled to room temperature and the liquid was decanted. Using aqueous extraction with distilled water and chloroform, the product was extracted in the chloroform and dried over calcium chloride for 1 h. This was filtered and the solvent removed *via* rotatory evaporation to yield a yellow solid

Synthesis for bis(η^3-2-methylallyl)dichlorodipalladium(II) $[Pd(\eta^3\text{-}C_4H_7)(\mu\text{-}Cl))]_2$: follow experimental above with sodium chloropalladate(II) (1.00 g, 3.40 mmol) and 2-methylallyl chloride (2-methyl-3-chloropropene) (1 cm^3) to yield a yellow solid.

6.451 Protonic allyl compounds

Synthesis for **17a**: compound **1a** (0.04 g, 0.27 mmol) and $[Pd(\eta^3\text{-}C_3H_5)(\mu\text{-}Cl))]_2$ (0.05 g, 0.14 mmol) were placed in a round bottom flask in a mixture of 50:50 DCM/MeOH (v/v) (50 ml). This was stirred for 1 h. followed by the addition of KOH (0.02 g, 0.41 mmol). The solution was stirred overnight and the precipitate collected by vacuum filtration, washed successively with methanol and air-dried to give a brown solid (0.04 g, 89 %). IR (KBr) *v*: 3431br, 3059m, 2908br, 2847m, 2365m, 1489s, 1427s, 1290m,

1227m, 1178m, 999m cm^{-1}; ^{1}H and ^{13}C NMR ($CDCl_3$): poor solubility; anal. calc. for $C_8H_{14}N_2S_2Pd_1$: C, 31.12; H, 4.57; N, 9.07. Found C, 26.04; H, 3.52; N, 6.07. Recalc. for $C_8H_{14}N_2S_2Pd_1.CHCl_3$: C, 25.25; H, 3.53; N, 6.54.

Synthesis for **17b**: follow experimental above with compound **1c** (0.04 g, 0.22 mmol), $[Pd(\eta^3\text{-}C_3H_5)(\mu\text{-}Cl))]_2$ (0.04 g, 0.11 mmol) and KOH (0.02 g, 0.33 mmol) to give a red solid (0.04 g, 55 %). IR (KBr) *v*: 2966m, 2930m, 1474m, 1425m, 1379m, 1328s, 1259br, 1169m, 1103m, 1051m, 941m cm^{-1}; ^{1}H NMR ($CDCl_3$): δ 5.12 (m, 2H, allyl-C*H*), 4.54 (d, 2H, J 13.1, CH_{eq}), 4.04 (d, 2H, J 6.7, allyl-CH_2), 3.26 - 3.42 (m, 4H, CH_{ax}), 2.78 (q, 4H, J 9.9, allyl-CH_2), 1.13 (d, 3H, J 3.6, *Me*), 1.11 (d, 3H, J 3.6, *Me*); mass spectrum (FAB): *m/z* 338 (M^+).

Synthesis for **17c**: follow experimental above with compound **1b** (0.04 g, 0.22 mmol), $[Pd(\eta^3\text{-}C_3H_5)(\mu\text{-}Cl))]_2$ (0.04 g, 0.11 mmol) and KOH (0.02 g, 0.33 mmol) to give a red solid (0.05 g, 60 %). IR (KBr) *v*: 3408br, 2957s, 2901m, 2806m, 2365s, 2339s, 1687br, 1632m, 1502m, 1434m, 1371m, 1317m, 1247m, 1158m, 1086m cm^{-1}; ^{1}H NMR ($CDCl_3$): δ 5.14 (sept, 1H, J 6.8, allyl-C*H*), 4.81 (d, 2H, J 12.8, CH_{eq}), 4.03 (t, 2H, J 5.1, allyl-CH_2), 2.87 (m, 2H, CH_{ax}), 2.77 (d, 2H, J 12.6, allyl-CH_2), 2.59 (m, 2H, CH_{ax}), 1.21 (d, 3H, J 3.6, *Me*), 1.17 (d, 3H, J 3.6, *Me*); mass spectrum (FAB): *m/z* 431 (M^+).

6.452 Methyl allyl compounds

Synthesis for **18a**: compound **1a** (0.03 g, 0.19 mmol) and $[Pd_2Cl_2(\eta^3\text{-}C_4H_7)_2]$ (0.04 g, 0.10 mmol) were placed in a round bottom flask in a mixture of 50:50 DCM/MeOH (v/v) (50 ml). This was stirred overnight and the precipitate collected by vacuum filtration, washed successively with methanol and air-dried to give a yellow solid (0.03

g, 93 %). IR (KBr) *v*: 3304br, 2926m, 2758m, 2704m, 2600m, 2459m, 2364s, 1582m, 1491s, 1435m, 1375br, 1258br, 1154m, 1043m, 997m cm^{-1}; ^1H NMR (D_2O): δ 4.14 (brs, 2H, N*H*$_2$), 4.03 (t, 2H, J 5.6, C*H*), 3,84 (s, 2H, allyl-C*H*$_2$), 3.25 (brd, 4H, J 4.8, C*H*), 3.12 (s, 2H, C*H*), 2.61 (s, 2H, allyl-C*H*$_2$), 1.77 (s, 3H, allyl-*Me*); mass spectrum (FAB): *m/z* 288 (M^+ - Cl); anal. calc. for $C_9H_{17}N_2S_2Pd_1$: C, 30.09; H, 4.77; N, 7.80. Found C, 27.44; H, 4.55; N, 7.36.

Synthesis for **18b**: compound **1a** (0.03 g, 0.19 mmol) and $[Pd(\eta^3\text{-}C_4H_7)(\mu\text{-}Cl))]_2$ (0.04 g, 0.10 mmol) were placed in a round bottom flask in a mixture of 50:50 DCM/MeOH (v/v) (50 ml). This was stirred for 15 min. followed by the addition of KOH (0.03 g, 0.48 mmol) and stirred overnight. The precipitate was collected by vacuum filtration, washed successively with methanol and air-dried to give a yellow solid (0.02, 56 %). IR (KBr) *v*: 3271s, 2945s, 2920m, 2816s, 1533m, 1437m, 1269m, 1126m, 1045m, 1018m, 1001m cm^{-1}; ^1H NMR ($CDCl_3$): δ 4.00 (m, 4H, N-C*H*$_2$), 3.39 (s, 2H, allyl-C*H*$_2$), 2.96 (m, 4H, N-C*H*$_2$), 2.67 (s, 2H, allyl-C*H*$_2$), 1.95 (s, 2H, allyl-C*H*$_2$).

Synthesis for **18c**: follow experimental above with compound **1b** (0.03 g, 0.15 mmol) and $[Pd(\eta^3\text{-}C_4H_7)(\mu\text{-}Cl))]_2$ (0.03 g, 0.08 mmol) were placed in a round bottom flask in a mixture of 50:50 DCM/MeOH (v/v) (50 ml). This was stirred for 1 h. followed by the addition of KOH (0.02 g, 0.30 mmol). The solution was stirred overnight and the precipitate collected by vacuum filtration, washed successively with methanol and air-dried to give a brown solid (0.02 g, 45 %). IR (KBr) *v*: 3244s, 3055s, 2964s, 2912m, 1501m, 1431m, 1371s, 1290s, 1242s, 1186s, 1107s, 1026s, 961s cm^{-1}; ^1H NMR ($CDCl_3$): δ 4.84 (d, 2H, J 10.8, C*H*$_{eq}$), 3.84 (s, 2H, allyl-C*H*$_2$), 2.89 (m, 2H, C*H*$_{ax}$), 2.67 (s, 2H, allyl-C*H*$_2$), 2.56 (m, 2H, C*H*$_{ax}$), 1.95 (s, 3H, allyl-CH*Me*), 1.13 (d, 6H, 2*Me*);

mass spectrum (FAB): *m/z* 350 (M^+); anal. calc. for $C_{11}H_{20}N_2S_2Pd_1$: C, 37.66; H, 5.74; N, 7.98. Found C, 37.17; H, 5.97; N, 7.17.

Synthesis for **18d**: follow experimental above with compound **1c** (0.03 g, 0.15 mmol), $[Pd(\eta^3\text{-}C_4H_7)(\mu\text{-}Cl))]_2$ (0.03 g, 0.08 mmol) and KOH (0.02 g, 0.30 mmol) to give an orange solid (0.03 g, 57 %). IR (KBr) *v*: 2964m, 2920m, 1487m, 1429s, 1379m, 1331s, 1313s, 1261s, 1171m, 1094m, 1051s, 941m cm^{-1}; ^1H NMR ($CDCl_3$): data too complex to identify individual peaks but can identify allyl protons; anal. calc. for $C_{11}H_{20}N_2S_2Pd_1$: C, 37.66; H, 5.74; N, 7.98. Found C, 32.96; H, 5.01; N, 6.53. Recalc. for $C_{11}H_{20}N_2S_2Pd_1.½CHCl_3$: C, 33.64; H, 5.03; N, 6.82.

Synthesis for **19a**: compound **2a** (0.13 g, 0.41 mmol) and $[Pd(\eta^3\text{-}C_4H_7)(\mu\text{-}Cl))]_2$ (0.08 g, 0.21 mmol) were placed in a round bottom flask in a mixture of 50:50 DCM/MeOH (v/v) (50 ml). This was stirred overnight and the precipitate collected by vacuum filtration, washed successively with methanol and air-dried to give a pale white solid (0.16 g, 89 %). IR (KBr) *v*: 3049s, 2974s, 2953m, 2910m, 2849m, 1485m, 1431m, 1377m, 1380m, 1273s, 1223m, 1161s, 1116m, 1003s, 904s cm^{-1}; ^1H and ^{13}C NMR ($CDCl_3$): poor solubility; anal. calc. for $C_{10}H_{15}N_2S_4K_1Pd_1$: C, 27.48; H, 3.46; N, 6.41. Found C, 22.69; H, 3.09; N, 4.62. Recalc. for $C_{10}H_{15}N_2S_4K_1Pd_1.2CH_2Cl_2$: C, 23.16; H, 3.16; N, 4.62.

Synthesis for **19b**: follow experimental above with compound **2b** (0.07 g, 0.20 mmol) and $[Pd(\eta^3\text{-}C_4H_7)(\mu\text{-}Cl))]_2$ (0.04 g, 0.10 mmol) to give a yellow solid (0.06 g, 66 %). IR (KBr) *v*: 3416br, 2964m, 2901m, 2813m, 2696br, 2451m, 1637m, 1574m, 1506m, 1435m, 1379m, 1185m, 1156m, 1100m, 1049m, 996m cm^{-1}; ^1H NMR ($CDCl_3$): δ 4.84

(brd, 2H, C*H*$_{eq}$), 3.83 (s, 2H, allyl-C*H*$_2$), 3.11 (brm, 2H, C*H*$_{ax}$), 2.89 (brm, 2H, C*H*$_{ax}$), 2.67 (s, 2H, allyl-C*H*$_2$), 1.94 (s, 3H, allyl-*Me*), 1.13 (d, 6H, 2*Me*); mass spectrum (FAB): *m/z* 425 (M^+ - K); anal. calc. for $C_{12}H_{19}N_2S_4K_1Pd_1$: C, 30.99; H, 4.12; N, 6.02. Found C, 32.81; H, 5.39; N, 9.65.

Synthesis for **19c**: follow experimental above with compound **2c** (0.07 g, 0.20 mmol) and $[Pd(\eta^3\text{-}C_4H_7)(\mu\text{-}Cl))]_2$ (0.04 g, 0.10 mmol) to give a yellow solid (0.07 g, 78 %). IR (KBr) *v*: 3439m, 3383m, 3051m, 2972s, 2908m, 2365m, 1475m, 1425s, 1379s, 1126m, 1278m, 1178m, 1102m, 1065s, 1051s cm^{-1}; ^1H NMR ($CDCl_3$): δ 5.42 (brm, 2H, C*H*$_{eq}$), 4.83 (t, 2H, J 14.7, C*H*$_{ax}$), 3.88 (s, 2H, allyl-C*H*$_2$), 3.93 (m, 2H, C*H*$_{ax}$), 2.70 (d, 2H, J 3.4, allyl-C*H*$_2$), 1.96 (d, 3H, J 5.5, allyl-*Me*), 1.33 (d, 3H, J 3.3, *Me*), 1.32 (d, 3H, J 3.3, *Me*); anal. calc. for $C_{12}H_{19}N_2S_4K_1Pd_1$: C, 30.99; H, 4.12; N, 6.02. Found C, 24.27; H, 3.41; N, 4.35. Recalc. for $C_{12}H_{19}N_2S_4K_1Pd_1.1½CHCl_3$: C, 25.17; H, 3.21; N, 4.35.

Synthesis for **20a**: compound **3a** (0.04 g, 0.20 mmol) and $[Pd(\eta^3\text{-}C_4H_7)(\mu\text{-}Cl))]_2$ (0.04 g, 0.10 mmol) were placed in a round bottom flask in a mixture of 50:50 DCM/MeOH (v/v) (50 ml). This was stirred for 1 h. and the precipitate collected by vacuum filtration, washed successively with methanol and air-dried to give a yellow solid (0.01 g, 41 %). IR (KBr) *v*: 3408br, 2988m, 2949s, 2908s, 2569m, 2538m, 2334m, 1628m, 1512s, 1466m, 1427m, 1352m, 1240s, 1198m, 1067m, 970m cm^{-1}; anal. calc. for $C_{10}H_{18}N_2S_2Pd_1$: C, 35.66; H, 5.39; N, 8.32. Found C, 26.70; H, 4.71; N, 9.81. Recalc. for $C_{12}H_{22}N_4S_4Pd_1.2CH_2Cl_2$: C, 26.82; H, 4.18; N, 9.94.

Synthesis for **20b**: follow experimental above with compound **3b** (0.05 g, 0.20 mmol) and $[Pd(\eta^3\text{-}C_4H_7)(\mu\text{-}Cl))]_2$ (0.04 g, 0.10 mmol) to give a yellow solid (0.07 g, 93 %).

IR (KBr) *v*: 3416br, 2980m, 2908m, 2569m, 2569m, 2451m, 2365s, 1637m, 1616m, 1504s, 1427m, 1269m, 1238m, 1156m, 1085m, 993m cm^{-1}; anal. calc. for $C_{11}H_{20}N_2S_2Pd_1$: C, 37.66; H, 5.75; N, 7.98. Found C, 25.95; H, 4.41; N, 8.33. Recalc. for $C_{14}H_{26}N_4S_4Pd_1.2CH_2Cl_2$: C, 29.34; H, 4.61; N, 8.55.

Synthesis for **21a**: compound **2a** (0.06 g, 0.20 mmol) and $[Pd(\eta^3\text{-}C_4H_7)(\mu\text{-}Cl))]_2$ (0.08 g, 0.20 mmol) were placed in a round bottom flask in a mixture of 50:50 DCM/MeOH (v/v) (50 ml). This was stirred for 1 h. then reduced using the rotatory evaporator. The precipitate was collected by vacuum filtration, washed successively with water and methanol and air-dried to give a white solid (0.07 g, 62 %). IR (KBr) *v*: 3029s, 2974s, 2952m, 2910m, 1842m, 1485m, 1431m, 1360s, 1273s, 1223m, 1161s, 1030m, 1003s, 905s cm^{-1}; ^1H and ^{13}C NMR ($CDCl_3$): poor solubility; anal. calc. for $Pd_2C_{14}H_{22}N_2S_4$: C, 30.06; H, 3.96; N, 5.01. Found C, 29.27; H, 3.88; N, 4.86.

Synthesis for **21b**: follow experimental above with compound **2c** (0.03 g, 0.10 mmol) and $[Pd(\eta^3\text{-}C_4H_7)(\mu\text{-}Cl))]_2$ (0.04 g, 0.10 mmol) to give a yellow solid (0.06 g, 30 %). IR (KBr) *v*: 2964m, 2903m, 2702m, 2442m, 1508m, 1433m, 1377m, 1258m, 1092m, 1024m cm^{-1}; ^1H NMR ($CDCl_3$): δ 5.06 (d, 2H, J11.6, CH_{eq}), 3.91 (s, 2H, allyl-CH_2), 3.42 (m, 4H, CH_{ax}), 2.76 (s, 2H, allyl-CH_2), 1.85 (s, 3H, allyl-*Me*), 1.64 (d, 6H, J 6.0, 2*Me*); mass spectrum (FAB): *m/z* 419 (M^+); anal. calc. for $C_{16}H_{26}N_2S_4Pd_2$: C, 32.71; H, 4.46; N, 4.77. Found C, 33.28; H, 5.41; N, 6.42. Recalc. for $C_{11}H_{20}N_2S_4Pd_1.2CH_2Cl_2$: C, 33.07; H, 5.09; N, 6.43.

Synthesis for **21c**: follow experimental above with compound **2b** (0.03 g, 0.10 mmol) and $[Pd(\eta^3\text{-}C_4H_7)(\mu\text{-}Cl))]_2$ (0.04 g, 0.10 mmol) to give a yellow solid (0.02 g, 30 %).

IR (KBr) *v*: 2959m, 2899m, 2827br, 2696m, 2590m, 2446m, 1566m, 1506m, 1434s, 1379m, 1256m, 1182m, 1163m, 1097s, 1049s, 1010m cm^{-1}; ^{1}H and ^{13}C NMR ($CDCl_3$): poor solubility: anal. calc. for $C_{16}H_{26}N_2S_4Pd_2$: C, 32.71; H, 4.46; N, 4.77. Found C, 29.34; H, 4.78; N, 7.86. Recalc. for $C_{14}H_{26}N_4S_4Pd_1.2CH_2Cl_2$: C, 29.34; H, 4.61; N, 8.55.

Synthesis for **22a**: follow experimental above with compound **9a** (0.06 g, 0.05 mmol) and $[Pd(\eta^3\text{-}C_4H_7)(\mu\text{-}Cl))]_2$ (0.01 g, 0.03 mmol) were placed in a round bottom flask in a mixture of 50:50 DCM/MeOH (v/v) (50 ml). This was stirred for 1 h. followed by the addition of aqueous $NaBF_4$ (0.01 g, 0.10 mmol) (5 ml). The solution was stirred overnight and the precipitate collected by vacuum filtration, washed successively with methanol and air-dried to give a yellow solid (0.02 g, 54 %). IR ν(KBr) 2910m, 2339m, 1483m, 1435s, 1358s, 1278s, 1217s, 1095s, 1055m, 1026m, 999s, 912m cm^{-1}; ^{1}H and ^{13}C NMR ($CDCl_3$): poor solubility but can identify allyl protons and PPh_2; ^{31}P NMR ($CDCl_3$): δ -4.1 (m, 2P, *P*Ph_2), -16.7 (m, 2P, *P*Ph_2); anal. calc. for $C_{60}H_{59}N_2S_4P_4B_1F_4Ru_1Pd_1$: C, 53.17; H, 4.39; N, 3.06. Found C, 41.96; H, 3.47; N, 159. Recalc. for $C_{60}H_{59}N_2S_4P_4B_1F_4Ru_1Pd_1.4CH_2Cl_2$: C, 41.96; H, 3.47; N, 1.53.

Synthesis for **22b**: follow experimental above with compound **9b** (0.06 g, 0.05 mmol), $[Pd(\eta^3\text{-}C_4H_7)(\mu\text{-}Cl))]_2$ (0.01 g, 0.03 mmol) and $NaBF_4$ (0.01 g, 0.10 mmol) to give a yellow solid (0.06 g, 90 %). IR (KBr) *v*: 3059m, 2962m, 2910m, 1490m, 1437m, 1267m, 1084m, 1059m, 1001m cm^{-1}; ^{1}H and ^{13}C NMR ($CDCl_3$): poor solubility but can identify allyl protons and PPh_2; anal. calc. for $C_{62}H_{63}N_2S_4P_4B_1F_4Ru_1Pd_1$: C, 53.86; H, 4.59; N, 2.03. Found C, 49.43; H, 4.44; N, 1.87. Recalc. for $C_{62}H_{63}N_2S_4P_4B_1F_4Ru_1Pd_1.2CH_2Cl_2$: C, 49.51; H, 4.35; N, 1.80.

Synthesis for **22c**: follow experimental above with compound **9c** (0.06 g, 0.05 mmol), $[Pd(\eta^3\text{-}C_4H_7)(\mu\text{-}Cl))]_2$ (0.01 g, 0.03 mmol) and $NaBF_4$ (0.01 g, 0.10 mmol to give a yellow solid (0.05 g, 65 %). IR (KBr) *v*: 3015m, 3274m, 2930m, 1585s, 1470m, 1435s, 1383m, 1327m, 1261s, 1173m, 1099m, 1051s, 999s cm^{-1}; ^1H and ^{13}C NMR ($CDCl_3$): poor solubility but can identify allyl protons and PPh_2; anal. calc. for $C_{62}H_{63}N_2S_4P_4B_1F_4Ru_1Pd_1$: C, 53.86; H, 4.59; N, 2.03. Found C, 52.70; H, 4.56; N, 1.67.

Synthesis for **23a**: compound **4b** (0.10 g, 0.23 mmol) was placed in a round bottom flask in a mixture of 50:50 DCM/MeOH (v/v) (50 ml) and CS_2 (3 drops, excess) was added dropwise. This was stirred for 15 min then reduced to dryness using the rotatory evaportator. This green solid was redissolved in a 50:50 DCM/MeOH solution and $[Pd(\eta^3\text{-}C_4H_7)(\mu\text{-}Cl))]_2$ (0.03 g, 0.09 mmol) was added and stirred overnight to give a red/drown solution. Next KOH (0.01 g, 0.26 mmol) was added to the solution (50 ml), which then turned green. This was reduced and the green precipitate was collected by filtration, washed successively with distilled water and methanol and air-dried to give a green solid (0.04 g, 70 %). IR (KBr) *v*: 3244m, 2963s, 2914m, 2810m, 1522m, 1437m, 1317m, 1244m, 1188m, 1153m, 1107m, 962m cm^{-1}; ^1H and ^{13}C NMR ($CDCl_3$): poor solubility but can identify allyl protons and substituted piperazine; mass spectrum (FAB): *m/z* 676 (M^+); anal. calc. for $C_{19}H_{31}N_4S_6Ni_1Pd_1$: C, 33.19; H, 4.64; N, 8.33. Found C, 28.39; H, 4.82; N, 8.86. Recalc. for $C_{19}H_{31}N_4S_6Ni_1Pd_1.CHCl_3$: C, 30.32; H, 4.07; N, 7.07.

6.5 References

[1] M. S. Vickers, J. Cookson, P. D. Beer, P. T. Bishop, B. Thiebaut, *Journal of Materials Chemistry* **2006**, *16*, 209.

[2] T. Trindade, P. O'Brien, *Journal of Materials Chemistry* **1996**, *6*, 343.

[3] M. Green, P. O'Brien, *Chemical Communications* **1999**, 2235.
[4] R. Roy, K. Bag, P. K. Santra, C. Sinha, *Transition Metal Chemistry* **2000**, *25*, 302.
[5] K. Unoura, A. Yamazaki, A. Nagasawa, Y. Kato, H. Itoh, H. Kudo, Y. Fukuda, *Inorganica Chimica Acta* **1998**, *269*, 260.
[6] S. Baitalik, S. Mohanta, B. Adhikary, *Polyhedron* **1996**, *16*, 983.
[7] K. K. Verma, J. Ahmed, M. P. Sahasrabuddhey, S. Bose, *Journal of the Indian Chemical Society* **1977**, *54*, 699.
[8] P. D. Beer, N. G. Berry, A. R. Cowley, E. J. Hayes, E. C. Oates, W. W. H. Wong, *Chemical Communications* **2003**, 2408.
[9] W. W. H. Wong, D. Curiel, A. R. Cowley, P. D. Beer, *Dalton Transactions* **2005**, 359.
[10] P. D. Beer, N. Berry, O. D. Fox, M. E. Padilla-Tosta, S. Patell, M. G. B. Drew, *Chemical Communications* **2001**, 199.
[11] M. E. Padilla-Tosta, O. D. Fox, M. G. B. Drew, P. D. Beer, *Angewandte Chemie, International Edition* **2001**, *40*, 4235.
[12] W. W. H. Wong, D. E. Phipps, P. D. Beer, *Polyhedron* **2004**, *23*, 2821.
[13] M. D. Pratt, P. D. Beer, *Tetrahedron* **2004**, *60*, 11227.
[14] O. D. Fox, M. G. B. Drew, P. D. Beer, *Angewandte Chemie-International Edition* **2000**, *39*, 136.
[15] O. D. Fox, J. Cookson, E. J. S. Wilkinson, M. G. B. Drew, E. J. MacLean, S. J. Teat, P. D. Beer, *Journal of the American Chemical Society* **2006**, *128*, 6990.
[16] N. G. Berry, M. D. Pratt, O. D. Fox, P. D. Beer, *Supramolecular Chemistry* **2001**, *13*, 677.
[17] J. D. E. T. Wilton-Ely, D. Solanki, G. Hogarth, *European Journal of Inorganic Chemistry* **2005**, 4027.
[18] G. Hogarth, *Progress in Inorganic Chemistry* **2005**, *53*, 71.
[19] B. P. Sullivan, T. J. Meyer, *Inorganic Chemistry* **1982**, *21*, 1037.
[20] M. Menon, A. Pramanik, N. Bag, A. Chakravorty, *Journal of the Chemical Society-Dalton Transactions* **1995**, 1543.
[21] A. E. Aliev, A. A. Fomichev, G. V. Grishina, Y. I. El'natanov, R. G. Kostyanovskii, *Izvestiya Akademii Nauk SSSR, Seriya Khimicheskaya* **1990**, 1760.
[22] G. Hogarth, J. D. E. T. Wilton-Ely, **2005**.
[23] I. Kovacs, A.-M. Lebuis, A. Shaver, *Organometallics* **2001**, *20*, 35.
[24] K. S. Siddiqi, F. R. Zaidi, S. A. A. Zaidi, *Synthesis and Reactivity in Inorganic and Metal-Organic Chemistry* **1980**, *10*, 569.
[25] http://chemviz.ncsa.uiuc.edu/content/doc-resources-bond.html
[26] Discussion with Dr. G. Hogarth and B. Harvey, **2001**.
[27] A. Keller, B. Jasionka, T. Glowiak, A. Ershov, R. Matusiak, *Inorganica Chimica Acta* **2003**, *344*, 49.

Chapter 7

Dithiocarbonates and Xanthates

7.1 Introduction

Following the extensive work on metallic dithiocarbamates in Chapter 6, we also considered metallic xathates[1-4] and dithiocarbonates[5-7]. The xanthate compounds are very common complexes that have enjoyed much attention due to their utility in mineral separation[8] and metal ore flotation[9]. Tetracoordinate metal xanthates have the general formula $[L_2M(S_2COR)]$ (R = alkyl; M = transition metal; L = various ligands e.g. phosphines) whereas dithiocarbonates are less well-known and have the formula $[L_2M(S_2C{=}O)]$. The reaction of carbon disulfide with metallic alkoxides in the presence of alcohols produces xanthate compounds[10]. Fackler *et al.* have formed a range of these complexes with various metals such as platinum, palladium, nickel and ruthenium[10, 11].

The formation of the metallic dithiocarbonates can be achieved using xanthates[10, 12-18] carbon disulfide[19] or phosphoiodithiocarboxylate[20]. For example, Alison *et al.*[12] formed platinium-based dithiocarbonate from the bis-xanthate complex (Scheme 1).

Scheme 1: Formation of metal dithiocarbonate from metal xanthates[12]

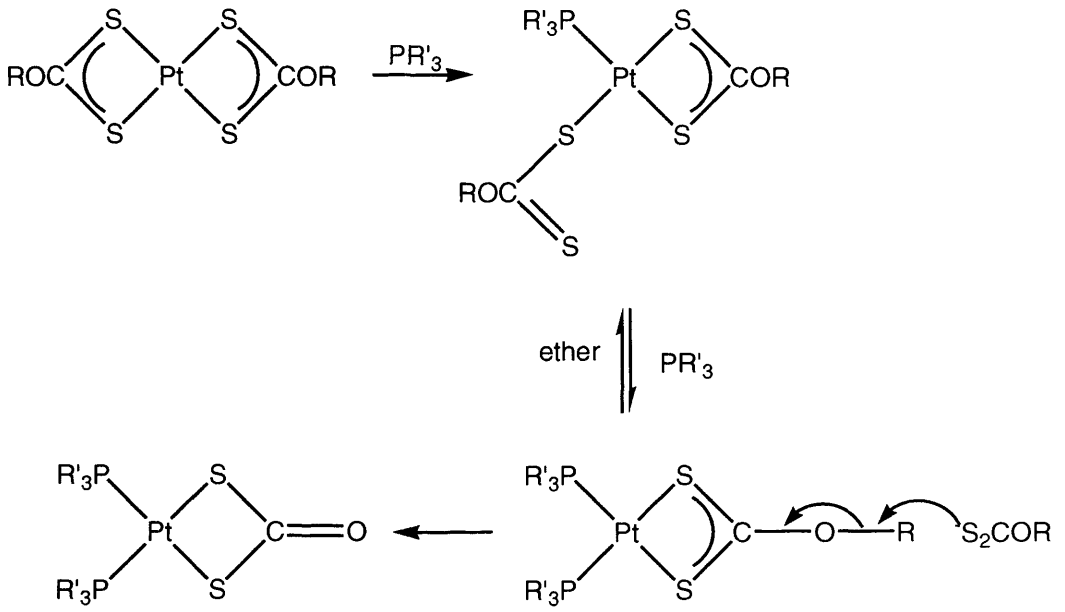

7.2 Results and Discussion

During our investigation of ruthenium dithiocarbamates, we found the reaction of *cis*-$[Ru(dppm)_2Cl_2]$ with CS_2 and NaOH produced the first known ruthenium dithiocarbonate, **1** in 94 % yield. To further investigate this, we considered the formation of xanthates and their intermediates forming three compounds, **1-3** (Figure 1).

Figure 1: Formation of dithiocarbonate (1) and xanthate complexes (2-3)

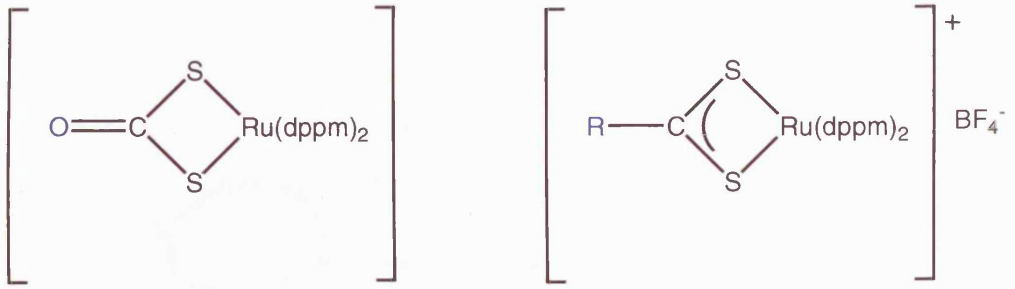

1

Compound	R
2	OH
3	OMe

Compound **1** was characterised using the standard techniques to establish the proposed dithiocarbonate structure. The ^1H NMR data clearly identified the phenyl as multiplets in the range δ 6.40 - 7.24 and dppm methylene protons appeared as multiplets at δ 4.26 and 4.72. The ^{13}C NMR data indicted the appropriate peaks with the key peak at δ 218.6, which represented the S_2CO carbon. The IR spectrum displayed the key stretch of ν(C=O) at 1568 cm^{-1} and the MS parent ion was 961 (M^+). In addition to all this data, the elemental analysis showed excellent agreement between the calculated percentages of C, 56.20; H, 4.30 and found values of C, 56.20 and H, 4.40.

Complex **1** was crystallised in different solvents and two single crystal modifications were determined, **1**.2CH_3OH and asymmetric **1**.3$CHCl_3$ (Δ and Λ-enantiomers). X-ray diffraction determined the crystal systems as monoclinic with the space group $C_{2/c}$ for **1**.2CH_3OH and P_{21} for **1**.3$CHCl_3$ (Figure 2).

Figure 2: Crystal structure of the ruthenium dithiocarbonate compound (1.2CH_3OH)

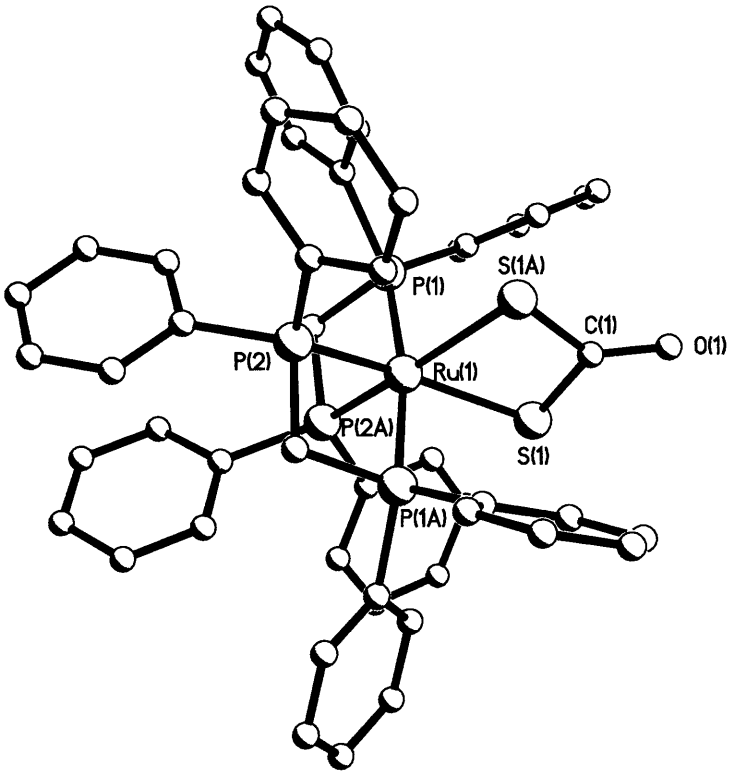

For the crystal **1**.2CH_3OH, the bonds of significance were the Ru-S bonds at 2.4198(10) Å (Ru(1)-S(1)), S-C at 1.764(3) Å (S(1)-C(1)) and the shorter carbonyl bond C-O (C(1)-O(1)) at 1.215(7) Å due to the double bond[10, 12-18]. The angles in this complex were similar to the other crystals[18, 21]. The S-Ru-S (S(1)-Ru(1)-S(1A) angle measured at 72.39(5)°, the S-C-S angle (S(1)-C(1)-S(1A)) at 108.20(3)° and the S-C-O angle (S(1)-C(1)-O(1)) 125.89(15)°.

Small variations were observed in **1**.3$CHCl_3$ when compared with the single structure **1**.2CH_3OH. The dithiocarbonate was observed to be marginally asymmetric in **1**.3$CHCl_3$ compared to the symmetrical dithiocarbonate in **1**.2CH_3OH. The Ru-S bond for **1**.3$CHCl_3$ was shorter at 2.4011(8) Å compared to 2.4198(10) Å of **1**.2CH_3OH. The S-C bond length was also shorter for **1**.3$CHCl_3$ at 1.749(4) Å compared to 1.764(3) Å. However, the C=O for **1**.3$CHCl_3$ was marginally longer at 1.226(4) Å compared to 1.215(7) Å.

These bonds were all in the expected ranges and compared well to [Ni(dippe)(S_2C=O)] (dippe = 1,2-bis(diisopropylphosphino)ethane)[18] and [Pt(S_2C=O){P(OMe)Ph_2}$_2$][21] (Table 1). Evaluation of the data from similar compounds found that the S-Ru-S bite angle was smaller than other metal complexes, suggesting at the dithiocarbonate unit was weakly bound and susceptible to distortions due to solvent molecules present. [Ru(dppm)$_2$(S_2CH_2)][22] was the isoelectronic analogue to **1** and was a point of comparison. In this structure, both the Ru-S and C-S bonds were observed to be longer than **1**, which was attributed to the double bond character of C=O of **1**.

It was proposed that **1** was formed from the *in situ* generation of Na[S_2COH] from NaOH and CS_2 in methanol. This was expected to react with *cis*-[Ru(dppm)$_2Cl_2$] to from the xanthate complex [Ru(dppm)$_2$(S_2COH)]$^+$ which would have been deprotonated under the basic conditions[23]. To prove this, **1** was protonated with HBF_4.OEt_2 to form [Ru(dppm)$_2$(S_2COH)]BF_4 (**2**). This was characterised by standard methods and shown to have some similarities with **1**. The phenyl and dppm protons in the ^{1}H NMR spectrum were observed along with an additional singlet at δ 3.83 attributed to the xanthate proton. The shift in ^{31}P NMR peaks and the lack of ν(C=O) in the IR spectrum

corroborated the proposed structure. This was further confirmed by the elemental analysis percentages calculated: C, 58.40; H, 4.30 and found values: C, 58.7; H, 4.50.

An alternative reaction pathway for the formation of **1** from *cis*-[Ru(dppm)$_2$Cl$_2$] would be the initial formation of *cis*-[RuCl(OH)(dppm)$_2$] which would be followed by insertion of CS_2 into the Ru-O bond and subsequent elimination of HCl[24]. The dithiocarbonate group in **1** was found to react with other electrophiles. The reaction of trimethyloxonium tetrafluoroborate with *cis*-[Ru(dppm)$_2$Cl$_2$] resulted in formation of the xanthate [Ru(dppm)$_2$(S$_2$COMe)][BF$_4$] (**3**), also prepared directly from the reaction of *cis*-[RuCl(OH)(dppm)$_2$] with NaS$_2$COMe (prepared *in situ* from NaOMe and CS_2) and $NaBF_4$. The ^{1}H NMR spectrum displayed a singlet at δ 3.80 which was assigned to the methyl group the structure was confirmed by MS with the parent ion at 977 (M^+) and elemental analysis.

The methyl xanthate ligand was found to have many similarities to the isopropyl xanthate moiety in [Ru(η^5-C$_5$Me$_5$)(S$_2$CO^{i}Pr)(PEt$_3$)][25]. The crystal structure of **3** was obtained as a yellow monoclinic plate with a space group of $C_{2/c}$ (Figure 3). The dppm fragment in this crystal structure closely resembled that of **9a** (Chapter 6). The interesting aspect of this structure was the bonding between the xanthate system. The bond lengths between Ru-S were almost identical at 2.4347(10) Å and longer than that of those of **1**.2CH$_3$OH. The S-C bond was also very similar at 1.691(3) Å. The carbonyl bond was measured to be 1.320(7) Å (C(1)-O(1)), longer than that of **1**.2CH$_3$OH and the O-Me length as 1.447(6) Å (O(1)- C(2)), consistent with other crystal structures[26-28].

Figure 3: Crystal structure of the xanthate complex 3

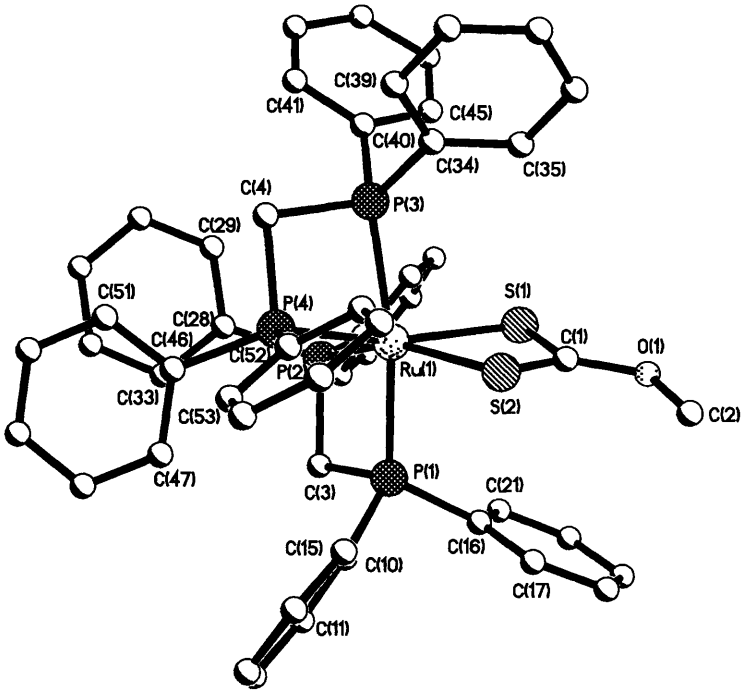

The angles of the dppm fragment were all in agreement with crystal structure **1**.2CH_3OH. The S-Ru-S angle was smaller at 71.72(19)° compared to 72.39(5)° of **1**.2CH_3OH and the S-C-S angle at 115.26(13)° (S(2)-C(1)-S(1)) was larger than **1**.2CH_3OH at 108.2(3)°. The angle between C-O-Me was bent at 118.30(2)° due to the sp^3 orbitals on the oxygen atom (Table 1).

The reactions of these ruthenium dithiocarbonate and xanthnate complexes can be summarised in the Scheme 2.

Scheme 2: Summary of reactions for the formation of dithiocarbonate (1) and xanthates (2-3)

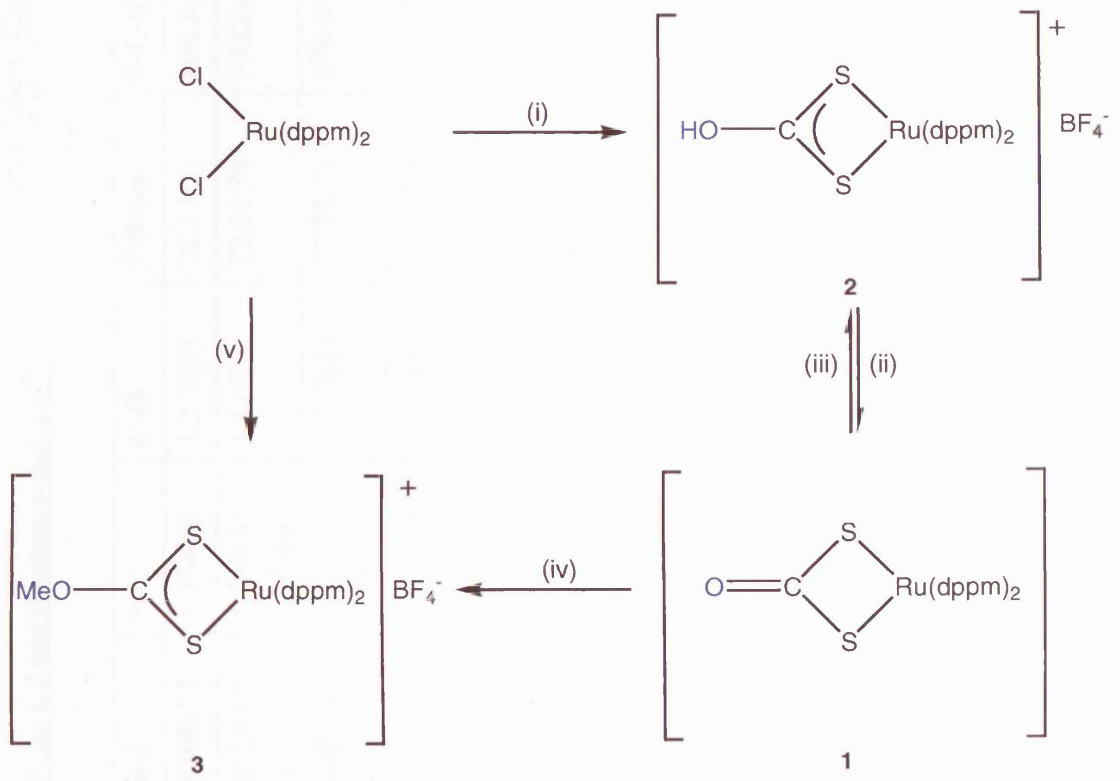

(i) CS_2, NaOH; (ii) NaOH or NEt_3; (iii) $HBF_4.OEt_2$; (iv) MeI, $[Me_3O]BF_4$;

(v) CS_2, NaOMe.

Reaction of **1** with methyl iodide also formed **3** with other products and ultimately led to the displacement of the xanthate ligand by iodide to give the known compound *cis*-$[Ru(dppm)_2I_2]$[29] similar to the reaction of $[Ni(dppe)(S_2C{=}O)]$ with methyl iodide to yield $[Ni(dppe)I_2]$[17].

Previous routes to dithiocarbonate complexes have frequently involved the reactions of xanthate complexes with bases such as phosphines[17]. However, treatment of **3** with NaOH in water and tetrahydrofuran (1:2) gave no reaction, suggesting that **3** is not an intermediate in the observed reaction between *cis*-$[Ru(dppm)_2Cl_2]$ and NaOH and CS_2 in methanol. Compound **3** also showed no reaction under acidic conditions.

Table 1: Selected bond lengths (Å) and angles (°) for 1, 3 and literature complexes[23]

Complex	Ru-P_{eq}	Ru-P_{ax}	Ru-S	S-C	C-O	S-Ru-S	S-C-S
[Ru(dppm)$_2$(S_2C=O)] (**1**·2CH_3OH)	2.3152(10)	2.3319(10)	2.4198(10)	1.764(3)	1.215(7)	72.39(5)	108.2(3)
Δ-[Ru(dppm)$_2$(S_2C=O)] (**1**·3$CHCl_3$)	2.3140(9) 2.3286(8)	2.3308(10) 2.3477(9)	2.4011(8) 2.4364(10)	1.749(4) 1.764(4)	1.226(4)	72.06(3)	108.21(19)
Λ-[Ru(dppm)$_2$(S_2C=O)] (**1**·3$CHCl_3$)	2.3138(9) 2.3323(9)	2.3280(9) 2.3429(10)	2.4157(9) 2.4353(9)	1.743(4) 1.765(4)	1.213(5)	71.78(3)	108.4(2)
[Ru(dppm)$_2$(S_2COMe)]$^+$ (**3**)	2.3124(6) 2.3200(6)	2.3342(6) 2.3721(6)	2.4347(6) 2.4398(6)	1.689(2) 1.691(2)	1.320(3)	71.715(19)	115.26(13)
[Ru(dppm)$_2$(S_2CH_2)][22]	2.3171(11) 2.3181(11)	2.3079(12) 2.3571(12)	2.4245(11) 2.4368(12)	1.812(5) 1.824(5)	-	72.96(4)	105.3(2)
[Ni(dippe)(S_2C=O)][18]	-	-	-	1.759(6) 1.769(5)	1.235(6)	79.72(6)	106.3(3)
[Pt{P(OMe)Ph_2}$_2$(S_2C=O)][21]	-	-	-	1.765(7) 1.767(7)	1.190(8)	75.2(1)	107.5(3)
[Ru(η^5-C_5Me_5)(S_2CO^iPr)(PEt_3)][26, 27]	-	-	2.393(2) 2.406(2)	1.678(5) 1.682(5)	1.315(6)	71.45(6)	113.0(3)
dippe = 1,2-bis(diisopropylphosphino)ethane							

7.3 Conclusions

In this final chapter, we examined the formation of ruthenium-based dithiocarbonates and xanthates. It has been proposed that reaction of CS_2 with NaOH leads to the formation of the intermediate xanthate complex $[Ru(dppm)_2(S_2COH)][BF_4]$ (**2**) which is deprotonated by the basic conditions to form $[Ru(dppm)_2(S_2C{=}O)]$ (**1**). We were able to form the ruthenium methyl xanthate complex, $[Ru(dppm)_2(S_2COMe)][BF_4]$ (**3**), *via* two routes. These compounds were fully characterised and single crystals X-ray diffraction determined structures of **1** and **3**. The $[Ru(dppm)_2(S_2C{=}O)]$ complex was found to form two modification, the single crystal **1**.$2CH_3OH$ and the two asymmetric enatiomers of **1**.$3CHCl_3$. These complexes were compared with similar literature complexes and displayed excellent agreement.

7.4 Experimental

All ^1H, ^{13}C and ^{31}P NMR spectra were obtained on a Bruker AMX300 (^1H 299.87 MHz, ^{31}P 121.39 MHz) and AMX400 (^1H 400.14 MHz, ^{31}P 161.97 MHz) spectrometer respectively. All spectra were recorded using $CDCl_3$ solutions unless otherwise specified and were referenced against internal standards. All IR spectra were recorded using a Shimaduz FT-IR 8700 spectrometer, operating in the region of 4000 - 400 cm^{-1}. The IR samples were prepared using KBr powder to make discs or as neat samples between NaCl plates. The mass spectra were obtained using a Micromass 70-SE magnetic sector mass spectrometer. Three different procedures were used to maximise accuracy of the data for individual samples. These were Electron Impact (EI) Mode with ionisation at 70 eV, Chemical Ionisation (CI) with methane reagent gas and Fast Atom Bombardment (FAB^+) using a caesium ion gun. The Elemental Analysis

(elemental analysis) was carried out using Elemental Analyzer (CE-440) (Exeter Analytical Inc).

Synthesis for **1** (a): NaOH (0.03 g, 0.80 mmol) was dissolved in methanol (10 ml) and CS_2 (0.06 g, 0.80 mmol) added. The reaction mixture was stirred for 10 min. followed by the addition of *cis*-[$Ru(dppm)_2Cl_2$] (0.20 mg, 0.16 mmol) dissolved in DCM (10 ml). The solution was stirred for 2 h. and then all the solvent was removed under reduced pressure. The residue was dissolved in a minimum quantity of DCM and filtered through diatomaceous earth. Ethanol (20 ml) was added and the solvent volume concentrated under reduced pressure until precipitation was complete. The pale green product was filtered and washed with ethanol (10 ml) and hexane (10 ml) (0.14 g, 94 %).

Synthesis for **1** (b): compound **2** (0.03 g, 0.03 mmol) was dissolved in DCM (10 ml) and treated with NEt_3 (4 drops, excess) and the reaction mixture stirred for 20 min. Ethanol (20 ml) was added and the solvent volume concentrated under reduced pressure until precipitation was complete. The pale green product was filtered and washed with ethanol (10 ml) and hexane (10 ml) (0.02 g, 82 %). IR (KBr) *v*: 1685s 1568s, 1312s, 1238s, 972s, 849s cm^{-1}; IR (CH_2Cl_2): 1605s, 1572s; ^1H NMR ($CDCl_3$): δ 6.4 - 7.24 (mm, 60H, *Ph*), 4.72 (m, 2H, dppm-CH_2), 4.26 (m, 2H, dppm-CH_2); ^{13}C NMR (CD_2Cl_2): δ 218.6, 129.6 - 134.2, 45.7; ^{31}P NMR ($CDCl_3$): δ -4.3 (t, 2P, J 32.6, *P*Ph_2), -19.5 (t, 2P, J 32.6, *P*Ph_2); mass spectrum (FAB): *m/z* 961 $(M)^+$; anal. calc. for $C_{51}H_{44}OP_4RuS_2$: C, 63.67; H, 4.61. Found C, 56.20; H, 4.40. Recalc. For $C_{51}H_{44}OP_4RuS_2 \cdot 2CH_2Cl_2$: C, 56.20; H, 4.30.

Synthesis for **2:** diethylether (10 ml) suspension of [Ru(κ^2-S_2C=O)(dppm)$_2$] (**1**) (0.03 g, 0.03 mmol) was treated with tetrafluoroboric acid diethyl ether complex (3 drops, excess) and the reaction mixture was stirred for 5 min. The precipitate was broken up by sonication in an ultrasound bath and then filtered and washed with diethylether (10 ml) and hexane (10 ml) to give product (0.03 g, 90 %). IR (KBr) *v*: 1339m, 1312m, 1236m, 1049m, 885m cm^{-1}; ^{1}H NMR ($CDCl_3$): δ 6.54 – 7.64 (mm, 40H, *Ph*), 5.03 (m, 2H, dppm-C*H*$_2$), 4.64 (m, 2H, dppm-C*H*$_2$), 3.83 (s, 1H, OH); ^{31}P NMR ($CDCl_3$): δ -4.4 (t, 2P, J 35.7, *P*Ph$_2$), -16.7 (t, 2P, J 35.7, *P*Ph$_2$); mass spectrum (FAB): *m/z* 979 (M + H_2O)$^+$; anal. calc. for $C_{51}H_{45}BF_4OP_4RuS_2$: C, 58.40; H, 4.30. Found: C, 58.70; H, 4.50.

Synthesis for **3** (a): NaOMe (0.02 g, 0.33 mmol) was dissolved in methanol (10 ml) and CS_2 (0.03 g, 0.33 mmol) added. The reaction mixture was stirred for 20 min. and the DCM solution (10 ml) of *cis*-[Ru(dppm)$_2$Cl$_2$] (0.10 g, 0.11 mmol) was added to give a white precipitate. The solution was treated with an aqueous solution (0.5 ml) of $NaBF_4$ (0.03 g, 0.22 mmol) and the reaction mixture was stirred for 1 h. All the solvent was removed under reduced pressure and the residue dissolved in a minimum quantity of DCM and filtered through diatomaceous earth. Methanol (20 ml) was added and the solvent volume concentrated under reduced pressure until precipitation was complete. The white product was filtered and washed with ethanol (10 ml) and hexane (10 ml) (0.08 g, 72 %).

Synthesis for **3** (b): compound **1** (0.03 g, 0.03 mmol) was dissolved in DCM (10 ml) and treated with trimethyloxonium tetrafluoroborate (4 drops, excess) and the reaction stirred for 30 min. Ethanol (20 ml) was added and the solvent volume concentrated under reduced pressure until precipitation was complete. The product was filtered and

washed with ethanol (10 ml) and hexane (10 ml) (0.02 g, 58 %). IR (KBr) *v*: 1335m, 1312m, 1248m, 1057m, 957m cm^{-1}; ^{1}H NMR ($CDCl_3$): δ 6.42 - 7.57 (mm, 40H, *Ph*), 4.90 (m, 2H, dppm-CH_2), 4.45 (m, 2H, dppm-CH_2), 3.80 (s, 3H, OCH_3); ^{31}P NMR ($CDCl_3$): δ -2.1 (t, 2P, J 35.8, PPh_2), -14.5 (t, 2P, J 35.8, PPh_2)]; mass spectrum (FAB): *m/z* 977 (M^+); anal. calc. for $C_{52}H_{47}BF_4OP_4RuS_2$: C, 58.70; H, 4.50. Found: C, 58.50; H, 4.40.

7.5 References

[1] C. R. Russell, R. A. Buchanan, C. E. Rist, B. T. Hofreiter, A. J. Ernst, *Tappi* **1962**, *45*, 557.
[2] D. J. Gannon, D. T. F. Fung, Application: ZA, 8004227, **1981**.
[3] R. J. Magee, *Reviews in Analytical Chemistry* **1973**, *1*, 335.
[4] R. F. McCleary, J. R. Morris, US, 2,363,884, **1944**.
[5] M. El-Khateeb, K. J. Asali, A. Lataifeh, *Polyhedron* **2006**, *25*, 1695.
[6] R. F. Struck, W. R. Waud, *Cancer Chemotherapy and Pharmacology* **2006**, *57*, 180.
[7] Y. Wang, L. Yan, J. Fu, M. Chai, *Huaxue Tongbao* **2005**, *68*, w036/1.
[8] A. Strong, D. Yan, R. Dunne, *Publications of the Australasian Institute of Mining and Metallurgy* **2005**, *5/2005*, 619.
[9] G. Winter, *Inorganic and Nuclear Chemistry Letters* **1975**, *11*, 113.
[10] J. P. Fackler, Jr., W. C. Seidel, J. A. Fetchin, *Journal of the American Chemical Society* **1968**, *90*, 2707.
[11] J. P. Fackler, Jr., W. C. Seidel, *Inorganic Chemistry* **1969**, *8*, 1631.
[12] J. M. C. Alison, T. A. Stephenson, *Journal of the Chemical Society, Dalton Transactions* **1973**, 254.
[13] D. J. Colehami, T. A. Stephens, *Journal of the Chemical Society-Dalton Transactions* **1974**, 1818.
[14] R. O. Gould, A. M. Gunn, T. E. M. Vandenhark, *Journal of the Chemical Society-Dalton Transactions* **1976**, 1713.
[15] M. C. Cornock, R. O. Gould, C. L. Jones, T. A. Stephenson, *Journal of the Chemical Society-Dalton Transactions* **1977**, 1307.
[16] J. Doherty, J. Fortune, A. R. Manning, F. S. Stephens, *Journal of the Chemical Society, Dalton Transactions* **1984**, 1111.
[17] M. F. Perpinan, L. Ballester, M. E. Gonzalez-Casso, A. Santos, *Journal of the Chemical Society, Dalton Transactions* **1987**, 281.
[18] M. J. Tenorio, M. C. Puerta, P. Valerga, *Journal of the Chemical Society, Dalton Transactions* **1996**, 1935.
[19] C. Bianchini, C. A. Ghilardi, A. Meli, A. Orlandini, *Journal of Organometallic Chemistry* **1985**, *286*, 259.
[20] C. Bianchini, C. Mealli, A. Meli, M. Sabat, *Journal of the Chemical Society, Chemical Communications* **1985**, 1024.

[21] R. Contreras, M. Valderrama, O. Riveros, R. Moscoso, D. Boys, *Polyhedron* **1996**, *15*, 183.
[22] T. Gandhi, M. Nethaji, B. R. Jagirdar, *Inorganic Chemistry* **2003**, *42*, 667.
[23] J. D. E. T. Wilton-Ely, D. Solanki, G. Hogarth, *Inorganic Chemistry* **2006**, *45*, 5210.
[24] M. J. Burn, M. G. Fickes, J. F. Hartwig, F. J. Hollander, R. G. Bergman, *Journal of the American Chemical Society* **1993**, *115*, 5875.
[25] A. Coto, M. J. Tenorio, M. C. Puerta, P. Valerga, *Organometallics* **1998**, *17*, 4392.
[26] A. R. Chakravarty, F. A. Cotton, W. Schwotzer, *Inorganica Chimica Acta* **1984**, *84*, 179.
[27] A. Keller, B. Jasionka, T. Glowiak, A. Ershov, R. Matusiak, *Inorganica Chimica Acta* **2003**, *344*, 49.
[28] A. A. Batista, C. Pereira, K. Wohnrath, S. L. Queiroz, R. H. D. Santos, M. T. D. Gambardella, *Polyhedron* **1999**, *18*, 2079.
[29] J. F. Bickley, A. A. La Pensee, S. J. Higgins, C. A. Stuart, *Journal of the Chemical Society, Dalton Transactions* **2003**, 4663.

Appendix

Appendix

Chapter 3

Crystal data and structure refinement for $[Cu(NH_3)_4][Ni(CN)_4]$ (**4a**)

Chemical formula	$C_4H_{12}CuN_8Ni$	
Formula weight	294.47	
Temperature	293(2) K	
Radiation, wavelength	MoKα, 0.71073 Å	
Crystal system, space group	orthorhombic, Pnma	
Unit cell parameters	a = 14.2309(9) Å	α = 90°
	b = 7.3114(5) Å	β = 90°
	c = 10.3602(7) Å	γ = 90°
Cell volume	1077.96(12) $Å^3$	
Z	4	
Calculated density	1.814 g/cm^3	
Absorption coefficient μ	3.696 mm^{-1}	
F(000)	596	
Crystal colour and size	blue, 0.16 × 0.12 × 0.09 mm^3	
Data collection method	Bruker SMART APEX diffractometer	
	ω rotation with narrow frames	
θ range for data collection	2.43 to 28.25°	
Index ranges	h −18 to 18, k −9 to 9, l −13 to 13	
Completeness to θ = 26.00°	99.5 %	
Reflections collected	8981	
Independent reflections	1414 (R_{int} = 0.0190)	
Reflections with $F^2>2\sigma$	1381	
Absorption correction	semi-empirical from equivalents	
Min. and max. transmission	0.5893 and 0.7321	
Structure solution	direct methods	
Refinement method	Full-matrix least-squares on F^2	
Weighting parameters a, b	0.0206, 0.3420	
Data / restraints / parameters	1414 / 0 / 103	
Final R indices [$F^2>2\sigma$]	R1 = 0.0159, wR2 = 0.0386	
R indices (all data)	R1 = 0.0165, wR2 = 0.0388	
Goodness-of-fit on F^2	1.093	
Largest and mean shift/su	0.001 and 0.000	
Largest diff. peak and hole	0.267 and −0.355 e $Å^{-3}$	

Bond lengths [Å] and angles [°].

Cu(1)–N(6A)	2.0148(11)	Cu(1)–N(6)	2.0148(11)
Cu(1)–N(5)	2.0237(10)	Cu(1)–N(5A)	2.0237(10)
Cu(1)–N(1)	2.3777(14)	Ni(1)–C(1)	1.8596(17)
Ni(1)–C(2)	1.8648(18)	Ni(1)–C(3)	1.8694(17)
Ni(1)–C(4)	1.8699(18)	N(1)–C(1)	1.151(2)
N(2)–C(2)	1.153(2)	N(3)–C(3)	1.153(2)
N(4)–C(4)	1.152(2)		

N(6A)–Cu(1)–N(6)	90.69(7)	N(6A)–Cu(1)–N(5)	172.06(5)
N(6)–Cu(1)–N(5)	89.51(5)	N(6A)–Cu(1)–N(5A)	89.51(5)
N(6)–Cu(1)–N(5A)	172.06(5)	N(5)–Cu(1)–N(5A)	89.20(6)
N(6A)–Cu(1)–N(1)	91.57(4)	N(6)–Cu(1)–N(1)	91.57(4)
N(5)–Cu(1)–N(1)	96.36(4)	N(5A)–Cu(1)–N(1)	96.36(4)
C(1)–Ni(1)–C(2)	90.08(7)	C(1)–Ni(1)–C(3)	179.85(7)
C(2)–Ni(1)–C(3)	90.07(7)	C(1)–Ni(1)–C(4)	87.41(7)
C(2)–Ni(1)–C(4)	177.49(7)	C(3)–Ni(1)–C(4)	92.44(7)
C(1)–N(1)–Cu(1)	124.48(12)	N(1)–C(1)–Ni(1)	177.00(14)
N(2)–C(2)–Ni(1)	179.73(15)	N(3)–C(3)–Ni(1)	176.52(14)
N(4)–C(4)–Ni(1)	175.08(15)		

Crystal data and structure refinement for $[Cu(en)_2][Ni(CN)_4].H_2O$ (**8a**)

Chemical formula	$C_8H_{10}CuN_8NiO$	
Formula weight	356.49	
Temperature	150(2) K	
Radiation, wavelength	MoKα, 0.71073 Å	
Crystal system, space group	triclinic, P1bar	
Unit cell parameters	a = 6.4602(11) Å	α = 106.289(2)°
	b = 7.1628(10) Å	β = 91.611(2)°
	c = 7.9585(11) Å	γ = 107.175(2)°
Cell volume	335.24(9) $Å^3$	
Z	2	
Calculated density	3.532 g/cm^3	
Absorption coefficient μ	5.988 mm^{-1}	
F(000)	358	
Crystal colour and size	purple, 0.12 × 0.12 × 0.03 mm^3	
Data collection method	Bruker SMART APEX diffractometer	
	ω rotation with narrow frames	
θ range for data collection	2.69 to 28.27°	
Index ranges	h −8 to 8, k −9 to 9, l −10 to 10	
Completeness to θ = 26.00°	98.2 %	
Reflections collected	2963	
Independent reflections	1533 (R_{int} = 0.0309)	
Reflections with $F^2>2\sigma$	1416	
Absorption correction	semi-empirical from equivalents	
Min. and max. transmission	0.5335 and 0.8408	
Structure solution	direct methods	
Refinement method	Full-matrix least-squares on F^2	
Weighting parameters a, b	0.0390, 0.0567	
Data / restraints / parameters	1533 / 0 / 101	
Final R indices [$F^2>2\sigma$]	R1 = 0.0258, wR2 = 0.0699	
R indices (all data)	R1 = 0.0274, wR2 = 0.0712	
Goodness-of-fit on F^2	1.077	
Largest and mean shift/su	0.000 and 0.000	
Largest diff. peak and hole	0.500 and −0.725 e $Å^{-3}$	

Bond lengths [Å] and angles [°].

Cu(1)–N(1)	2.0114(14)	Cu(1)–N(1A)	2.0114(14)
Cu(1)–N(2A)	2.0157(13)	Cu(1)–N(2)	2.0157(13)
Ni(1)–C(3B)	1.8636(15)	Ni(1)–C(3)	1.8636(15)
Ni(1)–C(4)	1.8726(15)	Ni(1)–C(4B)	1.8726(15)
N(1)–C(1)	1.480(2)	N(2)–C(2)	1.478(2)
N(3)–C(3)	1.148(2)	N(4)–C(4)	1.148(2)
C(1)–C(2)	1.510(2)		

N(1)–Cu(1)–N(1A)	180	N(1)–Cu(1)–N(2A)	95.44(6)
N(1A)–Cu(1)–N(2A)	84.56(6)	N(1)–Cu(1)–N(2)	84.56(6)
N(1A)–Cu(1)–N(2)	95.44(6)	N(2A)–Cu(1)–N(2)	180.00(8)
C(3B)–Ni(1)–C(3)	180	C(3B)–Ni(1)–C(4)	91.98(6)
C(3)–Ni(1)–C(4)	88.02(6)	C(3B)–Ni(1)–C(4B)	88.02(6)
C(3)–Ni(1)–C(4B)	91.98(6)	C(4)–Ni(1)–C(4B)	180.000(1)
C(1)–N(1)–Cu(1)	108.10(10)	C(2)–N(2)–Cu(1)	108.78(10)
N(1)–C(1)–C(2)	106.94(13)	N(2)–C(2)–C(1)	107.74(12)
N(3)–C(3)–Ni(1)	176.82(13)	N(4)–C(4)–Ni(1)	175.67(13)

Crystal data and structure refinement for[$Ni(en)_3$][$Ni(CN)_4$].H_2O (7)

Chemical formula	$C_{10}H_{26}N_{10}Ni_2O$	
Formula weight	419.83	
Temperature	150(2) K	
Radiation, wavelength	MoKα, 0.71073 Å	
Crystal system, space group	orthorhombic, Pbca	
Unit cell parameters	a = 11.5176(8) Å	α = 90°
	b = 15.6266(11) Å	β = 90°
	c = 19.7338(14) Å	γ = 90°
Cell volume	3551.7(4) $Å^3$	
Z	8	
Calculated density	1.570 g/cm^3	
Absorption coefficient μ	2.140 mm^{-1}	
F(000)	1760	
Crystal colour and size	pink, 0.34 × 0.32 × 0.05 mm^3	
Data collection method	Bruker SMART APEX diffractometer	
	ω rotation with narrow frames	
θ range for data collection	2.43 to 28.30°	
Index ranges	h −15 to 15, k −20 to 20, l −26 to 25	
Completeness to θ = 26.00°	99.9 %	
Reflections collected	29237	
Independent reflections	4329 (R_{int} = 0.0304)	
Reflections with $F^2>2\sigma$	3995	
Absorption correction	semi-empirical from equivalents	
Min. and max. transmission	0.5299 and 0.9006	
Structure solution	direct methods	
Refinement method	Full-matrix least-squares on F^2	
Weighting parameters a, b	0.0253, 1.3007	
Data / restraints / parameters	4329 / 0 / 264	
Final R indices [$F^2>2\sigma$]	R1 = 0.0203, wR2 = 0.0509	
R indices (all data)	R1 = 0.0225, wR2 = 0.0519	
Goodness-of-fit on F^2	1.042	
Largest and mean shift/su	0.004 and 0.000	
Largest diff. peak and hole	0.355 and −0.288 e $Å^{-3}$	

Bond lengths [Å] and angles [°].

Ni(1)–N(2)	2.1131(10)	Ni(1)–N(3)	2.1171(10)
Ni(1)–N(6)	2.1196(10)	Ni(1)–N(5)	2.1234(10)
Ni(1)–N(1)	2.1393(11)	Ni(1)–N(4)	2.1400(11)
Ni(2)–C(8)	1.8671(12)	Ni(2)–C(10)	1.8680(12)
Ni(2)–C(7)	1.8687(12)	Ni(2)–C(9)	1.8743(12)
N(1)–C(1)	1.4813(16)	N(2)–C(2)	1.4791(15)
N(3)–C(3)	1.4755(15)	N(4)–C(4)	1.4821(16)
N(5)–C(5)	1.4761(15)	N(6)–C(6)	1.4765(15)
N(7)–C(7)	1.1533(16)	N(8)–C(8)	1.1492(16)
N(9)–C(9)	1.1529(17)	N(10)–C(10)	1.1509(16)
C(1)–C(2)	1.5127(17)	C(3)–C(4)	1.5130(17)
C(5)–C(6)	1.5131(17)		

N(2)–Ni(1)–N(3)	91.36(4)	N(2)–Ni(1)–N(6)	95.28(4)
N(3)–Ni(1)–N(6)	171.34(4)	N(2)–Ni(1)–N(5)	172.63(4)
N(3)–Ni(1)–N(5)	92.11(4)	N(6)–Ni(1)–N(5)	81.94(4)
N(2)–Ni(1)–N(1)	81.75(4)	N(3)–Ni(1)–N(1)	94.75(4)
N(6)–Ni(1)–N(1)	91.70(4)	N(5)–Ni(1)–N(1)	91.48(4)
N(2)–Ni(1)–N(4)	92.70(4)	N(3)–Ni(1)–N(4)	81.59(4)
N(6)–Ni(1)–N(4)	92.53(4)	N(5)–Ni(1)–N(4)	94.25(4)
N(1)–Ni(1)–N(4)	173.30(4)	C(8)–Ni(2)–C(10)	178.07(5)
C(8)–Ni(2)–C(7)	88.44(5)	C(10)–Ni(2)–C(7)	89.64(5)
C(8)–Ni(2)–C(9)	90.76(5)	C(10)–Ni(2)–C(9)	91.15(5)
C(7)–Ni(2)–C(9)	177.22(5)	C(1)–N(1)–Ni(1)	108.40(7)
C(2)–N(2)–Ni(1)	107.14(7)	C(3)–N(3)–Ni(1)	106.81(7)
C(4)–N(4)–Ni(1)	109.33(7)	C(5)–N(5)–Ni(1)	108.82(7)
C(6)–N(6)–Ni(1)	107.38(7)	N(1)–C(1)–C(2)	108.10(10)
N(2)–C(2)–C(1)	108.16(10)	N(3)–C(3)–C(4)	108.64(10)
N(4)–C(4)–C(3)	109.24(9)	N(5)–C(5)–C(6)	108.84(9)
N(6)–C(6)–C(5)	108.57(10)	N(7)–C(7)–Ni(2)	177.79(11)
N(8)–C(8)–Ni(2)	176.79(11)	N(9)–C(9)–Ni(2)	178.85(12)
N(10)–C(10)–Ni(2)	178.88(12)		

Chapter 5

Crystal data and structure refinement for hexa(bromomethyl)benzene

Chemical formula	$C_6H_6Br_3$	
Formula weight	317.84	
Temperature	293(2) K	
Radiation, wavelength	MoKα, 0.71073 Å	
Crystal system, space group	hexagonal, R3bar	
Unit cell parameters	a = 16.3309(9) Å	α = 90°
	b = 16.3309(9) Å	β = 90°
	c = 5.3192(6) Å	γ = 120°
Cell volume	1228.56(17) $Å^3$	
Z	6	
Calculated density	2.578 g/cm^3	
Absorption coefficient μ	14.687 mm^{-1}	
F(000)	882	
Crystal colour and size	colorless, 0.04 × 0.02 × 0.01 mm^3	
Data collection method	Bruker SMART APEX diffractometer	
	ω rotation with narrow frames	
θ range for data collection	2.49 to 28.24°	
Index ranges	h −21 to 21, k −21 to 21, l −7 to 7	
Completeness to θ = 26.00°	99.6 %	
Reflections collected	3610	
Independent reflections	667 (R_{int} = 0.0247)	
Reflections with $F^2>2\sigma$	623	
Absorption correction	semi-empirical from equivalents	
Min. and max. transmission	0.5911 and 0.8670	
Structure solution	direct methods	
Refinement method	Full-matrix least-squares on F^2	
Weighting parameters a, b	0.0145, 0.9874	
Data / restraints / parameters	667 / 0 / 36	
Final R indices [$F^2>2\sigma$]	R1 = 0.0150, wR2 = 0.0365	
R indices (all data)	R1 = 0.0165, wR2 = 0.0370	
Goodness-of-fit on F^2	1.123	
Largest and mean shift/su	0.001 and 0.000	
Largest diff. peak and hole	0.390 and −0.762 e $Å^{-3}$	

Bond lengths [Å] and angles [°].

Br(1)–C(2)	1.9747(17)	C(1)–C(1A)	1.4079(16)
C(1)–C(1B)	1.4079(16)	C(1)–C(2)	1.490(2)
C(1A)–C(1)–C(1B)	119.979(7)	C(1A)–C(1)–C(2)	120.13(15)
C(1B)–C(1)–C(2)	119.87(15)	C(1)–C(2)–Br(1)	111.24(12)

Crystal data and structure refinement for 1,3,5-tris(bromomethyl)-2,4,6-trimethylbenzene with dimethyldithiocarbamate (**2a**)

Chemical formula	$C_{21}H_{33}N_3S_6$	
Formula weight	519.86	
Temperature	150(2) K	
Radiation, wavelength	MoKα, 0.71073 Å	
Crystal system, space group	monoclinic, P21/n	
Unit cell parameters	a = 11.5734(8) Å	α = 90°
	b = 12.1325(9) Å	β = 98.6920(10)°
	c = 18.2198(13) Å	γ = 90°
Cell volume	2528.9(3) $Å^3$	
Z	4	
Calculated density	1.365 g/cm^3	
Absorption coefficient μ	0.556 mm^{-1}	
F(000)	1104	
Crystal colour and size	colorless, 0.16 × 0.14 × 0.13 mm^3	
Data collection method	Bruker SMART APEX diffractometer	
	ω rotation with narrow frames	
θ range for data collection	1.96 to 28.27°	
Index ranges	h −14 to 15, k −16 to 16, l −24 to 24	
Completeness to θ = 26.00°	99.8 %	
Reflections collected	21921	
Independent reflections	6056 (R_{int} = 0.0180)	
Reflections with $F^2>2\sigma$	5531	
Absorption correction	semi-empirical from equivalents	
Min. and max. transmission	0.9164 and 0.9313	
Structure solution	direct methods	
Refinement method	Full-matrix least-squares on F^2	
Weighting parameters a, b	0.0830, 2.0566	
Data / restraints / parameters	6056 / 0 / 271	
Final R indices [$F^2>2\sigma$]	R1 = 0.0437, wR2 = 0.1286	
R indices (all data)	R1 = 0.0470, wR2 = 0.1320	
Goodness-of-fit on F^2	1.027	
Largest and mean shift/su	0.001 and 0.000	
Largest diff. peak and hole	0.597 and −0.536 e $Å^{-3}$	

Bond lengths [Å] and angles [°].

S(1)–C(13)	1.770(2)	S(1)–C(7)	1.817(2)
S(2)–C(13)	1.674(2)	S(3)–C(16)	1.776(2)
S(3)–C(9)	1.816(2)	S(4)–C(16)	1.664(2)
S(5)–C(19)	1.778(2)	S(5)–C(11)	1.817(2)
S(6)–C(19)	1.667(2)	N(1)–C(13)	1.333(3)
N(1)–C(15)	1.458(3)	N(1)–C(14)	1.464(3)
N(2)–C(16)	1.331(3)	N(2)–C(17)	1.467(3)
N(2)–C(18)	1.467(3)	N(3)–C(19)	1.337(3)
N(3)–C(21)	1.463(3)	N(3)–C(20)	1.467(3)
C(1)–C(2)	1.400(3)	C(1)–C(6)	1.400(3)
C(1)–C(7)	1.509(3)	C(2)–C(3)	1.406(3)
C(2)–C(8)	1.516(3)	C(3)–C(4)	1.404(3)
C(3)–C(9)	1.514(3)	C(4)–C(5)	1.406(3)
C(4)–C(10)	1.514(3)	C(5)–C(6)	1.403(3)
C(5)–C(11)	1.511(3)	C(6)–C(12)	1.510(3)

C(13)–S(1)–C(7)	103.41(9)	C(16)–S(3)–C(9)	104.59(9)
C(19)–S(5)–C(11)	102.96(10)	C(13)–N(1)–C(15)	121.62(18)
C(13)–N(1)–C(14)	122.85(17)	C(15)–N(1)–C(14)	115.42(17)
C(16)–N(2)–C(17)	123.28(17)	C(16)–N(2)–C(18)	121.83(18)
C(17)–N(2)–C(18)	114.79(17)	C(19)–N(3)–C(21)	120.69(18)
C(19)–N(3)–C(20)	122.19(18)	C(21)–N(3)–C(20)	117.10(18)
C(2)–C(1)–C(6)	120.91(18)	C(2)–C(1)–C(7)	120.19(18)
C(6)–C(1)–C(7)	118.88(18)	C(1)–C(2)–C(3)	119.10(18)
C(1)–C(2)–C(8)	119.29(18)	C(3)–C(2)–C(8)	121.61(18)
C(4)–C(3)–C(2)	120.59(17)	C(4)–C(3)–C(9)	119.85(17)
C(2)–C(3)–C(9)	119.55(18)	C(3)–C(4)–C(5)	119.51(17)
C(3)–C(4)–C(10)	120.90(18)	C(5)–C(4)–C(10)	119.59(18)
C(6)–C(5)–C(4)	120.22(18)	C(6)–C(5)–C(11)	119.04(18)
C(4)–C(5)–C(11)	120.71(18)	C(1)–C(6)–C(5)	119.55(17)
C(1)–C(6)–C(12)	120.02(18)	C(5)–C(6)–C(12)	120.43(18)
C(1)–C(7)–S(1)	108.54(13)	C(3)–C(9)–S(3)	107.04(13)
C(5)–C(11)–S(5)	110.79(14)	N(1)–C(13)–S(2)	124.30(15)
N(1)–C(13)–S(1)	112.94(14)	S(2)–C(13)–S(1)	122.76(11)
N(2)–C(16)–S(4)	124.83(15)	N(2)–C(16)–S(3)	112.45(14)
S(4)–C(16)–S(3)	122.67(12)	N(3)–C(19)–S(6)	123.33(16)
N(3)–C(19)–S(5)	113.23(15)	S(6)–C(19)–S(5)	123.44(12)

Crystal data and structure refinement for 1,3,5-tris(bromomethyl)-2,4,6-trimethylbenzene with diethyldithiocarbamate (**2b**)

Chemical formula	$C_{28}H_{46}Cl_{2.50}N_3S_6$	
Formula weight	705.66	
Temperature	150(2) K	
Radiation, wavelength	MoKα, 0.71073 Å	
Crystal system, space group	monoclinic, P21/n	
Unit cell parameters	a = 14.2534(10) Å	α = 90°
	b = 12.6279(9) Å	β = 101.4690(10)°
	c = 20.1945(14) Å	γ = 90°
Cell volume	3562.2(4) $Å^3$	
Z	4	
Calculated density	1.316 g/cm^3	
Absorption coefficient μ	0.595 mm^{-1}	
F(000)	1494	
Crystal colour and size	colorless, 0.08 × 0.05 × 0.05 mm^3	
Data collection method	Bruker SMART APEX diffractometer	
	ω rotation with narrow frames	
θ range for data collection	1.61 to 28.31°	
Index ranges	h −18 to 18, k −16 to 16, l −26 to 26	
Completeness to θ = 26.00°	99.7 %	
Reflections collected	31164	
Independent reflections	8545 (R_{int} = 0.0572)	
Reflections with $F^2>2\sigma$	6215	
Absorption correction	semi-empirical from equivalents	
Min. and max. transmission	0.9540 and 0.9709	
Structure solution	direct methods	
Refinement method	Full-matrix least-squares on F^2	
Weighting parameters a, b	0.1419, 13.4864	
Data / restraints / parameters	8545 / 3 / 338	
Final R indices [$F^2>2\sigma$]	R1 = 0.1076, wR2 = 0.2719	
R indices (all data)	R1 = 0.1401, wR2 = 0.2966	
Goodness-of-fit on F^2	1.057	
Largest and mean shift/su	0.066 and 0.002	
Largest diff. peak and hole	2.368 and −0.937 e $Å^{-3}$	

Bond lengths [Å] and angles [°].

S(1)–C(13)	1.745(6)	S(1)–C(7)	1.806(5)
S(2)–C(13)	1.639(7)	S(3)–C(18)	1.760(5)
S(3)–C(9)	1.817(5)	S(4)–C(18)	1.671(5)
S(5)–C(23)	1.781(5)	S(5)–C(11)	1.821(5)
S(6)–C(23)	1.658(5)	C(1)–C(2)	1.386(7)
C(1)–C(6)	1.405(6)	C(1)–C(7)	1.515(7)
C(2)–C(3)	1.413(7)	C(2)–C(8)	1.509(7)
C(3)–C(4)	1.408(7)	C(3)–C(9)	1.506(7)
C(4)–C(5)	1.407(7)	C(4)–C(10)	1.505(7)
C(5)–C(6)	1.384(7)	C(5)–C(11)	1.514(7)
C(6)–C(12)	1.517(7)	C(13)–N(1)	1.316(10)
C(14)–N(1)	1.491(14)	C(14)–C(15)	1.583(19)
C(16)–C(17)	1.258(18)	C(16)–N(1)	1.777(18)
C(18)–N(2)	1.334(6)	C(19)–N(2)	1.468(6)
C(19)–C(20)	1.493(10)	C(21)–N(2)	1.473(6)
C(21)–C(22)	1.490(9)	C(23)–N(3)	1.333(6)
C(24)–N(3)	1.473(7)	C(24)–C(25)	1.517(11)
C(26)–N(3)	1.468(7)	C(26)–C(27)	1.500(9)
C(40)–Cl(1)	1.785(14)	C(40)–Cl(2)	1.865(14)
C(40)–Cl(3)	1.909(16)	Cl(3)–C(40A)	1.909(16)

C(13)–S(1)–C(7)	104.2(3)	C(18)–S(3)–C(9)	104.5(2)
C(23)–S(5)–C(11)	103.3(2)	C(2)–C(1)–C(6)	120.7(4)
C(2)–C(1)–C(7)	119.0(4)	C(6)–C(1)–C(7)	120.3(4)
C(1)–C(2)–C(3)	119.5(4)	C(1)–C(2)–C(8)	120.5(5)
C(3)–C(2)–C(8)	120.0(5)	C(4)–C(3)–C(2)	119.8(4)
C(4)–C(3)–C(9)	120.0(5)	C(2)–C(3)–C(9)	120.1(4)
C(5)–C(4)–C(3)	119.4(5)	C(5)–C(4)–C(10)	120.2(5)
C(3)–C(4)–C(10)	120.4(5)	C(6)–C(5)–C(4)	120.5(4)
C(6)–C(5)–C(11)	120.1(5)	C(4)–C(5)–C(11)	119.5(5)
C(5)–C(6)–C(1)	119.9(4)	C(5)–C(6)–C(12)	120.1(4)
C(1)–C(6)–C(12)	120.0(5)	C(1)–C(7)–S(1)	106.2(3)
C(3)–C(9)–S(3)	106.0(3)	C(5)–C(11)–S(5)	106.8(3)
N(1)–C(13)–S(2)	123.0(5)	N(1)–C(13)–S(1)	113.7(5)
S(2)–C(13)–S(1)	123.3(4)	N(1)–C(14)–C(15)	113.9(13)
C(17)–C(16)–N(1)	93.2(14)	N(2)–C(18)–S(4)	124.3(4)
N(2)–C(18)–S(3)	114.1(3)	S(4)–C(18)–S(3)	121.6(3)
N(2)–C(19)–C(20)	112.7(6)	N(2)–C(21)–C(22)	112.7(5)
N(3)–C(23)–S(6)	125.2(4)	N(3)–C(23)–S(5)	113.6(4)
S(6)–C(23)–S(5)	121.2(3)	N(3)–C(24)–C(25)	111.6(5)
N(3)–C(26)–C(27)	111.5(5)	C(13)–N(1)–C(14)	121.7(8)
C(13)–N(1)–C(16)	118.6(9)	C(14)–N(1)–C(16)	115.0(9)

C(18)–N(2)–C(19)	124.4(4)	C(18)–N(2)–C(21)	121.4(4)
C(19)–N(2)–C(21)	114.2(4)	C(23)–N(3)–C(26)	120.5(4)
C(23)–N(3)–C(24)	123.9(4)	C(26)–N(3)–C(24)	115.6(4)
Cl(1)–C(40)–Cl(2)	103.8(8)	Cl(1)–C(40)–Cl(3)	116.4(9)
Cl(2)–C(40)–Cl(3)	118.7(8)	C(40)–Cl(3)–C(40A)	180.000(5)

Crystal data and structure refinement for hexasubstituted benzene with diisobutyldithiocarbamate (**4c**)

Chemical formula	$C_{66}H_{118}N_6S_{12}$	
Formula weight	1380.38	
Temperature	150(2) K	
Radiation, wavelength	MoKα, 0.71073 Å	
Crystal system, space group	monoclinic, P21/c	
Unit cell parameters	a = 30.801(11) Å	α = 90°
	b = 26.267(9) Å	β = 90.092(10)°
	c = 10.741(4) Å	γ = 90°
Cell volume	8690(5) Å^3	
Z	4	
Calculated density	1.055 g/cm^3	
Absorption coefficient μ	0.338 mm^{-1}	
F(000)	2992	
Crystal colour and size	colorless, 0.32 × 0.08 × 0.03 mm^3	
Data collection method	Bruker SMART APEX diffractometer	
	ω rotation with narrow frames	
θ range for data collection	1.02 to 28.33°	
Index ranges	h −41 to 41, k −33 to 33, l −14 to 14	
Completeness to θ = 26.00°	99.7 %	
Reflections collected	74156	
Independent reflections	20446 (R_{int} = 0.1947)	
Reflections with $F^2>2\sigma$	9329	
Absorption correction	semi-empirical from equivalents	
Min. and max. transmission	0.8997 and 0.9899	
Structure solution	direct methods	
Refinement method	Full-matrix least-squares on F^2	
Weighting parameters a, b	0.0680, 59.6535	
Data / restraints / parameters	20446 / 0 / 747	
Final R indices [$F^2>2\sigma$]	R1 = 0.1750, wR2 = 0.2877	
R indices (all data)	R1 = 0.2950, wR2 = 0.3327	
Goodness-of-fit on F^2	1.123	
Largest and mean shift/su	0.001 and 0.000	
Largest diff. peak and hole	0.676 and −0.685 e Å^{-3}	

Bond lengths [Å] and angles [°].

S(1)–C(7)	1.764(8)	S(1)–C(4)	1.823(8)
S(2)–C(7)	1.670(8)	S(3)–C(16)	1.761(9)
S(3)–C(5)	1.808(9)	S(4)–C(16)	1.655(10)
S(5)–C(25)	1.772(9)	S(5)–C(6)	1.819(7)
S(6)–C(25)	1.685(9)	S(7)–C(40)	1.791(9)
S(7)–C(38)	1.805(8)	S(8)–C(40)	1.669(9)
S(9)–C(49)	1.770(9)	S(9)–C(39)	1.815(9)
S(10)–C(49)	1.664(9)	S(11)–C(58)	1.762(9)
S(11)–C(37)	1.810(8)	S(12)–C(58)	1.658(9)
N(1)–C(7)	1.334(10)	N(1)–C(8)	1.460(12)
N(1)–C(12)	1.476(11)	N(2)–C(16)	1.378(11)
N(2)–C(17)	1.462(12)	N(2)–C(21)	1.463(12)
N(3)–C(25)	1.337(11)	N(3)–C(30)	1.463(13)
N(3)–C(26)	1.486(12)	N(4)–C(40)	1.330(11)
N(4)–C(45)	1.445(13)	N(4)–C(41)	1.480(11)
N(5)–C(49)	1.340(11)	N(5)–C(50)	1.477(12)
N(5)–C(54)	1.483(11)	N(6)–C(58)	1.360(11)
N(6)–C(59)	1.466(11)	N(6)–C(63)	1.477(13)
C(1)–C(3A)	1.394(11)	C(1)–C(2)	1.402(12)
C(1)–C(4)	1.524(11)	C(2)–C(3)	1.391(12)
C(2)–C(6)	1.517(11)	C(3)–C(1A)	1.394(11)
C(3)–C(5)	1.523(12)	C(8)–C(9)	1.521(18)
C(9)–C(10)	1.49(2)	C(9)–C(11)	1.59(2)
C(12)–C(13)	1.530(13)	C(13)–C(14)	1.512(13)
C(13)–C(15)	1.549(13)	C(17)–C(18)	1.542(14)
C(18)–C(19)	1.487(15)	C(18)–C(20)	1.514(16)
C(21)–C(22)	1.498(14)	C(22)–C(23)	1.467(16)
C(22)–C(24)	1.550(15)	C(26)–C(27)	1.533(17)
C(27)–C(29)	1.429(19)	C(27)–C(28)	1.532(17)
C(30)–C(31)	1.498(18)	C(31)–C(33)	1.12(2)
C(31)–C(32)	1.518(18)	C(34)–C(36B)	1.402(11)
C(34)–C(35)	1.407(12)	C(34)–C(37)	1.517(11)
C(35)–C(36)	1.392(11)	C(35)–C(38)	1.522(11)
C(36)–C(34B)	1.402(11)	C(36)–C(39)	1.514(11)
C(41)–C(42)	1.520(17)	C(42)–C(44)	1.422(19)
C(42)–C(43)	1.547(17)	C(45)–C(46)	1.489(17)
C(46)–C(48)	1.14(2)	C(46)–C(47)	1.519(17)
C(50)–C(51)	1.531(18)	C(51)–C(53)	1.47(2)
C(51)–C(52)	1.56(2)	C(54)–C(55)	1.529(13)
C(55)–C(57)	1.511(13)	C(55)–C(56)	1.556(13)
C(59)–C(60)	1.502(14)	C(60)–C(61)	1.486(16)
C(60)–C(62)	1.533(14)	C(63)–C(64)	1.526(14)

C(64)–C(65)	1.484(15)	C(64)–C(66)	1.485(15)
C(7)–S(1)–C(4)	103.6(4)	C(16)–S(3)–C(5)	103.3(4)
C(25)–S(5)–C(6)	102.5(4)	C(40)–S(7)–C(38)	102.5(4)
C(49)–S(9)–C(39)	103.2(4)	C(58)–S(11)–C(37)	103.4(4)
C(7)–N(1)–C(8)	121.4(8)	C(7)–N(1)–C(12)	122.4(7)
C(8)–N(1)–C(12)	116.2(7)	C(16)–N(2)–C(17)	121.6(8)
C(16)–N(2)–C(21)	118.3(8)	C(17)–N(2)–C(21)	120.1(8)
C(25)–N(3)–C(30)	123.7(8)	C(25)–N(3)–C(26)	120.5(8)
C(30)–N(3)–C(26)	115.8(8)	C(40)–N(4)–C(45)	125.0(8)
C(40)–N(4)–C(41)	120.1(8)	C(45)–N(4)–C(41)	114.8(8)
C(49)–N(5)–C(50)	120.2(8)	C(49)–N(5)–C(54)	123.0(7)
C(50)–N(5)–C(54)	116.8(8)	C(58)–N(6)–C(59)	119.2(8)
C(58)–N(6)–C(63)	122.3(8)	C(59)–N(6)–C(63)	118.5(8)
C(3A)–C(1)–C(2)	120.5(7)	C(3A)–C(1)–C(4)	119.9(7)
C(2)–C(1)–C(4)	119.5(8)	C(3)–C(2)–C(1)	119.8(8)
C(3)–C(2)–C(6)	120.8(8)	C(1)–C(2)–C(6)	119.4(8)
C(2)–C(3)–C(1A)	119.5(8)	C(2)–C(3)–C(5)	118.8(8)
C(1A)–C(3)–C(5)	121.6(8)	C(1)–C(4)–S(1)	105.9(5)
C(3)–C(5)–S(3)	105.2(6)	C(2)–C(6)–S(5)	108.4(5)
N(1)–C(7)–S(2)	124.6(6)	N(1)–C(7)–S(1)	113.8(6)
S(2)–C(7)–S(1)	121.6(5)	N(1)–C(8)–C(9)	112.8(10)
C(10)–C(9)–C(8)	113.2(11)	C(10)–C(9)–C(11)	109.2(13)
C(8)–C(9)–C(11)	108.3(15)	N(1)–C(12)–C(13)	114.2(8)
C(14)–C(13)–C(12)	112.8(8)	C(14)–C(13)–C(15)	109.4(8)
C(12)–C(13)–C(15)	108.3(8)	N(2)–C(16)–S(4)	125.0(7)
N(2)–C(16)–S(3)	112.0(7)	S(4)–C(16)–S(3)	122.9(5)
N(2)–C(17)–C(18)	113.4(8)	C(19)–C(18)–C(20)	111.5(10)
C(19)–C(18)–C(17)	111.9(10)	C(20)–C(18)–C(17)	109.1(10)
N(2)–C(21)–C(22)	112.8(9)	C(23)–C(22)–C(21)	114.7(11)
C(23)–C(22)–C(24)	109.4(11)	C(21)–C(22)–C(24)	109.5(9)
N(3)–C(25)–S(6)	125.1(7)	N(3)–C(25)–S(5)	113.9(7)
S(6)–C(25)–S(5)	121.0(5)	N(3)–C(26)–C(27)	112.3(8)
C(29)–C(27)–C(28)	109.6(14)	C(29)–C(27)–C(26)	112.6(12)
C(28)–C(27)–C(26)	107.0(12)	N(3)–C(30)–C(31)	114.6(9)
C(33)–C(31)–C(30)	128.4(17)	C(33)–C(31)–C(32)	121.4(18)
C(30)–C(31)–C(32)	109.2(11)	C(36B)–C(34)–C(35)	120.0(7)
C(36B)–C(34)–C(37)	120.9(8)	C(35)–C(34)–C(37)	119.1(8)
C(36)–C(35)–C(34)	120.6(7)	C(36)–C(35)–C(38)	119.5(7)
C(34)–C(35)–C(38)	119.8(7)	C(35)–C(36)–C(34B)	119.4(7)
C(35)–C(36)–C(39)	120.0(7)	C(34B)–C(36)–C(39)	120.7(7)
C(34)–C(37)–S(11)	104.7(6)	C(35)–C(38)–S(7)	108.9(5)
C(36)–C(39)–S(9)	105.1(6)	N(4)–C(40)–S(8)	126.1(7)
N(4)–C(40)–S(7)	113.4(6)	S(8)–C(40)–S(7)	120.4(5)

N(4)–C(41)–C(42)	112.3(9)	C(44)–C(42)–C(41)	112.4(13)
C(44)–C(42)–C(43)	109.3(14)	C(41)–C(42)–C(43)	107.1(11)
N(4)–C(45)–C(46)	116.7(9)	C(48)–C(46)–C(45)	127.4(16)
C(48)–C(46)–C(47)	121.1(17)	C(45)–C(46)–C(47)	110.6(11)
N(5)–C(49)–S(10)	125.1(7)	N(5)–C(49)–S(9)	113.1(6)
S(10)–C(49)–S(9)	121.7(5)	N(5)–C(50)–C(51)	111.6(10)
C(53)–C(51)–C(50)	113.9(12)	C(53)–C(51)–C(52)	109.4(13)
C(50)–C(51)–C(52)	105.1(14)	N(5)–C(54)–C(55)	114.7(8)
C(57)–C(55)–C(54)	111.4(8)	C(57)–C(55)–C(56)	109.3(8)
C(54)–C(55)–C(56)	108.2(8)	N(6)–C(58)–S(12)	125.1(7)
N(6)–C(58)–S(11)	112.4(6)	S(12)–C(58)–S(11)	122.5(5)
N(6)–C(59)–C(60)	113.0(8)	C(61)–C(60)–C(59)	113.1(10)
C(61)–C(60)–C(62)	109.4(10)	C(59)–C(60)–C(62)	110.3(9)
N(6)–C(63)–C(64)	115.0(8)	C(65)–C(64)–C(66)	111.3(10)
C(65)–C(64)–C(63)	110.0(9)	C(66)–C(64)–C(63)	109.7(10)

Chapter 6

Crystal data and structure refinement for $[((dppm)_2RuS_2C)_2C_4H_8][BF_4]_2$ (**11a**)

Chemical formula	$C_{109}H_{99}B_2Cl_9F_8N_2P_8Ru_2S_4$	
Formula weight	2507.71	
Temperature	150(2) K	
Radiation, wavelength	MoKα, 0.71073 Å	
Crystal system, space group	monoclinic, P21/c	
Unit cell parameters	a = 22.2606(14) Å	α = 90°
	b = 22.2816(14) Å	β = 80.1650(10)°
	c = 22.5341(14) Å	γ = 90°
Cell volume	11012.7(12) Å3	
Z	4	
Calculated density	1.512 g/cm^3	
Absorption coefficient μ	0.747 mm^{-1}	
F(000)	5096	
Crystal colour and size	pale yellow, 0.06 x 0.05 x 0.02 mm^3	
Data collection method	Bruker SMART APEX diffractometer	
	ω rotation with narrow frames	
θ range for data collection	1.29 to 28.60°	
Index ranges	h -29 to 29, k -29 to 28, l -29 to 28	
Completeness to θ = 26.00°	99.9 %	
Reflections collected	96717	
Independent reflections	26374 (R_{int} = 0.1914)	
Reflections with F2>2σ	10556	
Absorption correction	semi-empirical from equivalents	
Min. and max. transmission	0.9565 and 0.9852	
Structure solution	direct methods	
Refinement method	Full-matrix least-squares on F2	
Weighting parameters a, b	0.0709, 3.7897	
Data / restraints / parameters	26374 / 0 / 1297	
Final R indices [F2>2σ]	R1 = 0.1020, wR2 = 0.1675	
R indices (all data)	R1 = 0.2444, wR2 = 0.2180	
Goodness-of-fit on F2	1.003	
Largest and mean shift/su	0.020 and 0.000	
Largest diff. peak and hole	1.276 and -0.893 e Å^{-3}	

Bond lengths [Å] and angles [°].

Ru(1)-P(2)	2.304(2)	Ru(1)-P(3)	2.317(2)
Ru(1)-P(1)	2.322(2)	Ru(1)-P(4)	2.332(2)
Ru(1)-S(2)	2.432(2)	Ru(1)-S(1)	2.452(2)
Ru(2)-P(5)	2.307(2)	Ru(2)-P(6)	2.319(2)
Ru(2)-P(8)	2.340(2)	Ru(2)-P(7)	2.349(2)
Ru(2)-S(3)	2.426(2)	Ru(2)-S(4)	2.449(2)
S(1)-C(1)	1.701(8)	S(2)-C(1)	1.730(8)
S(3)-C(6)	1.720(8)	S(4)-C(6)	1.714(8)
P(1)-C(17)	1.821(8)	P(1)-C(11)	1.827(8)
P(1)-C(7)	1.829(8)	P(2)-C(23)	1.825(8)
P(2)-C(7)	1.839(8)	P(2)-C(29)	1.859(9)
P(3)-C(41)	1.810(9)	P(3)-C(35)	1.825(8)
P(3)-C(8)	1.855(8)	P(4)-C(47)	1.812(9)
P(4)-C(8)	1.843(8)	P(4)-C(53)	1.845(8)
P(5)-C(59)	1.807(10)	P(5)-C(9)	1.819(9)
P(5)-C(65)	1.841(9)	P(6)-C(77)	1.810(10)
P(6)-C(9)	1.823(9)	P(6)-C(71)	1.825(8)
P(7)-C(89)	1.824(9)	P(7)-C(10)	1.827(8)
P(7)-C(83)	1.828(8)	P(8)-C(101)	1.803(8)
P(8)-C(10)	1.816(8)	P(8)-C(95)	1.830(8)
N(1)-C(1)	1.340(9)	N(1)-C(4)	1.460(9)
N(1)-C(2)	1.483(9)	N(2)-C(6)	1.347(9)
N(2)-C(3)	1.459(9)	N(2)-C(5)	1.467(9)
C(2)-C(3)	1.493(11)	C(4)-C(5)	1.503(11)
C(11)-C(12)	1.389(11)	C(11)-C(16)	1.406(11)
C(12)-C(13)	1.397(12)	C(13)-C(14)	1.370(13)
C(14)-C(15)	1.366(14)	C(15)-C(16)	1.402(12)
C(17)-C(18)	1.372(11)	C(17)-C(22)	1.402(11)
C(18)-C(19)	1.375(11)	C(19)-C(20)	1.371(12)
C(20)-C(21)	1.377(12)	C(21)-C(22)	1.371(11)
C(23)-C(24)	1.380(11)	C(23)-C(28)	1.388(11)
C(24)-C(25)	1.401(11)	C(25)-C(26)	1.377(12)
C(26)-C(27)	1.323(12)	C(27)-C(28)	1.373(11)
C(29)-C(34)	1.360(11)	C(29)-C(30)	1.370(11)
C(30)-C(31)	1.407(12)	C(31)-C(32)	1.373(12)
C(32)-C(33)	1.367(12)	C(33)-C(34)	1.399(11)
C(35)-C(36)	1.370(11)	C(35)-C(40)	1.416(12)
C(36)-C(37)	1.404(11)	C(37)-C(38)	1.370(13)
C(38)-C(39)	1.369(13)	C(39)-C(40)	1.401(12)
C(41)-C(42)	1.374(11)	C(41)-C(46)	1.384(11)
C(42)-C(43)	1.392(12)	C(43)-C(44)	1.382(14)
C(44)-C(45)	1.355(14)	C(45)-C(46)	1.387(13)

C(47)-C(48)	1.389(11)	C(47)-C(52)	1.404(12)
C(48)-C(49)	1.371(12)	C(49)-C(50)	1.379(13)
C(50)-C(51)	1.367(14)	C(51)-C(52)	1.400(13)
C(53)-C(54)	1.363(11)	C(53)-C(58)	1.385(11)
C(54)-C(55)	1.400(11)	C(55)-C(56)	1.361(12)
C(56)-C(57)	1.354(12)	C(57)-C(58)	1.394(12)
C(59)-C(64)	1.386(13)	C(59)-C(60)	1.394(13)
C(60)-C(61)	1.391(17)	C(61)-C(62)	1.35(2)
C(62)-C(63)	1.368(19)	C(63)-C(64)	1.411(13)
C(65)-C(66)	1.377(12)	C(65)-C(70)	1.400(12)
C(66)-C(67)	1.406(13)	C(67)-C(68)	1.396(15)
C(68)-C(69)	1.364(15)	C(69)-C(70)	1.391(12)
C(71)-C(72)	1.371(11)	C(71)-C(76)	1.377(11)
C(72)-C(73)	1.379(11)	C(73)-C(74)	1.352(12)
C(74)-C(75)	1.348(12)	C(75)-C(76)	1.401(11)
C(77)-C(82)	1.343(14)	C(77)-C(78)	1.354(13)
C(78)-C(79)	1.406(14)	C(79)-C(80)	1.407(15)
C(80)-C(81)	1.302(18)	C(81)-C(82)	1.378(18)
C(83)-C(84)	1.393(11)	C(83)-C(88)	1.403(12)
C(84)-C(85)	1.375(12)	C(85)-C(86)	1.372(13)
C(86)-C(87)	1.401(13)	C(87)-C(88)	1.387(12)
C(89)-C(94)	1.386(11)	C(89)-C(90)	1.398(11)
C(90)-C(91)	1.396(12)	C(91)-C(92)	1.373(12)
C(92)-C(93)	1.396(12)	C(93)-C(94)	1.361(11)
C(95)-C(100)	1.375(11)	C(95)-C(96)	1.380(11)
C(96)-C(97)	1.407(12)	C(97)-C(98)	1.359(12)
C(98)-C(99)	1.363(12)	C(99)-C(100)	1.404(11)
C(101)-C(106)	1.355(11)	C(101)-C(102)	1.404(11)
C(102)-C(103)	1.386(11)	C(103)-C(104)	1.346(12)
C(104)-C(105)	1.385(12)	C(105)-C(106)	1.383(11)
C(108)-Cl(3)	1.726(11)	C(108)-Cl(2)	1.743(11)
C(108)-Cl(1)	1.762(12)	C(109)-Cl(6)	1.718(11)
C(109)-Cl(4)	1.740(12)	C(109)-Cl(5)	1.745(10)
C(110)-Cl(9)	1.722(12)	C(110)-Cl(8)	1.722(12)
C(110)-Cl(7)	1.778(13)	B(1)-F(1)	1.175(18)
B(1)-F(4)	1.25(2)	B(1)-F(2)	1.29(2)
B(1)-F(3)	1.368(16)	B(2)-F(8)	1.301(15)
B(2)-F(7)	1.306(14)	B(2)-F(5)	1.344(16)
B(2)-F(6)	1.347(15)		

P(2)-Ru(1)-P(3)	102.68(8)	P(2)-Ru(1)-P(1)	72.80(8)
P(3)-Ru(1)-P(1)	172.98(8)	P(2)-Ru(1)-P(4)	99.19(8)
P(3)-Ru(1)-P(4)	73.34(8)	P(1)-Ru(1)-P(4)	101.79(8)
P(2)-Ru(1)-S(2)	159.97(8)	P(3)-Ru(1)-S(2)	92.51(7)

P(1)-Ru(1)-S(2)	93.16(8)	P(4)-Ru(1)-S(2)	97.62(8)
P(2)-Ru(1)-S(1)	94.61(8)	P(3)-Ru(1)-S(1)	92.76(7)
P(1)-Ru(1)-S(1)	92.96(7)	P(4)-Ru(1)-S(1)	162.20(8)
S(2)-Ru(1)-S(1)	71.40(7)	P(5)-Ru(2)-P(6)	71.98(9)
P(5)-Ru(2)-P(8)	102.72(8)	P(6)-Ru(2)-P(8)	100.86(8)
P(5)-Ru(2)-P(7)	173.72(9)	P(6)-Ru(2)-P(7)	106.16(8)
P(8)-Ru(2)-P(7)	71.55(8)	P(5)-Ru(2)-S(3)	88.93(8)
P(6)-Ru(2)-S(3)	155.54(8)	P(8)-Ru(2)-S(3)	98.12(8)
P(7)-Ru(2)-S(3)	94.37(8)	P(5)-Ru(2)-S(4)	90.11(8)
P(6)-Ru(2)-S(4)	92.41(8)	P(8)-Ru(2)-S(4)	163.82(8)
P(7)-Ru(2)-S(4)	95.99(8)	S(3)-Ru(2)-S(4)	71.97(7)
C(1)-S(1)-Ru(1)	88.1(3)	C(1)-S(2)-Ru(1)	88.1(3)
C(6)-S(3)-Ru(2)	87.5(3)	C(6)-S(4)-Ru(2)	86.9(3)
C(17)-P(1)-C(11)	104.1(4)	C(17)-P(1)-C(7)	108.0(4)
C(11)-P(1)-C(7)	108.7(4)	C(17)-P(1)-Ru(1)	118.3(3)
C(11)-P(1)-Ru(1)	121.6(3)	C(7)-P(1)-Ru(1)	94.9(2)
C(23)-P(2)-C(7)	103.6(4)	C(23)-P(2)-C(29)	102.4(4)
C(7)-P(2)-C(29)	107.9(4)	C(23)-P(2)-Ru(1)	128.6(3)
C(7)-P(2)-Ru(1)	95.3(2)	C(29)-P(2)-Ru(1)	116.6(3)
C(41)-P(3)-C(35)	101.2(4)	C(41)-P(3)-C(8)	108.5(4)
C(35)-P(3)-C(8)	109.4(4)	C(41)-P(3)-Ru(1)	123.4(3)
C(35)-P(3)-Ru(1)	118.8(3)	C(8)-P(3)-Ru(1)	94.7(2)
C(47)-P(4)-C(8)	106.1(4)	C(47)-P(4)-C(53)	102.1(4)
C(8)-P(4)-C(53)	105.7(4)	C(47)-P(4)-Ru(1)	119.2(3)
C(8)-P(4)-Ru(1)	94.6(3)	C(53)-P(4)-Ru(1)	126.5(3)
C(59)-P(5)-C(9)	106.9(5)	C(59)-P(5)-C(65)	103.1(4)
C(9)-P(5)-C(65)	108.4(5)	C(59)-P(5)-Ru(2)	121.9(3)
C(9)-P(5)-Ru(2)	96.0(3)	C(65)-P(5)-Ru(2)	119.3(3)
C(77)-P(6)-C(9)	105.1(5)	C(77)-P(6)-C(71)	98.6(4)
C(9)-P(6)-C(71)	105.5(4)	C(77)-P(6)-Ru(2)	120.9(3)
C(9)-P(6)-Ru(2)	95.5(3)	C(71)-P(6)-Ru(2)	128.3(3)
C(89)-P(7)-C(10)	108.5(4)	C(89)-P(7)-C(83)	100.1(4)
C(10)-P(7)-C(83)	108.0(4)	C(89)-P(7)-Ru(2)	119.2(3)
C(10)-P(7)-Ru(2)	94.8(2)	C(83)-P(7)-Ru(2)	125.1(3)
C(101)-P(8)-C(10)	104.7(4)	C(101)-P(8)-C(95)	101.0(4)
C(10)-P(8)-C(95)	104.9(4)	C(101)-P(8)-Ru(2)	127.6(3)
C(10)-P(8)-Ru(2)	95.4(3)	C(95)-P(8)-Ru(2)	119.9(3)
C(1)-N(1)-C(4)	122.3(7)	C(1)-N(1)-C(2)	123.8(7)
C(4)-N(1)-C(2)	113.9(6)	C(6)-N(2)-C(3)	123.6(7)
C(6)-N(2)-C(5)	122.9(7)	C(3)-N(2)-C(5)	112.8(6)
N(1)-C(1)-S(1)	123.9(6)	N(1)-C(1)-S(2)	123.8(6)
S(1)-C(1)-S(2)	112.3(5)	N(1)-C(2)-C(3)	110.5(7)
N(2)-C(3)-C(2)	110.0(7)	N(1)-C(4)-C(5)	110.2(7)
N(2)-C(5)-C(4)	108.2(6)	N(2)-C(6)-S(4)	122.3(6)

N(2)-C(6)-S(3)	124.6(6)	S(4)-C(6)-S(3)	113.1(4)
P(1)-C(7)-P(2)	96.9(4)	P(4)-C(8)-P(3)	97.3(4)
P(5)-C(9)-P(6)	96.5(4)	P(8)-C(10)-P(7)	97.6(4)
C(12)-C(11)-C(16)	117.5(8)	C(12)-C(11)-P(1)	119.3(7)
C(16)-C(11)-P(1)	123.3(7)	C(11)-C(12)-C(13)	120.4(9)
C(14)-C(13)-C(12)	120.7(10)	C(15)-C(14)-C(13)	120.5(10)
C(14)-C(15)-C(16)	119.2(10)	C(15)-C(16)-C(11)	121.5(9)
C(18)-C(17)-C(22)	118.4(8)	C(18)-C(17)-P(1)	124.8(7)
C(22)-C(17)-P(1)	116.8(7)	C(17)-C(18)-C(19)	120.7(9)
C(20)-C(19)-C(18)	121.3(9)	C(19)-C(20)-C(21)	118.2(9)
C(22)-C(21)-C(20)	121.5(10)	C(21)-C(22)-C(17)	119.8(9)
C(24)-C(23)-C(28)	118.5(8)	C(24)-C(23)-P(2)	120.0(6)
C(28)-C(23)-P(2)	121.3(7)	C(23)-C(24)-C(25)	119.2(8)
C(26)-C(25)-C(24)	120.0(9)	C(27)-C(26)-C(25)	120.6(9)
C(26)-C(27)-C(28)	120.7(9)	C(27)-C(28)-C(23)	121.0(9)
C(34)-C(29)-C(30)	117.7(8)	C(34)-C(29)-P(2)	121.2(7)
C(30)-C(29)-P(2)	120.8(7)	C(29)-C(30)-C(31)	121.3(9)
C(32)-C(31)-C(30)	120.5(9)	C(33)-C(32)-C(31)	118.1(9)
C(32)-C(33)-C(34)	120.9(9)	C(29)-C(34)-C(33)	121.6(9)
C(36)-C(35)-C(40)	118.4(8)	C(36)-C(35)-P(3)	118.9(7)
C(40)-C(35)-P(3)	122.6(7)	C(35)-C(36)-C(37)	121.8(10)
C(38)-C(37)-C(36)	119.4(10)	C(39)-C(38)-C(37)	120.1(10)
C(38)-C(39)-C(40)	121.4(10)	C(39)-C(40)-C(35)	118.9(10)
C(42)-C(41)-C(46)	118.0(9)	C(42)-C(41)-P(3)	119.6(7)
C(46)-C(41)-P(3)	122.3(8)	C(41)-C(42)-C(43)	122.7(9)
C(44)-C(43)-C(42)	117.4(11)	C(45)-C(44)-C(43)	121.1(10)
C(44)-C(45)-C(46)	120.7(10)	C(41)-C(46)-C(45)	120.0(10)
C(48)-C(47)-C(52)	116.1(9)	C(48)-C(47)-P(4)	120.8(7)
C(52)-C(47)-P(4)	123.1(7)	C(49)-C(48)-C(47)	121.9(10)
C(48)-C(49)-C(50)	120.6(10)	C(51)-C(50)-C(49)	120.5(10)
C(50)-C(51)-C(52)	118.3(10)	C(51)-C(52)-C(47)	122.6(10)
C(54)-C(53)-C(58)	118.4(8)	C(54)-C(53)-P(4)	120.3(7)
C(58)-C(53)-P(4)	121.3(7)	C(53)-C(54)-C(55)	120.6(8)
C(56)-C(55)-C(54)	120.3(9)	C(57)-C(56)-C(55)	119.8(9)
C(56)-C(57)-C(58)	120.3(9)	C(53)-C(58)-C(57)	120.5(9)
C(64)-C(59)-C(60)	117.8(10)	C(64)-C(59)-P(5)	120.1(8)
C(60)-C(59)-P(5)	122.1(10)	C(61)-C(60)-C(59)	119.8(13)
C(62)-C(61)-C(60)	120.4(14)	C(61)-C(62)-C(63)	123.1(16)
C(62)-C(63)-C(64)	116.2(14)	C(59)-C(64)-C(63)	122.7(11)
C(66)-C(65)-C(70)	118.5(9)	C(66)-C(65)-P(5)	124.6(8)
C(70)-C(65)-P(5)	116.8(7)	C(65)-C(66)-C(67)	120.7(11)
C(68)-C(67)-C(66)	119.8(11)	C(69)-C(68)-C(67)	119.6(10)
C(68)-C(69)-C(70)	120.6(12)	C(69)-C(70)-C(65)	120.8(10)
C(72)-C(71)-C(76)	116.8(8)	C(72)-C(71)-P(6)	120.3(7)

C(76)-C(71)-P(6)	122.8(7)	C(71)-C(72)-C(73)	122.6(9)
C(74)-C(73)-C(72)	118.6(9)	C(75)-C(74)-C(73)	121.9(9)
C(74)-C(75)-C(76)	118.7(9)	C(71)-C(76)-C(75)	121.3(9)
C(82)-C(77)-C(78)	115.8(11)	C(82)-C(77)-P(6)	124.8(10)
C(78)-C(77)-P(6)	118.9(8)	C(77)-C(78)-C(79)	122.0(11)
C(78)-C(79)-C(80)	118.4(12)	C(81)-C(80)-C(79)	119.2(14)
C(80)-C(81)-C(82)	120.2(14)	C(77)-C(82)-C(81)	124.4(14)
C(84)-C(83)-C(88)	120.0(8)	C(84)-C(83)-P(7)	123.0(7)
C(88)-C(83)-P(7)	117.0(6)	C(85)-C(84)-C(83)	118.8(10)
C(86)-C(85)-C(84)	122.3(10)	C(85)-C(86)-C(87)	119.2(10)
C(88)-C(87)-C(86)	119.6(10)	C(87)-C(88)-C(83)	119.9(9)
C(94)-C(89)-C(90)	118.2(8)	C(94)-C(89)-P(7)	120.0(7)
C(90)-C(89)-P(7)	121.6(7)	C(91)-C(90)-C(89)	119.7(9)
C(92)-C(91)-C(90)	120.7(9)	C(91)-C(92)-C(93)	119.5(9)
C(94)-C(93)-C(92)	119.6(9)	C(93)-C(94)-C(89)	122.2(9)
C(100)-C(95)-C(96)	118.4(8)	C(100)-C(95)-P(8)	119.8(7)
C(96)-C(95)-P(8)	121.7(6)	C(95)-C(96)-C(97)	120.3(9)
C(98)-C(97)-C(96)	120.7(9)	C(97)-C(98)-C(99)	119.3(9)
C(98)-C(99)-C(100)	120.6(9)	C(95)-C(100)-C(99)	120.5(9)
C(106)-C(101)-C(102)	117.3(8)	C(106)-C(101)-P(8)	121.3(7)
C(102)-C(101)-P(8)	121.4(7)	C(103)-C(102)-C(101)	121.2(8)
C(104)-C(103)-C(102)	120.1(9)	C(103)-C(104)-C(105)	119.6(9)
C(106)-C(105)-C(104)	120.1(9)	C(101)-C(106)-C(105)	121.6(8)
Cl(3)-C(108)-Cl(2)	108.2(6)	Cl(3)-C(108)-Cl(1)	111.2(6)
Cl(2)-C(108)-Cl(1)	111.3(6)	Cl(6)-C(109)-Cl(4)	109.8(6)
Cl(6)-C(109)-Cl(5)	110.0(6)	Cl(4)-C(109)-Cl(5)	111.4(7)
Cl(9)-C(110)-Cl(8)	112.2(7)	Cl(9)-C(110)-Cl(7)	111.6(7)
Cl(8)-C(110)-Cl(7)	109.0(7)	F(1)-B(1)-F(4)	109(2)
F(1)-B(1)-F(2)	114.6(19)	F(4)-B(1)-F(2)	95.7(16)
F(1)-B(1)-F(3)	114.6(14)	F(4)-B(1)-F(3)	106.8(17)
F(2)-B(1)-F(3)	113.8(18)	F(8)-B(2)-F(7)	109.8(13)
F(8)-B(2)-F(5)	105.5(12)	F(7)-B(2)-F(5)	112.6(14)
F(8)-B(2)-F(6)	108.2(14)	F(7)-B(2)-F(6)	111.0(13)
F(5)-B(2)-F(6)	109.5(12)		

Chapter 7

Crystal data and structure refinement for $[(dppm)_2RuS_2C{=}O]$ (**1**.$2CH_3OH$)

Chemical formula	$C_{53}H_{44}O_3P_4RuS_2$	
Formula weight	1017.95	
Temperature	150(2) K	
Radiation, wavelength	MoKα, 0.71073 Å	
Crystal system, space group	monoclinic, C2/c	
Unit cell parameters	a = 16.834(4) Å	α = 90°
	b = 15.592(4) Å	β = 95.004(4)°
	c = 17.693(4) Å	γ = 90°
Cell volume	4626(2) $Å^3$	
Z	4	
Calculated density	1.462 g/cm^3	
Absorption coefficient μ	0.612 mm^{-1}	
F(000)	2088	
Crystal colour and size	yellow, 0.15 × 0.08 × 0.08 mm^3	
Data collection method	Bruker SMART APEX diffractometer	
	ω rotation with narrow frames	
θ range for data collection	1.78 to 28.37°	
Index ranges	h −21 to 21, k −20 to 20, l −23 to 23	
Completeness to θ = 26.00°	99.8 %	
Reflections collected	19290	
Independent reflections	5530 (R_{int} = 0.0813)	
Reflections with $F^2>2\sigma$	4676	
Absorption correction	semi-empirical from equivalents	
Min. and max. transmission	0.9138 and 0.9527	
Structure solution	Patterson synthesis	
Refinement method	Full-matrix least-squares on F^2	
Weighting parameters a, b	0.1373, 0.0000	
Data / restraints / parameters	5530 / 0 / 286	
Final R indices [$F^2>2\sigma$]	R1 = 0.0713, wR2 = 0.1842	
R indices (all data)	R1 = 0.0796, wR2 = 0.1924	
Goodness-of-fit on F^2	1.016	
Largest and mean shift/su	0.005 and 0.000	
Largest diff. peak and hole	2.192 and −2.899 e $Å^{-3}$	

Bond lengths [Å] and angles [°].

Ru(1)–P(2)	2.3152(10)	Ru(1)–P(2A)	2.3152(10)
Ru(1)–P(1A)	2.3319(10)	Ru(1)–P(1)	2.3319(10)
Ru(1)–S(1)	2.4198(10)	Ru(1)–S(1A)	2.4198(10)
S(1)–C(1)	1.764(3)	P(1)–C(3)	1.818(4)
P(1)–C(9)	1.824(4)	P(1)–C(2)	1.842(4)
P(2)–C(15)	1.826(4)	P(2)–C(21)	1.835(4)
P(2)–C(2A)	1.850(4)	O(1)–C(1)	1.215(7)
C(1)–S(1A)	1.764(3)	C(2)–P(2A)	1.850(4)
C(3)–C(4)	1.383(5)	C(3)–C(8)	1.397(5)
C(4)–C(5)	1.393(6)	C(5)–C(6)	1.368(6)
C(6)–C(7)	1.381(6)	C(7)–C(8)	1.381(6)
C(9)–C(14)	1.384(5)	C(9)–C(10)	1.389(5)
C(10)–C(11)	1.383(5)	C(11)–C(12)	1.390(6)
C(12)–C(13)	1.371(6)	C(13)–C(14)	1.388(5)
C(15)–C(20)	1.384(5)	C(15)–C(16)	1.396(5)
C(16)–C(17)	1.378(5)	C(17)–C(18)	1.377(6)
C(18)–C(19)	1.383(6)	C(19)–C(20)	1.380(6)
C(21)–C(22)	1.388(5)	C(21)–C(26)	1.392(5)
C(22)–C(23)	1.381(6)	C(23)–C(24)	1.374(6)
C(24)–C(25)	1.376(7)	C(25)–C(26)	1.395(6)
O(2)–C(27)	1.27(3)	O(2)–C(27B)	1.92(3)
C(27)–C(27B)	1.58(3)	C(27)–O(2B)	1.92(3)

P(2)–Ru(1)–P(2A)	97.40(5)	P(2)–Ru(1)–P(1A)	71.90(3)
P(2A)–Ru(1)–P(1A)	102.16(3)	P(2)–Ru(1)–P(1)	102.16(3)
P(2A)–Ru(1)–P(1)	71.90(3)	P(1A)–Ru(1)–P(1)	171.30(5)
P(2)–Ru(1)–S(1)	161.63(3)	P(2A)–Ru(1)–S(1)	96.67(4)
P(1A)–Ru(1)–S(1)	93.61(3)	P(1)–Ru(1)–S(1)	93.41(3)
P(2)–Ru(1)–S(1A)	96.67(4)	P(2A)–Ru(1)–S(1A)	161.63(3)
P(1A)–Ru(1)–S(1A)	93.41(3)	P(1)–Ru(1)–S(1A)	93.61(3)
S(1)–Ru(1)–S(1A)	72.39(5)	C(1)–S(1)–Ru(1)	89.69(15)
C(3)–P(1)–C(9)	100.00(16)	C(3)–P(1)–C(2)	108.13(17)
C(9)–P(1)–C(2)	105.30(17)	C(3)–P(1)–Ru(1)	122.60(11)
C(9)–P(1)–Ru(1)	123.37(12)	C(2)–P(1)–Ru(1)	95.54(11)
C(15)–P(2)–C(21)	102.99(17)	C(15)–P(2)–C(2A)	105.85(16)
C(21)–P(2)–C(2A)	103.78(17)	C(15)–P(2)–Ru(1)	125.32(12)
C(21)–P(2)–Ru(1)	119.75(12)	C(2A)–P(2)–Ru(1)	95.89(11)
O(1)–C(1)–S(1)	125.89(15)	O(1)–C(1)–S(1A)	125.89(15)
S(1)–C(1)–S(1A)	108.2(3)	P(1)–C(2)–P(2A)	95.28(17)
C(4)–C(3)–C(8)	119.1(3)	C(4)–C(3)–P(1)	124.3(3)
C(8)–C(3)–P(1)	116.5(3)	C(3)–C(4)–C(5)	120.1(4)
C(6)–C(5)–C(4)	120.2(4)	C(5)–C(6)–C(7)	120.5(4)

C(6)–C(7)–C(8)	119.8(4)	C(7)–C(8)–C(3)	120.4(4)
C(14)–C(9)–C(10)	119.4(3)	C(14)–C(9)–P(1)	119.2(3)
C(10)–C(9)–P(1)	121.4(3)	C(11)–C(10)–C(9)	120.4(4)
C(10)–C(11)–C(12)	119.8(4)	C(13)–C(12)–C(11)	119.9(4)
C(12)–C(13)–C(14)	120.5(4)	C(9)–C(14)–C(13)	120.0(4)
C(20)–C(15)–C(16)	118.6(3)	C(20)–C(15)–P(2)	122.4(3)
C(16)–C(15)–P(2)	119.0(3)	C(17)–C(16)–C(15)	120.7(4)
C(18)–C(17)–C(16)	120.3(4)	C(17)–C(18)–C(19)	119.2(4)
C(20)–C(19)–C(18)	120.8(4)	C(19)–C(20)–C(15)	120.3(4)
C(22)–C(21)–C(26)	118.9(4)	C(22)–C(21)–P(2)	123.0(3)
C(26)–C(21)–P(2)	118.0(3)	C(23)–C(22)–C(21)	120.6(4)
C(24)–C(23)–C(22)	120.5(4)	C(23)–C(24)–C(25)	119.6(4)
C(24)–C(25)–C(26)	120.5(4)	C(21)–C(26)–C(25)	119.8(4)
C(27)–O(2)–C(27B)	54.9(10)	O(2)–C(27)–C(27B)	84(2)
O(2)–C(27)–O(2B)	125.1(10)	C(27B)–C(27)–O(2B)	41.4(18)

Crystal data and structure refinement for $[(dppm)_2RuS_2C{=}O]$ (**1**.$3CHCl_3$)

Chemical formula	$C_{54}H_{47}Cl_9OP_4RuS_2$	
Formula weight	1320.04	
Temperature	150(2) K	
Radiation, wavelength	MoKα, 0.71073 Å	
Crystal system, space group	monoclinic, $P2_1$	
Unit cell parameters	a = 14.8972(17) Å	α = 90°
	b = 18.274(2) Å	β = 91.065(2)°
	c = 21.145(2) Å	γ = 90°
Cell volume	5755.4(11) $Å^3$	
Z	4	
Calculated density	1.523 g/cm^3	
Absorption coefficient μ	0.912 mm^{-1}	
F(000)	2672	
Crystal colour and size	yellow, 0.28 × 0.28 × 0.20 mm^3	
Data collection method	Bruker SMART APEX diffractometer	
	ω rotation with narrow frames	
θ range for data collection	1.47 to 28.28°	
Index ranges	h −19 to 19, k −24 to 24, l −28 to 27	
Completeness to θ = 26.00°	99.6 %	
Reflections collected	50105	
Independent reflections	26107 (R_{int} = 0.0188)	
Reflections with $F^2>2\sigma$	24659	
Absorption correction	semi-empirical from equivalents	
Min. and max. transmission	0.7842 and 0.8386	
Structure solution	Patterson synthesis	
Refinement method	Full-matrix least-squares on F^2	
Weighting parameters a, b	0.0569, 4.8323	
Data / restraints / parameters	26107 / 1 / 1279	
Final R indices [$F^2>2\sigma$]	R1 = 0.0369, wR2 = 0.0981	
R indices (all data)	R1 = 0.0393, wR2 = 0.1002	
Goodness-of-fit on F^2	1.032	
Absolute structure parameter	0.186(18)	
Largest and mean shift/su	0.011 and 0.000	
Largest diff. peak and hole	1.618 and −0.761 e $Å^{-3}$	

Bond lengths [Å] and angles [°]

Ru(1)–P(2)	2.3140(9)	Ru(1)–P(3)	2.3286(8)
Ru(1)–P(1)	2.3308(10)	Ru(1)–P(4)	2.3477(9)
Ru(1)–S(1)	2.4011(8)	Ru(1)–S(2)	2.4364(10)
Ru(2)–P(8)	2.3138(9)	Ru(2)–P(6)	2.3280(9)
Ru(2)–P(5)	2.3323(9)	Ru(2)–P(7)	2.3429(10)
Ru(2)–S(4)	2.4157(9)	Ru(2)–S(3)	2.4353(9)
S(1)–C(3)	1.749(4)	S(2)–C(3)	1.764(4)
S(3)–C(6)	1.765(4)	S(4)–C(6)	1.743(4)
P(1)–C(20)	1.829(4)	P(1)–C(10)	1.832(4)
P(1)–C(1)	1.850(4)	P(2)–C(30)	1.814(4)
P(2)–C(40)	1.823(3)	P(2)–C(1)	1.839(4)
P(3)–C(60)	1.826(4)	P(3)–C(50)	1.831(4)
P(3)–C(2)	1.862(4)	P(4)–C(70)	1.820(4)
P(4)–C(80)	1.824(4)	P(4)–C(2)	1.845(3)
P(5)–C(90)	1.828(3)	P(5)–C(100)	1.842(4)
P(5)–C(4)	1.850(3)	P(6)–C(120)	1.818(4)
P(6)–C(110)	1.824(4)	P(6)–C(4)	1.836(3)
P(7)–C(140)	1.810(4)	P(7)–C(130)	1.830(4)
P(7)–C(5)	1.848(4)	P(8)–C(160)	1.829(3)
P(8)–C(150)	1.830(4)	P(8)–C(5)	1.852(4)
O(1)–C(3)	1.226(4)	O(2)–C(6)	1.213(5)
C(10)–C(15)	1.377(6)	C(10)–C(11)	1.395(6)
C(11)–C(12)	1.398(6)	C(12)–C(13)	1.355(8)
C(13)–C(14)	1.402(7)	C(14)–C(15)	1.403(5)
C(20)–C(21)	1.381(6)	C(20)–C(25)	1.393(6)
C(21)–C(22)	1.385(6)	C(22)–C(23)	1.384(8)
C(23)–C(24)	1.360(8)	C(24)–C(25)	1.406(6)
C(30)–C(35)	1.395(5)	C(30)–C(31)	1.408(5)
C(31)–C(32)	1.379(5)	C(32)–C(33)	1.384(6)
C(33)–C(34)	1.347(7)	C(34)–C(35)	1.386(6)
C(40)–C(41)	1.351(6)	C(40)–C(45)	1.376(6)
C(41)–C(42)	1.387(7)	C(42)–C(43)	1.352(7)
C(43)–C(44)	1.331(7)	C(44)–C(45)	1.364(6)
C(50)–C(51)	1.381(5)	C(50)–C(55)	1.394(5)
C(51)–C(52)	1.397(5)	C(52)–C(53)	1.383(6)
C(53)–C(54)	1.377(7)	C(54)–C(55)	1.385(5)
C(60)–C(61)	1.392(5)	C(60)–C(65)	1.399(5)
C(61)–C(62)	1.389(5)	C(62)–C(63)	1.366(6)
C(63)–C(64)	1.381(7)	C(64)–C(65)	1.378(6)
C(70)–C(75)	1.382(5)	C(70)–C(71)	1.393(5)
C(71)–C(72)	1.399(6)	C(72)–C(73)	1.355(6)
C(73)–C(74)	1.384(6)	C(74)–C(75)	1.384(6)

C(80)–C(81)	1.378(5)	C(80)–C(85)	1.390(5)
C(81)–C(82)	1.400(5)	C(82)–C(83)	1.379(6)
C(83)–C(84)	1.368(6)	C(84)–C(85)	1.388(6)
C(90)–C(91)	1.397(5)	C(90)–C(95)	1.402(5)
C(91)–C(92)	1.381(5)	C(92)–C(93)	1.392(6)
C(93)–C(94)	1.390(6)	C(94)–C(95)	1.382(5)
C(100)–C(105)	1.383(5)	C(100)–C(101)	1.400(5)
C(101)–C(102)	1.386(6)	C(102)–C(103)	1.388(6)
C(103)–C(104)	1.368(7)	C(104)–C(105)	1.409(6)
C(110)–C(115)	1.386(6)	C(110)–C(111)	1.386(6)
C(111)–C(112)	1.407(6)	C(112)–C(113)	1.363(8)
C(113)–C(114)	1.363(8)	C(114)–C(115)	1.396(6)
C(120)–C(125)	1.389(5)	C(120)–C(121)	1.394(5)
C(121)–C(122)	1.383(6)	C(122)–C(123)	1.385(7)
C(123)–C(124)	1.362(6)	C(124)–C(125)	1.390(6)
C(130)–C(131)	1.389(5)	C(130)–C(135)	1.398(5)
C(131)–C(132)	1.389(6)	C(132)–C(133)	1.386(7)
C(133)–C(134)	1.360(6)	C(134)–C(135)	1.379(5)
C(140)–C(141)	1.397(6)	C(140)–C(145)	1.406(5)
C(141)–C(142)	1.399(6)	C(142)–C(143)	1.362(8)
C(143)–C(144)	1.382(8)	C(144)–C(145)	1.374(6)
C(150)–C(155)	1.386(5)	C(150)–C(151)	1.390(5)
C(151)–C(152)	1.385(5)	C(152)–C(153)	1.407(7)
C(153)–C(154)	1.371(6)	C(154)–C(155)	1.390(5)
C(160)–C(161)	1.374(5)	C(160)–C(165)	1.386(5)
C(161)–C(162)	1.401(5)	C(162)–C(163)	1.382(6)
C(163)–C(164)	1.377(6)	C(164)–C(165)	1.389(5)
C(200)–Cl(2)	1.719(7)	C(200)–Cl(3)	1.732(6)
C(200)–Cl(1)	1.769(8)	C(201)–Cl(4)	1.727(6)
C(201)–Cl(5)	1.745(5)	C(201)–Cl(6)	1.81(5)
C(202)–Cl(9)	1.739(5)	C(202)–Cl(7)	1.765(5)
C(202)–Cl(8)	1.771(6)	C(203)–Cl(10)	1.746(6)
C(203)–Cl(11)	1.747(5)	C(203)–Cl(12)	1.756(5)
C(204)–Cl(14)	1.604(11)	C(204)–Cl(13)	1.748(8)
C(204)–Cl(15)	1.752(10)	C(205)–Cl(17)	1.732(4)
C(205)–Cl(18)	1.744(5)	C(205)–Cl(16)	1.745(5)

P(2)–Ru(1)–P(3)	95.06(3)	P(2)–Ru(1)–P(1)	71.39(3)
P(3)–Ru(1)–P(1)	99.85(3)	P(2)–Ru(1)–P(4)	103.31(3)
P(3)–Ru(1)–P(4)	71.49(3)	P(1)–Ru(1)–P(4)	169.74(3)
P(2)–Ru(1)–S(1)	93.83(3)	P(3)–Ru(1)–S(1)	164.71(3)
P(1)–Ru(1)–S(1)	94.78(3)	P(4)–Ru(1)–S(1)	94.35(3)
P(2)–Ru(1)–S(2)	157.92(3)	P(3)–Ru(1)–S(2)	102.67(3)
P(1)–Ru(1)–S(2)	92.46(3)	P(4)–Ru(1)–S(2)	94.81(3)

S(1)–Ru(1)–S(2)	72.06(3)	P(8)–Ru(2)–P(6)	100.66(3)
P(8)–Ru(2)–P(5)	95.07(3)	P(6)–Ru(2)–P(5)	71.68(3)
P(8)–Ru(2)–P(7)	71.66(3)	P(6)–Ru(2)–P(7)	169.58(3)
P(5)–Ru(2)–P(7)	101.50(3)	P(8)–Ru(2)–S(4)	95.76(3)
P(6)–Ru(2)–S(4)	93.02(3)	P(5)–Ru(2)–S(4)	162.67(3)
P(7)–Ru(2)–S(4)	94.73(3)	P(8)–Ru(2)–S(3)	159.95(3)
P(6)–Ru(2)–S(3)	95.74(3)	P(5)–Ru(2)–S(3)	101.00(3)
P(7)–Ru(2)–S(3)	93.28(3)	S(4)–Ru(2)–S(3)	71.78(3)
C(3)–S(1)–Ru(1)	90.61(12)	C(3)–S(2)–Ru(1)	89.12(13)
C(6)–S(3)–Ru(2)	89.34(13)	C(6)–S(4)–Ru(2)	90.50(13)
C(20)–P(1)–C(10)	100.84(17)	C(20)–P(1)–C(1)	106.31(18)
C(10)–P(1)–C(1)	108.67(18)	C(20)–P(1)–Ru(1)	121.94(13)
C(10)–P(1)–Ru(1)	122.69(12)	C(1)–P(1)–Ru(1)	94.81(12)
C(30)–P(2)–C(40)	102.10(17)	C(30)–P(2)–C(1)	106.11(17)
C(40)–P(2)–C(1)	106.10(17)	C(30)–P(2)–Ru(1)	125.92(12)
C(40)–P(2)–Ru(1)	118.60(13)	C(1)–P(2)–Ru(1)	95.67(13)
C(60)–P(3)–C(50)	101.80(16)	C(60)–P(3)–C(2)	105.02(17)
C(50)–P(3)–C(2)	104.69(16)	C(60)–P(3)–Ru(1)	120.30(12)
C(50)–P(3)–Ru(1)	126.58(11)	C(2)–P(3)–Ru(1)	95.09(10)
C(70)–P(4)–C(80)	100.21(16)	C(70)–P(4)–C(2)	107.03(16)
C(80)–P(4)–C(2)	107.34(17)	C(70)–P(4)–Ru(1)	122.05(12)
C(80)–P(4)–Ru(1)	123.55(12)	C(2)–P(4)–Ru(1)	94.93(12)
C(90)–P(5)–C(100)	101.29(16)	C(90)–P(5)–C(4)	105.47(16)
C(100)–P(5)–C(4)	104.63(16)	C(90)–P(5)–Ru(2)	127.29(11)
C(100)–P(5)–Ru(2)	120.12(11)	C(4)–P(5)–Ru(2)	94.70(10)
C(120)–P(6)–C(110)	99.74(16)	C(120)–P(6)–C(4)	107.75(16)
C(110)–P(6)–C(4)	107.24(17)	C(120)–P(6)–Ru(2)	122.79(13)
C(110)–P(6)–Ru(2)	122.61(12)	C(4)–P(6)–Ru(2)	95.24(11)
C(140)–P(7)–C(130)	100.87(15)	C(140)–P(7)–C(5)	105.51(17)
C(130)–P(7)–C(5)	106.74(17)	C(140)–P(7)–Ru(2)	121.08(12)
C(130)–P(7)–Ru(2)	125.00(12)	C(5)–P(7)–Ru(2)	95.24(11)
C(160)–P(8)–C(150)	103.73(16)	C(160)–P(8)–C(5)	104.10(16)
C(150)–P(8)–C(5)	105.85(16)	C(160)–P(8)–Ru(2)	117.85(12)
C(150)–P(8)–Ru(2)	126.08(11)	C(5)–P(8)–Ru(2)	96.12(11)
P(2)–C(1)–P(1)	94.55(16)	P(4)–C(2)–P(3)	94.97(16)
O(1)–C(3)–S(1)	125.5(3)	O(1)–C(3)–S(2)	126.3(3)
S(1)–C(3)–S(2)	108.21(19)	P(6)–C(4)–P(5)	95.51(16)
P(7)–C(5)–P(8)	94.91(16)	O(2)–C(6)–S(4)	126.3(3)
O(2)–C(6)–S(3)	125.3(3)	S(4)–C(6)–S(3)	108.4(2)
C(15)–C(10)–C(11)	119.1(4)	C(15)–C(10)–P(1)	117.3(3)
C(11)–C(10)–P(1)	123.5(4)	C(10)–C(11)–C(12)	120.2(5)
C(13)–C(12)–C(11)	120.7(5)	C(12)–C(13)–C(14)	119.9(4)
C(13)–C(14)–C(15)	119.4(5)	C(10)–C(15)–C(14)	120.7(4)
C(21)–C(20)–C(25)	121.1(4)	C(21)–C(20)–P(1)	119.3(3)

C(25)–C(20)–P(1)	119.5(3)	C(20)–C(21)–C(22)	118.8(4)
C(23)–C(22)–C(21)	121.1(5)	C(24)–C(23)–C(22)	119.7(4)
C(23)–C(24)–C(25)	120.8(5)	C(20)–C(25)–C(24)	118.4(5)
C(35)–C(30)–C(31)	117.7(4)	C(35)–C(30)–P(2)	123.2(3)
C(31)–C(30)–P(2)	119.0(3)	C(32)–C(31)–C(30)	121.0(4)
C(31)–C(32)–C(33)	119.4(4)	C(34)–C(33)–C(32)	120.6(4)
C(33)–C(34)–C(35)	121.2(4)	C(34)–C(35)–C(30)	120.1(4)
C(41)–C(40)–C(45)	115.9(4)	C(41)–C(40)–P(2)	124.2(3)
C(45)–C(40)–P(2)	119.9(3)	C(40)–C(41)–C(42)	121.9(4)
C(43)–C(42)–C(41)	120.8(5)	C(44)–C(43)–C(42)	117.4(4)
C(43)–C(44)–C(45)	122.5(5)	C(44)–C(45)–C(40)	121.3(4)
C(51)–C(50)–C(55)	118.4(3)	C(51)–C(50)–P(3)	122.7(3)
C(55)–C(50)–P(3)	118.8(3)	C(50)–C(51)–C(52)	120.9(4)
C(53)–C(52)–C(51)	119.4(4)	C(54)–C(53)–C(52)	120.5(4)
C(53)–C(54)–C(55)	119.6(4)	C(54)–C(55)–C(50)	121.1(4)
C(61)–C(60)–C(65)	117.9(4)	C(61)–C(60)–P(3)	118.6(3)
C(65)–C(60)–P(3)	123.5(3)	C(62)–C(61)–C(60)	120.3(4)
C(63)–C(62)–C(61)	121.0(4)	C(62)–C(63)–C(64)	119.4(4)
C(65)–C(64)–C(63)	120.4(4)	C(64)–C(65)–C(60)	121.0(4)
C(75)–C(70)–C(71)	118.7(4)	C(75)–C(70)–P(4)	117.6(3)
C(71)–C(70)–P(4)	123.7(3)	C(70)–C(71)–C(72)	119.7(4)
C(73)–C(72)–C(71)	120.6(4)	C(72)–C(73)–C(74)	120.3(4)
C(73)–C(74)–C(75)	119.5(4)	C(70)–C(75)–C(74)	121.1(4)
C(81)–C(80)–C(85)	119.0(3)	C(81)–C(80)–P(4)	118.3(3)
C(85)–C(80)–P(4)	122.7(3)	C(80)–C(81)–C(82)	120.5(4)
C(83)–C(82)–C(81)	119.6(4)	C(84)–C(83)–C(82)	120.2(4)
C(83)–C(84)–C(85)	120.4(4)	C(84)–C(85)–C(80)	120.3(4)
C(91)–C(90)–C(95)	118.7(3)	C(91)–C(90)–P(5)	119.1(3)
C(95)–C(90)–P(5)	122.2(3)	C(92)–C(91)–C(90)	120.7(4)
C(91)–C(92)–C(93)	120.4(4)	C(94)–C(93)–C(92)	119.3(3)
C(95)–C(94)–C(93)	120.6(4)	C(94)–C(95)–C(90)	120.4(4)
C(105)–C(100)–C(101)	119.0(3)	C(105)–C(100)–P(5)	122.6(3)
C(101)–C(100)–P(5)	118.4(3)	C(102)–C(101)–C(100)	120.7(4)
C(103)–C(102)–C(101)	119.7(4)	C(104)–C(103)–C(102)	120.4(4)
C(103)–C(104)–C(105)	120.1(4)	C(100)–C(105)–C(104)	120.1(4)
C(115)–C(110)–C(111)	119.6(4)	C(115)–C(110)–P(6)	123.9(3)
C(111)–C(110)–P(6)	116.5(3)	C(110)–C(111)–C(112)	118.7(5)
C(113)–C(112)–C(111)	121.5(5)	C(114)–C(113)–C(112)	119.4(4)
C(113)–C(114)–C(115)	120.9(5)	C(110)–C(115)–C(114)	119.9(4)
C(125)–C(120)–C(121)	119.0(3)	C(125)–C(120)–P(6)	121.3(3)
C(121)–C(120)–P(6)	119.7(3)	C(122)–C(121)–C(120)	120.5(4)
C(121)–C(122)–C(123)	119.3(4)	C(124)–C(123)–C(122)	121.1(4)
C(123)–C(124)–C(125)	119.8(4)	C(120)–C(125)–C(124)	120.4(4)
C(131)–C(130)–C(135)	118.7(3)	C(131)–C(130)–P(7)	123.1(3)

C(135)–C(130)–P(7)	118.0(3)	C(132)–C(131)–C(130)	120.3(4)
C(133)–C(132)–C(131)	119.9(4)	C(134)–C(133)–C(132)	120.0(4)
C(133)–C(134)–C(135)	120.9(4)	C(134)–C(135)–C(130)	120.2(4)
C(141)–C(140)–C(145)	119.1(4)	C(141)–C(140)–P(7)	118.4(3)
C(145)–C(140)–P(7)	122.5(3)	C(140)–C(141)–C(142)	119.8(4)
C(143)–C(142)–C(141)	119.9(5)	C(142)–C(143)–C(144)	121.0(4)
C(145)–C(144)–C(143)	120.3(5)	C(144)–C(145)–C(140)	119.8(5)
C(155)–C(150)–C(151)	119.2(3)	C(155)–C(150)–P(8)	119.3(3)
C(151)–C(150)–P(8)	121.4(3)	C(152)–C(151)–C(150)	120.1(4)
C(151)–C(152)–C(153)	120.4(4)	C(154)–C(153)–C(152)	118.9(4)
C(153)–C(154)–C(155)	120.7(4)	C(150)–C(155)–C(154)	120.5(3)
C(161)–C(160)–C(165)	119.3(3)	C(161)–C(160)–P(8)	121.5(3)
C(165)–C(160)–P(8)	118.9(3)	C(160)–C(161)–C(162)	119.9(3)
C(163)–C(162)–C(161)	120.6(4)	C(164)–C(163)–C(162)	119.4(3)
C(163)–C(164)–C(165)	120.0(3)	C(160)–C(165)–C(164)	120.8(3)
Cl(2)–C(200)–Cl(3)	110.7(3)	Cl(2)–C(200)–Cl(1)	111.1(4)
Cl(3)–C(200)–Cl(1)	110.1(4)	Cl(4)–C(201)–Cl(5)	110.2(3)
Cl(4)–C(201)–Cl(6)	109.5(3)	Cl(5)–C(201)–Cl(6)	109.9(3)
Cl(9)–C(202)–Cl(7)	110.0(3)	Cl(9)–C(202)–Cl(8)	110.1(3)
Cl(7)–C(202)–Cl(8)	109.6(3)	Cl(10)–C(203)–Cl(11)	111.4(3)
Cl(10)–C(203)–Cl(12)	111.2(3)	Cl(11)–C(203)–Cl(12)	109.2(3)
Cl(14)–C(204)–Cl(13)	116.8(7)	Cl(14)–C(204)–Cl(15)	115.3(6)
Cl(13)–C(204)–Cl(15)	106.6(5)	Cl(17)–C(205)–Cl(18)	110.2(2)
Cl(17)–C(205)–Cl(16)	109.9(3)	Cl(18)–C(205)–Cl(16)	111.4(3)

Crystal data and structure refinement for $[(dppm)_2RuS_2COMe][BF_4]$ (**3**)

Chemical formula	$C_{53}H_{51}BF_4O_2P_4RuS_2$	
Formula weight	1095.82	
Temperature	150(2) K	
Radiation, wavelength	MoKα, 0.71073 Å	
Crystal system, space group	monoclinic, C2/c	
Unit cell parameters	a = 35.754(2) Å	α = 90°
	b = 11.8150(7) Å	β = 109.9030(10)°
	c = 24.7544(14) Å	γ = 90°
Cell volume	9832.5(10) $Å^3$	
Z	8	
Calculated density	1.481 g/cm^3	
Absorption coefficient μ	0.591 mm^{-1}	
F(000)	4496	
Crystal colour and size	yellow, 0.64 × 0.64 × 0.42 mm^3	
Data collection method	Bruker SMART APEX diffractometer	
	ω rotation with narrow frames	
θ range for data collection	1.76 to 28.32°	
Index ranges	h −45 to 45, k −15 to 15, l −32 to 32	
Completeness to θ = 26.00°	99.8 %	
Reflections collected	42408	
Independent reflections	11725 (R_{int} = 0.0186)	
Reflections with $F^2>2\sigma$	10896	
Absorption correction	semi-empirical from equivalents	
Min. and max. transmission	0.7036 and 0.7894	
Structure solution	Patterson synthesis	
Refinement method	Full-matrix least-squares on F^2	
Weighting parameters a, b	0.0598, 25.3068	
Data / restraints / parameters	11725 / 0 / 604	
Final R indices [$F^2>2\sigma$]	R1 = 0.0382, wR2 = 0.1047	
R indices (all data)	R1 = 0.0409, wR2 = 0.1069	
Goodness-of-fit on F^2	1.043	
Largest and mean shift/su	0.003 and 0.000	
Largest diff. peak and hole	1.336 and −0.748 e $Å^{-3}$	

Bond lengths [Å] and angles [°].

Ru(1)–P(2)	2.3124(6)	Ru(1)–P(4)	2.3200(6)
Ru(1)–P(1)	2.3342(6)	Ru(1)–P(3)	2.3721(6)
Ru(1)–S(1)	2.4347(6)	Ru(1)–S(2)	2.4398(6)
S(1)–C(1)	1.691(2)	S(2)–C(1)	1.689(2)
P(1)–C(16)	1.819(2)	P(1)–C(10)	1.821(2)
P(1)–C(3)	1.837(2)	P(2)–C(28)	1.822(2)
P(2)–C(22)	1.825(2)	P(2)–C(3)	1.841(2)
P(3)–C(34)	1.822(2)	P(3)–C(40)	1.824(2)
P(3)–C(4)	1.837(2)	P(4)–C(46)	1.826(2)
P(4)–C(52)	1.832(2)	P(4)–C(4)	1.848(2)
O(1)–C(1)	1.320(3)	O(1)–C(2)	1.447(3)
C(10)–C(15)	1.389(3)	C(10)–C(11)	1.404(3)
C(11)–C(12)	1.391(4)	C(12)–C(13)	1.386(4)
C(13)–C(14)	1.385(4)	C(14)–C(15)	1.399(3)
C(16)–C(21)	1.383(4)	C(16)–C(17)	1.392(4)
C(17)–C(18)	1.395(4)	C(18)–C(19)	1.365(5)
C(19)–C(20)	1.375(6)	C(20)–C(21)	1.401(4)
C(22)–C(27)	1.386(3)	C(22)–C(23)	1.394(3)
C(23)–C(24)	1.384(4)	C(24)–C(25)	1.375(5)
C(25)–C(26)	1.373(5)	C(26)–C(27)	1.398(4)
C(28)–C(33)	1.393(3)	C(28)–C(29)	1.395(3)
C(29)–C(30)	1.388(3)	C(30)–C(31)	1.392(4)
C(31)–C(32)	1.373(4)	C(32)–C(33)	1.397(3)
C(34)–C(35)	1.392(3)	C(34)–C(39)	1.395(3)
C(35)–C(36)	1.391(4)	C(36)–C(37)	1.387(4)
C(37)–C(38)	1.373(4)	C(38)–C(39)	1.391(4)
C(40)–C(41)	1.393(3)	C(40)–C(45)	1.396(3)
C(41)–C(42)	1.392(4)	C(42)–C(43)	1.383(4)
C(43)–C(44)	1.381(5)	C(44)–C(45)	1.389(4)
C(46)–C(51)	1.393(3)	C(46)–C(47)	1.399(3)
C(47)–C(48)	1.388(3)	C(48)–C(49)	1.385(4)
C(49)–C(50)	1.377(4)	C(50)–C(51)	1.395(3)
C(52)–C(53)	1.393(3)	C(52)–C(57)	1.399(3)
C(53)–C(54)	1.394(3)	C(54)–C(55)	1.385(4)
C(55)–C(56)	1.386(4)	C(56)–C(57)	1.391(3)
B(1)–F(2)	1.337(5)	B(1)–F(1)	1.377(5)
B(1)–F(4)	1.381(6)	B(1)–F(3)	1.398(5)
C(60)–O(2)	1.421(8)		

P(2)–Ru(1)–P(4)	95.58(2)	P(2)–Ru(1)–P(1)	71.74(2)
P(4)–Ru(1)–P(1)	101.55(2)	P(2)–Ru(1)–P(3)	102.64(2)
P(4)–Ru(1)–P(3)	71.411(19)	P(1)–Ru(1)–P(3)	170.85(2)

P(2)–Ru(1)–S(1)	96.31(2)	P(4)–Ru(1)–S(1)	164.32(2)
P(1)–Ru(1)–S(1)	91.87(2)	P(3)–Ru(1)–S(1)	95.98(2)
P(2)–Ru(1)–S(2)	156.12(2)	P(4)–Ru(1)–S(2)	100.49(2)
P(1)–Ru(1)–S(2)	87.72(2)	P(3)–Ru(1)–S(2)	99.19(2)
S(1)–Ru(1)–S(2)	71.715(19)	C(1)–S(1)–Ru(1)	86.28(8)
C(1)–S(2)–Ru(1)	86.15(8)	C(16)–P(1)–C(10)	104.29(11)
C(16)–P(1)–C(3)	109.08(12)	C(10)–P(1)–C(3)	105.01(11)
C(16)–P(1)–Ru(1)	118.62(8)	C(10)–P(1)–Ru(1)	122.62(8)
C(3)–P(1)–Ru(1)	95.44(7)	C(28)–P(2)–C(22)	100.17(10)
C(28)–P(2)–C(3)	107.54(11)	C(22)–P(2)–C(3)	105.00(11)
C(28)–P(2)–Ru(1)	124.45(7)	C(22)–P(2)–Ru(1)	121.47(8)
C(3)–P(2)–Ru(1)	96.05(7)	C(34)–P(3)–C(40)	98.51(10)
C(34)–P(3)–C(4)	106.95(11)	C(40)–P(3)–C(4)	107.38(10)
C(34)–P(3)–Ru(1)	121.76(7)	C(40)–P(3)–Ru(1)	126.47(7)
C(4)–P(3)–Ru(1)	93.85(7)	C(46)–P(4)–C(52)	103.36(10)
C(46)–P(4)–C(4)	104.64(10)	C(52)–P(4)–C(4)	105.71(10)
C(46)–P(4)–Ru(1)	127.70(7)	C(52)–P(4)–Ru(1)	117.05(7)
C(4)–P(4)–Ru(1)	95.26(7)	C(1)–O(1)–C(2)	118.3(2)
O(1)–C(1)–S(2)	126.01(18)	O(1)–C(1)–S(1)	118.72(17)
S(2)–C(1)–S(1)	115.26(13)	P(1)–C(3)–P(2)	95.51(11)
P(3)–C(4)–P(4)	96.01(10)	C(15)–C(10)–C(11)	120.0(2)
C(15)–C(10)–P(1)	120.30(18)	C(11)–C(10)–P(1)	119.23(19)
C(12)–C(11)–C(10)	119.3(2)	C(13)–C(12)–C(11)	120.5(3)
C(14)–C(13)–C(12)	120.2(2)	C(13)–C(14)–C(15)	119.9(3)
C(10)–C(15)–C(14)	120.0(2)	C(21)–C(16)–C(17)	119.4(2)
C(21)–C(16)–P(1)	121.8(2)	C(17)–C(16)–P(1)	118.4(2)
C(16)–C(17)–C(18)	120.0(3)	C(19)–C(18)–C(17)	120.3(3)
C(18)–C(19)–C(20)	120.2(3)	C(19)–C(20)–C(21)	120.2(3)
C(16)–C(21)–C(20)	119.8(3)	C(27)–C(22)–C(23)	119.8(2)
C(27)–C(22)–P(2)	120.30(18)	C(23)–C(22)–P(2)	119.68(19)
C(24)–C(23)–C(22)	119.7(3)	C(25)–C(24)–C(23)	120.4(3)
C(26)–C(25)–C(24)	120.4(3)	C(25)–C(26)–C(27)	120.1(3)
C(22)–C(27)–C(26)	119.6(3)	C(33)–C(28)–C(29)	119.2(2)
C(33)–C(28)–P(2)	124.06(17)	C(29)–C(28)–P(2)	116.72(17)
C(30)–C(29)–C(28)	120.8(2)	C(29)–C(30)–C(31)	119.6(2)
C(32)–C(31)–C(30)	119.9(2)	C(31)–C(32)–C(33)	120.9(2)
C(28)–C(33)–C(32)	119.6(2)	C(35)–C(34)–C(39)	119.1(2)
C(35)–C(34)–P(3)	118.48(18)	C(39)–C(34)–P(3)	122.03(19)
C(36)–C(35)–C(34)	120.0(2)	C(37)–C(36)–C(35)	120.5(3)
C(38)–C(37)–C(36)	119.6(2)	C(37)–C(38)–C(39)	120.6(2)
C(38)–C(39)–C(34)	120.2(2)	C(41)–C(40)–C(45)	119.0(2)
C(41)–C(40)–P(3)	123.37(18)	C(45)–C(40)–P(3)	117.53(19)
C(42)–C(41)–C(40)	120.5(2)	C(43)–C(42)–C(41)	119.8(3)
C(44)–C(43)–C(42)	120.2(3)	C(43)–C(44)–C(45)	120.3(3)

C(44)–C(45)–C(40)	120.1(3)	C(51)–C(46)–C(47)	118.4(2)
C(51)–C(46)–P(4)	121.88(17)	C(47)–C(46)–P(4)	119.70(17)
C(48)–C(47)–C(46)	120.7(2)	C(49)–C(48)–C(47)	120.3(2)
C(50)–C(49)–C(48)	119.6(2)	C(49)–C(50)–C(51)	120.7(2)
C(46)–C(51)–C(50)	120.3(2)	C(53)–C(52)–C(57)	118.5(2)
C(53)–C(52)–P(4)	123.16(18)	C(57)–C(52)–P(4)	118.30(16)
C(52)–C(53)–C(54)	120.8(2)	C(55)–C(54)–C(53)	119.8(2)
C(54)–C(55)–C(56)	120.2(2)	C(55)–C(56)–C(57)	119.9(2)
C(56)–C(57)–C(52)	120.7(2)	F(2)–B(1)–F(1)	112.1(4)
F(2)–B(1)–F(4)	111.4(3)	F(1)–B(1)–F(4)	104.2(4)
F(2)–B(1)–F(3)	109.1(4)	F(1)–B(1)–F(3)	105.4(3)
F(4)–B(1)–F(3)	114.5(4)		

Papers Resulting From This Thesis

Inorg. Chem. **2006**, *45*, 5210–5214

Synthesis and Reactivity of the Ruthenium(II) Dithiocarbonate Complex [Ru(κ^2-S_2C=O)(dppm)$_2$] (dppm = Bis(diphenylphosphino)methane)

James D. E. T. Wilton-Ely,*,† Dina Solanki,‡ and Graeme Hogarth‡

Chemistry Research Laboratory, University of Oxford, Mansfield Road, Oxford OX1 3TA, United Kingdom, and Department of Chemistry, University College London (UCL), 20 Gordon Street, London WC1H 0AJ, United Kingdom

Received February 8, 2006

Reaction of *cis*-[$RuCl_2$(dppm)$_2$] (dppm = bis(diphenylphosphino)methane) with CS_2 and NaOH yields the first ruthenium dithiocarbonate complex, [Ru(κ^2-S_2C=O)(dppm)$_2$]. Protonation with tetrafluoroboric acid affords the xanthate complex [Ru(κ^2-S_2COH)(dppm)$_2$]BF_4 in a reversible manner, suggesting that this may be an intermediate in dithiocarbonate formation. [Ru(κ^2-S_2C=O)(dppm)$_2$] reacts with methyl iodide or [Me_3O]BF_4 to give [Ru(κ^2-S_2COMe)(dppm)$_2$]$^+$, also obtained from the reaction of *cis*-[$RuCl_2$(dppm)$_2$] with CS_2 and NaOMe. Two modifications of [Ru(κ^2-S_2C=O)(dppm)$_2$] were examined crystallographically and the structure of [Ru(κ^2-S_2COMe)(dppm)$_2$]BF_4 and a new modification of *cis*-[$RuCl_2$(dppm)$_2$] are also reported.

Introduction

Interest in mononuclear complexes with sulfur-containing ligands has been sustained by their relevance as models for redox-active metalloproteins.[1] Compared, for example, to dithiocarbamate complexes,[2] dithiocarbonate complexes are less well-known, although examples have been reported for a number of metals.[3−10] The most-detailed study of the reactivity of these species to date has been that of [Rh(κ^2-S_2C=O)(triphos)]$^-$ (triphos = $MeC(CH_2PPh_2)_3$) by Bianchini and co-workers, who found that this complex displays a substantial and diverse reactivity.[10]

Existing synthetic routes to dithiocarbonate complexes involve the use of xanthate,[3−8] carbon disulfide,[9] or phosphoniodithiocarboxylate[10] compounds. For example, xanthates, [M(κ^2-S_2COR)$_2$] (M = Ni, Pd, Pt; R = alkyl), when treated with phosphines or phosphites (L), liberate *S*-alkyl *O*-alkyl dithiocarbonates $ROCS_2R$ to give dithiocarbonate complexes [M(κ^2-S_2C=O)L_2].[6b,8] Herein, we report the synthesis and reactivity of the first ruthenium dithiocarbonate complex, [Ru(κ^2-S_2C=O)(dppm)$_2$]. This is readily accessible in one step from the reaction of *cis*-[$RuCl_2$(dppm)$_2$][11] with NaOH and CS_2, a transformation proposed to involve a RuS_2COH intermediate.

Results and Discussion

Addition of *cis*-[$RuCl_2$(dppm)$_2$] (**1**) to a solution of NaOH and CS_2 led cleanly to the isolation of a single new product

* To whom correspondence should be addressed. E-mail: james.wilton-ely@chem.ox.ac.uk.
† University of Oxford.
‡ University College London.

(1) Blower, P. G.; Dilworth, J. R. *Coord. Chem. Rev.* **1987**, *76*, 121.
(2) Hogarth, G. *Prog. Inorg. Chem.* **2005**, *53*, 71.
(3) (a) Fackler, J. P., Jr.; Seidel, W. C.; Fetchin, J. A. *J. Am. Chem. Soc.* **1968**, *90*, 2707. (b) Fackler, J. P., Jr.; Seidel, W. C. *Inorg. Chem.* **1969**, *8*, 1631. (c) Burke, J. M.; Fackler, J. P., Jr. *Inorg. Chem.* **1972**, *11*, 2744.
(4) (a) Alison, J. M. C.; Stephenson, T. A. *J. Chem. Soc., Dalton Trans.* **1973**, 254. (b) Cole-Hamilton, D. J.; Stephenson, T. A. *J. Chem. Soc., Dalton Trans.* **1974**, 1818. (c) Gould, R. O.; Gunn, A. M.; Van den Hark, T. E. M. *J. Chem. Soc., Dalton Trans.* **1976**, 1713. (d) Cornock, M. C.; Gould, R. O.; Jones, C. L.; Owen, J. D.; Steele, D. F.; Stephenson, T. A. *J. Chem. Soc., Dalton Trans.* **1977**, 496. (e) Cornock, M. C.; Gould, R. O.; Jones, C. L.; Stephenson, T. A. *J. Chem. Soc., Dalton Trans.* **1977**, 1307.
(5) Doherty, J.; Fortune, J.; Manning, A. R.; Stephens, F. S. *J. Chem. Soc., Dalton Trans.* **1984**, 1111.
(6) (a) Perpiñán, M. F.; Ballester, L.; González-Casso, M. E.; Santos, A. *J. Chem. Soc., Dalton Trans.* **1987**, 281. (b) Tenorio, M. J.; Puerta, M. C.; Valerga, P. *J. Chem. Soc., Dalton Trans.* **1996**, 1935. (c) Travnicek, Z.; Pastorek, R.; Sindelar, Z.; Klicka, R.; Marek, J. *Transition Met. Chem.* **1996**, *21*, 81.
(7) Marchi, A.; Marvelli, L.; Rossi, R.; Magon, L.; Uccelli, L.; Bertolasi, V.; Ferretti, V.; Zanobini, F. *J. Chem. Soc., Dalton Trans.* **1993**, 1281.
(8) Contreras, R.; Valderrama, M.; Riveros, O.; Moscoso, R.; Boys, D. *Polyhedron* **1996**, *15*, 183.
(9) Bianchini, C.; Ghilardi, C. A.; Meli, A.; Orlandini, A. *J. Organomet. Chem.* **1985**, *286*, 259.
(10) (a) Bianchini, C.; Mealli, C.; Meli, A.; Sabat, M. *Chem. Commun.* **1985**, 1024. (b) Bianchini, C.; Meli, A.; Vizza, F. *Angew. Chem., Int. Ed.* **1987**, *26*, 767. (c) Bianchini, C.; Meli, A. *Inorg. Chem.* **1987**, *26*, 1345. (d) Bianchini, C.; Meli, A.; Laschi, F.; Vizza, F.; Zanello, P. *Inorg. Chem.* **1989**, *28*, 227. (e) Bianchini, C.; Meli, A. *Inorg. Synth.* **1990**, *27*, 287.
(11) Sullivan, B. P.; Meyer, T. J. *Inorg. Chem.* **1982**, *21*, 1037.

10.1021/ic060223b CCC: $33.50
Published on Web 06/01/2006

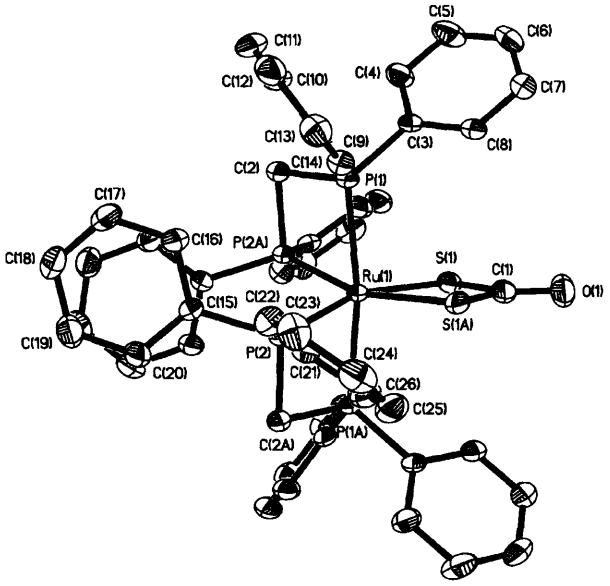

Figure 1. Structure of [Ru(κ²-S₂C=O)(dppm)₂] (**3**) (only Λ enantiomer shown). Selected bond lengths (Å) and angles (deg): P2−Ru1−P2A = 97.40(5), P2−Ru1−P1 = 102.16(3), P2A−Ru1−P1 = 71.90(3), P2A−Ru1−S1 = 96.67(4), P1A−Ru1−S1 = 93.61(3), P1−Ru1−S1 = 93.41(3). Other bond lengths are collected in Table 1.

in 94% yield that was identified as [Ru(κ²-S₂C=O)(dppm)₂] (**3**). Initial characterization was made on the basis of spectroscopic data, with key features being a resonance at 218.6 ppm in the $^{13}C\{^1H\}$ NMR spectrum and a ν(C=O) absorption at 1568 cm^{-1} in the solid-state IR spectrum (1572 cm^{-1} in CH_2Cl_2 solution). In the FAB mass spectrum, a molecular ion was observed at *m/z* = 961, with the only major fragmentation ion resulting from loss of SCO. To confirm the formation of a dithiocarbonate ligand, we carried out crystallographic studies on two crystal modifications; the results of one of these (**3**·2CH_3OH) are shown in Figure 1.

It is plausible that dithiocarbonate **3** results from the in situ generation of Na[S_2COH] from NaOH and CS_2 in methanol. This, in turn, reacts with *cis*-[$RuCl_2$(dppm)₂] (**1**) to afford the xanthate complex, [Ru(κ²-S_2COH)(dppm)₂]⁻, which is deprotonated under the prevailing basic conditions. To test this hypothesis, we protonated **3** with HBF_4·OEt_2 to obtain [Ru(κ²-S_2COH)(dppm)₂]BF_4 (**2**) (Scheme 1). In addition to the observed chemical shift changes in the $^{31}P\{^1H\}$ NMR spectrum, no ν(C=O) absorptions were observed in the IR spectrum of the product; the presence of the BF_4^- anion was noted as a broad band centered at 1049 cm^{-1} in the solid-state infrared spectrum. A singlet at 3.83 ppm in the ^1H NMR spectrum was tentatively assigned to the xanthate proton, and the overall composition was further supported by elemental analysis. To probe the formation of **2** further, we used NMR spectroscopy to monitor the protonation of **3** with trifluoroacetic acid. This led to a clean reaction but formed only the trifluoroacetate complex, [Ru(κ²-O_2CCF_3)(dppm)₂][CF_3CO_2], which has previously been reported by Robinson and co-workers.[13] It seems that although protonation does occur under these conditions, displacement of the xanthate by the coordinating anion

Scheme 1[a]

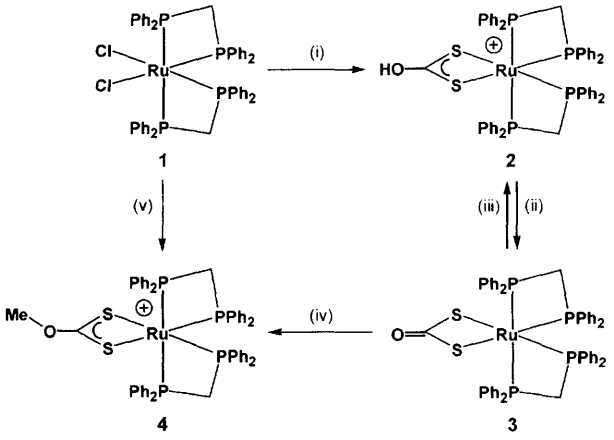

[a] (i) CS_2, NaOH; (ii) NaOH or NEt_3; (iii) HBF_4·OEt_2; (iv) MeI, [Me_3O]BF_4; (v) CS_2, NaOMe.

proceeds in a faster step. The free xanthate is unstable under acidic conditions, decomposing to liberate CS_2, which was easily identified from the pungent odor upon opening the NMR tube.

It appears that no examples of this parent xanthate have been reported previously.[12] Fackler and Seidel have shown that treatment of [Pt(κ²-S_2C=O)(PPh_2Me)₂] with HCl yields [$PtCl_2$(PPh_2Me)₂];[3b] however, the reaction with acids involving noncoordinating anions was not explored.

An alternative reaction pathway for the formation of **3** from **1** is the initial formation of *cis*-[RuCl(OH)(dppm)₂], which could be followed by insertion of CS_2 into the Ru−O bond and subsequent elimination of HCl. Although relatively rare, hydroxide complexes of ruthenium such as *trans*-[RuH(OH)(dmpm)₂] (dmpm = bis(dimethylphosphino)methane)[14a] and [RuCl(OH)(OH_2)₂(PPh_3)₂][14b] are known, but as far as we are aware, the insertion of CS_2 into such species has not been observed.

The dithiocarbonate group in **3** was found to react with other electrophiles. Treatment with trimethyloxonium tetrafluoroborate resulted in the formation of [Ru(κ²-S_2COMe)(dppm)₂]BF_4 (**4**), which was also prepared from the direct reaction of **1** with NaS_2COMe (prepared in situ from NaOMe and CS_2) and $NaBF_4$ (Scheme 1). A singlet resonance in the ^1H NMR spectrum at 3.80 ppm was assigned to the methyl group, and the overall composition was supported by a molecular ion at *m/z* = 977 in the FAB mass spectrum and elemental analysis. A crystallographic study was also undertaken (Figure 2).

Alkylation of **3** with methyl iodide also led to the formation of **4** (among other products), ultimately leading to displacement of the xanthate ligand by iodide to give the

(12) (a) Coucouvanis, D. *Prog. Inorg. Chem.*, **1970**, *11*, 233. (b) Coucouvanis, D. *Prog. Inorg. Chem.* **1979**, *26*, 301. (c) Tiekink, E. R. T.; Winter, G. *Rev. Inorg. Chem.* **1992**, *12*, 183.
(13) Boyar, E. B.; Harding, P. A.; Robinson, S. D.; Brock, C. P. *J. Chem. Soc., Dalton Trans.* **1986**, 1771.
(14) (a) Burn, M. J.; Fickes, M. G.; Hartwig, J. F.; Hollander, F. J.; Bergman, R. G. *J. Am. Chem. Soc.* **1993**, *115*, 5875. (b) Chaudret, B. N.; Cole-Hamilton, D. J.; Nohr, R. S.; Wilkinson, G. *J. Chem. Soc., Dalton Trans.* **1977**, 1546.

Table 1. Selected Bond Lengths (Å) and Angles (deg) for **3**, **4**, and Literature Complexes

complex	Ru−P_{eq}	Ru−P_{ax}	Ru−S	S−C	C−O	S−Ru−S	S−C−S
[Ru(κ^2-S_2C=O)(dppm)$_2$] (**3**·2CH_3OH)	2.3152(10)	2.3319(10)	2.4198(10)	1.764(3)	1.215(7)	72.39(5)	108.2(3)
Δ-[Ru(κ^2-S_2C=O)(dppm)$_2$] (**3**·3$CHCl_3$)	2.3140(9)	2.3308(10)	2.4011(8)	1.749(4)	1.226(4)	72.06(3)	108.21(19)
	2.3286(8)	2.3477(9)	2.4364(10)	1.764(4)			
Λ-[Ru(κ^2-S_2C=O)(dppm)$_2$] (**3**·3$CHCl_3$)	2.3138(9)	2.3280(9)	2.4157(9)	1.743(4)	1.213(5)	71.78(3)	108.4(2)
	2.3323(9)	2.3429(10)	2.4353(9)	1.765(4)			
[Ru(κ^2-S_2COMe)(dppm)$_2$]$^+$ (**4**)	2.3124(6)	2.3342(6)	2.4347(6)	1.689(2)	1.320(3)	71.715(19)	115.26(13)
	2.3200(6)	2.3721(6)	2.4398(6)	1.691(2)			
[Ru(κ^2-S_2CH_2)(dppm)$_2$][16]	2.3171(11)	2.3079(12)	2.4245(11)	1.812(5)	-	72.96(4)	105.3(2)
	2.3181(11)	2.3571(12)	2.4368(12)	1.824(5)			
[Ni(κ^2-S_2C=O)(dippe)][a,6b]	-	-	-	1.759(6)	1.235(6)	79.72(6)	106.3(3)
				1.769(5)			
[Pt(κ^2-S_2C=O){P(OMe)Ph_2}$_2$][8]	-	-	-	1.765(7)	1.190(8)	75.2(1)	107.5(3)
				1.767(7)			
[Ru(η^5-C_5Me_5)(κ^2-S_2CO^{i}Pr)(PEt_3)][18]	-	-	2.393(2)	1.678(5)	1.315(6)	71.45(6)	113.0(3)
			2.406(2)	1.682(5)			

[a] dippe = 1,2-bis(diisopropylphosphino)ethane.

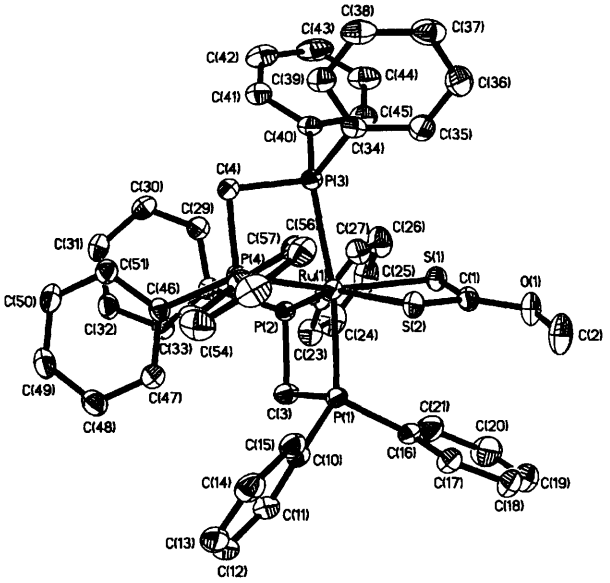

Figure 2. Structure of [Ru(κ^2-S_2COMe)(dppm)$_2$]BF_4 (**4**) (only Λ enantiomer shown). Selected bond lengths (Å) and angles (deg): O1−C2 = 1.447(3), P2−Ru1−P4 = 95.58(2), P2−Ru1−P1 = 71.74(2), P4−Ru1−P1 = 101.55(2), P2−Ru1−P3 = 102.64(2), P4−Ru1−P3 = 71.411(19), P2−Ru1−S1 = 96.31(2), P1−Ru1−S1 = 91.87(2), P3−Ru1−S1 = 95.98(2), P4−Ru1−S2 = 100.49(2), P1−Ru1−S2 = 87.72(2), P3−Ru1−S2 = 99.19(2), C1−S1−Ru1 = 86.28(8), C1−O1−C2 = 118.3(2), O1−C1−S2 = 126.01(18), O1−C1−S1 = 118.72(17). Other bond lengths are collected in Table 1.

known compound *cis*-[RuI_2(dppm)$_2$].[15] The dithiocarbonate ligand is lost in a similar manner in the reaction of [Ni(κ^2-S_2C=O)(dppe)] with methyl iodide to yield [NiI_2(dppe)].[6a]

Previous routes to dithiocarbonate complexes have frequently involved the reactions of xanthate complexes with bases such as phosphines.[3−8] However, treatment of **4** with NaOH in water and tetrahydrofuran (1:2) gave no reaction, suggesting that **4** is not an intermediate in the observed reaction between **1** and NaOH and CS_2 in methanol. Compound **4** also showed no reaction under acidic conditions (excess trifluoroacetic acid).

Crystallographic Studies

During the course of this work, crystal structures were determined for two crystal modifications of **3** (**3**·2CH_3OH and **3**·3$CHCl_3$), **4**·CH_3OH, and **1**·PrOH, the results of which are summarized in Figures 1 and 2 and Table 1. Figures depicting the other structures are included in the Supporting Information, along with a brief discussion of the structure of **1**·PrOH.

In **3**·3$CHCl_3$ there are two independent molecules in the asymmetric unit (Δ and Λ enantiomers), whereas **3**·2CH_3OH contains a single dithiocarbonate complex. Gross structural features of all three are similar, each containing a distorted octahedral geometry with cis-interligand angles ranging between 71.90(3) and 102.16(3)°. In **3**·2CH_3OH, the dithiocarbonate is symmetrically bound to ruthenium, whereas the same feature in both molecules in **3**·3$CHCl_3$ shows a slight asymmetry. The Ru−S bond lengths vary between 2.4364(10) and 2.4011(8) Å, with both extremes being observed in the Δ isomer in **3**·3$CHCl_3$; C−S (1.765(4)−1.743(4) Å) and C−O (1.226(4)−1.213(5) Å) bonds vary within much smaller ranges. These bond lengths are comparable to those found in [Ni(κ^2-S_2C=O)(dippe)] (dippe = 1,2-bis(diisopropylphosphino)ethane)[6b] and [Pt(κ^2-S_2C=O){P(OMe)Ph_2}$_2$];[8] however, the ligand bite angles in **3** (S−Ru−S = 72.39(5)−1.78(3)°) are significantly smaller than those found in related nickel or platinum complexes (Table 1). These observations indicate that the RuS_2C=O unit is softly bound to the ruthenium center, allowing for significant distortions depending on the structure modification.

The closest structural analogue to **3** is the isoelectronic complex [Ru(κ^2-S_2CH_2)(dppm)$_2$] reported recently by Jagirdar and co-workers.[16] The Ru−S lengths in the methanedithiolate compound are at the longer end of those seen in **3**, whereas the C−S bond distances are appreciably greater than those found in **3**. This may be due to the partial double-bond character resulting from the resonance forms shown in Chart 1. In **3**, the C−O distance shows double-bond character, which it has in common with all reported dithiocarbonate complexes,[3−10] and the bond length compares well with the average of 1.210 Å found in ketones.[17]

(15) Bickley, J. F.; La Pensée, A. A.; Higgins, S. J.; Stuart, C. A. *J. Chem. Soc., Dalton Trans.* **2003**, 4663.

(16) Gandhi, T.; Nethaji, M.; Jagirdar, B. R. *Inorg. Chem.* **2003**, *42*, 667.

Chart 1. Resonance Forms for the Dithiocarbonate Ligand

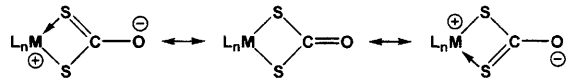

The Ru−S bond lengths in [Ru(κ²-S₂COMe)(dppm)₂]BF₄ (**4**) are slightly longer than those found in **3**, whereas the C−S distances are considerably shorter, reflecting the partial double-bond character present. The C−O bond length is relatively short, although the multiple-bond character is not as pronounced as that in **3**. The S−C−S angle of the xanthate ligand in **4** is substantially larger than that found in **3**, whereas the S−Ru−S bite angle is only marginally smaller than the corresponding feature in **3**. Apart from this slightly larger S−Ru−S angle, the structural features of the methyl xanthate ligand are similar to those found for the isopropyl xanthate moiety in [Ru(η⁵-C₅Me₅)(κ²-S₂CO^{i}Pr)(PEt₃)][18] (Table 1).

Conclusions

The first dithiocarbonate compound of ruthenium, [Ru(κ²-S₂C=O)(dppm)₂] (**3**), has been prepared from the reaction of carbon disulfide and hydroxide in methanol with *cis*-[RuCl₂(dppm)₂] (**1**). The reactivity of **3** centers on the oxygen of the dithiocarbonate ligand, which can be alkylated or protonated to yield either alkyl or parent xanthate products, respectively. The latter is a plausible intermediate in the formation of **3** and is the first such example of this ligand to be reported, to the best of our knowledge.

Experimental Section

General Procedures. All manipulations were carried out under aerobic conditions using commercially available solvents and reagents as received. Infrared and NMR spectroscopy were carried out at 25 °C using Shimadzu FTIR 8700 (KBr plates with Nujol) and Bruker AMX-300 (^{1}H, 299.87 MHz; ^{31}P, 121.39 MHz) or AMX-400 (^{1}H, 400.14 MHz; ^{31}P, 161.97 MHz) spectrometers, respectively. Infrared spectroscopic features due to the bis(diphenylphosphino)methane ligands have been omitted to aid clarity. FAB-MS spectra (nitrobenzyl alcohol matrixes) were measured using a VG 70-SB magnetic sector mass spectrometer. Elemental microanalyses were performed at UCL. Solvates were determined by ^{1}H NMR spectroscopy. *cis*-[RuCl₂(dppm)₂] (**1**) was prepared according to a published procedure.[11]

[Ru(κ²-S₂COH)(dppm)₂]BF₄ (2). A diethyl ether (10 mL) suspension of [Ru(κ²-S₂C=O)(dppm)₂] (**3**) (33 mg, 0.034 mmol) was treated with tetraflouroboric acid diethyl ether complex (3 drops, excess), and the reaction mixture was stirred for 5 min. The precipitate was broken up by sonication in an ultrasound bath and then filtered and washed with diethyl ether (10 mL) and hexane (10 mL). Yield: 32 mg (90%). IR (KBr/Nujol): 1339, 1312, 1236, 1049 (ν(BF)), 885 cm^{-1}. ^{31}P NMR ($CDCl_3$): δ −4.4, −16.7 (t × 2, J_{PP} = 35.7 Hz, dppm). ^{1}H NMR ($CDCl_3$): δ 3.83 (s, 1H, OH), 4.64, 5.03 (m × 2, 2 × 2H, PCH_2P), 6.54, 7.00, 7.06, 7.30, 7.64 (m × 5, PC_6H_5, 40H). FAB-MS *m/z* (abundance): 979 (38) [M + H_2O]$^+$. Anal. Calcd for $C_{51}H_{45}BF_4OP_4RuS_2$: C, 58.4; H, 4.3. Found: C, 58.7; H, 4.5.

[Ru(κ²-S₂C=O)(dppm)₂] (3). (a) NaOH (32 mg, 0.800 mmol) was dissolved in methanol (10 mL), and carbon disulfide (61 mg, 0.801 mmol) was added. The reaction mixture was stirred for 10 min. *cis*-[RuCl₂(dppm)₂] (**1**) (150 mg, 0.159 mmol) was dissolved in dichloromethane (10 mL) and added to the mixture. The solution was stirred for 2 h. All solvent was removed under reduced pressure; the residue was taken up in a minimum quantity of dichloromethane and filtered through diatomaceous earth. Ethanol (20 mL) was added, and the solvent volume was concentrated under reduced pressure until precipitation was complete. The pale green product was filtered and washed with ethanol (10 mL) and hexane (10 mL). Yield: 144 mg (94%). (b) Complex **2** (30 mg, 0.029 mmol) was dissolved in dichloromethane (10 mL) and treated with triethylamine (4 drops, excess) and the reaction mixture was stirred for 20 min. Ethanol (20 mL) was added, and the solvent volume was concentrated under reduced pressure until precipitation was complete. The pale green product was filtered and washed with ethanol (10 mL) and hexane (10 mL). Yield: 23 mg (82%). IR (CH_2Cl_2): 1605, 1572 (ν(C=O)). IR (KBr/Nujol): 1685, 1568 (ν(C=O)), 1312, 1238, 972, 849 cm^{-1}. ^{31}P NMR ($CDCl_3$): δ −4.3, −19.5 (t × 2, J_{PP} = 32.6 Hz, dppm). ^{1}H NMR ($CDCl_3$): 4.26, 4.72 (m × 2, 2 × 2H, PCH_2P), 6.40, 6.85, 7.17, 7.26, 7.49, 7.24 (m × 6, 40H, PC_6H_5). ^{13}C NMR (CD_2Cl_2): δ 45.7 (m, CH_2), 129.6−134.2 (C_6H_5), 218.6 (s, CO). FAB-MS *m/z* (abundance): 961 (53) [M]$^+$, 902 (100) [M − SCO]$^+$. Anal. Calcd for $C_{51}H_{44}OP_4RuS_2{\cdot}2CH_2Cl_2$: C, 56.2; H, 4.3. Found: C, 56.2; H, 4.4%.

[Ru(κ²-S₂COMe)(dppm)₂]BF₄ (4). (a) NaOMe (17 mg, 0.325 mmol) was dissolved in methanol (10 mL), and carbon disulfide (25 mg, 0.328 mmol) was added. The reaction mixture was stirred for 20 min. *cis*-[RuCl₂(dppm)₂] (**1**) (100 mg, 0.106 mmol) was dissolved in dichloromethane (10 mL) and added to give a colorless precipitate. The solution was treated with an aqueous solution (0.5 mL) of $NaBF_4$ (24 mg, 0.219 mmol), and the reaction mixture was stirred for 1 h. All solvent was removed under reduced pressure; the residue was taken up in a minimum quantity of dichloromethane and filtered through diatomaceous earth. Methanol (20 mL) was added, and the solvent volume was concentrated under reduced pressure until precipitation was complete. The colorless product was filtered and washed with ethanol (10 mL) and hexane (10 mL). Yield: 81 mg (72%). (b) Complex **3** (30 mg, 0.031 mmol) was dissolved in dichloromethane (10 mL) and treated with trimethyloxonium tetrafluoroborate (4 drops, excess); the reaction mixture was stirred for 30 min. Ethanol (20 mL) was added, and the solvent volume was concentrated under reduced pressure until precipitation was complete. The product was filtered and washed with ethanol (10 mL) and hexane (10 mL). Yield: 19 mg (58%). IR (KBr/Nujol): 1335, 1312, 1248, 1057 (ν(BF)), 957 cm^{-1}. ^{31}P NMR ($CDCl_3$): δ −2.1, −14.5 (t × 2, J_{PP} = 35.8 Hz, dppm). ^{1}H NMR ($CDCl_3$): δ 3.80 (s, 3H, OCH_3), 4.45, 4.90 (m × 2, 2 × 2H, PCH_2P), 6.42, 6.95, 7.05, 7.23, 7.36, 7.57 (m × 6, 40H, PC_6H_5). FAB-MS *m/z* (abundance): 977 (100) [M]$^+$. Anal. Calcd for $C_{52}H_{47}BF_4OP_4RuS_2$: C, 58.7; H, 4.5. Found: C, 58.5; H, 4.4.

X-ray Crystallography. Crystals of **1**·PrOH were grown by slow diffusion of ethanol into a dichloromethane solution of the complex (containing small amounts of propanol), whereas crystals of **3**·2CH_3OH were obtained from slow diffusion of methanol into a dichloromethane solution of the complex. Slow evaporation of a concentrated chloroform solution of **3** led to crystals of **3**·3$CHCl_3$ being obtained. Although crystals of **4**·CH_3OH were obtained by layering a chloroform solution of the complex with hexane, a molecule of methanol was retained. Single crystals were mounted

(17) Allen, F. H.; Kennard, O.; Watson, D. G.; Brammer, L.; Orpen, A. G.; Taylor, R. *J. Chem. Soc., Perkin Trans.* **1987**, S1.
(18) Coto, A.; Tenorio, M. J.; Puerta, M. C.; Valerga, P. *Organometallics* **1998**, *17*, 4392.

Table 2. Crystal Data for Compounds **3** (Two Modifications) and **4**

	3·2CH_3OH	**3**·3$CHCl_3$	**4**·CH_3OH
chemical formula	$C_{52}H_{44}O_3P_4RuS_2$	$C_{54}H_{47}Cl_9OP_4RuS_2$	$C_{53}H_{51}BF_4O_2P_4RuS_2$
fw	1017.95	1320.04	1095.82
cryst syst	monoclinic	monoclinic	monoclinic
cryst color	yellow	yellow	yellow
cryst size (mm^3)	0.15 × 0.08 × 0.08	0.28 × 0.28 × 0.20	0.64 × 0.64 × 0.42
space group	*C*2/*c*	*P*2/1	*C*2/*c*
a (Å)	16.834(4)	14.8972(17)	35.754(2)
b (Å)	15.592(4)	18.274(2)	11.8150(7)
c (Å)	17.693(4)	21.145(2)	24.7544(14)
α (deg)	90	90	90
β (deg)	95.004(4)	91.065(2)	109.9030(10)
γ (deg)	90	90	90
V (Å^3)	4626(2)	5755.4(11)	9832.5(10)
Z	4	4	8
D_{calcd} (g/cm^3)	1.462	1.523	1.481
T (K)	150(2)	150(2)	150(2)
μ(Mo Kα) (mm^{-1})	0.612	0.912	0.591
F(000)	2120	2672	4496
no. of reflns collected	19290	50105	42408
no. of unique reflns (R_{int})	5530 (0.0813)	26107 (0.0188)	11725 (0.0186)
R1 ($I > 2\sigma(I)$)	0.0713	0.0369	0.0382
wR′2 (all data)	0.1924	0.1002	0.1069

on glass fibers, and all geometric and intensity data were taken from these samples on a Bruker SMART APEX CCD diffractometer using graphite-monochromated Mo Kα radiation (λ = 0.71073 Å) at 150 ± 2 K. Data reduction and integration were carried out with SAINT+ and absorption corrections were applied using the SADABS program. The structures were solved by direct methods and developed using alternating cycles of least-squares refinement and difference Fourier synthesis. All non-hydrogen atoms were refined anisotropically. Hydrogen atoms were placed in calculated positions and their thermal parameters were linked to those of the atoms to which they were attached (riding model). Structure solution and refinement used the SHELXTL PLUS version 6.10 program package.[19] Selected crystal data are given in Table 2 (see the Supporting Information for crystal data for **1**·PrOH).

Crystallographic data for the structure of complexes **1**·PrOH, **3**·2CH_3OH, **3**·3$CHCl_3$, and **4**·CH_3OH have been deposited with the Cambridge Crystallographic Data Centre as CCDC 278731, CCDC 278732, CCDC 278733, and CCDC 283230, respectively. Copies of the data can be obtained free of charge on application to The Director, CCDC, 12 Union Road, Cambridge CB2 1EZ, U.K. (Fax: 44 (1223) 336-033. E-mail for inquiry: fileserv@ccdc.cam.ac.uk.)

Acknowledgment. J.D.E.T.W.-E. gratefully acknowledges Merton College for a Fitzjames Research Fellowship and the Ramsay Memorial Trust for a Research Fellowship. We thank EPSRC for a studentship (D.S.); the UCL Department of Chemistry, the University of London Central Research Fund, and the UCL Graduate School for funding for consumables; and Johnson Matthey Ltd. for a generous loan of ruthenium salts and Cognis Ltd. for funding.

Supporting Information Available: Crystal data and structural discussion for **1**·PrOH and figures depicting the crystal structures of **1**·PrOH and **3**·3$CHCl_3$. This material is available free of charge via the Internet at http://pubs.acs.org.

IC060223B

(19) *SHELXTL*, version 6.10; Bruker AXS: Madison, WI, 2000.